



# THE UNIVERSITY *of* EDINBURGH

This thesis has been submitted in fulfilment of the requirements for a postgraduate degree (e.g. PhD, MPhil, DClinPsychol) at the University of Edinburgh. Please note the following terms and conditions of use:

This work is protected by copyright and other intellectual property rights, which are retained by the thesis author, unless otherwise stated.

A copy can be downloaded for personal non-commercial research or study, without prior permission or charge.

This thesis cannot be reproduced or quoted extensively from without first obtaining permission in writing from the author.

The content must not be changed in any way or sold commercially in any format or medium without the formal permission of the author.

When referring to this work, full bibliographic details including the author, title, awarding institution and date of the thesis must be given.

**Investigating the role of *eef1a2* in zebrafish as a  
potential disease model.**

**Nwamaka Juliana Idigo**



**THE UNIVERSITY  
*of* EDINBURGH**

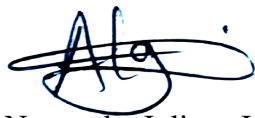
**A thesis submitted for the degree of  
Doctor of Philosophy**

**The University of Edinburgh**

**2018**

## Declaration

I declare that this thesis has been written by me and that all the work presented within is my own and was performed by me unless stated otherwise. All sources of information and other individuals' contributions have been appropriately acknowledged. This work has not been submitted for any other degree or professional qualification

A handwritten signature in blue ink, appearing to read 'Nwamaka', with a large, stylized flourish extending to the right.

Nwamaka Juliana Idigo

## **Dedication**

This thesis is dedicated to all women juggling motherhood with a career in science. Having faced it myself during the course of writing this thesis, I am only full of admiration for you and say keep going!

## Acknowledgements

I would like to thank my supervisor Prof. Cathy Abbott in a very special way for all her support, understanding and guidance throughout the course of my PhD. I won't have been able to complete this thesis if not of the great love and encouraging messages which kept me motivated. You were not just a supervisor but also a mentor, a friend and a teacher to me. I would also like to thank past and present members of my thesis committee; Dr Toby Hurd, Prof. David Fitzpatrick, Dr. Dinesh Soares and Dr. David Lyons for all their contributions and support along the way.

To all the members of the Abbott group, past and present, and all my other research colleagues; Faith, Fiona, Francis, Vesa, Shane and Katerina, thank you for all the small chats and goodies you shared with me. They really brightened up my days. To my wonderful IGMM Dream Team ladies; Elena, Jilly, Marion and Rodanthi, thank you for making N4.10 very homely when we were all in there and for always giving me the extra push I needed to finish up with my writing. Rodanthi, thank you for your patience in answering my endless silly questions about the zebrafish. You are free of them now!

I am immensely grateful to members of the MRC, HGU zebrafish facility; Dr. Cameron Wyatt, Wei Qing and Lori Tighe (past member) for all your help with zebrafish husbandry and embryo injections. I would also like to thank Dr. Liz Patton and her team especially Zhiqiang Zeng and past member Witold Rybski for their help in the generation of the *eef1a2* mutant lines and also for their readiness to assist me and provide me with reagents and working protocols. To Dr. Therese Bergendahl, thank you for giving me a crash course on comparative homology modeling for proteins. The seizure behaviour analysis would not have been possible if not of Craig Nicol. Thank you for turning your precious studio into a mini laboratory for my video recording. I would also like to thank Dr. Pia Lundegaard for analysing the videos. I would also like to thank Dr. Jorge del Pozo for his detailed histological examination of my mutant lines and also his guidance with my analysis.

I would like to thank Rosemary and Andrew Milligan for being wonderful and very supportive with Michael and giving me some 'me time' once in a while. Even though

you keep saying you are not doing enough, those times when you showed up was always just right. I am grateful to you for opening up your home to me as my study room and thank you, Peter Milligan for being such a great study buddy on some of those days. I would also like to thank all my other friends especially those at St Andrews Ravelston for your great show of concern and offers to help.

To all my family including my in-laws, I will like to thank you for your support. Mum and Dad, you have been amazing parents and I am forever grateful for the constant love, prayers and phone calls you made to keep me going. I love you all and I am proud to be your daughter. To my other half, Ife mi, Di m oma, Anthony Ojo, you have been the best as a husband and my thesis planner. Thank you for being by my side and making my journey more organised and stress-free. Finally and in a big way, I would like to thank my son Michael Tobechukwu Ojo, who showed me I was stronger than I could ever imagine. I am stronger and better at using my 24 hours because of you, for which mummy says Thank you Bobo!

## Lay summary

eEF1A is a molecule which plays a significant role in a process used by cells to make new proteins, which are important for them to survive. This molecule occurs in slightly different forms in many animals, for example, in mice and human, there are two forms called eEF1A1 and eEF1A2. Every cell contains only one form of eEF1A. eEF1A2 is present only in the nerve, heart and muscle cells, while eEF1A1 can be found in the rest of the other cells types. Mice that have no eEF1A2 show abnormal characteristics such as loss of nerve and muscle cells, deteriorate rapidly and die at 28 days old. Recently, eEF1A2 has been shown to cause epilepsy, autism and intellectual disability in humans. Our research focuses on providing better understanding of the role of eEF1A2 in these neurological disorders. Our approach involves the use of different models, as insights from them can lead to better treatment strategies.

One model that is increasingly becoming popular is the zebrafish. Zebrafish has many advantages, one in particular is the ease to use them for drug testing experiments. The main aim of my PhD was to try and generate a zebrafish model of these neurological disorders caused by eEF1A2. Zebrafish have four forms of eEF1A genes: *eef1a1lll*, *eef1a1a*, *eef1a1b* and *eef1a2*. As we do not know much about *eef1a* in zebrafish, I looked at different early stages and adult tissues for the different *eef1a* forms using some molecular techniques. My results showed *eef1a1lll* is seen first, followed by *eef1a1a* and *eef1a1b* and much later during development, *eef1a2*. To understand the role of *eef1a2* in zebrafish, I generated and characterised zebrafish with two mutant copies of *eef1a2*. These fish were healthy and did not show any neurological abnormality, and unlike the process seen in mice, they survive to adulthood. We think the fish remain healthy because of the presence of the other *eef1as* and so any deleterious effect that may have occurred by the loss of *eef1a2* is prevented. However, a pilot study suggests that loss of *eef1a2* might make zebrafish vulnerable to induced seizures similar to cases we have observed in mice.

In all, this study has provided us with valuable information of how eEF1A works in zebrafish which will help in further investigation.

## Abstract

Eukaryotic elongation factor (eEF1A) plays a vital role in protein synthesis. It recruits amino-acylated tRNAs and delivers them to the ribosome during protein translation. eEF1A is conserved throughout evolution and exists as independently encoded isoforms in many species. In mammals, there are two isoforms: eEF1A1 and eEF1A2. Unlike eEF1A1 which is widely expressed, expression of eEF1A2 is restricted to the brain, heart and skeletal muscle and is upregulated during development. In mice, homozygote deletion in *Eef1a2* gene resulting in the complete loss of function of eEF1A2 causes severe neurodegeneration, loss of muscle bulk and death by 28 days. Recently, *de novo* heterozygous missense mutation in *EEF1A2* has been identified in humans which cause epilepsy, autism and intellectual disability. The main aim of this project was to investigate the use of zebrafish as a model to better understand the role of eEF1A2 in neurological disorders. In addition to its many advantages, the zebrafish has been shown to be an excellent tool for *in vivo* drug screening. This is an attractive attribute for our studies as regards developing treatment strategies for these disorders. Zebrafish possess four *eef1a* genes: *eef1a1l1*, *eef1a1a*, *eef1a1b* and *eef1a2* which encodes separate highly similar proteins: eEF1A1L1, eEF1A1A, eEF1A1B and eEF1A2 respectively. The zebrafish eEF1A2 shares a 94% sequence identity with the mouse and human eEF1A2 at the amino acid level. In this work, characterisation of zebrafish eEF1A genes was first carried out, as there is currently little information available. Using conventional reverse transcriptase polymerase chain reaction (RT-PCR) and real time quantitative PCR (qPCR), I analysed the expression pattern of *eef1a* genes at different embryonic stages and adult tissues. These genes were differentially expressed with only *eef1a1l1* detected at earlier developmental stages, followed by *eef1a1a* and *eef1a1b*. Similar to mammals, *eef1a2* is detected much later (48 hpf) during development. Co-expression of *eef1a* mRNA was observed in the adult tissues analysed except in liver where *eef1a2* was not detected. An attempt to knock-in one of the epilepsy causing variant, G70S into the zebrafish genome using CRISPR/Cas9 technology was unsuccessful. However, I established two null *eef1a2* mutant lines using this technology. Homozygotes from these null lines showed no obvious phenotype and in contrast to null *Eef1a2* mice, they are fertile and viable through adulthood. No evidence of neurodegeneration was observed. These results



suggest the possibility of compensatory mechanisms activated by the other *eef1a* genes to buffer the loss of *eef1a2* in the mutants. However, preliminary findings suggest that *eef1a* null mutation might cause zebrafish to be susceptible to PTZ-induced seizures. Results from this work has provided vital information on functional redundancy of *eef1a* genes in zebrafish and a foundation for further validation of the zebrafish as a model system.

# Table of Contents

<b>Declaration</b> .....	ii
<b>Dedication</b> .....	iii
<b>Acknowledgements</b> .....	iv
<b>Lay summary</b> .....	vi
<b>Abstract</b> .....	vii
<b>List of figures</b> .....	xii
<b>List of tables</b> .....	xiv
<b>List of abbreviations</b> .....	xv
<b>Chapter 1: Introduction</b> .....	1
1.0 Protein synthesis .....	1
1.1 Eukaryotic elongation factor 1 alpha (eEF1A) .....	1
1.1.1 eEF1A exists as different isoforms that show reciprocal expression patterns.....	2
1.1.2 Isoform switching is conserved through evolution.....	3
1.1.3 Non-canonical roles of eEF1A .....	5
1.1.4 Post-translational modification .....	10
1.2 eEF1A2 role in diseases .....	13
1.2.1 The wasted mouse.....	13
1.2.2 eEF1A2 role in epilepsy, autism and intellectual disability .....	15
1.2.3 eEF1A2 in cancer.....	19
1.3 Zebrafish: a useful tool for modelling human diseases.....	22
1.3.1 Comparison of the zebrafish and human central nervous system with a focus on relevant regions in modelling human neurological disease .....	23
1.3.2 Zebrafish models for motor neuron disease.....	25
1.3.3 Zebrafish models of epilepsy .....	32
1.4 Local mRNAs translation in neurons .....	35
1.5 Previous studies of the eukaryotic elongation factor 1 alpha in zebrafish .....	38
1.6 Project aims .....	39
<b>Chapter 2: Materials and Methods</b> .....	40
2.1 Materials.....	40
2.1.1 Reagents.....	40
2.1.2 Oligonucleotides for gRNAs synthesis.....	42
2.1.3 Primers .....	42

2.1.4 Antibodies .....	44
2.2 Methods.....	45
2.2.1 Zebrafish model .....	45
2.2.2 Methods for RNA analysis .....	46
2.2.3 <i>eef1a</i> constructs preparation and expression analysis.....	53
2.2.4 Method for protein analysis .....	55
2.2.5 Generation of mutant lines using CRISPR/Cas9 .....	59
2.2.6 PCR protocol.....	63
2.2.7 General sequencing protocol .....	65
2.2.8 PTZ treatment and behavioural monitoring.....	65
2.2.9 Histology.....	67
2.2.10 Databases and online resources .....	68
<b>Chapter 3: Bioinformatics and expression analysis of Zebrafish eEF1A .....</b>	<b>70</b>
3.1 Introduction .....	70
3.2 Results.....	71
3.2.1 Bioinformatics analysis of <i>eef1a</i> in zebrafish.....	71
3.2.2 Expression analysis of <i>eef1a</i> isoforms during zebrafish development and adult tissues.....	95
3.3 Discussion .....	109
<b>Chapter 4: Modelling eEF1A2 disease-causing mutation in zebrafish .....</b>	<b>116</b>
4.1 Introduction .....	116
4.1.1 Guide RNA (gRNA) synthesis .....	117
4.1.2 CRISPR/Cas9-mediated HDR experimental design.....	120
4.1 Results.....	122
4.1.1 Microinjection and screening of founders for mutation .....	122
4.2 Discussion .....	125
<b>Chapter 5: Generation and characterisation of <i>eef1a2</i> knockout zebrafish model.....</b>	<b>129</b>
5.1 Introduction .....	129
5.2 Results.....	130
5.2.1 Generation of <i>eef1a2</i> null zebrafish lines .....	130
5.2.2 Germline transmission and establishing stable mutant lines .....	132
5.2.3 Del2 and Ins4 mutant lines show reduced <i>eef1a2</i> transcript levels. ....	135
5.2.4 Characterisation of mutant fish by histology.....	138

5.2.5 Transcript levels of the other <i>eef1a</i> genes .....	142
5.2.6 Behavioural characterisation of homozygous <i>Ins4</i> mutant larvae .....	144
5.3 Discussion .....	148
<b>Chapter 6: Summary and future directions</b> .....	155
6.1 Summary .....	155
6.1.1 Bioinformatics and expression analysis of Zebrafish eEF1A.....	155
6.1.2 Modelling an eEF1A2 disease-causing mutation in zebrafish.....	157
6.1.3 Generation and characterisation of <i>eef1a2</i> null zebrafish model.....	159
6.2 Future directions.....	160
6.2.1 Potential of using the zebrafish and its eEF1A isoforms to understand the functions of eEF1A in vertebrates .....	160
6.2.2 Translational validity of the <i>eef1a2</i> mutant lines for neurological diseases .....	163
6.3 Conclusion .....	167
<b>Appendices</b> .....	167
<b>References</b> .....	176

## List of figures

Figure 1.1. Schematic of eEF1A participation in protein translation.....	2
Figure 1.2: Expression pattern of eEF1A isoforms in adult <i>Xenopus laevis</i> .....	4
Figure 1.3: eEF1A isoforms generate F-actin bundles with different morphology....	7
Figure 1.4. 3-D structure of human eEF1A2 showing location of missense mutations with respect to known binding sites mapped onto its surface.....	19
Figure 3.1. Exon-intron organisation of the <i>eef1a</i> genes in zebrafish.....	70
Figure 3.2. Comparison of the intron-exon structure of the zebrafish eEF1A1L1 gene and eEF1A genes in human and mouse species.....	70
Figure 3.3. Molecular Phylogenetic analysis of eEF1A1 and eEF1A2 orthologues by Maximum Likelihood method.....	73
Figure 3.4. Conserved synteny analysis for zebrafish <i>eef1a</i> genes.....	76
Figure 3.5. Multiple sequence alignment of the zebrafish and human eEF1A isoforms with the yeast eEF1A as a template.....	81
Figure 3.6. Mapping of variant amino acids and known binding sites onto the surface of zebrafish eEF1A isoforms.....	85
Figure 3.7. Sequence alignment showing predicted phosphorylation sites for zebrafish eEF1A proteins.....	90
Figure 3.8. Location of isoform-specific potential phosphorylation sites on the 3-D structure of the eEF1A protein.....	92
Figure 3.9. Expression of <i>eef1a</i> genes during zebrafish development assayed by RT-PCR.....	95
Figure 3.10. Whole-mount <i>in situ</i> hybridisation analysis of <i>eef1a</i> expression in different developmental stages in zebrafish.....	96
Figure 3.11. Expression analysis of the four <i>eef1a</i> genes in adult tissues.....	100
Figure 3.12. eEF1A2 expression in zebrafish tissues using eEF1A2-Abcam antibody.....	104
Figure 3.13. Expression of eEF1A constructs confirmed by Western blot analysis.	106
Figure 3.14. Validation analysis of eEF1A2-Abcam antibody using the expression eEF1A constructs.....	106
Figure 4.1. Mutation rate analysis of gRNA3 and gRNA5 in CRISPR-Cas9 experiment.....	117
Figure 4.2. G70S zebrafish CRISPR/Cas9 experimental design.....	119

Figure 4.3. CRISPR/Cas9 experiment generated indels but failed to generate a G70S mutation in ssODN injected founders.....	122
Figure 5.1. PCR products amplified from F0 fish injected with gRNA3 or gRNA5 in the CRISPR-Cas9 experiment.....	129
Figure 5.2. Establishing <i>eef1a2</i> mutant zebrafish line.....	131
Figure 5.3. Reduced <i>eef1a2</i> transcript levels in Del2 and Ins4 mutants.....	135
Figure 5.4. Del2 and Ins4 characterisation by histology.....	138
Figure 5.5. Transcript levels of the other <i>eef1a</i> gene in del2 and Ins4 adult brain....	141
Figure 5.6. Locomotor activity analysis of Ins4 and wild-type zebrafish larvae exposed to 2.5mM PTZ or E3 medium.....	144
Figure 5.7. Seizure behaviour analysis in Ins4 and wild-type zebrafish larvae.....	145
Appendix figure 1: geNorm analysis for selecting reference genes for qPCR experiments.....	165
Appendix figure 2: Analysis of <i>eef1a2</i> transcripts in Ins4 and confirmation of the possibility of Del2 and Ins4 mutations leading to nonsense-mediated decay.....	166
Appendix figure 3: Preliminary histological examination of the brain from one homozygous Ins4 fish (5 months old) and age-matched wild-type zebrafish.....	167
Appendix figure 4: Time evolution of a representative larva showing a pattern of activity consistent with stage III seizure behaviour.....	168

## List of tables

Table 1.1 Summary of experimentally validated phosphorylated sites in eEF1A isoform.....	11
Table 1.2: Published cases of patients with missense mutations in <i>EEF1A2</i> and associated phenotypes.....	16
Table 1.3: Summary of some studies which showed overexpression of eEF1A2 in different human cancer types.....	20
Table 1.4: Most common genes linked to ALS with statistics obtained from the Amyotrophic lateral sclerosis online genetics database (accessed July 2018).....	27
Table 1.5: Nomenclature of the zebrafish eEF1A isoforms.....	37
Table 2.1: List of reagents used in this work and their recipe.....	38
Table 2.2: Oligonucleotide sequences used to generate gRNAs for CRISPR/Cas9 experiment.....	40
Table 2.3: Sequences of primers used in this work.....	41
Table 2.4: List of antibodies employed in this project.....	42
Table 2.5: Description of embryonic developmental stages used for expression analysis taken from ZFIN.....	44
Table 2.6: List of genes in the zebra fish geNorm kit (PrimerDesign, UK).....	46
Table 3.1. Main features of the <i>eef1a</i> genes in zebrafish.....	69
Table 3.2. Percentage identity matrix of zebrafish eEF1A variants at the nucleotide and amino acid sequence level calculated using Clustal Omega.....	71
Table 3.3: Predicted isoform-specific phosphorylation sites in zebrafish eEF1A proteins.....	91
Table 4.1: Mutagenesis efficiency of CRISPR/Cas9 genome editing to target <i>eef1a2</i> in zebrafish.....	116
Table 4.2: Number of surviving fish at different ages injected with 92ng/μl and 183ng/μl ssODN.....	120
Appendix Table 1: Positions with amino acid variation and the respective residues in the four zebrafish eEF1A isoforms.....	169
Appendix Table 2: Slope, intercept and correlation coefficient ( $R^2$ ) output from SDS software to estimate efficiency of primers used for qPCR analyses.....	172

## List of abbreviations

AEDs	Anti-epileptic drugs
ANOVA	Analysis of variance
ATP	Adenosine triphosphate
<i>ATPsynth</i>	ATP synthase (Zebrafish gene)
BLAST	Basic Local Alignment Search Tool
bp	Base pair
BSA	Bovine serum albumin
CCe	Corpus cerebelli
cDNA	Complementary DNA
CNS	Central nervous system
CRISPR	Clustered regularly interspaced short palindromic repeats
DIG	Digoxigenin
DMEM	Dulbecco's modified eagle medium
DNA	Deoxyribonucleic acid
dpf	days post fertilization
DSB	Double-stranded break
DTT	Dithiothreitol
EDTA	Ethylenediaminetetraacetic acid
eEF1A	Eukaryotic elongation factor 1 alpha (protein)
<i>EEF1A1</i>	Eukaryotic elongation factor 1 alpha 1 (Human gene)
<i>Eef1a1</i>	Eukaryotic elongation factor 1 alpha 1 (Mouse gene)
<i>eef1a1a</i>	Eukaryotic elongation factor 1 alpha 1A (Zebrafish gene)
<i>eef1a1b</i>	Eukaryotic elongation factor 1 alpha 1B (Zebrafish gene)
<i>eef1a1ll</i>	Eukaryotic elongation factor 1 alpha 1 like 1 (Zebrafish gene)
<i>EEF1A2</i>	Eukaryotic elongation factor 1 alpha 2 (Human gene)
<i>eef1a2</i>	Eukaryotic elongation factor 1 alpha 2 (Zebrafish gene)
<i>Eef1a2</i>	Eukaryotic elongation factor 1 alpha 2 (Mouse gene)
eEF1B	Eukaryotic elongation factor 1B
GDP	Guanosine diphosphate
GFAP	Glial fibrillary acidic protein
GFP	Green fluorescent protein
gRNA	Guide RNA
GTP	Guanosine triphosphate
H&E	Haematoxylin and eosin
HDR	Homology-directed repair
HEK293	Human embryonic kidney 293
HM	Hybridisation Mix
hpf	hours post fertilization
HRP	Horse radish peroxidase
IHC	Immunohistochemistry
MABT	Maleic acid buffer-Tween
MND	Motor neuron degeneration
mRNA	Messenger ribonucleic acid
NADH	Nicotinamide adenine dinucleotide (NAD) + hydrogen (H)



<i>NADH</i>	NADH dehydrogenase (Zebrafish gene)
NHEJ	Non-homologous end joining
NMD	Nonsense-mediated decay
NTMT	Alkaline phosphatase buffer
PAM	Protospacer adjacent motif
PBS	Phosphate buffered saline
PBS-T	PBS-Tween
PCR	Polymerase chain reaction
PFA	Paraformaldehyde
PTMs	Post-translational modifications
PTZ	Pentylentetrazole
qPCR	Quantitative PCR
RBH	Reciprocal best hit
RIPA	Radioimmunoprecipitation assay
RNA	Ribonucleic acid
RT-PCR	Reverse transcriptase PCR
SSC	Saline Sodium Citrate
ssODN	Single-stranded oligonucleotide
TALEN	Transcription activator-like effector nucleases
TBS-T	Tris-buffered saline, 0.1% Tween 20
tRNA	Transfer ribonucleic acid
UTR	Untranslated region
WB	Western blot
WISH	Whole mount in situ hybridisation
<i>Wst</i>	Wasted
WT	Wild-type
ZFN	Zinc finger nucleases

# Chapter 1: Introduction

## 1.0 Protein synthesis

Protein synthesis is one of the essential biological processes employed by cells to survive. During protein synthesis, cells use the information contained in the DNA to make specific proteins that help in the proper functioning of the cell. An important part of this process is translation, which is the actual stage where the protein is synthesised using mRNA as a template. Protein synthesis is divided into three phases; initiation, elongation and termination. During initiation, the initiation complex is formed by the binding of the ribosomal small unit and the initiator methionine-tRNA to the start codon (AUG) on the mRNA. Subsequently, the large ribosomal subunit binds to the initiator complex. The second phase, elongation, involves the assembling of amino acids which are carried by tRNAs to the growing polypeptide chain following the sequence contained in the mRNA. This phase is repeated and involves the same mechanism until any of the three stop codons, UAA, UAG and UGA, is reached in the mRNA and signals the start of the last phase, termination. At this phase, the newly synthesised protein is released from the ribosome which is then recycled and made available for another translation process. Each of these phases is coordinated by several protein factors to ensure the precise spatial and temporal levels of protein are synthesised for normal physiological functions (Livingstone *et al.*, 2010).

### 1.1 Eukaryotic elongation factor 1 alpha (eEF1A)

Eukaryotic elongation factor 1 alpha (eEF1A), formerly referred to as EF1 $\alpha$ , is a member of the G protein family and the second most abundant protein after actin, making up about 1-2% of the total protein in normal growing cells (Condeelis, 1995). Delivery of aminoacylated-tRNAs to the A-site of the ribosome during the elongation step of translation is catalysed by this protein. This process is GTP-dependent and is mediated by the guanine exchange factor, eEF1B. Once the anticodon region of the recruited aminoacylated-tRNA correctly matches the codon of the mRNA at the A-site of the ribosome, the GTP bound to eEF1A is hydrolysed. The inactive eEF1A-GDP complex is then reactivated by eEF1B which exchanges the GDP for GTP, to bind another aminoacylated-tRNA (Figure 1.1).

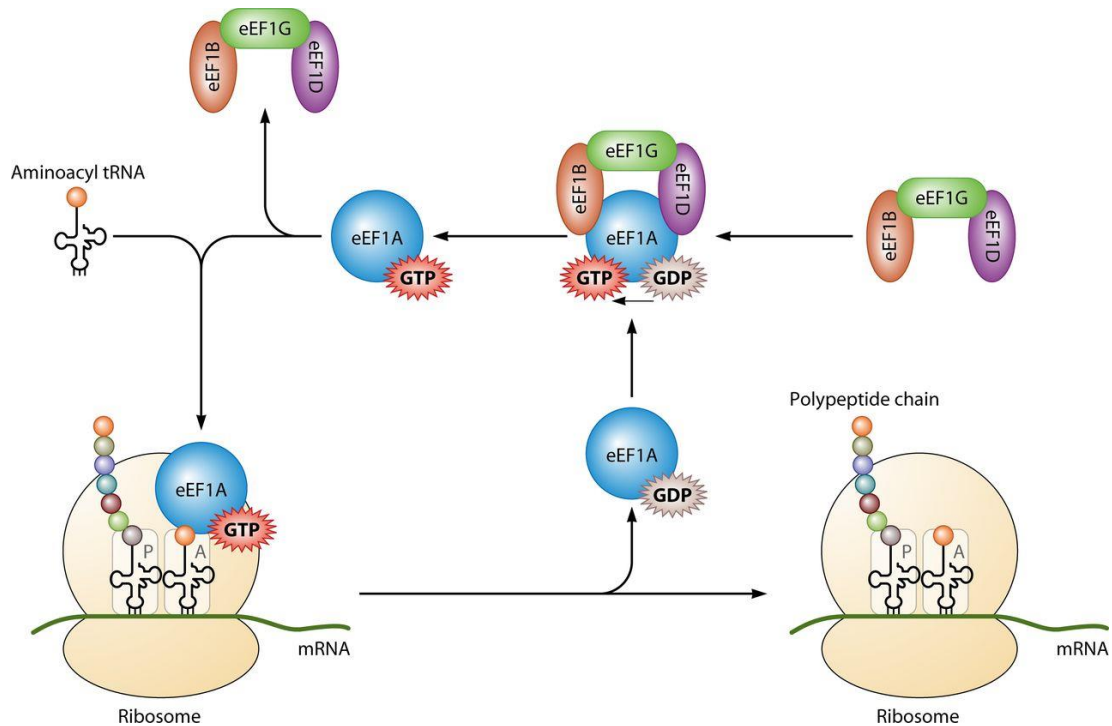


**Figure 1.1. Schematic of eEF1A participation in protein translation.** During elongation, the eEF1A in its active state (bound to GTP) recruits aminoacylated tRNA to the A site of the ribosome. Recognition of the anticodon region of the aminoacylated tRNA by the codon of the mRNA triggers the hydrolysis of GTP to GDP, releasing eEF1A-GDP from the ribosome to be recycled. To reactivate itself, eEF1A exchanges the bound GDP for GTP with the guanine exchange factor, eEF1B. The multi-unit eEF1B protein consists of three subunits: eEF1B is shown in orange, eEF1G in green, and eEF1D in purple. **Taken from** (Li *et al.*, 2013).

### 1.1.1 eEF1A exists as different isoforms that show reciprocal expression patterns

The presence of multiple eEF1A genes which are usually located on separate chromosomes has been described in different eukaryotic species. For example, two sequence-redundant eEF1A genes *TEF1* and *TEF2* are present in the yeast, *Saccharomyces cerevisiae* (Nagata *et al.*, 1984; Nagashima, Nagata and Kaziro, 1986). In *Drosophila melanogaster*, two genes, F1 and F2, have been described (Hovemann *et al.*, 1988) while in *Xenopus laevis*, four eEF1A genes, *EF-1aO*, *EF-1aS*, *42Sp50* and *eEF1A2*, have been reported so far (Djé *et al.*, 1990; Newbery *et al.*, 2011). In mammalian species, two eEF1A genes have been shown to be actively expressed (Ann *et al.*, 1992; Knudsen *et al.*, 1993; Chambers, Peters and Abbott, 1998; Kahns *et al.*, 1998; Svobodová *et al.*, 2015). In vertebrates, these genes encode different eEF1A proteins, eEF1A1 and eEF1A2, with amino acid sequences that are highly conserved.

Interestingly, eEF1A variants are more identical between species than they are when compared within the same species. For example, human eEF1A1 show a 99.8% sequence identity with its mouse orthologue but is only 92.4% identical to the human eEF1A2 isoform. This suggests that these duplicated eEF1A genes might have acquired some other functional differences which are biologically important, hence they were positively selected and retained in the genomes.

Another common feature of eEF1A genes is that they show a developmental and tissue-specific pattern of expression. In mammalian species where this has been extensively studied, eEF1A1 is widely expressed during development but is then down-regulated in the brain, heart and skeletal muscle postnatally and replaced with eEF1A2 in these tissues (Knudsen *et al.*, 1993; Lee, Wolfrain and Wang, 1993; Chambers, Peters and Abbott, 1998; Svobodová *et al.*, 2015). While a complete switch of eEF1A variants is observed in adult muscle tissues, eEF1A1 remains expressed in the glial cells, some small neuronal cells (most neurons show eEF1A2 expression) and white matter of the spinal cord in mice (Khalyfa *et al.*, 2001; Newbery *et al.*, 2007). In human and mice, eEF1A2 expression was also observed in the pancreatic islet cells, enteroendocrine cells in colon crypts and specific cells in the lungs using immunohistochemistry. A consistent expression pattern, except in the lungs, was observed between the two species suggesting the possible functional importance of eEF1A2 in these cells (Newbery *et al.*, 2007).

### **1.1.2 Isoform switching is conserved through evolution**

Although it is still not clear why there are two eEF1A isoforms with very high sequence identity in vertebrates, it is quite intriguing they show differential expression pattern and are developmentally regulated. The regulation of eEF1A variants was initially observed by different studies in mammalian species and was shown to occur at the mRNA level. Subsequent analysis in our laboratory using *Xenopus* confirmed the presence of eEF1A2 in non-mammalian vertebrates (Newbery *et al.*, 2011). Analysis of a range of adult tissues showed overlapping expression of eEF1A1 and eEF1A2 mRNA in the brain, heart and muscle tissues (Figure 1.2A). However, when the expression of eEF1A isoforms were investigated at the protein level, eEF1A1 was absent in the muscle and optic ganglion while eEF1A2 expression was observed in

these tissues (Figure 1.2B). The absence of eEF1A1 and the presence of eEF1A2 in the muscle at the protein level, with both mRNA present was also observed in *Xenopus tropicalis* in this study. Interestingly, translational regulation of eEF1A had been previously suggested to occur in *Xenopus laevis* during embryogenesis and in serum-deprived cultured *Xenopus* cell line (Loreni, Francesconi and Amaldi, 1993). Cell-specific expression data obtained using immunohistochemistry showed eEF1A2 to have widespread expression in cardiac muscle but was restricted to large neurons in the brain and spinal cord of *Xenopus laevis* (Figure 1.2C). This same expression pattern was also seen for eEF1A2 in mammals (Newbery *et al.*, 2007).

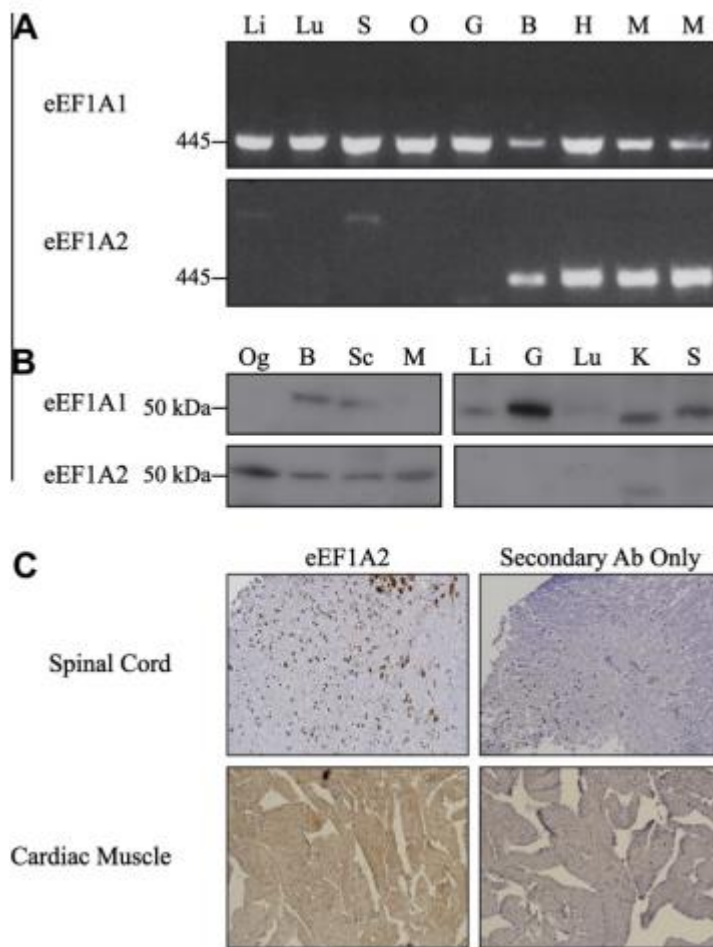


**Figure 1.2: Expression pattern of eEF1A isoforms in adult *Xenopus laevis*.** **A.** RT-PCR of eEF1A1 (top) and eEF1A2 (bottom) mRNA from Liver (Li), Lung (Lu), Spleen (S), oocytes (O), gall bladder (G), brain (B), heart (H) and muscle (M) **B.** Expression analysis using protein lysates from Og-optic ganglion, Brain (B), spinal cord (Sc), Muscle (M), Liver (Li), gall bladder (G), Lung (Lu), Kidney (K) and Spleen (S) for western blot for eEF1A1 (top) and eEF1A2 (bottom). The molecular weight of both protein is ~50kDa. **C.** Immunohistochemistry for eEF1A2 in the spinal cord (top panel) and cardiac muscle (bottom panel). In the spinal cord, eEF1A2 expression is restricted to the neuronal cells but is widespread in the cardiac muscle. **Taken from Newbery *et al.*, 2011.**

The observation that the tissue-specific expression of eEF1A2 and the down-regulation of eEF1A1, most notably in the muscle (where eEF1A2 replaces it), is conserved in vertebrates provides strong evidence to suggest this to have biologically important consequences. What the functional significance is, remains unclear. A plausible hypothesis is that these two isoforms might have other functional differences even though they share the same major role in translation. This is an attractive notion when the architecture of cells that express eEF1A2 only is considered. These cells are terminally differentiated and are more stable, therefore it is likely that some other functional roles of eEF1A1 in these cells might interfere with their overall structure. For this reason, eEF1A1 is replaced with eEF1A2 to avoid or modify these functions but at the same time ensure translational activities are maintained in the cells (Newbery *et al.* 2007). Interestingly, Khalyfa *et al.*, 2003 showed a dramatic upregulation of eEF1A1 in rats muscle after about one month of being subjected to permanent denervation. The level of the eEF1A1 remained high even after two years and could possibly stem from the unstable tissue environment caused by the injury. Similarly, a 165-fold increase of eEF1A1 mRNA was observed in the muscle tissues of trauma patients that were in catabolic conditions than in muscle samples obtained from age-matched healthy controls (Bosutti *et al.*, 2007). These studies further stress the possibility that the non-canonical functions of eEF1A1 might be needed at only a certain point in the development of these cell types that express only eEF1A2 in adults.

### **1.1.3 Non-canonical roles of eEF1A**

In addition to its central role in translation, there is growing evidence that shows eEF1A is a multifunctional protein with a role in a wide variety of biological processes ( reviewed in Ejiri, 2002; Mateyak and Kinzy, 2010). Some non-canonical roles of eEF1A include cytoskeleton interaction and remodelling, proteolysis, apoptosis, nuclear transport and heat shock response. It is still unclear if some of these non-canonical functions, except for heat shock which is eEF1A1 specific (see section 1.1.3.2), are shared by both eEF1A isoforms and how they perform these roles. Understanding this could provide insights into the biological significance of isoform switching in certain cell types. Unfortunately, detangling these ‘moonlighting’

functional relationship between eEF1A1 and eEF1A2 has been technically challenging mostly because of the high similarities in their amino sequence.

### **1.1.3.1 Cytoskeleton interaction and remodelling**

The association of eEF1A with the cytoskeleton is the most established non-canonical function of eEF1A as it has been demonstrated by numerous studies across species. The first direct evidence that showed eEF1A interaction with actin, an important protein of the cell cytoskeletal system, was demonstrated in *Dictyostelium discoideum* (Demma *et al.*, 1990; Yang *et al.*, 1990). Demma *et al.*, 1990 showed eEF1A (formerly known as ABP-50) isolated from *Dictyostelium discoideum* to have strong actin binding and bundling properties *in vitro*. Actin-binding activities of eEF1A, unlike its translational function, are not GTP-dependent but are modulated by pH changes (Edmonds, Murray and Condeelis, 1995). Although there is an obvious link between protein synthesis machinery and the cytoskeleton, the binding of aminoacylated-tRNA and the actin by eEF1A are biochemically separate events. Increasing the pH (from 6.5 to 7.0) favoured the binding of eEF1A to aminoacylated-tRNA and reduced its affinity for F-actin (Liu *et al.*, 1996). However, changes in pH did not affect the binding affinity of eEF1A for aminoacylated-tRNA. Interaction of eEF1A with actin was then demonstrated *in vivo* in the yeast, *Saccharomyces cerevisiae*. Using site-directed mutagenesis, different mutations were identified that reduced actin bundling and disorganisation induced by the overexpression of eEF1A (Gross and Kinzy, 2005, 2007). Some of the mutant strains showed normal elongation activities, while two mutations resulted in reduced translation rate in the yeast. However, aberrant protein synthesis observed in these mutants was due to a translation initiation defect (Gross and Kinzy, 2007). Their finding is consistent with the report of Liu *et al.*, 1996 that these two functions of eEF1A are distinct processes.

Although eEF1A2 has been less studied in terms of actin-related activities, it has been shown to have a role in actin remodelling through its interaction with the phosphatidylinositol-4 kinase III  $\beta$  (PI4IIIK $\beta$ ). Activation of PI4IIIK $\beta$  by eEF1A2 stimulates the formation of filopodia (slender projections that contain bundles of cross-linked actin filaments) *in vitro* (Jeganathan *et al.*, 2008). More efforts are now being made to better understand the actin activities of this variant especially as this can provide more insights into its implication in other processes in particular

transformation (further discussed in section 1.2.3). Recent studies by Novosylina *et al.*, 2017 demonstrated the actin-bundling activity of eEF1A2 *in vitro*. Interestingly, eEF1A1 and eEF1A2 generate actin bundles with different morphology (Figure 1.3), with eEF1A2 producing short, thick and splinter-like actin bundles (Novosylina *et al.*, 2017). The authors implicated the compact dimeric structure of eEF1A2 which was described by Timchenko *et al.*, 2013 as a possible explanation for their observation since it is most likely that eEF1A performs its actin bundling activities as a dimer (Vlasenko *et al.*, 2015). Interestingly, *in silico* analysis of the human eEF1A variants showed that almost all of the amino acid residues that differ between the two proteins were located on one side of the modelled structures away from the binding site of eEF1B $\alpha$  (Soares *et al.*, 2009). They also demonstrated that the residues were arranged in two clusters; a circular band of 12 residues within domain I and a swathe of 14 residues across domain II and III on the variable face of the 3D structures. The identification of eight residues that impact on actin binding properties from the yeast mutagenesis studies (Gross and Kinzy, 2005, 2007) which are also found within domain II and III together with the findings of Novosylina *et al.*, 2017 could suggest that eEF1A1 and eEF1A2 may differ in their actin-related functions.

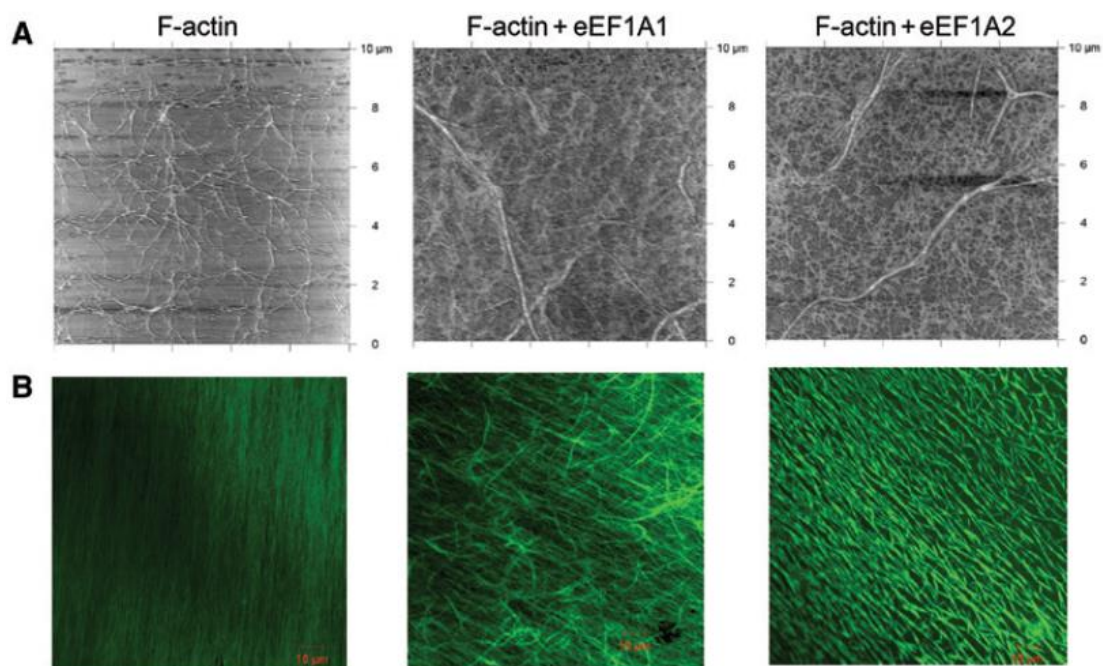


**Figure 1.3: eEF1A isoforms generate F-actin bundles with different morphology.** **A.** Atomic force microscopy (AFM) image showing phalloidin-stabilised F-actin only (Left panel), F-actin bundled with eEF1A1 (centre panel) and F-actin bundled with eEF1A2 (right panel). **B.** Confocal microscope images



showing only F-actin stabilised with phalloidin (bottom left panel), F-actin bundled with eEF1A1 (bottom centre panel) and F-actin bundled with eEF1A2 (bottom right panel). **Taken from Novosylna et al 2017**

In addition to actin, eEF1A has been shown to interact with other components of the cytoskeleton. For example, eEF1A has been reported to have both microtubule bundling and severing abilities. The microtubule bundling activity of eEF1A was demonstrated *in vitro* using eEF1A isolated from carrots (Durso and Cyr, 1994), while eEF1A was purified from *Xenopus* eggs as a rapid microtubule severing protein (Shiina et al., 1994). This study also demonstrated that human eEF1A displays quick microtubule severing function *in vitro* and by microinjecting the recombinant form of the protein into rat fibroblasts. The functional importance or regulation of these microtubule-related activities of eEF1A remains unclear.

### **1.1.3.2 Temperature induced stress**

In response to cold stress, enzymatic elongation factor activities were significantly enhanced in the liver, kidney, spleen, gill, white muscles of rainbow trout with the activity rate varying in these organs except in the red muscle where no compensatory enhancement was observed (Simon, 1987). Although no particular elongation factor was identified in this study, using hybrid protein synthetic systems from fish and rat, eEF1A from Antarctic fish was identified as a major component that was sufficient alone to protect the rat system from the effect of temperature breaks (Haschemeyer, 1985). Similarly, eEF1A was differentially expressed in maize under cold stress, with its mRNA level upregulated in the leaves and transiently reduced in the roots (Berberich et al., 1995).

In response to environmental stresses such as thermal stress, low oxygen and starvation, cells activate genes that encode the heat shock proteins (HSPs). This is known as the heat shock response and has been found to occur in every organism studied so far. Although some characteristics may vary, all organisms share many of the features of this response which include the rapid and intense production of HSPs (Lindquist and Craig, 1988). Induction of the heat shock response is regulated by the HS factors (HSFs) in eukaryotes, with numerous evidence supporting HSF1 as the master regulator in vertebrates (Shamovsky and Nudler, 2008). HSF1 is present in all cells but is only activated by environmental stress stimuli.

The first direct evidence of eEF1A playing a role in the heat shock response was demonstrated *in vitro* by Shamovsky *et al.*, 2006. In this study, eEF1A was identified as a co-activator of HSF1 alongside a non-coding RNA, which they termed heat shock RNA-1 (HSR1). They suggested that the shutdown of protein synthesis and the collapse of the cell cytoskeletal system in response to stress stimuli might cause the release of adequate amounts of eEF1A which is then available to activate the heat-shock response in cells. Although the variant of eEF1A was not indicated, the protein was isolated from rat liver which is known to express only eEF1A1 (Lee, Wolfrain and Wang, 1993).

Subsequent work by Vera *et al.*, 2014 provided a more detailed mechanism of the eEF1A heat-shock response activities. This study revealed a more multi-faceted role of eEF1A in coordinating the heat-shock response. In addition to activating HSF1 as observed in previous work, eEF1A was also responsible for the quick transcription, stabilisation and nuclear export of HSP70 mRNAs upon stress. Also, this study confirmed that eEF1A1 was the variant with heat shock function and that this is not shared by the eEF1A2 isoform. This was demonstrated by the use of short interfering RNA (siRNA) to knockdown eEF1A1 and eEF1A2. Only eEF1A1-deficient cells showed impaired induction of HSPs genes when stressed. This is consistent and provides a suitable explanation for the findings of Batulan *et al.*, 2003, who showed that HSP70 was only expressed in glial cells (express only eEF1A1) but not in cultured motor neuron cells (express eEF1A2 only) when heat-shocked.

### **1.1.3.3 Apoptosis**

Apoptosis, also referred to as programmed cell death, is a tightly controlled series of cellular events employed in multicellular organisms to remove unwanted or damaged cells. Work by Duttaroy *et al.*, 1998 showed that the changes in the expression levels in eEF1A affected the rate of apoptosis in serum-deprived cultured mice fibroblasts. According to this study, overexpression of eEF1A favoured apoptosis while cells were protected from this process with reduced eEF1A levels. In contrast, Talapatra *et al.*, 2002 identified eEF1A from a screen of cDNA libraries to confer apoptotic resistance to hematopoietic cells upon growth factors withdrawal during culture. Despite this discrepancy, the global rate of protein synthesis in the cells were observed to remain unaffected in both studies, suggesting the apoptotic and translational activities of

eEF1A are independent functions. However studies from Ruest *et al*, 2002 demonstrated that the eEF1A variants modulate apoptotic activities in different ways. While eEF1A1 was observed to be pro-apoptotic, eEF1A2, on the other hand, was anti-apoptotic increasing the survival rate of serum-deprived cultured differentiated myotubes. Their findings provide a reasonable explanation to the contradicting results described above especially as it is not clear which of the isoforms these two groups investigated. It is still not fully understood how these isoforms perform the opposite effects on apoptosis. However, it is likely they bind with different protein partners and exert differential regulation on genes involved in this process. For example, Chang and Wang, 2007 showed that eEF1A2 and not eEF1A1 interacts with peroxiredoxin 1 (Prdx-1) in yeast two-hybrid experiments. Mouse cell line NIH 3T3 fibroblasts transfected with both eEF1A2 and Prdx-1 were resistant to peroxide-induced cell death. In addition, activation of caspases 3 and 8, key proteins in the initiation and execution phase of apoptosis, were significantly reduced in these cells. Instead, levels of Akt protein, which promotes survival, increased 5-fold with a further half-fold increment observed when transfected cells were treated with peroxide.

#### **1.1.4 Post-translational modification**

Several post-translational modifications (PTMs) have been reported in the eEF1A protein across species. Interestingly, unlike the amino acid sequence, these modifications are less conserved in eukaryotes (Merrick *et al.*, 1990).

In the rabbit, seven PTMs were identified in eEF1A1 isolated from reticulocytes. These include the addition of ethanolamine to the glutamic amino acids at position 301 and 374, while the other five PTMs involved lysines amino acids with dimethylation at position 55 and 165 and trimethylation at position 36, 79 and 318 (Dever *et al.*, 1989). Chemical sequencing of eEF1A2 purified from rabbit skeletal muscle revealed the same PTMs as eEF1A1 at Glu301 and Glu374. However, Lys55 and Lys165 were trimethylated in this isoform and not dimethylated as observed in eEF1A1 (Kahns *et al.*, 1998).

*In silico* functional analysis by Soares and Abbott, 2013 identified 74 positions that could be post-translationally modified in human eEF1A isoforms. Similarly to the

rabbit eEF1A, there is evidence, as provided by several bioinformatics and experimental studies, that the human eEF1A isoforms may also show different PTM patterns. However, it is worth mentioning that most of the positions involve conserved residues and as such it is impossible to infer the specific isoform these peptides are derived from in most studies. Although most of the type of PTMs reported so far involves phosphorylation of serine, threonine and tyrosine residues, the addition of ethanolamine to Glu301 and Glu374 has been shown to occur in human eEF1A *in vitro* as seen in rabbit (Rosenberry *et al.*, 1989). Some experimentally reported phosphorylation sites in human eEF1A is summarised in table 1.1.

**Table 1.1 Summary of experimentally validated phosphorylated sites in eEF1A isoforms**

Residues	Isoform	Conserved?	Techniques	Reference
Tyr29, Tyr141	Ambiguous	Y	MS	Rush <i>et al.</i> , 2005
Tyr29, Ser163	eEF1A1	Y	MS	Molina <i>et al.</i> , 2007
Thr432	eEF1A1	Y	MS, SDM	Eckhardt <i>et al.</i> , 2007
Ser300	eEF1A1	Y	2D-phosphopeptide mapping, SDM	Lin <i>et al.</i> , 2010
Ser21	Both	Y	MS, SDM	Sanges <i>et al.</i> , 2012
Thr88	eEF1A1	Y	MS, SDM	Sanges <i>et al.</i> , 2012
Ser205	eEF1A2	Y	MS, immunoblot with Ab against S358 phospeptide	Gandi <i>et al.</i> , 2013
Ser358	eEF1A2	N	MS, immunoblot with Ab against S358 phospeptide	Gandi <i>et al.</i> , 2013

Y- Yes, N- No, MS- Mass spectrometry, SDM- Site directed mutagenesis

Although no functional importance has been assigned to most PTMs residues, a few studies have shown that these modifications are capable of regulating the human eEF1A isoforms affecting its translational and/or non-canonical activities. Lin *et al.*, 2010 showed that phosphorylation of Ser300 by type 1 TGF- $\beta$  receptor (T $\beta$ R-1) inhibited the translation activities of eEF1A1 by interfering with its binding ability with aminoacylated-tRNAs (Lin *et al.*, 2010), whereas phosphorylation of Ser21 was shown to modulate the stability of both eEF1A isoforms as well as regulate their apoptotic functions. Mutation of this residue in eEF1A1 resulted in an increase of early apoptosis while an increase of late apoptosis in eEF1A2 mutants was observed in transfected H1355 cell lines (Sanges *et al.*, 2012). Interaction of eEF1A2 with newly synthesised polypeptides intended for degradation was found to be enhanced when its Ser205 and Ser358 residues were phosphorylated by stress-activated c-Jun N-terminal kinase (Gandin *et al.*, 2013).

Another common form of PTMs that has been reported in the human eEF1A isoform is lysine methylation. Using mass spectrometry, two studies identified methylated lysine residues; 36, 55,79,165 and 318, in the human eEF1A which corresponded to those previously reported in the rabbit eEF1A (Cao, Arnaudo and Garcia, 2013; Guo *et al.*, 2014). An additional site; K313, was found to be dimethylated in eEF1A2 (Guo *et al.*, 2014). All of these residues are conserved between the two eEF1A isoforms. The lysine (K)-specific methyltransferase (KMTs) enzymes responsible for the methylation of four of these sites; K36, K79, K165 and K318 have been identified (Dzialo *et al.*, 2014; Shimazu *et al.*, 2014; Jakobsson *et al.*, 2017; Małeck *et al.*, 2017). The effect of methylation on the human eEF1A isoforms is still poorly understood but it is likely to be of functional importance as suggested by the conservation of the methylation of two of these sites; K79 and K318 over a large evolutionary distance from yeast eEF1A to human eEF1A isoforms and by orthologues of the same KMTs in yeast and human (Lipson, Webb and Clarke, 2010; Dzialo *et al.*, 2014; Hamey *et al.*, 2016). Also, investigations by Jakobsson *et al.*, 2017 showed that methylation of K36 modulates mRNA translation by affecting the dynamics as well translation speed of distinct codons using ribosome profiling. Using the same technique, they also demonstrated that methylation of K165 impacted the translation of certain mRNA (Małeck *et al.*, 2017). This study also revealed a difference in the methylation pattern

of K165 in eEF1A1 between tissues and cancer cell lines, with a significantly higher methylation level in human cancer cell lines compared to different rat organs and a variation of K165 methylation between the different organs were also noted (Małecki *et al.*, 2017). It therefore possible that the structure of the eEF1A isoforms, in addition to their tiny differences in amino acid residues, has been further strengthened by their difference in PTMs making them more functionally divergent, and hence allowed them to be retained in the genome.

## 1.2 eEF1A2 role in diseases

### 1.2.1 The wasted mouse

A deletion spanning 15.8 kilobases involving the promoter and first exon of eEF1A2 was identified to cause a wasted (*wst*) phenotype in mice (Chambers, Peters and Abbott, 1998). This mutation which occurred spontaneously in the Jackson laboratory in 1972, eliminated the transcription of *Eef1a2*. Mice which are homozygous for this mutation appear normal earlier in development. However, abnormal phenotypes such as tremors, weight loss and uncoordinated gait become visible from around 21 days of age. The severity of the wasted phenotypes increases, leading to paralysis and death of the mouse at around 30 days of age (Shultz, L.D, Sweet, H.O, Davisson, 1982). Despite having low levels of eEF1A2, heterozygous mice (*+/wst*) show no neuromuscular dysfunction or spinal cord abnormalities (Griffiths *et al.*, 2012).

Further works from our laboratory confirmed that the eEF1A2 gene was solely responsible for the phenotypes observed in the wasted mice. This was demonstrated using transgenic experiments. Newbery *et al*, 2007 generated two different sets of transgenic mice carrying mouse bacterial artificial chromosome (BAC) with either intact *Eef1a2* or a loss of function mutation in *Eef1a2*. Only the BAC transgene containing intact *Eef1a2* was able to rescue the wasted phenotypes. The mutant *Eef1a2* containing BAC was unable to correct the wasted phenotypes even though it carried another candidate gene, *C20orf149*, which was expressed at normal levels in wasted mice.

Prominent neurological features of the wasted mouse include vacuolar degeneration of motor neurons located in the anterior horn of the spinal cord and the accumulation of phosphorylated neurofilaments (Lutsep and Rodriguez, 1989). Detailed analysis of the pathology of the wasted mouse showed that neurological abnormalities occur as early as 17 days postnatal and start in the spinal cord (Newbery *et al.*, 2005). Elevated GFAP staining, indicative of reactive gliosis, in the spinal cord and a reduction in the number of innervated endplates in the thoracic muscles, were first seen. This was then followed by axon and motor neuron degeneration and weak synaptic input from muscle fibres. These pathologies occur in a rostrocaudal manner starting at the cervical level and progressing caudally. Muscle wasting which results in significant loss of total body weight in wasted mice begins at about 21 days of age. When subjected to rotarod activity, an assay for testing motor function, wasted mice performed progressively less compared to their wild-type littermates from 21 days.

The onset of the neuromuscular abnormalities in wasted mice falls within the period when *Eef1a1* is down-regulated and is gradually replaced with *Eef1a2* in the brain, heart and skeletal muscle (Chambers, Peters and Abbott, 1998, Khalyfa *et al.*, 2001). A more dramatic effect is seen in the skeletal muscles for the wasted mouse. Since eEF1A2 completely replaces eEF1A1 in the muscle, homozygous wasted mice do not have any form of eEF1A in their muscles resulting in the total loss of protein synthesis activities in these tissues. However, *in vivo* studies from our laboratory have demonstrated that the characteristic muscle wasting phenotype in these null mutants has a neurogenic origin (Doig *et al.*, 2013). This was shown using tissue-specific eEF1A2 constructs to restore expression of eEF1A2 in the neurons or muscle of wasted mice. Although generating transgenic wasted mice with eEF1A2 expression only in the neurons was unsuccessful, the presence of eEF1A2 in the muscle only and not the neurons was shown to be insufficient to correct the wasted phenotypes in the transgenic wasted mice. Their results were consistent and fit well with the findings of Newbery *et al.*, 2005 where the first signs of abnormalities in these mutants are observed at the neurological levels.

### 1.2.2 eEF1A2 role in epilepsy, autism and intellectual disability

The use of whole exome sequencing to investigate the underlying genetic cause of some neurodevelopmental disorder has identified several missense mutations in *EEF1A2* (see table 1.2). Most of these mutations reported are *de novo* and occur in the heterozygous state. More recently, Cao *et al.*, 2017 reported a homozygous missense *EEF1A2* mutation (P333L) which they identified in two siblings who died in early childhood of dilated cardiomyopathy (DCM). Diagnosis of DCM is unique to this study as it was not reported in the *de novo* cases. Although Cao *et al.*, 2017 postulated that this might be because cardiac function was not evaluated in the patients in these other studies, it is possible that DCM was absent because mutations identified in these other patients are heterozygous and/or it could manifest later in life. The DNA from both parents were also sequenced and are shown to be heterozygous for the mutation. While the mother appeared normal, the father was described to smile in an inappropriate manner and avoided eye contact during a medical examination session. He also has relatives with a history of neurodevelopmental problems such as learning disability, speech delay and seizure disorder (Cao *et al.*, 2017).

In all cases, individuals with eEF1A2 missense mutations presented with intellectual disability (ID) and developmental delay and in almost all cases, epilepsy or abnormal EEG. Many of the individuals also displayed autistic behaviours, while in some cases, facial dimorphic features such as tented upper lip and broad nasal bridge were noted. The effect of these different mutations varies ranging from extremely severe to mild phenotypes presented by the individuals. For example, a case described by Lam *et al.*, 2016 of a 9 years old patient with a heterozygous F98L mutation. She presented with very severe hypotonia and global developmental delay and daily seizures. She is nonverbal and is unable to move her head, sit or stand. A much milder case is a 10 years old patient with a heterozygous E124K mutation who showed no sign of hypotonia and is capable of walking unaided. Although she shows significant delays in language and comprehension, she can communicate in sentences. Unlike the case of the patient with a F98L mutation, her seizures are well controlled with anti-epileptic drugs (Lam *et al.*, 2016).



**Table 1.2: Published cases of patients with missense mutations in *EEF1A2* and associated phenotypes.**

<b>Mutation</b>	<b>Sex (Age)</b>	<b>Epilepsy</b>	<b>ID and development phenotype</b>	<b>Autism</b>	<b>Hypotonia</b>	<b>Facial features</b>	<b>Others</b>	<b>Reference</b>
G70S	F (22y)	Onset at 4 months with myoclonic seizures, absences and grand mal	SID, GDD, very limited speech development	Y	Y	N	Head circumference normal at 22 years old	de Ligt <i>et al.</i> , 2012
G70S	M (14y)	Onset at 10 weeks with myoclonic seizures, infantile spasms, GTC, refractory	Severe delay, Non-verbal, incoordination and gait instability	NM	Y	NM	Acquired microcephaly	Veeramah <i>et al.</i> , 2014
G70S	F (3y)	Onset at 2 months with myoclonic and tonic-clonic seizures, now absence seizures	GDD	NM	Y	Y	No microcephaly at 9 months, dysphagia	Lam <i>et al.</i> , 2016
E122K	F (12y)	Onset at 4 months with infantile spasms, controlled	SID, Non-verbal, motor delay, ataxic gait	Y	Y	Y	Progressive microcephaly, cerebral atrophy	Nakajima <i>et al.</i> , 2014
E122K	F (2y)	Onset at 10 months with myoclonic seizures, atypical absence, uncontrolled	SID, development stagnated during seizure episodes, non-verbal, cannot roll over at 2 years	NM	NM	Y	Normal head circumference at birth	Inui <i>et al.</i> , 2016
E122K	M (2y)	Onset at 8 months with myoclonic seizures and myoclonic-atonic seizures, uncontrolled	SID, developmental delay, non-verbal and cannot stand unaided at 2 years	NM	NM	Y	Cerebral atrophy	Inui <i>et al.</i> , 2016
E122K	F (6y)	Infantile spasm onset from 10 weeks, controlled	Gross motor delay, unsteady gait, non-verbal but vocalizes uses signs	N	Y	Y	Small head circumference	Lam <i>et al.</i> , 2016

<b>Mutation</b>	<b>Sex (Age)</b>	<b>Epilepsy</b>	<b>ID and development phenotype</b>	<b>Autism</b>	<b>Hypotonia</b>	<b>Facial features</b>	<b>Others</b>	<b>Reference</b>
E124K	F (10y)	Onset at 3 months with myoclonic seizures, now absence seizures, controlled	Normal but immature gait, verbal but significant delay in language, mild ID	N	N	Y	Normal MRI, head circumference at 25th centile at 5 years	Lam <i>et al</i> , 2016
D252H	F (8y)	Onset at 8y with generalised tonic seizures	SID, Significant psychomotor developmental delay, non-verbal,	Y	Y	Y	Progressive microcephaly, mild cerebral atrophy at 2 and 4 years	Nakajima <i>et al.</i> , 2014
A92T	F (6y)	Seizure onset at 1 months	ID, Significant developmental delay	Y	NM	NM		Lopes <i>et al.</i> , 2016
I71L	M (9y)	Seizures	Severe GDD, non-verbal but uses signs	NM	NM	Y	Head circumference >9 <sup>th</sup> centile, brachycephaly	Lam <i>et al</i> , 2016
D91N	F (14y)	Onset at 2y with head drops, eye rolling and arm extension seizures, uncontrolled	GDD, non-verbal, unable to walk unaided at 14 years	NM	Y	Y	Head circumference <50 <sup>th</sup> centile, brachycephaly, reduced bone density accompanied with fractures	Lam <i>et al</i> , 2016
F98L	F (9y)	Onset at infant with focal seizures, now myoclonic, tonic and occasional tonic-clonic seizures	Severe GDD, non-verbal, unable to sit or stand	N	Y	Y	Head circumference 85 <sup>th</sup> centile at 6 months, poor bone density	Lam <i>et al</i> , 2016
R423C	M (5y)	Onset at 4 months, multiple seizure types daily	GDD, non-verbal, can't walk at 5 years	NM	Y	Y	MRI showed mild hypoplasia of corpus callosum and mild	Lam <i>et al</i> , 2016

							progressive global volume loss	
<b>Mutation</b>	<b>Sex (Age)</b>	<b>Epilepsy</b>	<b>ID and development phenotype</b>	<b>Autism</b>	<b>Hypotonia</b>	<b>Facial features</b>	<b>Others</b>	<b>Reference</b>
*P333L	M	Onset at 7 months, febrile seizures, eye deviation, tonic-clonic, absences	GDD, non-verbal, unable to walk	NM	Y	Y	FTT, progressive DCM leading to early death at 29 months	Cao <i>et al</i> , 2017
*P333L	F	Onset at 12 months, febrile, tonic-clonic	SID, GDD	NM	Y	Y	Microcephaly, FTT, progressive DCM leading to early death at 5 years	Cao <i>et al</i> , 2017

Y- Yes, N- No, NM- Not mentioned, DCM- Dilated cardiomyopathy, FTT- Failure to thrive, GTC- Generalised tonic-clonic, GDD- Global developmental delay, SID- Severe intellectual disability. \* indicate mutation is homozygous recessive in patients and not *de novo* heterozygous as the other mutations. Adapted from Lam *et al*, 2016.

These missense mutations are not present in online databases including the Exome Aggregation Consortium (ExAC) and Genome Aggregation Database (gnomAD) which contain data set from 60,706 unrelated individuals and 123,136 exome sequences respectively (Lam *et al*, 2016, Cao *et al*, 2017). They involve residues that are shared between both eEF1A isoforms and are evolutionarily conserved across species. Mapping of these mutations on the surface of the 3-D modelled structure of the human eEF1A2 shows that most of them are clustered around the binding sites critical for protein elongation. Some of these residues which are buried in the modeled structure lie in close proximity to the eEF1B binding sites or located at or close to residues involved in domain-domain contacts (Figure 1.4).

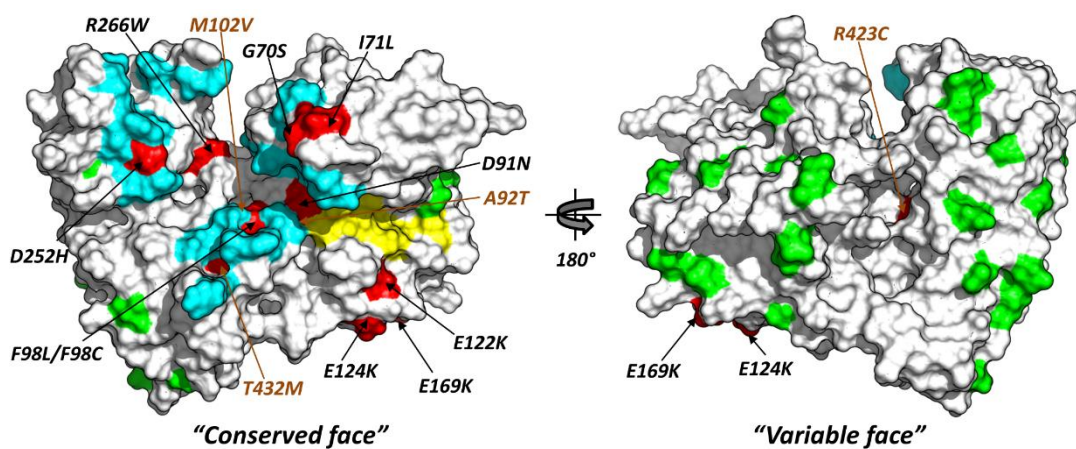


**Figure 1.4. 3-D structure of human eEF1A2 showing location of missense mutations with respect to known binding sites mapped onto its surface.** Two views rotated by 180° about the y-axis of the eEF1A2 structure with the equivalent location of eEF1B $\alpha$  (cyan) and GTP/GDP binding site (yellow) from yeast eEF1A crystal structure. Variant residues between the human eEF1A1 and eEF1A2 are also indicated (green). Mutations are shown in red with residues with buried side-chains labelled in brown. A92T, M102V, T432M also lie in close proximity to the eEF1B $\alpha$  binding site, while M102V, R423C and T432M are located at or adjacent to inter-domain contacts. *Modelling and figure made by Dinesh Soares.*

### 1.2.3 eEF1A2 in cancer

Several studies have implicated eEF1A2 as an oncogene consistent with its overexpression in tumour cells derived from different tissues as summarised in table 1.3 (Reviewed in (Lee and Surh, 2009; Abbas, Kumar and Herbein, 2015). Most importantly, functional analysis carried out by most of these studies showed that indeed eEF1A2 has the ability to transform cells. For example, Anand *et al*, 2002 demonstrated the transformation ability of eEF1A2 *in vivo* by injecting nude mice with

*EEF1A2*-expressing NIH3T3 cells. These cells grew as tumours on the mice, while no tumour was seen in the parental mice or those injected with vector-transfected NIH3T3 cells only. It is still not yet clear how the expression of eEF1A2 is enhanced in tumour cells. Working with primary ovarian tumour cells, Anand *et al*, 2002 showed that *EEF1A2* amplification may elevate its expression in most, but not all, tumour cells. Tomlinson *et al*, 2007, however, demonstrated a lack of correlation between *EEF1A2* copy number and its expression in ovarian tumours. Interestingly, they found the highest *EEF1A2* copy number in a tumour that did not express eEF1A2. Although they did not find any functional mutation or differential methylation modification of the *EEF1A2* locus in normal and tumour cells, their findings suggest there are other alternative ways by which eEF1A2 is upregulated. The authors postulated the improper expression of a trans-acting factor in some tumours as a likely cause for eEF1A2 overexpression.

**Table 1.3: Summary of some studies which showed overexpression of eEF1A2 in different human cancer types**

Cancer type	Methods of eEF1A2 detection	Relevant findings	Reference
Ovarian cancer	Northern blot	Increased <i>EEF1A2</i> expression in ~30% primary ovarian tumours while it was detected in normal ovarian tissues	Anand <i>et al.</i> , 2002
Ovarian cancer	RT-PCR, WB, IHC	~75% of ovarian clear cell carcinomas showed overexpression of eEF1A2 using IHC	Tomlinson <i>et al.</i> , 2007
Breast cancer	RT-PCR, IHC	40 out of 63 breast tumours showed increased expression of eEF1A2 with more significant observed in ER-positive tumours	Tomlinson <i>et al.</i> , 2005

Breast cancer	DNA microarray, IHC	Upregulation of eEF1A2 found in ~30% of ductal and lobular carcinomas and tumour metastases	Kulkarni <i>et al.</i> , 2007
Lung cancer	CGH	Overexpression of eEF1A2 was related to gene amplification and stage of the disease	Li <i>et al.</i> , 2006
Lung cancer	CGH	<i>EEF1A2</i> suggested as a strong oncogene with a marked upregulation of 127.9-fold increase	Zhu <i>et al.</i> , 2007
Hepatocellular carcinoma	qRT-PCR	Overexpression of eEF1A2 partially dependent on gene amplification	Grassi <i>et al.</i> , 2007
Hepatocellular carcinoma (HCC)	CGH, qRT-PCR, WB, IHC	Increased expression of eEF1A2 in about half HCC cell lines.	Schlaeger <i>et al.</i> , 2008
Pancreatic cancer	qRT-PCR, WB, IHC	Upregulation of eEF1A2 in 83% of pancreatic cancer tissues	Cao <i>et al.</i> , 2009
Prostate cancer (PCa)	qRT-PCR, IHC	Enhanced expression of eEF1A2 in 26/30 (86.7%) PCa tissues	Sun <i>et al.</i> , 2014

How eEF1A2 promotes tumorigenesis is still poorly understood. Thornton *et al.*, 2003 suggested that increased protein synthesis as a result of eEF1A overexpression occurs in these cells. This, in turn, leads to the excessive production of protein which then promotes cell growth and proliferation. Another possibility could relate to the other non-canonical functions of eEF1A2, in particular, its cytoskeletal remodelling and anti-apoptotic role which has obvious implications for tumour progression. Different studies have shown that the promoting effect of eEF1A2 in the migration, invasion and metastasis of tumour cells occurs in an Akt and P13K (phosphatidylinositol-3-kinase) dependent manner (Pecorari *et al.*, 2009; Li *et al.*, 2010; Xu, Hu and Zhu, 2013). Using

both bioinformatics and experimental approaches, it has been shown that only eEF1A1 interact with calmodulin (Kanibolotsky *et al.*, 2008; Novosylina *et al.*, 2017). In their study, Novosylina *et al.* 2017 also demonstrated that calmodulin interfered with the tRNA-binding ability of eEF1A1 and also had an inhibitory effect on its actin-bundling activity. This made the authors suggest that eEF1A2, when present in these tissues, might escape eEF1A1-specific regulation. This then leads to the inappropriate behaviour of the cells which makes them become oncogenic. This hypothesis is strengthened by the fact that only eEF1A1 is normally expressed in most of the tissues.

### **1.3 Zebrafish: a useful tool for modelling human diseases**

The zebrafish (*Danio rerio*) is a small freshwater vertebrate that is undoubtedly becoming a popular choice of animal model for understanding human diseases. As a model, the zebrafish has several advantages that make it suitable for this purpose. The breeding and maintenance of these animals is not only easy but also space and cost-efficient. A single mating pair of the zebrafish produces large clutch sizes of fertilised eggs within a range of 200-300 in a week, with the generation time relatively rapid. More so, the embryos develop *ex utero* in a transparent chorion. This, together with the embryo being translucent up till early larval stages make it ideal for visualising different aspects of development using different techniques including conventional light microscopy. For example, monitoring of motor neuron axonal length and branching pattern, which is a marker indicating motor neuron degeneration in zebrafish, can be carried out in embryos as early as 24 hours post fertilisation (Kabashi, Brustein, *et al.*, 2011).

Zebrafish are genetically tractable models, a feature which is further strengthened by the continuous development of advanced and more precise genome-editing techniques such as TALEN and CRISPR-Cas9. Fortunately, the complete sequence of the zebrafish genome is now available and shows that approximately 70% of human genes have at least one clear orthologue in its genome (K. Howe *et al.*, 2013). Another important and very attractive feature of the zebrafish is the ease to use them as an *in vivo* model to carry out high-throughput chemical screening for drug discovery researches for different human diseases such as neurological disorders and cancers (Reviewed in (Lieschke and Currie, 2007; Booterabi *et al.*, 2017). Due to their small

size, larvae can be placed into a 96-well plate containing water-soluble drugs, allowing large numbers of fish to be tested simultaneously. This benefit and others mentioned above not only makes zebrafish a suitable complement to rodent models but also helps in reducing the number of rodents used for research purposes, as unprotected (larval) stages can also be used in experiments, therefore, adhering to the 3Rs (replacement, refinement and reduction) principles.

### **1.3.1 Comparison of the zebrafish and human central nervous system with a focus on relevant regions in modelling human neurological disease**

The central nervous system (CNS) is the most complex tissue in vertebrates, as such raising questions as to the suitability of using the zebrafish to model neurological disorders. Although the human CNS is much more complex and some of the structures, for example, the cerebral hemisphere, are bigger than that of the zebrafish, the overall organisation of their CNS is similar. As in other vertebrates, the CNS of the zebrafish is divided into forebrain, midbrain, hindbrain and spinal cord.

The zebrafish brain shares some similarities with that of mammals. For example, the cerebellum which plays a key role in motor control has the typical three-cell layer structure; molecular layer, Purkinje cell layer and granule cell layer as seen in the mammalian cerebellum. Using *in situ* hybridisation, Bae *et al.*, 2009 also showed similar expression profiles of most of the key genetic markers for GABAergic and glutamatergic neurons in the cell types found in these layers. As suggested by the authors, this could indicate that the development and functioning of the cerebellum may be the same in these species, as such the zebrafish could also provide insights to understand cerebellar development. However, the major difference between the teleost and the mammalian cerebellum is the presence of teleost-specific eurydendroid cells identified by Nieuwenhuys, Pouwels and Smulders-Kersten, 1974; these are located in the Purkinje layer. These cells are homologous to the deep cerebellar nuclei (DCN) found in mammals which are located further away from the Purkinje layer. These two cell types are efferent neurons and receive inputs from the Purkinje cells and transmit them to other regions of the brain. As shown by Bae *et al.*, 2009, the expression of VGLUT2 which also has preferential expression for DCN is conserved in the



eurycytoplasmic cells. However, it is still not clear if these different cell types develop or perform their function in the same manner.

Other parts such as the medulla, tectum and olfactory system of the zebrafish brain also show some structural similarities to the corresponding regions in the human brain. Deterioration of the olfactory system has been noted to correlate to the progression of some neurodegenerative diseases in preclinical studies suggesting it has some clinical importance (Aguilar Martínez *et al.*, 2017). The sensory pathway of the olfactory system of the zebrafish shares homology with that of mammals (Tropepe and Sive, 2003). For example, the olfactory nerves project through the olfactory bulb to targets within the telencephalon and diencephalon in teleost as well as in mammals (Wullimann, 1997). However, caution should be taken when interpreting data on homologies from the forebrain regions as the forebrain is much smaller and less developed in the zebrafish. In addition, unlike mammals which have an evaginated telencephalon, the teleost telencephalon is everted. Although, there are now various studies aimed at providing more insights into the structural and functional homologies of this region between the zebrafish and mammals. For example, tracing studies using neuronal tracers has identified the dorsal nucleus of the zebrafish ventral telencephalic area to be homologous to part of the mammalian striatum (Rink and Wullimann, 2004). The striatum is one of the main input regions for the basal ganglia which is also involved with neurodegenerative diseases in human.

Most of the descending neural pathway originating from the brainstem down to the spinal cord appears to be phylogenetically conserved in teleost and mammals (reviewed in (Yamamoto, Nakayama and Hagio, 2017)). However, an important difference is the lack of descending projections referred to as corticospinal tract (CST) in the homologous telencephalic area in teleost species. In mammals, the CST is sent out from the motor cortex to the spinal cord and has been suggested to play a role in skilled movement of the forelimbs in primates (Iwaniuk and Whishaw, 2000). This is an important difference to consider particularly when modelling neurodegenerative diseases associated with the upper motor neurons.

Apart from the neurons, major glial cell types such as oligodendrocytes (Kirby *et al.*, 2006) and microglia (Peri and Nüsslein-Volhard, 2008) are present in the brain and

spinal cord parenchyma of the zebrafish and show similar development and function as in mammalian species (reviewed in (Lyons and Talbot, 2015). With the recent findings implicating glial cells in neurodegenerative diseases (Kurosinski, Biol and Götz, 2002), this also strengthens the suitability of the zebrafish as a model system. Although stellate-shaped astrocytes have been reported to be found in the adult zebrafish spinal cord (Kawai, Arata and Nakayasu, 2001) and adult rainbow trout brain (Alunni *et al.*, 2005), this has not been supported by other studies. However radial cells, which usually transform to astrocytes during the maturation of the mammalian nervous system are found in abundance in the zebrafish. There are studies that provide evidence that the radial glial cells have the capabilities to subserve some of the roles which have been described for the mammalian differentiated astrocytes (Lyons and Talbot, 2015). One function of the astrocytes is their involvement in the maintenance and modulation of the blood-brain barrier (BBB) in mammals (Janzer and Raff, 1987; Daneman *et al.*, 2010). Interestingly, it has recently been demonstrated that a functional endothelial tight junction BBB, similar to that of higher vertebrates is also present in the zebrafish brain (Jeong *et al.*, 2008). As the BBB also presents a challenge for the efficient delivery of therapeutic compounds, this finding suggests that a better understanding of the BBB can also be achieved using the zebrafish. This, therefore, strengthens its utility as an *in vivo* model for chemical screening for the purpose of developing treatments for neurological disorders.

Although investigations of the comparative homologies between the zebrafish and human CNS are still ongoing, there is enough evidence that suggests the conservation of the overall structure and function of the CNS in these species, thereby validating the use of the zebrafish model to contribute to the understanding and treatment of these complex neurological disorders. This is further supported by the findings of numerous studies that have noted phenotypes in zebrafish models of some neurological disorders to parallel those of rodent models.

### **1.3.2 Zebrafish models for motor neuron disease**

Motor neuron disease (MND) is a collective term which is used to describe a heterogeneous group of neurodegenerative disorders that results in the selective death of motor neurons resulting in the increasing weakness and wasting of the associated

muscles. MND can be categorised depending on whether the disease affects the upper motor neurons (UMNs), which start in the motor cortex of the brain and end within the spinal cord and/or the lower motor neurons (LMNs) which are located from the spinal cord or brainstem to the skeletal muscles. There are different types of MND such as spinal muscular atrophy (SMA), hereditary spastic paraplegia and amyotrophic lateral sclerosis (ALS), which is the most common form of the disease and will be the focus of this review.

ALS, which is also referred to as MND in the UK (henceforth will be used interchangeably with ALS), is a late-onset neurodegenerative disorder that affects both UMNs and the LMNs. It has been found in different populations with an incidence rate ranging between 0.9-2.4 per 100,000 depending on the population (Sathasivam, 2010). While 90% of ALS cases occur sporadically, about 5-10% of cases are inherited in a Mendelian fashion, although a systematic meta-analysis suggests 5.1% as the accurate rate of familial ALS (Byrne *et al.*, 2011). Most cases of ALS are diagnosed in people between the ages of 40-70, although a much rarer form known as juvenile ALS can occur in younger individuals below 25 years of age. A study in a combined European cohort by Logroscino *et al.*, 2010 shows that the incidence of ALS rapidly increases after the age of 40 years and peaks at the early 70s for men and late 60s for women, after which it falls. The location of the onset of the disease varies, with ~70% ALS patients presenting with limb-onset, ~20% with bulbar-onset and ~5% with trunk and respiratory involvement and spread to other region of the body (Kiernan *et al.*, 2011). The neuropathological hallmarks of ALS include the disappearance of the pyramidal and Betz cells which results in retrograde axonal degeneration, loss of the anterior horn cells of the spinal cord as well as the lower cranial nerve motor nuclei of the brain stem, accumulation of intracellular inclusions such as phosphorylated neurofilaments and ubiquitinated inclusions within the anterior horn cells, and gliosis (Hirano, 1996; Maragakis and Galvez-Jimenez, 2018). The disease rapidly progresses and deteriorates, leading to the death of most patients within 2-5 years of diagnosis often due to respiratory failure (Van Damme, Robberecht and Van Den Bosch, 2017).

Although there is currently no cure, the growing interest in this condition has provided valuable insights into the aetiology of ALS which is still essentially unknown. About 20 genes have been identified over the last decade, most of which are associated with

the familial form of the disease (Corcia *et al.*, 2017). Most of these genes are involved in different biological pathways reflecting the multifactorial cause of this disease. The first causative gene implicated in ALS is the Superoxide dismutase 1 (*SOD1*) identified in 1993 (Rosen *et al.*, 1993) with the frequency of 12-23.5%. Other most common genes linked to ALS are *C9ORF72*, *TARDBP* and *FUS* with frequencies of 39.3% (Familial ALS), 5% and 4.1% respectively (Al Sultan *et al.*, 2016). Most of the ALS-causing mutations in these genes were identified in patients with the familial form of ALS (see Table 1.4 below).

**Table 1.4: Most common genes linked to ALS with statistics obtained from the Amyotrophic lateral sclerosis online genetics database (accessed July 2018)**

Gene	FALS	SALS	Most frequent mutation reported
<i>CORF72</i>	60	46	HREM
<i>FUS</i>	77	27	Arg521His
<i>SOD1</i>	286	44	Cys6Ser
<i>TARDBP</i>	58	40	Ala382Thr

FALS- Familial Amyotrophic lateral sclerosis, SALS- Sporadic Amyotrophic lateral sclerosis, HREM - hexanucleotide repeat expansion mutation

The heterogeneous clinical presentation of ALS in patients even within individuals from the same family and the same causative gene stresses the need to better understand this disease as this has implications for identifying potential therapeutic targets (Van Damme, Robberecht and Van Den Bosch, 2017). Different animal models have been generated to recapitulate the neurological abnormalities or the genetic aspects of the condition (reviewed in (Van Damme, Robberecht and Van Den Bosch, 2017)). Although there is no perfect animal model displaying all the clinical features of the disease, they have no doubt served as a valuable tool in providing insights into the mechanism of motor neuron disease. An example is the wasted mouse, which is one of the several spontaneous mouse strains (reviewed in (Doble and Kennel, 2000)) and a model that our laboratory has worked extensively on. In terms of neurological abnormalities, the wasted mouse (described in section 1.2.1) presents with clinical features that more closely resemble ALS in humans than the other spontaneous mice models. More recently, different zebrafish models for ALS have been described in

several studies (reviewed in (Babin, Goizet and Raldúa, 2014; Patten *et al.*, 2014). However, most of the approaches used in generating these models involve the injection of mRNA for overexpression of ALS-related genes or morpholinos to knockdown these genes in the embryos. Expression of genes in these models is only transient, limiting the time to perform any phenotypic assay. This poses a challenge for this condition which has a late onset (Kabashi *et al.*, 2011) as well as having the potential for off-target effects associated with the use of morpholinos, therefore results from these studies should be interpreted with caution. However, due to the ease and speed of these methods, models generated with these approaches have been used to confirm the usefulness of the zebrafish as a tool for understanding the pathogenesis of motor neuron disease as well as for screening small molecules to be used for treatment for the condition in combination with other animal models.

The first ALS disease zebrafish model was generated by Lemmens *et al.*, 2007 using an overexpression approach. Microinjection of embryos with three different ALS-causing mutations of the human *SOD1* mRNA induced axonal abnormalities that were specific to the motor neuron and were reminiscent of those seen in transgenic *SOD1* rodent models. It has been reported that the phenotype associated with the mutation of *SOD* is modified by two factors; wild-type *SOD1* and the vascular endothelial growth factor (VEGF) gene in rodents. VEGF has been suggested to have a protective effect on motor neuron in humans and rodents models of ALS (Lambrechts *et al.*, 2003; Storkebaum *et al.*, 2005). Wild-type *SOD1* worsens the ALS phenotype in transgenic *SOD1* mutant mice and even cause these phenotypes to appear in mice carrying a mutation, *SOD1*<sup>A4V</sup> that has been previously shown to not induce any ALS phenotypes in mice even after 2 years, consistent with a toxic gain of function effect (Deng *et al.*, 2006). Lemmens *et al.*, 2007 investigated the effect of VEGF and wild-type *SOD1* on their mutant embryos and their findings were consistent with those observed in mice. This not only validated the zebrafish model for studying motor neurodegeneration but has led to the development of transient zebrafish models as well as stable transgenic lines carrying mutations in different genes involved in MND by different groups; these have been reviewed in Babin, Goizet and Raldúa, 2014. As a result of this work, the interactions between these genes are now being studied in the hope that this will provide a complete picture of the pathogenesis of MND and better inform the

development of effective therapeutic strategies for the different gene mutations. A good example is that demonstrated by Kabashi, Bercier, *et al.*, 2011, where the interactions of *FUS* with *TARDBP* and *SOD1* was investigated. They showed that human wild-type *FUS* was able to rescue phenotypes such as motor neuron branching and swimming abnormalities induced by the knockdown of zebrafish *tardbp* but not vice versa while the wild-type form of both human *FUS* and *TARDBP* genes had no effect on fish injected with the human G93A mutant *SOD1* mRNAs. Also, human wild-type *SOD1* had no effect on phenotypes induced by the overexpression of human mutant *FUS* and *TARDBP* or knockdown of the zebrafish *fus* and *tardbp*. However, a more severe phenotype was observed in injected embryos co-expressing human mutant *SOD1* with either human mutant forms of *FUS* or *TARDBP*. Their findings suggested that *FUS* shares a common pathway with *TARDBP*, although the latter acts upstream and hence was unable to rescue the phenotype induced when the zebrafish *fus* was knockdown. On the other hand, *SOD1* might act independently of *FUS* and *TARDBP* (Kabashi, Bercier, *et al.*, 2011). Consistent with these findings, Laird *et al.*, 2010 had previously shown that overexpression of human progranulin gene had a neuroprotective effect on the axonopathy induced by mutant *TARDBP* but not mutant *SOD1* expression. Interestingly, the zebrafish models are now being used to identify other gene modifiers that could serve as a potential target for therapeutic interventions. Van Hoecke *et al.*, 2012 identified the ephrin receptor, *epha4*, as a modifier of ALS using a morpholino-based modifier screen approach with embryos overexpressing human mutant *SOD1*. They then confirmed that this factor was also a modifier in rodents ALS models as well as in ALS patients, with lower *EPHA4* expression resulting in later disease onset and reduced severity and progression of the disease. Pharmacological inhibition of the *Epha4* signalling pathway also completely rescued the axonopathy induced by mutant *SOD1* in zebrafish and delayed onset of the disease as well as increased the survival rate of ALS rat models (Van Hoecke *et al.*, 2012).

Despite the fact that zebrafish was only recently validated as a suitable model for investigating MND pathogenesis, the fish models are already being used to carry out chemical screenings for drug discovery purposes confirming their advantage, particularly as regards economic issues, over rodent models. The first *in vivo* chemical screening was performed using three compounds; lithium chloride, methylene blue

(MB) and riluzole which are known for their neuroprotective potential, first in transgenic mutant TDP-43 (mTDP-43) and mFUS *Caenorhabditis elegans* ALS models and then later with transgenic zebrafish models, referred to as mTDP-43 and mFUS by the authors, using only MB which showed more promise in worms (Vaccaro *et al.*, 2012). In both their worm and fish models, motor neuron abnormalities induced by TDP-43 and FUS mutations such as paralysis in *C. elegans* and swimming deficits with shortened and unbranched axons in zebrafish were significantly improved with MB, with earlier rather than late administration of MB being more effective in worms. This study also identified the molecular mechanism of MB as the oxidative stress levels in mTDP-43 and mFUS zebrafish and *C. elegans* models were reduced using dihydrofluorescein diacetate (DHF) assay. In the presence of intracellular peroxide which is a marker of oxidative stress, DHF produces a strong fluorescent signal which was observed in mTDP-43 and mFUS zebrafish and *C. elegans*. When both mutant models were treated with either MB and *ero-1* (ER oxidoreductin 1) RNAi, the intensity of the fluorescent signal was significantly reduced (Vaccaro *et al.*, 2012, 2013). This suggests that MB exerted a neuroprotective effect through the endoplasmic reticulum (ER) stress pathway that is activated in response to the accumulation of the unfolded mutant proteins (UPR<sup>ER</sup>) which was demonstrated with only mTDP-43 zebrafish models (Vaccaro *et al.*, 2013). Understanding the mode of action of MB led to the identification of three other candidate compounds with therapeutic potential which were structurally similar to MB in the same study. Two of these compounds, salubrinal and guanabenz have previously been demonstrated to be active in the UPR<sup>ER</sup> (Boyce *et al.*, 2005; Tsaytler *et al.*, 2011) while the first evidence of the neuroprotective ability of phenazine through this pathway was reported in the study of Vaccaro *et al.*, 2013. Interestingly, salubrinal was also found to reduce disease onset and delay its progression through the ER stress pathway in the transgenic FALS mouse model expressing the human *SOD1*<sup>G93A</sup> mutation (Saxena, Cabuy and Caroni, 2009). These three compounds act through different branches within the UPR<sup>ER</sup> pathway and proved to be more efficient when combined with MB (Vaccaro *et al.*, 2013). Validation of the suitability of Vaccaro *et al.*, 2013 mTDP-43 zebrafish model for drug screening subsequently led to a high-throughput screening for other drugs for MND which has now been translated to patients with ALS (Patten *et al.*, 2017). In this recent study,

3,850 small molecules were first screened using mTDP-43 *C. elegans* models and 13 lead compounds, all neuroleptics, were identified as positive hits. Using the mTDP-43 zebrafish model, only 10 of these compounds were confirmed, with pimozone being the lead compound with neuroprotective abilities which was also observed in zebrafish overexpressing the mutant form of human SOD1 and FUS. Pimozone was next tested in mutant SOD1 mice where it was shown to restore neuromuscular synaptic transmission. This study also demonstrated the safety and promise of using pimozone in patients with SALS in a pilot randomised controlled trial (RCT), allowing a second RCT trial with 100 patients to be approved for further investigation (Patten *et al.*, 2017).

Some other studies have also validated the use of mutant *sod1* zebrafish models for small molecules screening. McGown *et al.*, 2013 demonstrated the effectiveness of riluzole, the only approved drug for MND, in their transgenic *sod1* mutant and also identified a new role of the drug in reducing neuronal stress in interneurons. Another antioxidant drug, olesoxime was also shown to protect against SOD1 neurotoxicity in a T701 *sod1* zebrafish model generated using TILLING (targeting induced local lesions in genomes) by Da Costa and colleagues, 2014. Interestingly, apomorphine was also found to be effective in reducing oxidative stress in the different *sod1* zebrafish mutants in both studies (McGown *et al.*, 2013; Da Costa *et al.*, 2014). This drug has also been demonstrated to reduce motor dysfunction in *SOD1*<sup>G93A</sup> transgenic mice as well as attenuate oxidative stress and increase the survival rate in fibroblasts derived from ALS patients subjected to oxidative insult *in vitro* (Mead *et al.*, 2013). Apomorphine is an activator of the nuclear factor erythroid 2-related factor (NRF2), which drives the expression of several neuroprotective genes by interacting with the antioxidant response elements (ARE). Further investigation of this compound as well as of the NRF2-ARE pathway, which has been shown to be impaired in SOD1 mutant mice models and brain and spinal cord tissues from ALS patients (Sarlette *et al.*, 2008; Vargas *et al.*, 2008), can now be done using the zebrafish in combination with the other available animal models. This could potentially speed the translatability of research findings to individuals with motor neuron disease.



### 1.3.3 Zebrafish models of epilepsy

Epilepsy is a complex neurological disorder marked by unprovoked and recurrent seizures that are caused by abnormal electrical activity in the brain. This disorder is common, affecting approximately 1% of the general population. Despite the wide range of anti-epileptic drugs (AEDs), epileptic seizures in around one-third of these patients cannot be controlled with the available treatment (Cunliffe, 2016). Also, some of these AEDs have been shown to have an adverse effect, for example, increased rate of congenital malformation and developmental and cognitive impairment in children with *in utero* exposure to valproate, a widely used AED, has been reported (Adab *et al.*, 2004; Morrow *et al.*, 2006). It is therefore important that new drugs with better efficacy for drug-resistant epilepsy and with fewer side effects are developed.

Several factors, for example, genetic mutations or head trauma can cause epilepsy; however, the cause is still unknown in at least 40% of cases (Shorvon, 2011). The number of these cases is gradually diminishing, especially for childhood cases of epilepsy, with the advent of whole exome sequencing (WES). Exome sequencing of patient-parents trios has identified many *de novo* mutations in genes that have never previously been implicated in neurological disorders. These patients present with other cognitive and behavioural deficits such as autism and intellectual disability (ID) along with the seizures. This in itself is no surprise, as it is known that there is a strong association between epilepsy, ID, autism and even motor impairment in infants (Tuchman and Cuccaro, 2011). However, it is still not clear if these other neurodevelopmental disorders are as a result of the damage caused by the seizure itself, as implied by the term epileptic encephalopathy, or independent of the presence of seizures but with a common underlying cause. Most studies seem to point to the latter, especially in the development of autism, which will suggest that these disorders might share a common molecular pathway that these genes are involved in (Tuchman and Cuccaro, 2011). The development of animal models which recapitulate some of these phenotypes has been and is still extremely valuable in understanding the contribution of these genetic mutations to neurodevelopmental disorders especially as more new genes, whose causal role have to be validated, are being discovered.

The zebrafish has again been employed in epilepsy research and has contributed immensely to the growing information currently available (recently reviewed in Cunliffe, 2016). One of the attractive features of using the zebrafish is the ability to effectively model epilepsy using both larval and adult stages. While the larvae can be used to model early-onset epilepsy, other more complex seizure-related behaviours can be further investigated using the adult fish (Stewart *et al.*, 2012). Epileptic seizures can be investigated in zebrafish models using pharmacological induced and/or genetic manipulation methods. Chemically induced seizure was first demonstrated by Baraban *et al.*, 2005 using pentylenetetrazole (PTZ), a common convulsant drug also used in rodent models. In this study, they found PTZ induced locomotor convulsive behaviour, abnormal electrical discharges in the brain and increased expression of *c-fos*, a biomarker for neuronal activity, in the brain of PTZ treated zebrafish larvae, 7 days post fertilization (dpf). All these changes were similar to those seen in the rodent seizure models and were readily suppressed using valproate and diazepam, two AEDs that are also known to be effective in PTZ-induced seizure in rodents. The well-established scoring system of seizure behaviour of PTZ treated fish from this study has paved the way for other uses of the PTZ assay. The assay was used to perform the first large-scale genetic screening in N-ethyl-N-nitrosourea (ENU) mutagenized larvae which identified six candidate genes that conferred resistance to seizure (Baraban *et al.*, 2007). Interestingly, this study showed that PTZ can also be used to induce seizures effectively in larvae at earlier developmental stages from 3-5 dpf which are not regulated (unlike 7 dpf larvae) and will not require a license to carry out these experiments, an added benefit of this model. In 3dpf larvae, Teng and colleagues used this assay in combination with morpholinos to demonstrate that knockdown of *lgila* or *lgilb*, both of which encode ion channel proteins, increased the susceptibility of their *Lgi1a* and *Lgi1b* zebrafish morphants to PTZ-induced seizures (Teng *et al.*, 2010, 2011). Other convulsant drugs used in mammals have now been shown to be equally effective in inducing seizures in zebrafish, but PTZ still remains the most widely used (reviewed in Stewart *et al.*, 2012).

Zebrafish have been shown to be sensitive to mutations in genes shown to cause epilepsy in humans and rodents. An example is the sodium channel subunit *scn1La* zebrafish mutation which was identified from an ENU mutagenesis screen (Baraban,

Dinday and Hortopan, 2013). Heterozygous missense mutations in *SCN1A*, most of which are *de novo* (85%), account for the underlying cause of Dravet syndrome (DS) in about 70- 80% of individuals with this disorder (Rosander and Hallböök, 2015). DS is a severe form of epilepsy marked by prolonged frequent generalised seizures that may or not be caused by a fever. These seizures begin within the first year of life, usually around 5 months of age and are poorly controlled by the available AEDs (Bender *et al.*, 2012). In addition to epilepsy, these patients also present with developmental delay, cognitive and behavioural problems towards the second year of life. Some other neurological abnormalities such as hypotonia, ataxia and gait abnormalities accompany these other features in some infants with DS (Dravet, 2011). Another example is the *KCNQ3* gene which encodes for the voltage-gated potassium channel, kv7.3. Mutation in this gene and another of this gene family, *KCNQ2*, are associated with a range of early-onset epilepsies with varying severity from the mild inherited epilepsy benign familial neonatal seizures (BFNS) to the severe epileptic encephalopathy usually caused by *de novo* mutations in these genes (Charlier *et al.*, 1998; Singh *et al.*, 1998; Miceli *et al.*, 2015). Using morpholinos, knockdown of *KCNQ3* expression in zebrafish induced seizure-like activities shown by the abnormal electrical discharges obtained from the brains of larval morphants using electrophysiology (Chege *et al.*, 2012).

Most of the pro and anti-convulsant drugs are water soluble and can easily be administered by placing in a small volume of the normal bathing medium of the fish. Combined with the small size and genetic amenability of the zebrafish larvae, this makes the larval form excellent for high-throughput screening to identify new AEDs drugs. This has been further strengthened with the development of devices for automated compound delivery with in-built software for automated behavioural analyses that are compatible with a 96-well plate allowing large number of larvae to be tested simultaneously (for example, [www.noldus.com](http://www.noldus.com)). A good example where these benefits have been employed is seen in the study of Baraban *et al.*, 2013. They performed a relatively large screen using a chemical library made up of 320 compounds in the *scn1La* zebrafish Dravet syndrome models and found that clemizole was effective in reducing seizure activity in 5dpf larval mutants. A larger screening of about 2000 small molecules has also been performed using PTZ-induced seizure wild

type larvae at 2dpf with similar equipment (Baxendale *et al.*, 2012). The authors also demonstrated the change of *c-fos* expression associated with seizure activities in zebrafish was robust enough to be used as another *in vivo* criterion for assessing the anti-convulsant properties of compounds in high-throughput chemical screens. The ability to use zebrafish larvae to carry out chemical screening not only identifies the effective doses of potential compounds but also allows for the simultaneous evaluation of their toxicity *in vivo* to determine if they are safe to be used for treatment of epilepsy. Goldsmith *et al.*, 2007 showed that GBR12909, a dopamine reuptake inhibitor, although having an anti-convulsant effect on zebrafish and rodent models of generalised epilepsy, has a cardiac side effect as it induced abnormal heart rhythms in zebrafish even at the effective dose concentration for treating epilepsy. Interestingly, this finding parallels data from two phase 1 clinical studies that suggested the potential QT prolongation of GBR12909 in humans (Goldsmith *et al.*, 2007). Their study demonstrates that the zebrafish could be used as the first *in vivo* platform to assess safety of a drug, once it has been identified as a hit, to determine if it should be developed further and then tested in the mammalian system. This could help avoid a waste of time and resources (and welfare issues) in the development of drugs that might be found to have serious side effects in the long run. Taken together, these studies demonstrate that zebrafish larvae present an excellent platform for identifying new and safe AEDs drugs for pharmocoresistant seizures, as well as seizures that are currently controlled by AEDs shown to have major side effects in the long term e.g valproate.

## **1.4 Local mRNAs translation in neurons**

mRNA localisation is a highly conserved mechanism that allows for the spatiotemporal control of the synthesis of specific proteins in cells. Using differentiated neurons separated into neurites and soma fractions, Zappulo *et al.*, 2017 showed that mRNA localisation accounted for half of the neurite-localised proteome. This finding together with those from a number of studies support the idea that mRNA localisation underlie the establishment and maintenance of dendrites and axons which are functionally specialised compartments of the neuron (reviewed in (Holt and Schuman, 2013)). The mRNAs localised to these compartments fall into diverse

functional categories such as translation, cytoskeleton, degradation and channel/receptor formation. This further reflects the ability of axons and dendrites to function independently as they are able to coordinate and regulate the translation of these mRNAs locally when needed. Interestingly, this has already been demonstrated *in vivo* in a study by Harris and Colleagues in 1987. Using time-lapse video recordings, they showed that axons isolated from the soma were able to grow and navigate correctly to the optic tectum in *Xenopus* embryos (Harris, Holt and Bonhoeffer, 1987).

There is much evidence that demonstrates the role of axonal mRNA translation in axon growth and navigation, synapse formation as well as the survival of axons and deficits in this process can lead to neurodevelopmental and neurodegenerative disorders (reviewed in (Cioni, Koppers and Holt, 2018; Costa and Willis, 2018). Interestingly, there are studies that link eEF1A to local protein synthesis during synaptic formation. It was demonstrated that eEF1A is important for the maintenance of newly formed synapses using sensory neurons isolated from *Aplysia* (Giustetto *et al.*, 2003). In this study, it was observed that applying serotonin (5-HT) increases the level of eEF1A protein and mRNA but its mRNA was only enriched in the axonal processes when applied to both the cell body and the synapse. Blocking the expression of eEF1A using antisense oligonucleotides or antibodies resulted in the failure of the long-term facilitation (LTF) induced by 5-HT to last beyond 24 hrs. LTF is the major form of synaptic plasticity in invertebrates and has been suggested to underlie long-term learning behaviour and memory in *Aplysia* (Frost *et al.*, 1985).

Long-term potentiation (LTP) and long-term depression (LDP) which describes the long-lasting increase or decrease in synaptic strength respectively are the most studied form of synaptic plasticity, which is also believed to underlie learning and memory in human. Similarly, these processes require *de novo* protein synthesis suggesting that local mRNA translation at the synapses is important for their maintenance. There are studies that show the local translation of eEF1A2 mRNA at the synapses is required for LTP and LDP. Using microarray, eEF1A was identified as part of a subset of dendritic mRNAs from rat hippocampal neurons (Zhong, Zhang and Bloch, 2006). Another study demonstrated that eEF1A2 binds the alpha-2 subunit of the glycine receptor (GlyR) in a pull-down assay using extracts from adult rat brain (Bluem *et al.*, 2007). Immunofluorescence microscopy also showed eEF1A to colocalise with GlyR

from the soma into the dendrites and at inhibitory synapses in cultured hippocampal and spinal cord neurons from rat. Stimulation of hippocampal LTP in dendrites that have been severed from the cell body led to the increased expression of eEF1A, suggesting its translation is locally regulated at the dendrites. This effect was absent when the rat hippocampal slices were then treated with rapamycin, an inhibitor of the mammalian target of rapamycin (mTOR) pathway, and also blocked the maintenance of LTP (Tsokas *et al.*, 2005). In another study, induction of LTP in rat hippocampal slices resulted in the enhanced expression levels of eEF1A protein in the dendrites (Huang, Chotiner and Steward, 2005).

These findings provide strong evidence for the conserved role of eEF1A in maintaining long-term synaptic plasticity and possible in learning and memory. Interestingly, expression of eEF1A protein is reduced in the hippocampus, in particular the CA1 and dentate, but not in the cerebellum or midfrontal gyrus in *post mortem* brain samples obtained from patients diagnosed with Alzheimer disease (AD) (Beckelman, Zhou, *et al.*, 2016). AD is a neurodegenerative disorder with memory loss as one of the first symptom in patients. This group also showed that impaired LTP characteristic to AD is attenuated by the upregulation of eEF1A in hippocampal slices obtained from transgenic AD mice models (Beckelman, Day, *et al.*, 2016). Similarly, dysregulation of eEF1A was found to underlie the impaired synaptic elimination observed in Fragile X syndrome, the major form of inherited learning disability. Tsai *et al.*, 2012 showed that reducing eEF1A levels which is found to be elevated in *Fmr1* knockout neurons restore synaptic elimination in mice. FMR1 protein participates in the spatial and temporal control of local protein synthesis during synaptic development. This protein represses translation of certain neuronal mRNAs whose levels are elevated in its absence (Bagni *et al.*, 2012). Although not all these mRNAs are known, a direct interaction between eEF1A mRNA and FMR1 protein has been demonstrated (Sung *et al.*, 2003; Darnell *et al.*, 2011) which could explain the enhanced levels in individuals with this disorder and *Fmr* knockout mice models.

## 1.5 Previous studies of the eukaryotic elongation factor 1 alpha in zebrafish

Before the complete sequence of the zebrafish genome was available, the zebrafish was thought to have only one gene copy of eEF1A. The structure of the zebrafish eEF1A gene was first reported by Gao *et al.*, 1997. They described this gene to be made up of 8 exons interspersed with 7 introns. The exon-intron organisation of the eEF1A gene was found to be identical to the human and displayed the same splice pattern and exon sizes with the human eEF1A gene. Differential expression levels of eEF1A mRNA was observed when compared in different developmental stages and cultured cells derived from adult fish tissue. This led to the suggestion that eEF1A was developmentally regulated in the zebrafish. Another study then identified this eEF1A gene to be important for embryonic development based on the results from a large insertional mutagenesis screen carried out in zebrafish (Golling *et al.*, 2002; Amsterdam *et al.*, 2004). Homozygous *eef1a* mutants develop abnormally with phenotypes becoming visible from 2 days post fertilisation (dpf). At 3 dpf, they have small heads and eyes and grow slowly compared to their wild type siblings. At 4 and 5 dpf, their swim bladders fail to inflate and they then die by day 5. In this study, this gene was identified as the orthologue of the human *EEF1A1*. On the contrary, Clark *et al.*, 2011 found that homozygous *eef1a* mutants did not show any abnormal phenotype and were viable till adulthood. In their study, mutants were generated using a gene-break transposon mutagenesis system which resulted in the knockdown of most transcripts by >99%. Only the gene ID, zgc:73138 was mentioned, but it was also identified as the orthologue of the human *EEF1A1*, with a paralogue gene identified as zgc:110335 in the zebrafish genome. These two studies were carried out at the time when the zebrafish sequencing project was still in its early stage. However, with the complete sequence now available, it is now obvious that the zebrafish has more than one eEF1A gene. The reason for the discrepancy between the two studies was actually due to the groups identifying different eEF1A genes. While the gene reported by Amsterdam *et al.*, 2004 is now known as *eef1aIII*, zgc:73138 and zgc:110335 have been renamed *eef1aIa* and *eef1aIb* respectively (ZFIN). The zebrafish eEF1A isoforms are described in more details in chapter 3 of this thesis.

A guide to the past and current nomenclature of the zebrafish eEF1A is summarised in table 1.5. However, for the sake of clarity, the mammalian naming convention for proteins will be used when referring to eEF1A proteins from all species in this thesis.

**Table 1.5: Nomenclature of the zebrafish eEF1A isoforms**

<b>Current gene symbol</b>	<b>Previous gene names</b>	<b>Protein</b>
<i>ef1a1l1</i>	ef-1 alpha, ef1 alpha, ef1a, EFL1-alpha,	eEF1A1L1
<i>ef1a1a</i>	j64c02, wu:fj64c02, zgc:73138	eEF1A1A
<i>ef1a1b</i>	ef1a1, wu:fj34g08, zgc:110335	eEF1A1B
<i>ef1a2</i>	zgc:92085	eEF1A2

## 1.6 Project aims

With the growing evidence that supports the utility and the contribution of the zebrafish in understanding different human disease pathogenesis, the main aim of this project was to investigate the potential of using the zebrafish as a model to understand the role of eEF1A2 in neurological disorders. The objectives of this project include:

1. To characterise eEF1A isoforms in zebrafish using bioinformatics and gene expression analyses
2. To recreate the G70S eEF1A2 mutation in the zebrafish to investigate the mechanisms by which it causes the observed human phenotype
3. To generate and characterise eEF1A2 null zebrafish model for complementary use with mice models with the intention of using the zebrafish model as an *in vivo* platform for chemical screening. This would help in the identification of potential compounds that could ameliorate any observed phenotype(s) caused by eEF1A2 for further investigation.



## Chapter 2: Materials and Methods

### 2.1 Materials

#### 2.1.1 Reagents

The recipe for the different reagents used throughout this work is listed in table 2.1 below.

**Table 2.1: List of reagents used in this work and their recipe**

<b>Whole mount <i>in situ</i> hybridisation (WISH) experiment</b>	
<b>Name</b>	<b>Composition</b>
1M Lithium chloride	4 $\mu$ l of 10M LiCl (Fluka) diluted in 36 $\mu$ l of DEPC-treated water
0.003% PTU (Sigma-Aldrich)	100x stock solution of 0.3% PTU (w/v) dissolved in distilled water was diluted in E3 to working concentration of 0.003% PTU (v/v)
4% PFA	4g of PFA (Sigma-Aldrich) dissolved in 1x PBS
<sup>a</sup> PBS-T	1ml of Tween 20 (Thermo Fisher Scientific) diluted in 1L of 1x PBS
Hybridisation Mix (HM+)	50% Formamide, 5X SSC, 0.1% Tween 20, 50 $\mu$ g/ml Heparin, 500 $\mu$ g/ml RNase free tRNA
Hybridisation Mix (HM-)	Same as above without RNase free tRNA and heparin
10x Maleic acid buffer (MAB)	58g Maleic acid, 43.5g NaCl, 20g NaOH, 400ml distilled water, pH adjusted to 7.5
MABT	10x MAB diluted to 1x in distilled water, 0.1% Tween 20

Blocking buffer	10% stock blocking reagent powder (Roche) diluted to 1% in MABT
Alkaline phosphatase buffer (NTMT)	5ml 1M Tris HCl pH 9.5 2.5ml 1M MgCl <sub>2</sub> 1ml 5M NaCl 250µl 20% Tween 20 Distilled water up to 50ml
Staining solution	200µl of NBT/BCIP stock solution diluted in 10ml NTMT
<b>Protein detection using western blot<sup>a</sup></b>	
RIPA lysis buffer	1.5ml 1M NaCl, 0.1ml Nonidet P-40, 50µl 0.5% Sodium deoxycholate, 50µl 20% SDS, 5ml 50mM Tris, pH8.0, dH <sub>2</sub> O up to 10ml. 1 Complete Protease inhibitor tablet (Roche) added prior use
10% separating gel	8ml 1.5M Tris pH8.8, 10.4ml 30% acrylamide/bis (Bio-Rad), 160µl 20% SDS, 20µl TEMED, 80µl 25% AMPS, 13.4ml dH <sub>2</sub> O
4.3% stacking gel	5ml 0.5M Tris-HCl pH6.8, 2.9ml 30% acrylamide/bis (Bio-Rad), 100µl 20% SDS, 10µl TEMED, 100µl 25% AMPS, 11.9ml dH <sub>2</sub> O
TBS-T	1ml of Tween 20 (Thermo Fisher Scientific) diluted in 1L of 1x TBS
Blocking buffer	5% dried skimmed milk (Marvel) dissolved in TBS-T
<b>Histology</b>	
3% hydrogen peroxide	100ml 30% stock H <sub>2</sub> O <sub>2</sub> diluted in 900ml distilled water

<sup>a</sup> same recipe for PBS-T used for WISH and protein detection applications

### 2.1.2 Oligonucleotides for gRNAs synthesis

Sequences of oligonucleotides used in the cloning of gRNA into the expression vector, pDR274 for the CRISPR/Cas9 experiments are listed in table 2.2 below. All oligonucleotides were purchased from Integrated DNA Technologies (IDT) with a 5' phosphate modification to improve ligation efficiency.

**Table 2.2: Oligonucleotide sequences used to generate gRNAs for CRISPR/Cas9 experiment**

Name	Sequence (5' to 3')
eef1a2 CR F1	[P] TAGTGATCGGCCATGTTGATTC
eef1a2 CR R1	[P] AAACGAATCAACATGGCCGATC
eef1a2 CR F2	[P] TAGGGCATCTCATCTACAAATG
eef1a2 CR R2	[P] AAACCATTTGTAGATGAGATGC
gRNA3 1	[P] TAGGATAAGTTGAAGGCTGAGA
gRNA3 2	[P] AAACTCTCAGCCTTCAACTTAT
gRNA5 1	[P] TAGGTTTGAGAAAGAGGCAGCTG
gRNA5 2	[P] AAACCAGCTGCCTCTTTCTCAA
gRNA7 1	[P] TAGGTAAACCCTGATGCTTCCTG
gRNA7 2	[P] AAACCAGGAAGCATCAGGGTTTA

### 2.1.3 Primers

Sequences of primers used in this project are listed in Table 2.3 below together with the applications they were used for indicated by the subheadings. Primers were purchased from Sigma-Aldrich unless otherwise indicated.

Please note that primers highlighted in grey were obtained from the Primerdesign gene detection kit and their sequences are copyrighted and may not be used to synthesise new primers from a different source.

**Table 2.3: Sequences of primers used in this work**

<b>Expression analysis of <i>eef1a</i> during development and adult tissues</b>	
<i>eef1a111</i> RT-PCR F	ACCTACCCTCCTCTTGGTCG
<i>eef1a111</i> RT-PCR R	GGAACGGTGTGATTGAGGGA
<i>eef1a1a</i> RT-PCR F	TCCTCCTCTGGGTCGTTTTG
<i>eef1a1a</i> RT-PCR R	GTAACCTTCCGCTTGTCGC
<i>eef1a1b</i> RT-PCR F	TCCTCTTGGTCGTTTTGCAGT
<i>eef1a1b</i> RT-PCR R	TGTGGCTGACCCAAGTGTTT
<sup>a</sup> <i>eef1a2</i> RT-PCR F	TACTGTTCTCTCTTGCCGCC
<sup>a</sup> <i>eef1a2</i> RT-PCR R	TTTTCCCATCTCAGCTGCCT
<i>actb2</i> F	GATCAAGATCATTGCCCCACC
<i>actb2</i> R	GAGTCGGCGTGAAGTGGTAA
<b>Sequencing primers for CRISPR/Cas9 experiments</b>	
<i>eef1a2</i> CR GENO F (IDT)	TGCAGACAGAAGAAAGCACCT
<i>eef1a2</i> CR GENO R (IDT)	TTTGAGAAAGAGGCAGCTGAG
gRNA3 GENO F	CACCTTTATTTTTGCGTGAACA
gRNA3 GENO R	TCAAAAACATGATCACTGGGAC
gRNA5 GENO F	TCAACATGGGGAAAGAGAAGAT
gRNA5 GENO R	CACTTGCATCTTCCATTTTGAA
gRNA7 GENO F	TTTAATGTGAAGAACGTGTCCGTAA
gRNA7 GENO R	AGGTCATCATTTTGAATCACCC
G70S New F	GGTAGGCCCGGTCTATAAA
G70S New R	CTTGTTTGAATGTACCGTTAGT
<b>Expression analyses in Del and Ins4 <i>eef1a2</i> mutant lines<sup>a</sup></b>	
<i>eef1a2</i> F (Primerdesign)	AGGCGGATTGTGCTGTCTT
<i>eef1a2</i> R (Primerdesign)	GGCGTGTCCCTTGTTTGG
<i>eef1a111</i> F (Primerdesign)	GAGGAAATCACCAAGGAAGTCA
<i>eef1a111</i> R (Primerdesign)	GTTGTCACCGTGCCATCC
<i>eef1a1a</i> F (Primerdesign)	GATTGTGCTGTGCTGATTGTG
<i>eef1a1a</i> R (Primerdesign)	GTAAGCCAGAAGAGCGTGTT
<i>eef1a1b</i> F (Primerdesign)	CTTGCTGGCGTACACTCTC
<i>eef1a1b</i> R (Primerdesign)	GACTTCCTTCACAATCTCCTCAT
3' <i>eef1a2</i> RT-PCR F	AGTATCCTCCACTGGGACGC
3' <i>eef1a2</i> RT-PCR R	AGCTGATTTGGTCACTCTCCC
<b>Probe synthesis for ISH experiment</b>	
<i>eef1a11</i> 3'UTR AntiF	AGAAGGCTGCCAAGACCAAG
<i>eef1a11</i> 3'UTR AntiR	[T7]TTATTCATCAGCGTTTCCAAATTGT

<b>ee1a1a 3'UTR AntiF</b>	TGTTGTGTTTGACTGCCAACTC
<b>ee1a1a 3'UTR AntiR</b>	[T7]ACAAGTGCTTGTGCAGGGTT
<b>ee1a1b 3'UTR AntiF</b>	AAACACTTGGGTCAGCCACA
<b>ee1a1b 3'UTR AntiR</b>	[T7]TGAGTGCAAGTGCAAACAAGAT
<b>ee1a2 3'UTR AntiF</b>	TGAATCTCCAAGACAGTCACCTT
<b>ee1a2 3'UTR AntiR</b>	[T7]TTGTCACAGGTTTGAGCAGC

<sup>a</sup>- Primers used in two different experiments, [T7] promoter sequence-TAATACGACTCACTATAGGG, Grey highlight- indicate primer sequences are copyrighted by Primerdesign Ltd.

## 2.1.4 Antibodies

The antibodies used in this project is listed in the table below together with the concentration and the application they were used.

**Table 2.4: List of antibodies employed in this project**

<b>Antibody name</b>	<b>Host species</b>	<b>Application and dilution</b>	<b>Company</b>
EEF1A2 (1°)	Rabbit	WB 1:500	GeneTex
EEF1A2 (1°)	Rabbit	WB 1:500	Proteintech
Anti-EEF1A2 (1°)	Rabbit	WB 1:1000	Abcam
Anti-EF1 $\alpha$ (1°)	Mouse	WB 1:1000	Merck Milipore
Anti-EF1A (1°)	Rabbit	WB 1:1000	GeneTex
eEF1A2-2 (1°)	Sheep	WB 1:50	Made in-house
GFAP (1°)	Rabbit	IHC 1:500	Dako
IRDye® anti-rabbit (2°)	Goat	WB 1:5000	LICOR
IRDye® anti-mouse (2°)	Goat	WB 1:5000	LICOR
Anti-rabbit biotinylated (2°)	Goat	IHC 1:500	Dako

Anti-goat HRP	IgG- (2°)	Rabbit	WB 1:2000	Dako
Anti-rabbit HRP	IgG- (2°)	Goat	WB 1:2000	Cell signaling

## 2.2 Methods

### 2.2.1 Zebrafish model

#### 2.2.1.1 Animal Husbandry

Zebrafish were maintained in the Yamuna fish room, MRC Human Genetics Unit (HGU) University of Edinburgh. They were raised in re-circulating in closed water system (Aquatic Habitats UK) at ~ 28.5°C with a pH range of 7.0 - 7.2. Room temperature was maintained at ~ 25°C on a diurnal light schedule of 14 hours of day (9 am to 11 pm) and 10 hours of night (11 pm to 9 am). AB zebrafish strains were used and were established from embryos collected from adult fish from within the facility using either the pairing or marbling mating methods.

Embryos were placed in E3 solution in batches of 50 per 9cm Petri dishes or 100 in 15cm Petri dishes and kept in the incubator at ~ 28.5°C until they become free swimming larvae at 5 days old. To ensure a healthy clutch was maintained, unfertilised, deformed or dead embryos were removed and the embryos were placed in fresh E3 solution every day. At 5 days old, the larvae were introduced into the water system and fed 3-4 times a day; one daily feed of paramecia, one feed of Artemia and one or two feed of dry food. Around 6 weeks of age, the fish are fed twice a day with adult dry food and live Artemia.

#### 2.2.1.2 Experimental procedures

All procedures carried out was done in accordance with the UK Home Office regulations. Permission to perform all experiments was granted to Personal Project License (PPL) number 60/4418 (updated to PA3527EC3) and Personal Individual License (IF3D4F532).

## 2.2.2 Methods for RNA analysis

### 2.2.2.1 Collection and extraction of RNA from embryos and adult tissues

Adult zebrafish were killed by immersing in tricaine for 10mins or until the cessation of gill movement. Tissues were quickly dissected and stored at -70°C in RNAlater® solution until RNA extraction. Zebrafish embryos were collected by natural spawning and raised in Petri dishes at 28.5°C until the desired developmental stages were reached according to Kimmel *et al.*, 1995. Embryos were collected at the following stages: 1-cell, 2-cell, 4-cell, 8-cell, 16-cell, 256-cell, high, 50%-epiboly, 90%-epiboly, 24 hours, 48 hours and 72 hours post fertilisation (hpf). A brief description of these developmental stages is summarised in table 2.5.

**Table 2.5: Description of embryonic developmental stages used for expression analysis taken from ZFIN ([https://zfin.org/zf\\_info/zfbook/stages/index.html](https://zfin.org/zf_info/zfbook/stages/index.html)).**

Stage	Period	Begins (hpf)	Landmark feature
1-cell	Zygote	0.00	Cytoplasm streams toward animal pole to form blastodisc
2-cell	Cleavage	0.75	Partial cleavage
4-cell		1.00	2X2 array of blastomeres
8-cell		1.25	2X4 array of blastomeres
16-cell		1.50	4X4 array of blastomeres
256-cell	Blastula	2.50	7 blastomere tiers
High		3.33	Blastodisc flattening starts
50%-epiboly	Gastrula	5.25	Uniformity of Blastoderm thickness remains

90%-epiboly	Gastrula	9.00	Brain and notochord rudiments
24hpf	Pharyngula	24	Early pigmentation, heartbeat
48hpf	Hatching	48	Elongated pectoral fin buds
72hpf	Early larva	72	Protruding mouth

Total RNA from tissues and approximately 50 embryos were extracted by homogenising in TRIzol® using a cordless pestle motor and RNase free pestle (VWR international). Muscle tissues were further homogenised by passing the lysate through a 1ml syringe with a 25G needle. RNA clean-up was done using the RNeasy Mini Kit (Qiagen) with on-column DNase treatment (RNase-free DNase set, Qiagen) following the manufacturer's instructions. Concentration and integrity of extracted RNA were assessed using the Agilent 2100 Bioanalyzer.

#### 2.2.2.2 Synthesis of cDNA

RNA was synthesised into cDNA using the AffinityScript Multiple Temperature cDNA Synthesis Kit (Agilent Genomics), following the manufacturer's instructions. A combination of oligo (dT) and random primers were used for all reactions. A '-RT' control, containing all the reagents except the reverse transcriptase (Affinityscript RT) was also included to check for DNA contamination in the RNA preparation. cDNA was then stored at -20°C until required.

#### 2.2.2.3 RT-PCR

Genomic contamination was assessed first for all cDNA using a primer for *actb2*. The primers were designed such that it amplifies cDNA at a product size of 360 base pair and genomic DNA if present, at a size of 648 base pair. Once it was ascertained that cDNA was free of genomic DNA, samples were run in duplicate with gene-specific primers and primer that amplified *actb2* to serve as a loading control for the reaction. PCR was performed using the Phusion High-Fidelity DNA Polymerase (see table 2.3



for primer sequences and section 2.6.1 for PCR parameters). Products were run out on a 2% 0.5 x TBE agarose gel containing SYBRsafe and visualised on a transilluminator or a Fujifilm FLA-5100 imager.

#### 2.2.2.4 geNorm reference kit

For accurate mRNA quantification, it is important to normalise real-time PCR data to a fixed reference gene, one that is not influenced by the experimental conditions. Some important factors to consider when choosing reference genes are discussed in Bustin *et al.*, 2009. A study by Vandesompele *et al.*, 2002 demonstrated the importance of using the geometric mean of multiple reference genes that have been carefully chosen for a more accurate normalisation factor for qPCR analysis. To select the best reference genes for this study, I used the geNorm gene kit for zebrafish (PrimerDesign Ltd UK). This consists of custom designed primers for 12 reference genes (Table 2.6) from the zebrafish genome which were analysed using a representative set of the samples. Primer sequences are not disclosed by the company. PCR was run as described in section 2.2.2.5. Data were analysed using the qbase+ analysis software (Biogazelle) which ranks the reference genes in order of their expression stability.

**Table 2.6: List of genes in the zebrafish geNorm kit (PrimerDesign, UK)**

Gene name	Symbol
Eukaryotic translation initiation factor 1B	EIF1B
NADH dehydrogenase	NADH
Tyrosine 3-monooxygenase activation protein	YWHAZ
16S ribosomal RNA	16S
ATP synthase	ATPsynth
Cytochrome P450 monooxygenase	CYP2K17
Actin, beta 1	actb1
Glyseraldehyde-3-phosphate dehydrogenase	GAPDH
Ribosomal protein L13	RPL13
Topoisomerase (DNA) II alpha	TOP2
Succinate dehydrogenase	SDHA
Ubiquitin specific protease 5	USP5

### 2.2.2.5 Quantitative PCR (qPCR)

Gene expression levels of the genes studied in this project were examined using RNA extracted from adult fish. RNA and cDNA preparation was carried out as described in section 2.2.2.1 and 2.2.2.2. The cDNA templates were diluted 1:5 with RNase free water before it was used in the reaction. The qPCR reaction was performed using the Brilliant II SYBR Green qPCR Master Mix (Agilent Technologies) and the 7900HT Light Cycler (Roche). Primers sequences are given in Table 2.3. Custom designed primers from Primerdesign were prevalidated by the company using pooled full-length cDNA generated from whole adult zebrafish by me.

Reaction set-up contained 5 $\mu$ l 2x Brilliant II SYBR Green, 0.5 $\mu$ l 6 $\mu$ M Primer mix, 0.375 $\mu$ l reference dye diluted 1:50 in water and 0.125 $\mu$ l RNase free water for a final volume of 10 $\mu$ l which were assembled on ice. Cycling conditions used were as follows:

#### Thermocycling conditions for qPCR

Cycles	Duration of cycle	Temperature (°C)
1	10 minutes	95
50	30 seconds	95
	1 minute	60

A dissociation curve was carried out at the end of the program to assess the specificity of the PCR reaction.

Primer efficiency was assessed for all genes using seven 4-fold serial dilutions of cDNA pooled cDNA from whole adult fish (1:4, 1:16, 1:64, 1:256, 1:1024, 1:4096 and 1:16384), all carried out in triplicate. Data were used to construct a standard curve for each target gene and reference genes and the efficiency of the reaction was calculated from the slope of the standard curve determined in the HT7900 system SDS software (Applied Biosystems) which is summarised in appendix table 2. Quantity of transcripts levels in the different tissues was determined using the appropriate standard curve for each gene.

The mRNA quantity of each gene of interest was then normalised to three reference genes: *ATPsynth*, *NADH* and *16S* which were selected using the geNorm kit (PrimerDesign Ltd UK) described in section 2.2.2.5, by dividing each target gene by

the geometric mean of the reference genes. To compare the amount of each zebrafish *eef1a* transcripts, the Pfaffl method (Pfaffl, 2001) was used to calculate the gene expression ratio of each transcript relative to the geomean of the reference genes for each tissue. All reactions were performed with three biological replicates in triplicate and a no-template control was included for each gene.

GraphPad Prism v5 was used to make graphs and perform statistical analyses. To test for significance, Mann Whitney test or One-way ANOVA with Tukey Multiple Comparison tests was performed where appropriate.

### 2.2.2.6 Whole mount *in situ* hybridisation (WISH)

#### 2.2.2.6.1 Probe synthesis

DNA primers were used to amplify fragments from the 3'UTR region of each *eef1a* gene as this region shows less similarity across the gene families, thereby avoiding cross-hybridisation of probes. PCR was performed using Phusion HF DNA polymerase (see section 2.2.6.1 for protocol) and products were gel-purified using the QIAquick Gel Extraction Kit (QIAGEN) according to the manufacturer's instructions. For each *eef1a* gene, PCR templates for antisense (experimental) and sense (control) probes were amplified. Primer sequences for sense probes are the same as that listed for antisense probes in Table 2.3 except that the T7 promoter sequence is tagged to the 5' of the forward primer.

Digoxigenin (DIG)-labelled anti-sense and sense probed were generated with 1µg of purified PCR products as templates using T7 RNA-polymerase and DIG RNA labelling mix (Roche). Reaction setup was assembled at room temperature in the following order;

Component	Volume (µl)
Purified PCR product	X (1µg)
DEPC-treated water	Up to 20
10X transcription buffer	2
DIG-RNA labelling mix	2
T7 RNA polymerase	2
RNasein (Promega, 40U/µl)	1

The reaction was incubated for 2 hours at 37°C. To stop the reaction, 1µl of DNase (Turbo DNase, Ambion) was added to the mix and incubated at 37°C for 20 minutes. RNA probes were then precipitated from the reaction by adding 6µl of DEPC-treated water, 75µl of 100% ethanol and 10µl 1M lithium chloride (LiCl). Precipitation mix was left overnight at -20°C and was centrifuged at a speed of 12,000xg the next day at 4°C for 30 minutes. The pellet was washed with 70µl of 70% ethanol and centrifuged at room temperature at a speed of 8,000xg for 5 minutes, after which it was air dried for 5-10 minutes. Pellets were dissolved with Diethyl pyrocarbonate (DEPC)-treated water and 1µl of RNasein to protect the RNA from degradation. Concentration and integrity of the probes were measured using the NanoDrop 1000 spectrophotometer (Thermo Fisher Scientific). All probes were aliquoted and stored at -80°C until needed.

#### **2.2.2.6.2 Preparation of embryos**

Embryos were collected and staged using the same method described in section 2.2.2.1. At 9hpf, the embryos were dechorionated using forceps and gently transferred to E3 medium containing 0.003% phenylthiourea (PTU) to inhibit melanin synthesis. The medium containing PTU was replaced regularly until the desired stage was reached. After this they were fixed overnight in 4% paraformaldehyde (PFA) in 1X PBS. The next day, the embryos were dehydrated through an increasing series of methanol in 1X PBS (25%, 50% and 75% v/v) for 5 minutes each and three changes of 100% methanol for 10 minutes. Embryos were stored in 100% methanol at -20°C until needed.

#### **2.2.2.6.3 *In situ* hybridisation**

The hybridisation protocol used was modified from the method described by Thisse and Thisse, 2007 and was carried out in sterile 1.5ml Eppendorf tubes. Embryos were rehydrated through a decreasing series of methanol in 1X PBS (75%, 50% and 25% v/v) for 5 minutes and then 4 times in PBS-T for 5 minutes each. Embryos were then digested with 500µl of 10µg/ml Proteinase K diluted in PBS-T at room temperature to make them permeable and allow penetration of the RNA probes. Embryos at 24hpf were digested for 10 minutes, those at 48hpf for 20 minutes and larvae at 72hpf and 5dpf were digested for 30 minutes. To stop the reaction, embryos were incubated in 4% PFA in 1X PBS for 20 minutes. The embryos were then washed in five changes of 500µl PBS-T for 5 minutes per wash to get rid of residual PFA. The embryos were

then prehybridised in 250µl prewarmed (15 minutes at 67°C) Hybridisation Mix (HM+) in the water bath at 67°C for 3 hours. Antisense and sense RNA probes were diluted separately in 250 µl of HM+ and denatured in a thermal cycler at 95°C for 2mins and placed immediately on ice to prevent reannealing. The final concentration of probes used was in the range of 40-50ng. The HM+ was removed and was then replaced with the HM+ containing probes. The embryos were hybridised in the solution overnight in the water bath at 67°C.

The HM+ containing probe solution was removed and stored at -20°C to be reused. The embryos were then washed in a decreasing series of heparin-free and tRNA-free Hybridisation Mix (HM-) diluted in 2x SSC (75%, 50% and 25% HM-) for 10 minutes per wash and then for 10 minutes in 100% 2x SSC. The embryos were washed 3 times for 30 minutes per wash in 0.2x SSC to prevent non-specific hybridisation of the probes. All these washes were performed in a water bath set at 67°C with the solutions prewarmed to 67°C prior to use. The embryos were then washed twice in 1x maleic acid buffer (MABT) for 10 minutes per wash at room temperature. Embryos were then incubated in blocking buffer at room temperature for 2 hours to avoid non-specific binding by the anti-DIG antibody. They were then incubated with the anti-DIG-AP antibody (Roche) diluted at 1:5000 in blocking buffer overnight at 4°C on an orbital shaker set at 40 rpm.

The next day, the antibody solution was replaced with 1x MABT and the embryos were washed for 5 minutes. They were then washed four times with 1x MABT for 30 minutes per wash to remove excess antibody and then washed with four changes of NTMT solution for 15 minutes per wash. All these washes were performed at room temperature with gentle agitation. This was then followed by staining the embryos with freshly prepared staining solution and the reaction was monitored under a dissecting microscope illuminated from above every 10 minutes. Staining was performed in the dark and with multi-well plates wrapped with foil to avoid excess exposure to light. The reaction was stopped by washing the embryos in five changes of 1x PBS-T for 5 minutes per wash and then incubating in 0.1M EDTA for 20mins. They were again washed in five changes of 1x PBS-T for 5 minutes per wash to remove residual EDTA. Brightfield microscopy using a Zeiss upright microscope and the Micro-manager

imaging software was used to view and take pictures of stained embryos. Stained embryos were stored in 4% PFA at 4°C.

## 2.2.3 *eef1a* constructs preparation and expression analysis

### 2.2.3.1 Cloning of full-length *eef1a* transcripts

#### 2.2.3.1.1 Generation of full-length cDNA

Total RNA was extracted from whole adult fish and cDNA synthesised as described in section 2.2.2. Full-length cDNA of *eef1a* genes were cloned into a pcDNA6.2C-EmGFP vector using Gateway cloning technology. The forward and backward primers were designed to contain *attB* site to facilitate recombination. Kozak consensus sequence was included in the forward primer to allow protein expression in mammalian cells and stop codon removed from the reverse primer to allow for GFP expression. *attB*-PCR products were generated using the PCR reaction set-up and cycling parameters summarised below;

#### PCR reaction set-up and thermocycling parameters for full-length *eef1a* cDNA

Component	Volume (µl)
5X Q5 Reaction Buffer	10
10Mm dNTPs	1
10µM F Primer	2.5
10µM R Primer	2.5
cDNA	2
Q5 Hot Start High-fidelity DNA Polymerase	0.5
5X Q5 High GC Enhancer	10
Water	21.5

Step	Temperature (°C)	Time
Initial Denaturation	98	30 seconds
35 cycles	98 *59 ( <i>eef1a2</i> ), 64 ( <i>eef1a1a</i> and <i>eef1a1b</i> ), 62 ( <i>eef1a11l</i> ) 72	10 seconds 30 seconds 2 minutes
Final Extension	72	2 minutes

\*indicates the different T<sub>m</sub> temperature used for each gene.

#### **2.2.3.1.2 PCR product clean up**

After amplification, PCR products were run on a 1% TAE agarose gel. The amplified products were excised from the gel with a clean scalpel using a Safe Imager transilluminator and purified using the QIAquick Gel Extraction Kit (QIAGEN) according to the manufacturer's instructions. 5µl of the purified products were run on a 1% 0.5x TBE gel to check the integrity of the DNA. The concentration of DNA was determined using the Nanodrop 1000 spectrophotometer (Thermo Fisher Scientific).

#### **2.2.3.1.3 BP recombination reaction**

Purified *attB*-PCR products were cloned into a pDONR221 donor vector using the BP clonase kit following the manufacturer's instructions to create an entry clone. In brief, a reaction containing 2µl of BP clonase, 150ng of pDONR221, 100ng *attB*-PCR product and TE buffer to a final volume of 10µl was made in a 1.5ml tube and incubated overnight at room temperature.

#### **2.2.3.1.4 Transformation of competent cells**

Library Efficiency DH5α competent cells were thawed on ice and 50µl aliquoted to 1.5ml ice-cold tubes. One microliter of BP recombination reaction was added and incubated on ice for 30 minutes. Cells were heat-shocked for 30 seconds at 42°C and immediately transferred to ice. After 2 minutes, 450µl of SOC medium was added to each tube and the cells were agitated horizontally for 1 hour at 37°C.

For each transformation, two LB plates containing kanamycin were used. The plates were pre-warmed at 37°C and 20µl cells spread on one plate and 100µl on the other plate. The plates were sealed with paraffin to avoid drying out and incubated overnight at 37°C. The pUC19 DNA vector was included as a control.

#### **2.2.3.1.5 Colony screening**

Four colonies were randomly chosen for each transformation and inoculated in individual Falcon tubes containing 4ml of LB broth containing 50µg/ml kanamycin. Cells were grown overnight at 37°C with constant shaking. The plasmid was purified from 3.5ml of the cell culture using QIAprep Spin Miniprep Kit (QIAGEN) following the manufacturer's protocol. 10µl of the purified plasmids were sent to Technical Services, MRC HGU Unit for sequencing using M13 sequencing primer from the

facility. The remaining 500µl of all positive entry clones were mixed individually with 500µl 50% v/v glycerol and stored at -70°C to provide a glycerol stock.

#### **2.2.3.1.6 LR recombination reaction**

Each gene was transferred to the pcDNA6.2C-EmGFP destination vector using the LR clonase II enzyme mix kit according to the manufacturer's instructions. Transformation and screening of colonies for the correct insert were performed as described above. In this case, LB containing 100µg/ml ampicillin was used and T7 promoter primers used for sequencing.

#### **2.2.3.2 Transient transfection**

HEK293T cell line, a kind gift from Dr. Chloe Stanton, were used for transfection. Transfection was performed using TurboFect Transfection reagent (Thermo Fisher Scientific) according to the manufacturer's recommended protocol. Briefly, cells were seeded into 6-well cell culture plates at a seeding density of  $2.4 \times 10^4$  in 4ml of DMEM (Gibco) with 10% Fetal Bovine Serum (FBS) growth medium 24 hours prior to transfection. 4µg of purified plasmid DNA containing the relevant construct was mixed with 6µl of TurboFect in 400µl of serum-free DMEM and incubated for 15 minutes at room temperature. The transfection reagent/DNA mixture was added to the well and mixed gently. Cells were harvested after 24 hours and used for protein analysis as described in section 2.2.4.2.

### **2.2.4 Method for protein analysis**

#### **2.2.4.1 Protein extraction from tissues**

Tissues were immediately snap frozen in dry ice after dissection and stored at -70°C if not extracted immediately. Ice cold RIPA buffer (containing one EDTA-free protease inhibitor tablet per 10ml RIPA buffer) was added to the tissue. Tissues were homogenised on ice using a cordless pestle motor (VWR). Lysates were maintained under constant agitation at 4°C for 2 hours and then centrifuged for 20 minutes at 12,000rpm at 4°C. The supernatant was gently aspirated and placed in a fresh pre-chilled 1.5ml tube and the pellet discarded.



#### **2.2.4.2 Protein extraction from cell culture**

Protein lysates from cultured cells were prepared in multi-well plates placed on ice. Cell medium was carefully aspirated and then the cells were washed once with ice-cold PBS. Ice cold RIPA buffer (containing one EDTA-free protease inhibitor tablet per 10ml RIPA buffer) was added to each well and a cold plastic cell scraper was used to collect the cells at one side of the well. The cell suspension was transferred to a pre-chilled 1.5ml tube and maintained under constant agitation for 30 minutes at 4°C. The lysate was centrifuged for 20 minutes at 12,000 rpm at 4°C. The supernatant was gently aspirated and placed in a fresh pre-chilled 1.5ml tube and the pellet discarded.

#### **2.2.4.3 Protein concentration determination**

Protein concentrations were quantified using the Pierce BCA protein assay kit (Pierce) for cell lysates and the DC Protein Assay (Bio-Rad) for tissue lysates following the manufacturers' instructions. In brief, the Pierce BCA protein assay was carried out using the microplate method. Eight BSA standards were prepared by diluting 2mg/ml BSA stock in RIPA. 25µl of standards and samples were pipetted into the microplate wells in duplicate. Working reagent was prepared by mixing fifty parts of reagent A with one part of reagent B (50:1) and 200µl of the solution added to each well and mixed on a shaker for 30 seconds. The plate was incubated at 37°C for 30 minutes and cooled to room temperature. The absorbance was measured at 562nm using a FLUOstar Omega plate reader.

The DC Protein assay was performed using individual cuvettes. The working reagent was prepared by mixing 20µl of reagent S to each ml of reagent A and 125µl added per cuvette. Five protein standards were made from a stock of 1.52mg/ml of BSA diluted in RIPA as follows: 0.25mg/ml, 0.5mg/ml, 0.75mg/ml, 1mg/ml and 1.5mg/ml. 2µl of standards and samples were added and the cuvette vortexed briefly and left for 5 minutes at room temperature. Absorbance was measured at 750nm using a Biomate 3 Spectrophotometer (Thermo Fisher Scientific).

The protein concentration of unknown samples was determined using a standard curve prepared from the BSA standards for both assays.

#### **2.2.4.4 SDS-PAGE**

All samples were prepared at equal protein concentration using the results obtained from the protein concentration assay kits. Laemelli loading buffer was added to each sample at a 1:1 ratio. Samples were denatured by placing in a heat block at 100°C for 5 minutes and then 10% (v/v) 1M dithiothreitol (DTT) was added.

Precast gel (4-15% Mini-Protean TGX stain-free gel, Bio-Rad) or homemade gels were used. Homemade gels were prepared using the Bio-Rad mini-Protean glass plates. The glass plates were cleaned using 70% ethanol, assembled into the casting frame and clamped to the casting stand. A 10% separating gel was poured into the gap between the plates and overlaid with isopropanol until it overflowed to ensure the top of the gel was horizontal. Once the separating gel had set, the isopropanol was discarded and 4.3% stacking gel pipetted between the glass plates until it overflowed. The comb was gently inserted to avoid trapping air under the teeth and the gel left to set.

Up to 20µl of samples were loaded into each well, with the first lane containing 10µl of a protein marker. Gels were run in a Bio-Rad Protean III tank with running buffer at 200V for precast gel or 100V through the stacking gel and then 150V through the separating gel when using homemade gels. Gels were run until the blue dye front reached the bottom of the gel.

#### **2.2.4.5 Protein transfer**

Two pieces of Whatman filter paper and one piece of PVDF membrane (Millipore) were cut to the size of the gel. The membrane was activated by wetting it with 100% methanol for 15 seconds. The membrane and gel were equilibrated in the transfer buffer in different trays for 15 minutes. The transfer sandwich was assembled in a tray containing transfer buffer as follows: the gel holder cassette, placed with the black side facing down, sponge, filter paper, gel, filter paper and sponge. Air bubbles were removed using a glass pipette and the cassette carefully closed and locked. The cassette was placed in the module and put into a tank along with an ice pack and magnet. The tank was filled with transfer buffer, placed on a magnetic stirrer and transfer performed at 100V for 1 hour at 4°C.

#### **2.2.4.6 Sypro Ruby Protein Blot Stain**

To determine if protein transfer was successful, membranes were stained using Sypro Ruby Blot Stain (Invitrogen) following the manufacturer's instructions. In brief, membranes were allowed to dry completely after transfer and then washed faced down in a solution of 7% acetic acid with 10% methanol on a shaker for 15 minutes. Membranes were washed four times in water for 5 minutes each and incubated in Sypro Ruby Blot Stain for 15 minutes with rocking in an opaque box to prevent light. Finally, the membranes were washed 2-3 times for 1 minute each to remove excess stain. Protein bands were visualised using the Odyssey Fc imager (LI-COR Biosciences, UK).

#### **2.2.4.7 Immunoblotting using HRP-conjugated secondary antibodies**

Membranes were blocked for 1 hour in blocking buffer containing 0.1% v/v Tween 20 and 5% w/v dried skimmed milk in TBS-T at room temperature. They were then incubated in primary antibody diluted in blocking buffer overnight at 4°C. Membranes were washed three times with TBS-T and incubated with the appropriate HRP-conjugated secondary antibody diluted in blocking buffer for 1 hour at room temperature. Membranes were again washed in TBS-T three times for five minutes each and detected using Clarity Western ECL Substrate (Bio-Rad) according to the manufacturer's instructions.

#### **2.2.4.8 Immunoblotting using LI-COR**

Membranes were blocked in Odyssey blocking reagent (LI-COR Biosciences, UK) for 1 hour at room temperature. Membranes were incubated overnight at 4°C with primary antibodies diluted to an appropriate concentration in Odyssey blocking buffer. They were washed three times in PBS-T for 5 minutes each wash and then incubated in secondary antibodies diluted 1:5000 in Odyssey blocking buffer. Membranes were washed three times with PBS-T for 5 minutes and photographed using the Odyssey Fc imager.

## **2.2.5 Generation of mutant lines using CRISPR/Cas9**

### **2.2.5.1 Cloning of guide RNA into guide RNA expression vector**

For the CRISPR/Cas9 experiment, guide RNAs (gRNAs) were designed to target the zebrafish *eef1a2*. The gRNA expression vectors were constructed by cloning a pair of annealed oligonucleotides into a Bsal (New England Biolabs) digested pDR274 (Addgene) backbone. Oligonucleotides corresponding to five different gRNA sequences (see Table 2.2) were annealed by mixing 9µl each of 100µM top and bottom strand with 2µl of annealing buffer (0.01M Tris-HCl pH 7.5, 0.05M NaCl, 1mM EDTA). The mixture was heated for 5 minutes at 95°C and cooled down slowly to room temperature. The pDR274 (a kind gift from Dr. Rodanthi Lyraiki) was linearized by digesting it with Bsal in CutSmart buffer for 1 hour at 37°C and the enzyme was heat inactivated for 20 minutes at 65°C. The vector was dephosphorylated using Antarctic phosphatase (New England Biolabs) to prevent it from self-annealing and purified using the QIAquick PCR Purification Kit (QIAGEN) according to the manufacturer's protocol. Annealed oligonucleotides were ligated to the digested vector by mixing 10nM of annealed oligonucleotide with ~ 50ng of purified linearized vector and incubating the reaction with 1µl of Quick ligase and 10µl of ligase buffer (New England Biolabs) at room temperature for 15 minutes. Library Efficiency DH5α competent cells were transformed with the ligation mix using the same method described in section 2.2.3.1.4. The presence of the correct insert was confirmed as described in section 2.2.3.1.5.

### **2.2.5.2 *In vitro* transcription of gRNA**

gRNA sequences were first amplified from purified gRNA expression vector with the cloned insert using Phusion High-Fidelity DNA Polymerase and primers which were a gift from Zhiqiang Zeng. The cycling conditions used were 98°C for 30 seconds, 30 cycles of 98°C for 30 seconds, 58°C for 30 seconds and 72°C for 20 seconds, followed by 10 minutes at 72°C. PCR product was confirmed by running 5µl on a 2% 0.5x TBE agarose gel and purified using the QIAquick PCR Purification Kit (QIAGEN) according to the manufacturer's instructions.

*In vitro* transcription of gRNA was carried out using the Ambion MAXIscript T7 kit (Thermo Fisher Scientific) and 1µg of the purified PCR product as a template. The

reaction was incubated for 1 hour at 37°C and treated with Turbo DNase for 15 minutes at 37°C to get rid of the template DNA. The gRNAs were purified using the SigmaSpin sequencing reaction clean-up kit (Sigma Aldrich). They were aliquoted in RNase-free 0.2ml tubes and stored at -80°C until use.

#### **2.2.5.3 Preparation of the nCas9 mRNA**

Purified pCS2-nCas9n vector (Addgene) plasmid was obtained from Dr. Rodanthe Lyraki. This plasmid contains the insert nuclear localised signal zebrafish codon-optimised Cas9 (nls-zCas9-nls) and an SP6 promoter for *in vitro* transcription. The vector was linearized with NotI-HF (New England Biolabs) for 1.5 hours at 37°C and purified using the PCR column purification kit (QIAGEN). Approximately 370ng of the linearized vector was used as a template for *in vitro* transcription using the SP6 mMACHINE kit (Thermo Fisher Scientific) following the manufacturer's instructions producing capped nCas9 mRNA molecules. The Cas9 mRNA was purified using the RNaseasy kit (QIAGEN) following the 'RNA cleanup' protocol. Poly(A) tailing of the nCas9 mRNA was then carried out using *E. Coli* Poly(A) polymerase (E-PAP) and purified again using the RNaseasy kit (QIAGEN) and eluted in RNase-free water. Capping and poly(A) tailing of the mRNA is important for stabilising the nCas9 mRNA molecules, therefore increasing translation efficiency once injected into the zebrafish embryo.

The other nls-zCas9-nls mRNA molecules used was prepared by Zhiqiang Zeng (Patton lab). The same preparation method described above was used excluding the poly(A) tailing procedure as *in vitro* transcription from the plasmid SP6 or T3 promoter already produces a capped, polyadenylated mRNA.

#### **2.2.5.4 Microinjection of embryos**

A solution containing the nCas9 mRNA (300ng/μl) and gRNA were mixed in a 1:1 ratio and microinjected directly into the cell of one-cell stage AB zebrafish eggs to generate *ee1a2* null cells. Injections were carried out by Witold Rybski (Patton's lab) and by me. For the CRISPR/Cas9-mediated HDR experiment, two test concentrations, 92ng/μl and 183ng/μl of ssODN repair template (IDT) were used to increase the chances of the G70S mutation being incorporated. ssODN at these concentrations were co-injected separately with nCas9 mRNA (300ng/μl) and gRNA3 (92ng/μl) mixed in

a 1:1:1 ratio. Injections were conducted by Dr. Cameron Wyatt (Zebrafish Manager, IGMM).

#### **2.2.5.5 Genomic DNA isolation from zebrafish embryos and adult fish**

Isolation of genomic DNA was conducted using either single or pooled whole embryos and clipping from tail fins of individual adult fish. Extraction of genomic DNA from these materials was performed using either DNA Releasy reagent (Nippon Genetics) or 50mM NaOH.

When using DNA Releasy reagent, embryos or tail fin clippings were placed in a 0.2ml PCR tube and covered with 20 $\mu$ l of DNA Releasy reagent. The tubes were then placed in a thermal cycler and DNA extracted using the following conditions: 65°C for 20 minutes, 96°C for 2 minutes, 65°C for 4 minutes, 96°C for 1 minute, 65°C at 1 minute, 96°C for 30 seconds and hold at 20°C.

Protocol for extracting DNA using 50mM NaOH was described by Meeker *et al.*, 2007. Tail fin clip or embryos were placed into 0.2ml PCR tubes containing 50 $\mu$ l of 50mM NaOH and incubated for 20 minutes at 95°C. The tubes were cooled to 4°C and 5 $\mu$ l of 1M Tris-HCL, pH 8, was added to neutralise the basic solution. In both methods, the tubes were centrifuged to pellet the debris, and the supernatant which contained the genomic DNA was stored at -20°C until use.

#### **2.2.5.6 TOPO cloning of PCR products to identify individual mutations**

Mutagenic efficiency of gRNAs and nCas9 mRNA were assessed after injection using DNA extracted from 5-10 pooled 2 days post fertilisation injected embryos. The target site was amplified using appropriate primers flanking target sites (see Table 2.3) and Taq DNA polymerase. PCR products were confirmed by gel electrophoresis and purified using a QIAquick PCR purification kit (QIAGEN).

As it is likely that amplified DNA fragments would be heterogeneous, purified PCR products were cloned into the TOPO vector using the TOPO-TA cloning kit (Invitrogen) before sequencing. Two microliters of purified PCR products was mixed with 2 $\mu$ l of water, 1 $\mu$ l of water and 1 $\mu$ l of TOPO vector. The ligation mixture was gently mixed and left to incubate for 30 minutes at room temperature. The ligation reaction was used to transform One Shot TOP10 chemically competent *E. coli* cells

(Invitrogen). The presence of the lacZ $\Delta$ M15 gene in these cells makes them a good choice as it allows for a more accurate selection of positive clones using the blue/white colour screening method. For this reason, 40 $\mu$ g of X-gal was spread on LB-Kanamycin plates 1 hour before use. Cells were thawed on ice and 25 $\mu$ l of cells aliquoted to ice-cold 1.5ml tubes. 2 $\mu$ l of the appropriate transformation reaction was added to each tube. The tubes were swirled gently to mix and incubated for 25 minutes on ice. Cells were heat shocked at 42°C for 1 minute and placed immediately on ice for 2 minutes. Room temperature SOC medium (275 $\mu$ l) was added to each tube and the tubes were incubated at 37°C for 1 hour under constant agitation of 225rpm. Two LB-Kanamycin plates with X-gal were used for each transformation. The plates were pre-warmed at 37°C and 50 $\mu$ l cells spread on one plate and 100 $\mu$ l on the other plate. The plates were sealed with paraffin to avoid drying out and incubated overnight at 37°C. Positive colonies, indicated by their white colour, were inoculated in individual wells containing 1ml of LB-Kanamycin broth in a 96-well deep well culture plate. The plates were sent to the Technical services, MRC HGU Unit for processing. T7 primers provided by the technical services were used for Sanger sequencing.

#### **2.2.5.7 Founder (F0) screening for mutation**

Genomic DNA extracted from tail fin clippings of injected fish at 3 months old were used to identify putative founder fish. Target sites were amplified using Taq DNA polymerase. Wild-type and no template controls were included in each reaction. 2 $\mu$ l of PCR product was sent off for analysis to Technical Services, MRC HGU using the Agilent 2100 Bioanalyzer.

#### **2.2.5.8 Germline transmission and establishing stable lines**

Putative founders were outcrossed with wild-type AB to confirm if the mutation could be passed to their offspring. Genomic DNA was extracted from 10-16 individual embryos and the target site amplified using Taq DNA polymerase and sequenced. When mutations were recovered, the rest of the F1 embryos were raised to adults.

Genomic DNA was isolated from tail fin clippings of 3 months old F1 fish and the target site was amplified with the Phusion High Fidelity (HF) DNA polymerase and sequenced to identify the mutant fish. F1x F1 crosses between fish with identical mutations were carried out. Fish from these crosses were then screened by PCR using

the Phusion HF DNA Polymerase and Sanger sequencing to identify homozygous null F2 fish. Phusion HF DNA polymerase was used for the PCR experiments because of its proof-reading capacity so as to ensure the correct sequences of mutant alleles were identified.

#### **2.2.5.9 Restriction enzyme digestion to screen for G70S incorporation in F0 fish**

Genomic DNA around the target site for the G70S incorporation amplified with Phusion HF DNA polymerase was digested with two restriction enzymes; EcoRI High fidelity (HF) and MnlI. Using EcoRI, a digest of the G70S allele is expected to produce two products of sizes, 429 and 60 base pairs. Since the EcoRI site was engineered in the G70S repair template and is absent in the wild-type allele, PCR products containing the wild-type remains uncut. Using MnlI, a digest of the wild-type allele is expected to generate three products; 291bp, 190bp and 8bp, whereas the G70S will remain uncut as the incorporation of the G70S mutation and the PAM-blocking silent mutation disrupts the MnlI recognition sites.

Reaction set-up for both enzymes was as follows:

<b>Component</b>	<b>15µl reaction</b>
Cutsmart buffer (NEB)	1.5
H <sub>2</sub> O	8
Restriction enzyme (NEB)	0.5
DNA	5

Samples were incubated for 2 hours at 37°C in a BioRad C1000 Touch thermal cycler.

#### **2.2.6 PCR protocol**

DNA amplification was performed by polymerase chain reaction (PCR) using either the proof-reading Phusion High Fidelity DNA Polymerase (New England Biolabs) or Taq DNA Polymerase (Invitrogen).

##### **2.2.6.1 PCR with Phusion High Fidelity (HF) DNA Polymerase**

A typical reaction setup which was assembled on ice when using the Phusion HF DNA polymerase is as follows:



<b>Component</b>	<b>25µl reaction</b>
10µM F Primer	1.25
10µM R Primer	1.25
cDNA/DNA/-RT/NTC	2
2X Phusion Master mix	12.5
H <sub>2</sub> O	8

The PCR tubes containing the reaction mix were centrifuged briefly and transferred to a Bio-Rad C1000 Touch thermal cycler and processed with the following conditions;

<b>Step</b>	<b>Temperature</b>	<b>Time</b>
Initial Denaturation	98°C	30 seconds
Denaturation	98°C	10 seconds
Annealing	<b>X</b>	30 seconds
Extension	72°C	15-30secs per kb
Final Extension	72°C	10mins
Hold	4°C	

The annealing temperature used for each primer set was determined using the NEB Tm calculator (<https://tmcalculator.neb.com/#!/main>).

#### **2.2.6.2 PCR with Taq DNA Polymerase**

DNA amplification was mostly performed using Taq DNA polymerase for routine genotyping experiments. The reaction setup assembled on ice was as follows:

<b>Component</b>	<b>X1 (µl) for 25ul</b>
10X PCR Buffer	2.5
50mM MgCl <sub>2</sub>	0.75
10mM dNTPs	0.5
10µM F Primer	1.25
10µM R Primer	1.25
DNA/NTC	2
Taq Polymerase	0.5
H <sub>2</sub> O	16.25

The following thermocycling conditions were used to process the amplification reaction:

Step	Temperature	Time
Initial Denaturation	94°C	3mins
Denaturation Annealing Extension	94°C 63°C 72°C	45s 30s 60s
	<b>35 cycles</b>	
Final Extension	72°C	10mins
Hold	12°C	

### 2.2.7 General sequencing protocol

When the sequencing reaction was carried out by me, the following protocol was used. Once the target site has been amplified and confirmed, the PCR product was treated with ExoSAP-IT (Affymetrix) to remove excess primers and incorporated dNTPs. Five microliters of PCR product were incubated with 1µl of ExoSAP-IT at 37°C for 15 minutes, and then at 80°C for another 15 minutes to inactivate the ExoSAP-IT. The DNA sequencing reaction was carried out using the BigDye Terminator v3.1 Cycle Sequencing kit (Thermo Fisher Scientific). The reaction was set up as follows: 4µl clean PCR product, 1.5µl primer, 1µl Big Dye, 1.5µl Big Dye and 2µl water. The sequencing reaction was then run using the following program: 96°C for 1 minute and 24 cycles of 96°C for 1 minute, 50°C for 15 seconds and 64°C for 4 minutes.

The sequencing reaction was cleaned up by adding 2.5µl of 125mM EDTA and 30µl of absolute ethanol to each well. The reaction was mixed by inverting the sealed plate gently four times and the plate incubated at room temperature for 5 minutes. The plate was then centrifuged for 15 minutes at 3000 rpm. The ethanol was removed and replaced with 30µl 70% ethanol. The plate was again centrifuged for 15 minutes at 3000 rpm and the ethanol removed. The plate was left to air dry at room temperature for 10 minutes. Plates were sent off to the Technical services, MRC Human Genetic Unit (HGU) for processing using a 3730 Genetic Analyser (Applied Biosystems). Chromatograms were viewed using the SnapGene Viewer (version 2.8.2, GSL, Biotech).

### 2.2.8 PTZ treatment and behavioural monitoring

Zebrafish larvae were sorted and placed individually in a 96-well plate (Greiner CELLSTAR) 24 hours before the experiment and then placed in an incubator at 28.5°C

until they were needed. Each well contained 70µl of E3 medium and one 5 dpf larva. Before starting the recording session, larvae were allowed to habituate for 10 minutes to minimise disturbance due to handling and transporting of the plate. Baseline recordings of 20 minutes were then obtained from the fish while in normal E3 medium. Experimental fish were then treated with 2.5mM PTZ (Sigma-Aldrich) diluted in E3 medium while controls were left in normal E3 medium. Swimming behaviour of the fish was monitored for 80 minutes.

Video recordings were performed with the assistance of Craig Nicol using a Nikon D800 camera with an attached 60mm macro lens mounted on a copy stand. The experiment was carried out in a quiet location with restricted access to avoid exposing the fish to unintended stimuli. Recording session (80 minutes) was done at intervals of 20 minutes which is the recording limit of the camera. For Locomotion analysis, swimming behaviour of the fish was tracked using EthoVision XT9, an automated locomotion tracking software, by Dr. Pia Lundegaard. For seizure analysis, the video was scored according to Baraban *et al.*, 2005 (summarised below) by Dr. Rodanthi Lyraki blind to the genotype and treatment of the fish. Graphs and statistical analysis were performed using GraphPad Prism 5. To test for significance, One-way ANOVA with Tukey Multiple Comparison tests or repeated measures ANOVA were performed where appropriate.

**Description of seizure stages according to Baraban *et al.*, 2005 used for seizure analysis**

<b>Seizure stage</b>	<b>Description</b>
I	Dramatic increase in swim activity
II	Rapid ‘whirlpool-like’ circling swim behaviour
III	Clonus-like convulsions followed by brief loss of posture

## **2.2.9 Histology**

### **2.2.9.1 H & E staining**

Adult zebrafish were culled in an overdose of tricaine for 10 minutes or until the cessation of gill movement. Using a forceps, a longitudinal incision was made on the ventral side of the fish to allow for the introduction of the fixative into the body. The fish were fixed in 10% neutral buffered formalin (Sigma-Aldrich) and sent to the Easter Bush Pathology labs for processing. Sections were cut at a thickness of 3  $\mu$ M and haematoxylin and eosin (H&E) staining were performed by staff at the Easter Bush Pathology department.

### **2.2.9.2 Immunohistochemistry**

Spinal cord sections were dewaxed in two changes of xylene for 5 minutes each and were rehydrated through a decreasing series of alcohol solutions, with 5 minutes in two changes of 100% ethanol and 5 minutes in two changes of 70% ethanol. Sections were then washed under running tap water for 5 minutes. Antigen retrieval was carried out by treating sections with Proteinase K (Dako) at room temperature for 10 minutes. Sections were then treated with 3% hydrogen peroxide to block endogenous peroxidase activity. They were again washed in water, followed by PBS for 5 minutes each. Slides were transferred to a Sequenza (Shandon) and washed briefly with PBS. They were treated for 10 minutes with 100 $\mu$ l goat blocking serum (Bethyl Laboratories) diluted 1:5 in PBS to prevent non-specific binding of the secondary antibody. 100 $\mu$ l GFAP antibody (Dako) diluted 1:500 in PBS was then added and the slides incubated overnight. The slides were washed twice with PBS for 5 minutes and incubated for 30 minutes with 100 $\mu$ l goat anti-rabbit biotinylated secondary antibody (Dako) diluted 1:500 in PBS. They were then washed for 5 minutes in PBS and treated with 3 drops of Strept ABC reagent (Vector Laboratories) for 30 minutes. Slides were again washed in PBS for 5 minutes, removed from the Sequenza and treated with DAB (Abcam) for 10 minutes. Excess DAB was removed by washing slides under running tap water. Sections were counterstained in haematoxylin solution (Shandon) for 5 minutes, rinsed in water to remove excess stain and then differentiated in saturated lithium carbonate for few seconds. Sections were washed briefly in water and then dehydrated through two changes of 70% ethanol, 100% ethanol and xylene for 5

minutes. Slides were mounted using DPX (VWR) and imaged using an Olympus BX60 light microscope.

### **2.2.10 Databases and online resources**

The two main online databases used in this work were Ensembl (<https://www.ensembl.org/index.html>) and ZFIN (<http://zfin.org/>) genome browsers (D. G. Howe *et al.*, 2013; Flicek *et al.*, 2014). BLAST search and design of primers for qRT-PCR were performed using tools from the NCBI homepage (<https://www.ncbi.nlm.nih.gov/>). Other primers were designed using Primer3 (<http://primer3.ut.ee/>) (Untergasser *et al.*, 2012). Multiple alignments of DNA and protein sequences were done using Clustal Omega (<https://www.ebi.ac.uk/Tools/msa/clustalo/>) (Sievers *et al.*, 2011). The phylogenetic tree was constructed by Dr. Dinesh Soares with the MEGA version 6 software (Tamura *et al.*, 2013) using a maximum likelihood method. Conserved synteny analysis was conducted using the Synteny Database (Catchen, Conery and Postlethwait, 2009).

Comparative modeling and visualisation of the 3-D structures of the zebrafish eEF1A isoforms were carried out through the Chimera-Modeller interface (Pettersen *et al.*, 2004; Webb and Sali, 2016). The coarse packing quality of the models was evaluated using the WHAT IF server (<https://swift.cmbi.umcn.nl/servers/html/index.html>). This checks the normality of the local environment of amino acids and assigns a score. A residue with a score of -0.5 or lower indicates something is 'wrong' with its packing quality within the model (Vriend and Sander, 1993). Solvent-accessibility of variant amino acid residues and those within a distance of 5 Å of a known binding site was calculated under Chimera (Sanner, Olson and Spehner, 2018). Phosphorylation site prediction was performed using the NetPhos version 3.1 server (<http://www.cbs.dtu.dk/services/NetPhos/>) (Blom, Gammeltoft and Brunak, 1999) using a threshold set at 0.5 so that only positive predicted phosphorylation sites are displayed. The NetPhos 3.1 server performs both generic and kinase specific predictions of serine, threonine or tyrosine phosphorylation sites in eukaryotic proteins using ensembles of neural networks. It then assigns a score to each sites with the confidence of its prediction indicated by how high the score is from 0.5, which is the threshold for showing only positive potential phosphorylation sites in the result output.

For the CRISPR/Cas9 experiments, the target finder tools CHOPCHOP (<http://chopchop.cbu.uib.no/>) and <http://crispr.mit.edu/> were used to design guide RNAs and primers (CHOPCHOP) to amplify target sites for the zebrafish *eef1a2*. These target finder tools also search for potential off-target sites for each gRNA in the zebrafish genome. Sanger sequencing results were viewed using the SnapGene Viewer version 2.8.2. Double peak regions in the sequencing chromatograms were separated into wild-type and alternative sequences using the Poly Peak Parser software to identify indel mutations (<http://yosttools.genetics.utah.edu/PolyPeakParser/>) (Hill *et al.*, 2014).

# Chapter 3: Bioinformatics and expression analysis of Zebrafish eEF1A

## 3.1 Introduction

As detailed in chapter 1, eEF1A is important for protein translation where it helps recruit aminoacylated-tRNA to the acceptor site of the ribosome during protein synthesis. This process is GTP-dependent and is facilitated by its interaction with eEF1B, a GTP-exchange factor. Apart from this function, eEF1A also has other non-canonical roles such as binding and bundling actin (see section 1.1.3 in chapter 1 for details). Different numbers of *eEF1A* genes are found in individual eukaryotic species. In the yeast *Saccharomyces cerevisiae*, two sequence-redundant genes, *TEF1* and *TEF2* are present. In *Xenopus*, four different genes; *eef1a1* which is the somatic form, *eef1a1o* which is the oocyte form, *42Sp50*, expressed only in the oocytes and *eef1a2* are present. While many pseudogenes exist in mammalian genomes, only two *EEF1A* genes, *EEF1A1* and *EEF1A2*, has been shown to be actively expressed in human, rat, mouse, rabbit and pig (Knudsen *et al.*, 1993; Chambers, Peters and Abbott, 1998; Kahns *et al.*, 1998; Svobodová *et al.*, 2015). They encode distinct proteins, eEF1A1 and eEF1A2 which has been implicated in neurological diseases. Extensive studies of eEF1A in mammals revealed the differential expression of these two genes, with eEF1A1 widely expressed and eEF1A2 expression restricted to the brain, heart and skeletal muscle, where it gradually replaces eEF1A1 during development in these cell types. Although, eEF1A has been studied less extensively in non-mammalian vertebrates, studies by Newbery *et al.* 2011 in *Xenopus* species show a similar pattern of expression of eEF1A2 and that variant switching is conserved with the regulation of expression occurring at the post-transcriptional level rather than transcriptional as seen in vertebrates.

The emergence of the zebrafish as an excellent tool for modelling disease processes has resulted in tremendous progress of the sequencing of its genome. Previous studies reported only one actively expressed *eef1a* gene in zebrafish (Gao *et al.* 1997). However, the zebrafish genomic sequence has developed to the point where it is clear that the zebrafish has more than one *eef1a* gene. This chapter describes work providing

an updated studies of eEF1A in zebrafish. Zebrafish eEF1A was investigated using bioinformatics and gene expression analysis approaches to confirm the existence of each eEF1A gene and investigate if they are functionally active.

## 3.2 Results

### 3.2.1 Bioinformatics analysis of *eef1a* in zebrafish

#### 3.2.1.1 Identification of *eef1a* genes in zebrafish

To investigate the *eef1a* genes in zebrafish, its genome was searched using the Ensembl (Zv9, release 79) and ZFIN databases (Bradford *et al.*, 2011; Flicek *et al.*, 2014). Four *eef1a* genes, referred to as *eef1a11l*, *eef1a1a*, *eef1a1b* and *eef1a2* were identified which are located on different chromosome in the zebrafish genome. Table 3.1 summarises some of the features of the *eef1a* genes. All of them contained eight exons, seven introns and an open reading frame (ORF) that encodes different proteins 462 (eEF1A1L1, eEF1A1A and eEF1A1B) or 463 (eEF1A2) amino acid long. The exon-intron organisation for each *eef1a* gene is shown in figure 3.1. Exon 1 together with part of exon 2 form the 5'UTR, and part of exon 8 makes up the 3'UTR in all four *eef1a* genes. While the sizes of exons 3-7 are the same for all the genes, some of the introns of *eef1a1a*, *eef1a1b* and *eef1a2* genes are greatly expanded compared to *eef1a11l* which has smaller introns similar to eEF1A1 gene in human and mouse species (Figure 3.2). The *eef1a* genes shared high sequence homology at the nucleotide level in the coding region and also at amino acid level, with *eef1a1a* and *eef1a1b* being highly related to one another as shown in table 3.2.

**Table 3.1. Main features of the *eef1a* genes in zebrafish**

Gene	Chromosome	Transcript length (bps)	Number of exons	Translation length (aa)	Protein encoded
<i>eef1a11l</i>	19	1745	8	462	eEF1A1L1
<i>eef1a1a</i>	13	2170	8	462	eEF1A1A
<i>eef1a1b</i>	1	2160	8	462	eEF1A1B
<i>eef1a2</i>	23	2030	8	463	eEF1A2



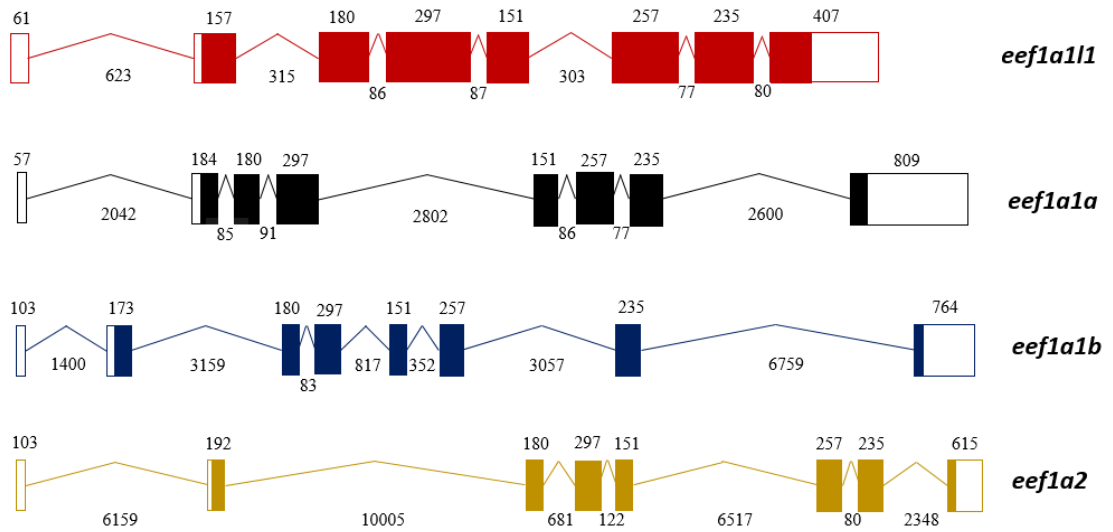


**Figure 3.1. Exon-intron organisation of the *eef1a* genes in zebrafish.** Schematic representation of *eef1a1l1* (red), *eef1a1a* (black), *eef1a1b* (blue) and *eef1a2* (yellow) gene structures obtained from the Ensembl database. Exons are represented with blocks while introns are represented with lines. Untranslated regions (UTRs) in exons are shown with empty blocks. Length (in base pairs) of exons and introns, which are not drawn to scale, are indicated above and below respectively.

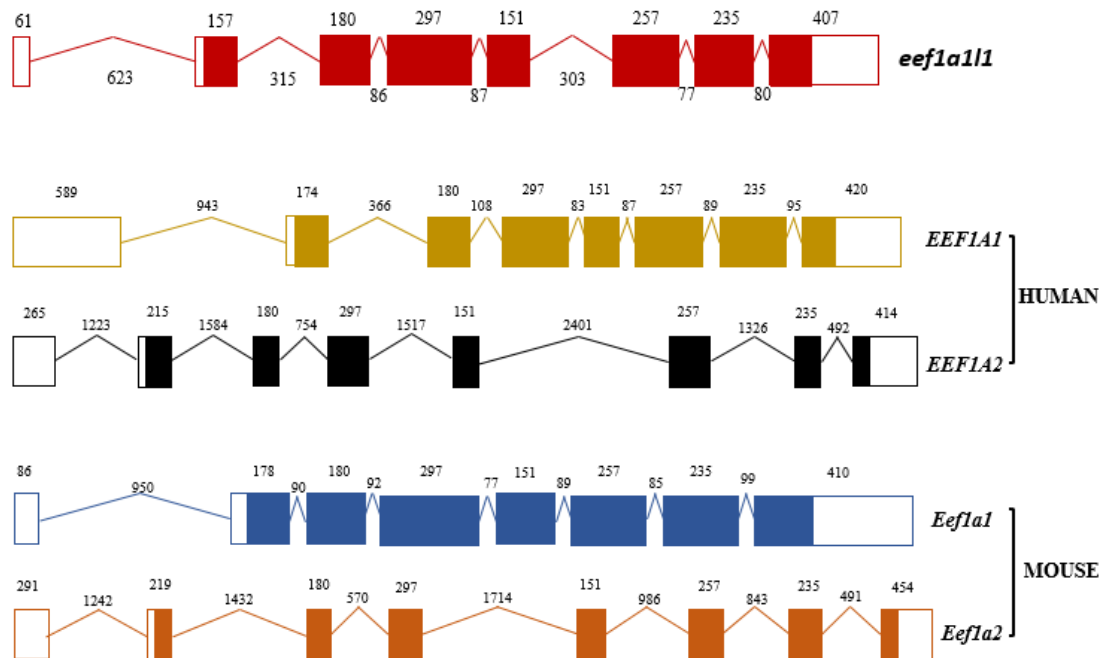


**Figure 3.2. Comparison of the intron-exon structure of the zebrafish *eEF1A1L1* gene and *eEF1A* genes in human and mouse species.** Gene structures of zebrafish *eef1a1l1* (red), human *EEf1A1* (gold) and *EEf1A2* (black), mouse *Eef1a1* (blue) and *Eef1a2* (orange) obtained from the Ensembl genome browser. The zebrafish *eef1a1l1* gene architecture is much more similar to that *eEF1A1* gene of both vertebrate species. Exons are represented with blocks while introns are represented with lines. Untranslated regions (UTRs) in exons are shown with empty blocks. Length (in base pairs) of exons and introns, which are not drawn to scale, are indicated.

**Table 3.2. Percentage identity matrix of zebrafish eEF1A variants at the nucleotide and amino acid sequence level calculated using Clustal Omega**

	<i>eef1a1l1</i>	<i>eef1a1a</i>	<i>eef1a1b</i>	<i>eef1a2</i>
<i>eef1a1l1</i>	100 (100)	80 (92)	79 (91)	75 (89)
<i>eef1a1a</i>	80 (92)	100 (100)	83 (97)	77 (91)
<i>eef1a1b</i>	79 (91)	83 (97)	100 (100)	77 (90)
<i>eef1a2</i>	75 (89)	77 (91)	77 (90)	100(100)

*\*Numbers in bracket indicate the percentage identity at the amino acid sequence level.*

### 3.2.1.2 Orthology assignment of zebrafish *eef1a* to human *EEF1A* genes

Three different approaches were used to assign the zebrafish *eef1a* genes to their appropriate human orthologue. Firstly, a reciprocal best hit (RBH) BLAST was employed using each of the human protein eEF1A variants as the query sequence against the zebrafish genome using the reference sequence (RefSeq) protein database on the NCBI BLAST browser. A BLAST search of the human eEF1A1 protein against the zebrafish genome produced eEF1A1A and eEF1A1B as its top two hits with approximately the same magnitude of alignments with the following BLAST results;

	Score	Expect	Identities	Positives	Gaps
eEF1A1A	905 bits (2338)	0.0	438/462(95%)	448/462 (96%)	0/462 (0%)
eEF1A1B	901 bits (2329)	0.0	436/462 (94%)	447/462 (96%)	0/462 (0%)

A retro-BLAST with the zebrafish eEF1A1A and eEF1A1B against the human genome both found eEF1A1 as their best hit. Similar BLAST searches were done for eEF1A2 protein. The human and zebrafish eEF1A2 produced each other as their top hit with the results;

	Score	Expect	Identities	Positives	Gaps
eEF1A2	910 bits (2351)	0.0	436/463(94%)	454/463 (98%)	0/463 (0%)

However, an eEF1A1L1 BLAST search hit the human eEF1A1 and eEF1A2 with approximately the same magnitude. The BLAST results are summarised below.

	<b>Score</b>	<b>Expect</b>	<b>Identities</b>	<b>Positives</b>	<b>Gaps</b>
eEF1A1	882 bits (2279)	0.0	425/462(92%)	441/462 (95%)	0/462 (0%)
eEF1A2	875 bits (2262)	0.0	417/460(91%)	448/460 (95%)	0/460 (0%)

Secondly, a phylogenetic analysis was performed with the MEGA6 software (Tamura *et al.*, 2013) using all four zebrafish eEF1A protein sequences and those from other vertebrate species. The phylogenetic tree was built by Dr. Dinesh Soares using the maximum likelihood method (see figure 3.3 legend for details). Result from this analysis showed that zebrafish eEF1A1A is paralogous to eEF1A1B, and both of them are co-orthologous to human eEF1A1. The phylogenetic tree also suggests that zebrafish eEF1A2 is orthologous to the human eEF1A2. However, eEF1A1L1 did not segregate with the eEF1A1 clade and appears to possess sequence features similar to both eEF1A1 and eEF1A2.

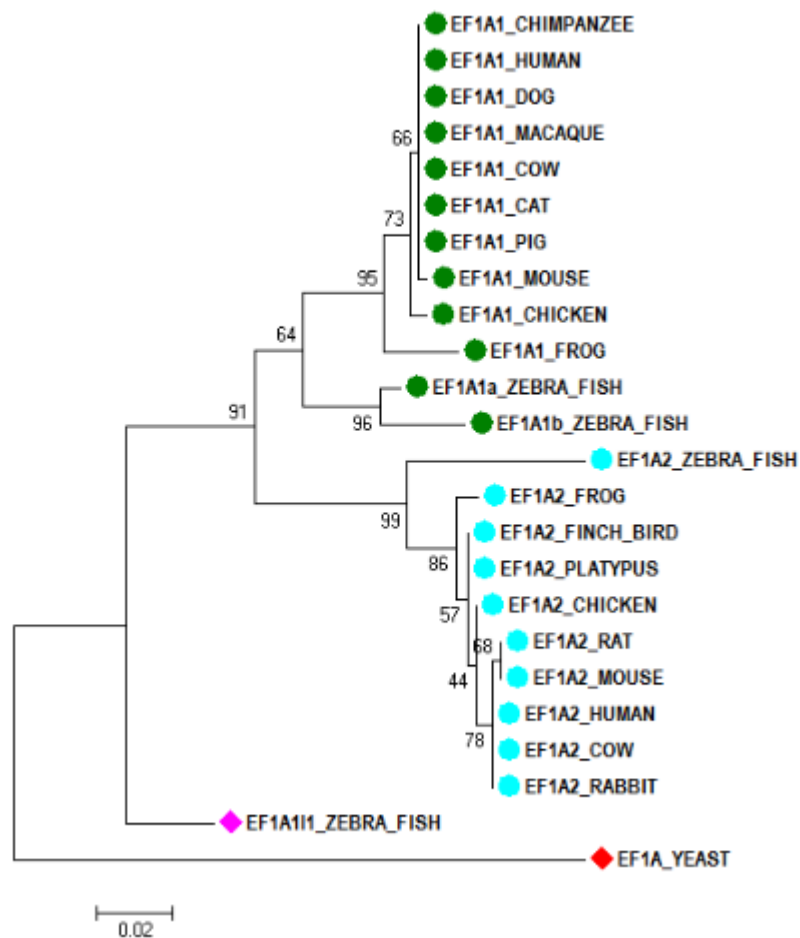


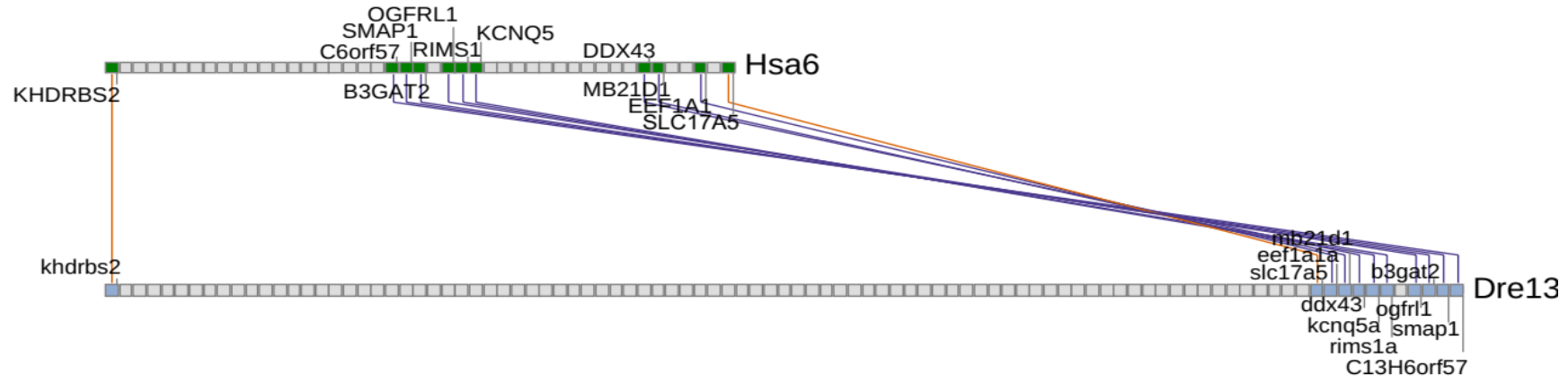
**Figure 3.3. Molecular Phylogenetic analysis of eEF1A1 and eEF1A2 orthologues by Maximum Likelihood method.** The evolutionary history was inferred by using the Maximum Likelihood method based on the Poisson correction model (Zuckerkandl and Pauling, 1965). The tree with the highest log likelihood (-2809.8575) is shown. The percentage of trees in which the associated taxa clustered together is shown next to the branches. Initial tree(s) for the heuristic search were obtained automatically by applying Neighbour-Join and BioNJ algorithms to a matrix of pairwise distances estimated using a JTT model, and then selecting the topology with superior log likelihood value. The tree is drawn to scale, with branch lengths measured in the number of substitutions per site. The reliability of each branch was assessed using 1,000 bootstrap replicates and reliable assignment values indicated. The analysis involved 24 amino acid sequences. All positions with less than 95% site coverage were eliminated. That is, fewer than 5% alignment gaps, missing data, and ambiguous amino acids were allowed at any position. There were a total of 462 positions in the final dataset. Evolutionary analyses were conducted in MEGA6 (Tamura *et al.*, 2013). The orthologues of eEF1A1 and eEF1A2 sequences fall into well-supported clades, consistent with their known paralogous classification and functional divergence. The eEF1A1I1 sequence from zebrafish on the other hand appears to be more divergent, does not fall into the eEF1A1 group of sequences and appears to possess sequence features of both eEF1A1 and eEF1A2. (*Phylogenetic tree and figure legend by Dr. Dinesh Soares*)

The third approach involved the use of the Synteny Database (Catchen, Conery and Postlethwait, 2009) to identify conserved synteny regions between the zebrafish and human genomes. Conserved synteny make use of gene position and order to identify orthologous chromosomal regions in different species, unlike RBH BLAST and phylogenetic analyses which infers orthologous genes based on sequence similarities. Therefore, conserved synteny served as an independent line of evidence to confirm results obtained using the other two approaches. The Synteny Database was used to search for conserved regions between the *eef1a* genes region in zebrafish and in humans using the recommended sliding window size of 100-gene. A gene trace clearly showed strong conservation between zebrafish *eef1a1a* gene located on chromosome 13 (Dre13) and the human *EEF1A1* on chromosome 6 (Hsa6) with ten pairs of orthologous genes surrounding the *EEF1A1/eef1a1a* orthologues with *SLC17A5*, *MB21D1* and *DDX43* genes as near neighbours in both species (Figure 3.4A). The orthologous syntenic cluster associated with zebrafish *eef1a1b* (Dre1) showed only *RIMS1* and *KCNQ5* as the orthologous genes surrounding the *EEF1A1/eef1a1a* orthologues (Figure 3.4B). However, a paralogous syntenic cluster for zebrafish *eef1a1a* and *eef1a1b* showed a strong local conservation between these regions and contained 13 paralogous gene pairs including *eef1a1a* and *eef1a1b*, as well as the directly adjacent paralogues of *rims1* and *kcnq5* as their near neighbours (Figure 3.4C). This confirms *eef1a1a* and *eef1a1b* as paralogues and indicates *eef1a1b* arose from the duplication of the genomic region containing the *eef1a1a* gene.

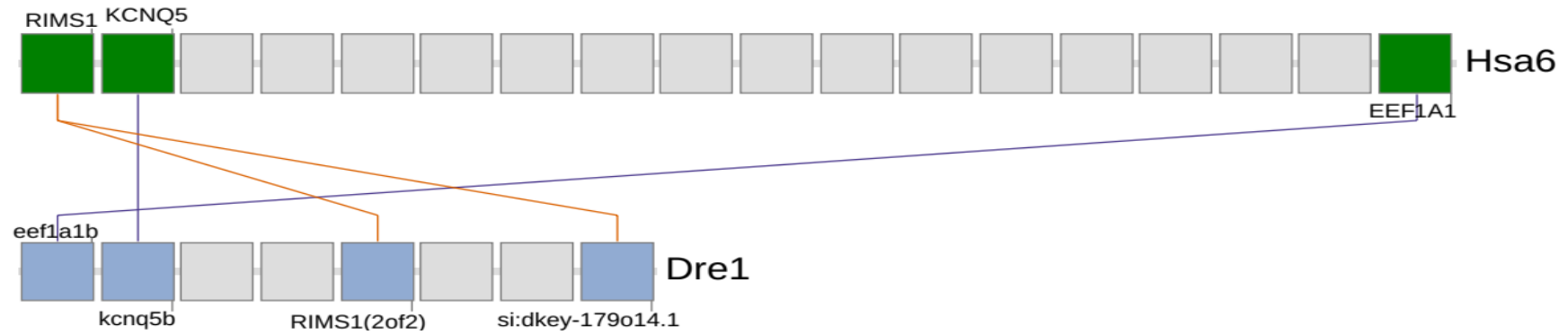
Similar analysis was carried out for zebrafish *eef1a2*. The orthologous syntenic cluster between the zebrafish *eef1a2* and human *EEF1A2* showed a strong conservation with a total of 96 pairs of orthologues between the two species using a 100-gene sliding window. However, the gene trace (shown in Figure 3.4E) was drawn using a 25-gene sliding window for the sake of clarity and shows 22 pairs of orthologues, with *NKAIN4* and *EEF1A2* forming a subcluster in both species. Searching for any conserved region for *eef1a111* between zebrafish and the human genomes produced an orthologous syntenic cluster for a region on human chromosome 6 (Hsa6) containing the *EEF1A1* gene. However, this region did not contain any pair of orthologous genes but only related genes that belonged to the same family; *EEF1A1/eef1a111*, *TFAP2B/tfap2e* and *SLC17A5/slc17a3* (Figure 3.4D).

Taken together, these results show that zebrafish *eef1a1a* and *eef1a1b* are paralogues and are co-orthologues to human *EEF1A1*, while *eef1a2* is the orthologue of the human *EEF1A2* gene. However, zebrafish *eef1a111* did not appear to have any orthologous *EEF1A* gene in the human genome.

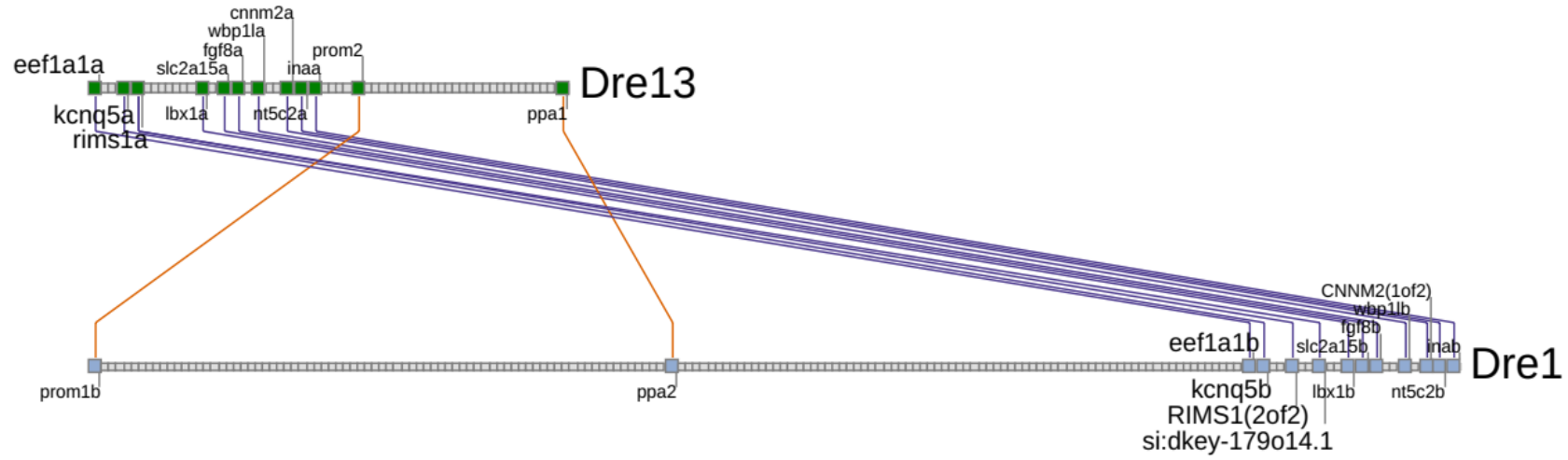
**A**



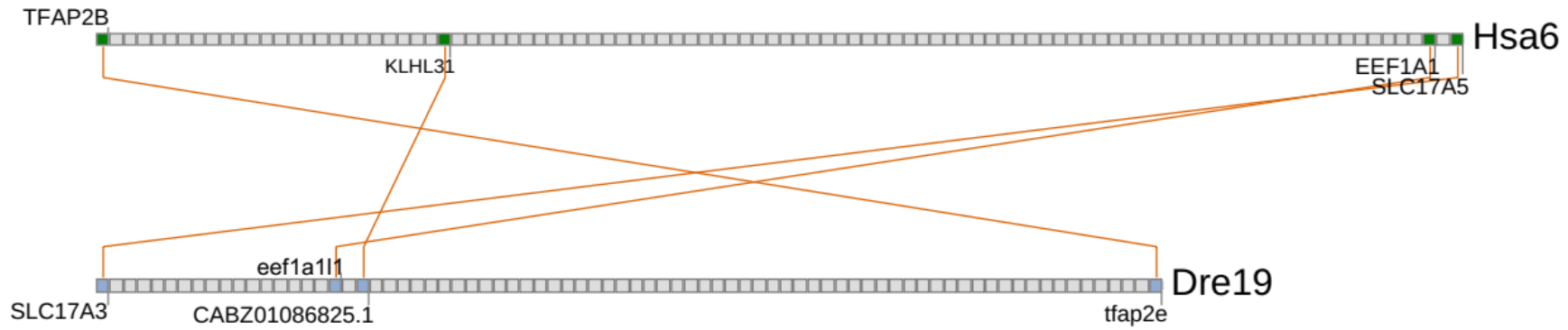
**B**



**C**



**D**





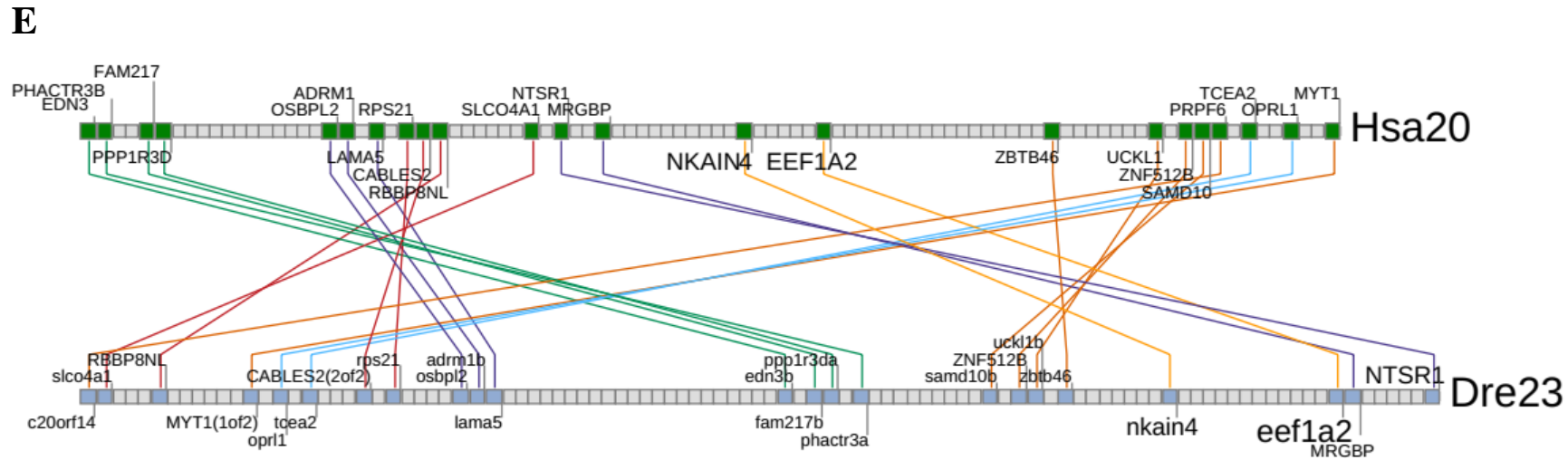


**Figure 3.4. Conserved syntenies analysis for zebrafish *eefla* genes.** Gene trace representation of the conserved syntenies between zebrafish *eefla* genes and the human *EEFlA* genes were generated using the Synteny DB discovered using a 100-gene sliding window. Orders of the genes (indicated as squares) but not their physical location are preserved. Coloured squares indicate genes that belong to the cluster while grey squares show genes within the region but not members of the cluster. Lines connecting coloured squares between the two clusters represent orthologous or paralogous gene pairs. Lines of the same colours (referred to as subclusters) indicate strong local conservation. **A-B.** Orthologous syntenic cluster for *eefla1a* and *eefla1b* showing syntenic conservation between the human chromosome 6 (Hsa6) which contain *EEFlA1* and zebrafish chromosome 13 (Dre13) for *eefla1a* and Dre1 (*eefla1b*) **C.** The *eefla1a* and *eefla1b* paralogous syntenic cluster showing a strong conserved region between Dre13 and Dre1 which contains *eefla1a* and *eefla1b* respectively. **D.** Orthologous syntenic cluster generated for *eefla111* shows a weak conservation with Hsa6, but genes from the two clusters are not orthologous pairs but belong to the same family. **E.** The zebrafish *eefla2* orthologous gene trace showing a very strong conservation with the Hsa20 which contains *EEFlA2*, both of which form a subcluster with *NKAIN4*. For clarity, the window size used in generating the gene trace was reduced to 25. Syntenic cluster using a 100-gene sliding window size discovered 97 orthologous gene pairs in this region between the two species.

### 3.2.1.3 Comparative analysis of zebrafish eEF1A sequence

Although, it is still not understood why two near-identical eEF1A isoforms exist, it is clear that there are some functional differences between the two isoforms in humans. It was therefore hypothesised that some form of functional divergence might also have occurred among the zebrafish eEF1A isoforms. To investigate this, a comparative analysis of zebrafish eEF1A was carried out using a similar approach to that described in the study by Soares *et al.*, 2009. A multiple sequence alignment of the zebrafish eEF1A protein (Figure 3.5) show the number of variant amino acid residues in eEF1A1L1 from eEF1A1A, eEF1A1B and eEF1A2 to be 37, 42 and 53 respectively, while eEF1A1A differ from eEF1A1B and eEF1A2 at 12 and 44 positions respectively out of 462 (for eEF1A1A/eEF1A1B) and 463 ( for eEF1A1A/eEF1A2). Also, eEF1A1B differ from eEF1A2 at 48 positions out of 463. The position and the residues present for each of the eEF1A proteins are summarised in appendix table 1, while figure 3.6 shows their location on the 3-D models. Alignment of the human eEF1A protein sequences together with the zebrafish eEF1A protein sequences show some variant residues to be wholly conserved, such that eEF1A1 from the two species have the same amino acid residue as do eEF1A2 from human and zebrafish at that same position. Zebrafish eEF1A1L1 which has no orthologue in human fall more in the eEF1A1 cluster at these positions than with the eEF1A2 orthologues, with eEF1A1L1 having the same amino acid as the eEF1A1 orthologues in 13 out of the 16 wholly conserved positions.

Published data obtained from the study of Soares *et al.* 2009 were then mapped onto the aligned sequences (Figure 3.5). These data include functional annotations, some of which have been confirmed *in vivo*, which shows translational and actin-related activities based on the yeast eEF1A protein. Yeast eEF1A shows high sequence identity with the zebrafish eEF1A proteins (~82% (eEF1A1L1), ~81% (eEF1A1A and eEF1A1B) and ~79% for eEF1A2) which is similar to both human eEF1A variants (~81%). Twenty six residues shown to be involved in the binding of the yeast eEF1A with the C-terminal of eEF1B $\alpha$  are highly conserved in the zebrafish eEF1A with only 2 (out of 26) variations for eEF1A1A, eEF1A1B and eEF1A2 and 1 (out of 26) variation for eEF1A1L1. The residues Ala76 and Val89 in yeast are substituted with Ser76 in eEF1A1A, eEF1A1B and eEF1A2 and Ile89 in all the zebrafish proteins.

However, these substitutions are conserved with the human proteins. Also, the equivalent residues involved in the binding of aminoacyl-tRNA in the zebrafish eEF1A, (His295, His296 and Arg322), are conserved in all the eEF1A variants. Similarly, residues Gly19, Lys20, Ser21, Thr22, Asn153, Lys154 and Asp156 which are shown to be essential for forming the guanine-binding pocket for GDP/GTP binding were also conserved. Three positions, 296, 329 and 333 (298, 331 and 335 in zebrafish eEF1A) demonstrated to bind actin through site mutagenesis studies in yeast are variable in the zebrafish eEF1A variants. Both 331 and 335 positions are also variable between the two human eEF1A variants. The eEF1A1 orthologues (and eEF1A1L1) have asparagine at position 331, while eEF1A2 orthologues have serine at this position. At position 335, eEF1A1A, eEF1A1B and eEF1A2 all have a glutamine residue as seen in human eEF1A2, while eEF1A1L1 shares the same methionine residue seen in human eEF1A1. Position 298 involved a non-conservative change of Ala298 in eEF1A1B and eEF1A1B (same as both human eEF1A variants) to Ser298 in eEF1A2 and eEF1A1L1.

eEfl1a1a	1	MGKEK	HINIVVIGHVDSGKSTTTGHLIYKCGGIDKRTIEKFEKEAAEMGKGSFKYAWVL
eEfl1a1b	1	MGKEK	HINIVVIGHVDSGKSTTTGHLIYKCGGIDKRTIEKFEKEAAEMGKGSFKYAWVL
eEfl1A1_HUMAN	1	MGKEK	HINIVVIGHVDSGKSTTTGHLIYKCGGIDKRTIEKFEKEAAEMGKGSFKYAWVL
eEfl1a2	1	MGKEK	HINIVVIGHVDSGKSTTTGHLIYKCGGIDKRTIEKFEKEAAEMGKGSFKYAWVL
eEfl1A2_HUMAN	1	MGKEK	HINIVVIGHVDSGKSTTTGHLIYKCGGIDKRTIEKFEKEAAEMGKGSFKYAWVL
eEfl1a111	1	MGKEK	HINIVVIGHVDSGKSTTTGHLIYKCGGIDKRTIEKFEKEAAEMGKGSFKYAWVL
eEfl1A_YEAST	1	MGKEK	HINIVVIGHVDSGKSTTTGHLIYKCGGIDKRTIEKFEKEAAEMGKGSFKYAWVL

eEfl1a1a	61	DKLKAERERGITIDISLWK	FETSKYYVTIIDAPGHRDFIKNMITGTSQADCAVLIVAAGV
eEfl1a1b	61	DKLKAERERGITIDISLWK	FETSKYYVTIIDAPGHRDFIKNMITGTSQADCAVLIVAAGV
eEfl1A1_HUMAN	61	DKLKAERERGITIDISLWK	FETSKYYVTIIDAPGHRDFIKNMITGTSQADCAVLIVAAGV
eEfl1a2	61	DKLKAERERGITIDISLWK	FETSKYYVTIIDAPGHRDFIKNMITGTSQADCAVLIVAAGV
eEfl1A2_HUMAN	61	DKLKAERERGITIDISLWK	FETSKYYVTIIDAPGHRDFIKNMITGTSQADCAVLIVAAGV
eEfl1a111	61	DKLKAERERGITIDISLWK	FETSKYYVTIIDAPGHRDFIKNMITGTSQADCAVLIVAAGV
eEfl1A_YEAST	61	DKLKAERERGITIDISLWK	FETSKYYVTIIDAPGHRDFIKNMITGTSQADCAVLIVAAGV

eEfl1a1a	121	GEFEAGISKNGQTR	EHALLAYTLGVKQLIVGVNKM	DSTEP	SY	SQKRYEEIVKEV	STYIKK
eEfl1a1b	121	GEFEAGISKNGQTR	EHALLAYTLGVKQLIVGVNKM	DSTEP	NY	SQKRYEEIVKEV	STYIKK
eEfl1A1_HUMAN	121	GEFEAGISKNGQTR	EHALLAYTLGVKQLIVGVNKM	DSTEP	PY	SQKRYEEIVKEV	STYIKK
eEfl1a2	121	GEFEAGISKNGQTR	EHALLAYTLGVKQLIVGVNKM	DSTEP	SY	SEKRYEEIVKEV	SAYIKK
eEfl1A2_HUMAN	121	GEFEAGISKNGQTR	EHALLAYTLGVKQLIVGVNKM	DSTEP	PY	SEKRYEEIVKEV	SAYIKK
eEfl1a111	121	GEFEAGISKNGQTR	EHALLAYTLGVKQLIVGVNKM	DSTEP	PY	SQARFEEITKEV	SAYIKK
eEfl1A_YEAST	121	GEFEAGISKNGQTR	EHALLAYTLGVKQLIVGVNKM	DSTEP	SY	SEKRYEEIVKEV	SAYIKK

eEfl1a1a	181	IGYNPD	TVAFVPI	SGWNGDN	MLEAS	PNM	SWFKGWK	ITRKEG	NAAG	TTLEALDA	IQPPTR	
eEfl1a1b	181	IGYNPD	TVAFVPI	SGWNGDN	MLEAS	PNM	SWFKGWK	ITRKEG	NAAG	TTLEALDA	IQPPTR	
eEfl1A1_HUMAN	181	IGYNPD	TVAFVPI	SGWNGDN	MLEAS	PNM	SWFKGWK	ITRKEG	NAAG	TTLEALDA	IQPPTR	
eEfl1a2	181	IGYSPAS	VFFVPI	SGWHGDN	MLEPSS	NMP	WFKGWK	LDLDRKE	HHAC	GVTTLEALD	TI	PPTR
eEfl1A2_HUMAN	181	IGYNPA	TVEFVPI	SGWHGDN	MLEPSS	NMP	WFKGWK	VERKEG	NAAG	SVLLEALD	TI	PPTR
eEfl1a111	181	IGYNPAS	VAFVPI	SGWHGDN	MLEAS	NM	WFKGWK	ITRKEG	NAAG	TTLLDALDA	IQPPSR	
eEfl1A_YEAST	179	VGYNPK	TVEFVPI	SGWNGDN	MLEAS	NM	WFKGWK	ITRKEG	NAAG	TTLEALDA	IQPPSR	

eEfl1a1a	241	PTDKPLRLPLQDVYK	IGGIGTVPVGRVETG	ILKPGMVVTFAPVNV	TTTEVKS	VEMHHEALS
eEfl1a1b	241	PTDKPLRLPLQDVYK	IGGIGTVPVGRVETG	ILKPGMVVTFAPVNV	TTTEVKS	VEMHHEALS
eEfl1A1_HUMAN	241	PTDKPLRLPLQDVYK	IGGIGTVPVGRVETG	ILKPGMVVTFAPVNV	TTTEVKS	VEMHHEALS
eEfl1a2	241	PTDKPLRLPLQDVYK	IGGIGTVPVGRVETG	ILRPGMVVTFAPVNV	TTTEVKS	VEMHHEALS
eEfl1A2_HUMAN	241	PTDKPLRLPLQDVYK	IGGIGTVPVGRVETG	ILRPGMVVTFAPVNV	TTTEVKS	VEMHHEALS
eEfl1a111	241	PTDKPLRLPLQDVYK	IGGIGTVPVGRVETG	ILKPGMVVTFAPVNV	TTTEVKS	VEMHHEALS
eEfl1A_YEAST	239	PTDKPLRLPLQDVYK	IGGIGTVPVGRVETG	ILKPGMVVTFAPVNV	TTTEVKS	VEMHHEALS

eEfl1a1a	301	EALPGDNVGFNVK	NSVKDIRRGNVAG	DSKNDPPQEAAN	F	TAQV	IILNHPGQIS	SAGYAPV
eEfl1a1b	301	EALPGDNVGFNVK	NSVKDIRRGNVAG	DSKNDPPQEAAN	F	TAQV	IILNHPGQIS	SAGYAPV
eEfl1A1_HUMAN	301	EALPGDNVGFNVK	NSVKDIRRGNVAG	DSKNDPPQEAAN	F	TAQV	IILNHPGQIS	SAGYAPV
eEfl1a2	301	EALPGDNVGFNVK	NSVKDIRRGNVAG	DSKSDPPQEAAN	F	TAQV	IILNHPGQIS	SAGYAPV
eEfl1A2_HUMAN	301	EALPGDNVGFNVK	NSVKDIRRGNVAG	DSKSDPPQEAAN	F	TAQV	IILNHPGQIS	SAGYAPV
eEfl1a111	301	EALPGDNVGFNVK	NSVKDIRRGNVAG	DSKNDPPQEAAN	F	TAQV	IILNHPGQIS	SAGYAPV
eEfl1A_YEAST	299	QGVPGDNVGFNVK	NSVKDIRRGNVAG	DSKNDPPQEAAN	F	TAQV	IILNHPGQIS	SAGYAPV

eEfl1a1a	361	LDCHTAHIACKFAEL	KEKIDRRSGKKLED	NP	PKSLKSGDAA	IVDMIPGKPMCVES	SFS	YPP
eEfl1a1b	361	LDCHTAHIACKFAEL	KEKIDRRSGKKLED	NP	PKSLKSGDAA	IVDMIPGKPMCVES	SFS	YPP
eEfl1A1_HUMAN	361	LDCHTAHIACKFAEL	KEKIDRRSGKKLED	NP	PKSLKSGDAA	IVDMIPGKPMCVES	SFS	YPP
eEfl1a2	361	LDCHTAHIACKFAEL	KEKIDRRSGKKLED	NP	PKSLKSGDAA	IVDMIPGKPMCVES	SFS	YPP
eEfl1A2_HUMAN	361	LDCHTAHIACKFAEL	KEKIDRRSGKKLED	NP	PKSLKSGDAA	IVDMIPGKPMCVES	SFS	YPP
eEfl1a111	361	LDCHTAHIACKFAEL	KEKIDRRSGKKLED	NP	PKSLKSGDAA	IVDMIPGKPMCVES	SFS	YPP
eEfl1A_YEAST	359	LDCHTAHIACKFAEL	KEKIDRRSGKKLED	NP	PKSLKSGDAA	IVDMIPGKPMCVES	SFS	YPP

eEfl1a1a	421	LGRFAVRDMRQT	VAVGVIK	VEKKT	TS	SGKVT	KSQAQAQ	AK
eEfl1a1b	421	LGRFAVRDMRQT	VAVGVIK	VEKKT	TS	SGKVT	KSQAQAQ	AK
eEfl1A1_HUMAN	421	LGRFAVRDMRQT	VAVGVIK	VEKKT	TS	SGKVT	KSQAQAQ	AK
eEfl1a2	421	LGRFAVRDMRQT	VAVGVIK	VEKKT	TS	SGKVT	KSQAQAQ	SSK
eEfl1A2_HUMAN	421	LGRFAVRDMRQT	VAVGVIK	VEKKT	TS	SGKVT	KSQAQAQ	AGK
eEfl1a111	421	LGRFAVRDMRQT	VAVGVIK	VEKKT	TS	SGKVT	KSQAQAQ	AK
eEfl1A_YEAST	419	LGRFAVRDMRQT	VAVGVIK	VEKKT	TS	SGKVT	KSQAQAQ	AK

**Figure 3.5. Multiple sequence alignment of the zebrafish and human eEF1A isoforms with the yeast eEF1A as a template.** Results of the alignment were shaded using BoxShade v3.21 where black, grey and white background indicates strictly conserved, conservative substituted or non-conserved regions respectively. Functional annotations obtained for yeast eEF1A is shown using different symbols. Domains are shown with filled rectangles, with domain I, II and III indicated with aqua, green and pink respectively. Circles show domain-domain contacts, with the red ● and yellow ● circles indicating conserved and non-identical residues respectively. Also shown on the yeast sequence are □; -residues in the disordered region of the yeast crystal structure, □ - involved in the binding of the C-terminal region of eEF1B $\alpha$ . Residues identified in yeast mutagenesis studies to be □-actin bundling/disorganisation, □-affect translational fidelity, □-reduce dependence on eEF1B $\alpha$ . \*- human eEF1A2 mutations which are completely conserved in the four zebrafish eEF1A isoforms. **Adapted from Soares *et al.* 2009.**

### 3.2.1.4 Variant residues analysis using the 3-D models of zebrafish, human and yeast eEF1A proteins

Functional analysis of the variant residues based on their position in the 3-D structure provides better insight than analysis of the linear sequence, especially when comparing highly homologous proteins. To this end, I constructed structural models of the zebrafish eEF1A proteins using the Modeller software through the Chimera interface (Pettersen *et al.*, 2004). The yeast eEF1A (1F60) structure was used as a template and the variant residues analysed further. As with yeast, all the zebrafish eEF1A proteins models are made up of three domains; domain I (1-240), domain II (241-336) and domain III (337-443). Residues at position 444-462 (463 for eEF1A2) are equivalent to the disordered residues of the yeast eEF1A and so were not included in the resulting models. The variant residues within the zebrafish eEF1A proteins are spread across the three domains. Six variable positions are found to be completely buried in all the eEF1A models. Positions 87 and 361 are conservative changes and are wholly conserved within orthologues, with eEF1A1L1 falling into the eEF1A1 group. Two other positions, 189 and 326, did not involve conservative substitutions but were also wholly conserved within the eEF1A and eEF1A2 orthologues, with eEF1A1L1 in the eEF1A1 group again. While eEF1A1L1 and eEF1A2 has the same residue as the yeast eEF1A at positions 118 and 151 respectively, the others have the same residues with both human eEF1A variants at these sites. Positions 216, 161 and 339 are found to be completely buried only in the zebrafish eEF1A1A, eEF1A1B and eEF1A2 modeled structures respectively. Position 216 involves a conservative change (Ile216 for eEF1A1L1, eEF1A1A and eEF1A1B, Leu261 for eEF1A2). On the other hand, changes at position 161 and 339 are not conservative, therefore the quality of the

packing properties of the residues was evaluated using the WHAT IF server (see section 2.2.10 in chapter 2). Asn161 (eEF1A1B) and Gly339 (eEF1A2) has a packing score of -1.1 and 0.6 respectively. Packing scores of -0.5 or lower indicates something is 'going on' with the packing quality of that residue. However, judging from the good packing scores, these residues likely fit into the protein interior and suggests that eEF1A1B and eEF1A2 do not have different domain structures from the other eEF1A variants.

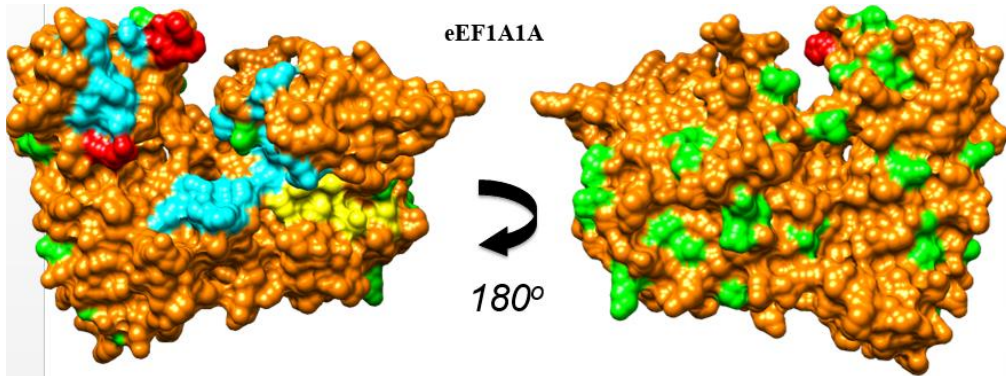
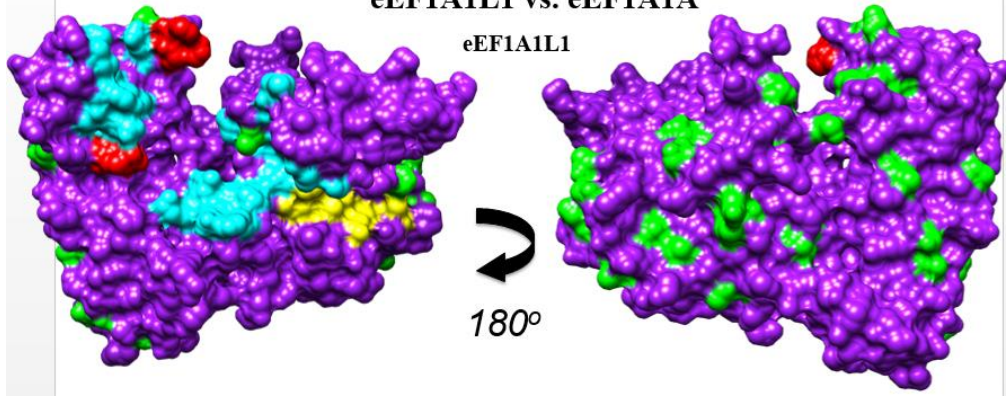
Existing structural data for the domain contacts for the yeast structure from the study of Soares *et al.* 2009 were also mapped on the multiple aligned sequences shown in figure 3.5. This showed 40 out of 42 residues involved in domain-domain contact to be absolutely conserved among the zebrafish eEF1A variants, yeast eEF1A and the two human eEF1A variants. Two positions; 335 and 417 (K333 and Glu415 in yeast) with residues that connects domain II and III are variable in zebrafish. It is worth mentioning that a two sequence insertion in vertebrate eEF1A isoforms relative to the yeast eEF1A is found between position 159 and 160 in the yeast eEF1A, thereby leading to a discrepancy in the numbering of residues after position 159. The glutamine residue is present at position 335 for eEF1A1A, eEF1A1B and eEF1A2 (same as human eEF1A2), while eEF1A1L1 has a methionine, as in human eEF1A1. Zebrafish eEF1A1A and eEF1A1B share the same residue (Glu417) with yeast (Glu415 in yeast) and a conservative change of aspartic acid (Asp417) is present in human eEF1A1. While eEF1A2 has Gln417, as in human eEF1A2, eEF1A1L1 is the only zebrafish variant with threonine at this position. However, the main-chain oxygen atom of all the variant residues at these two positions maintained their inter-domain H-bond interaction with the side-chains of residues Cys411 for residues at position 335 and Lys244 for position 417. This suggest that all the eEF1A proteins are predicted to have the same conformation as that seen in yeast, at least in the context of the eEF1B $\alpha$ -bound structure.

Similar to what is seen for human eEF1A isoforms, the majority of the variable residues between the zebrafish eEF1A isoforms are present on one side and show similar clustering arrangement as the variable amino acid between the human eEF1A isoforms (Figure 3.6). The Chimera software was then used to check if any of the positions containing variant amino acid residues were in close proximity (within 5Å)

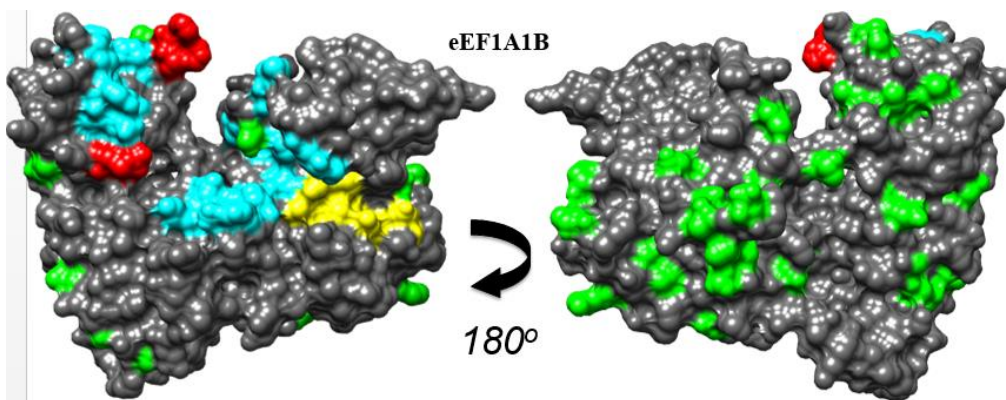
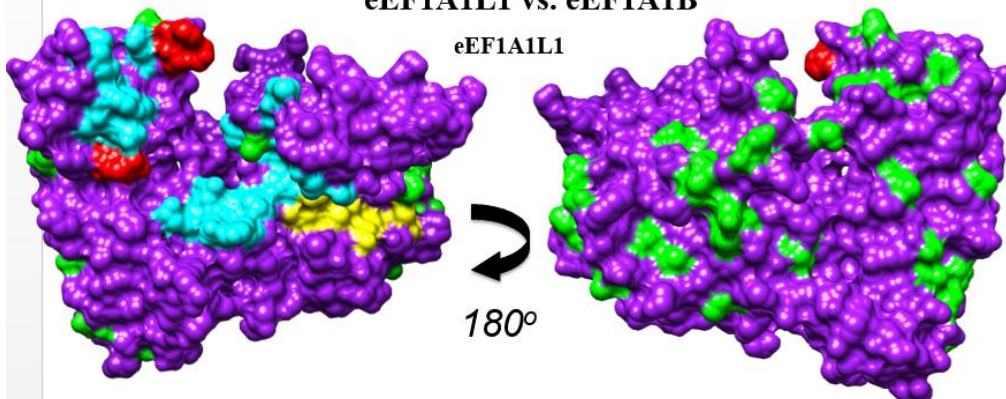
to some of the functional annotations shown in figure 3.4. Position 298, which involved a non-conservative change of Ala298 in eEF1A1A and eEF1A1B (same as both human eEF1A variants) to Ser298 in eEF1A2 and eEF1A1L1, was found to lie within 5Å of Glu293 and His296, (equivalent to yeast Glu291 and His294) which are involved in eEF1B $\alpha$  and aminoacyl-tRNA binding respectively. A double mutant form of yeast eEF1A with a H294A Q296R mutation (equivalent to position 296 and 298 in zebrafish eEF1A isoforms) was shown to promote actin cable formation when overexpressed in yeast cells but did not affect the total translation in the cells (Gross and Kinzy, 2007). Another variant position 355 which also entails a non-conservative substitution of Ala355 (eEF1A1A, eEF1A1B and both human eEF1A variants) with Ser355 (eEF1A2) and Gln355 (eEF1A1L1) lies within 5Å of Tyr357. The Tyr357 residue is equivalent to the yeast Tyr355 which is also implicated in actin-related functions in yeast (Gross and Kinzy, 2007). Tyr357 is also in close proximity with another variable position, 358. This position is wholly conserved within the eEF1A orthologues with Ala358 for the eEF1A family (and eEF1A1L1) and Ser358 for the eEF1A2 family in human and zebrafish. Position 326 close to Phe310 (equivalent to yeast eEF1A Phe308) also involved in actin organisation, is variable between eEF1A isoforms in the zebrafish (Ala326 in eEF1A1A, eEF1A1B and eEF1A1L1, Cys326 in eEF1A2 only) but is wholly conserved within the eEF1A orthologues in both species. Close to Asp156, one of the residues important for GDP/GTP binding, is another variant position, 197, which has Asn in eEF1A1A and eEF1AB (same as human eEF1A1) and His197 in eEF1A2 and eEF1A1L1 (as with human eEF1A2).



**eEF1A1L1 vs. eEF1A1A**

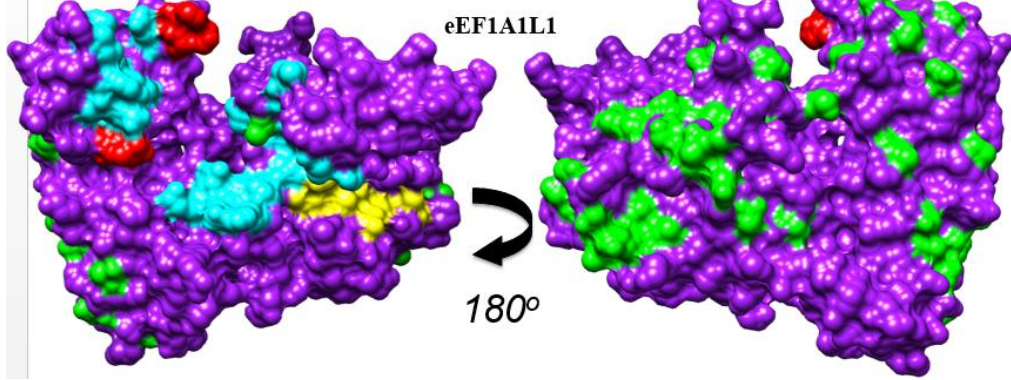


**eEF1A1L1 vs. eEF1A1B**

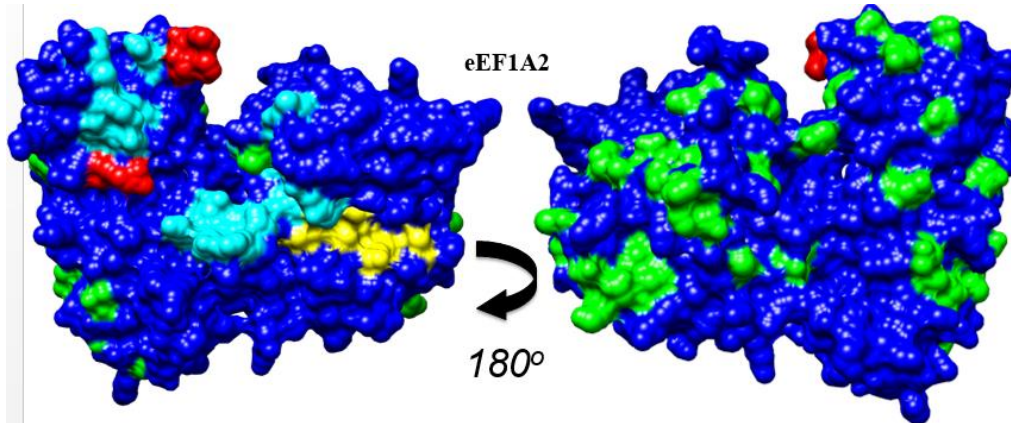




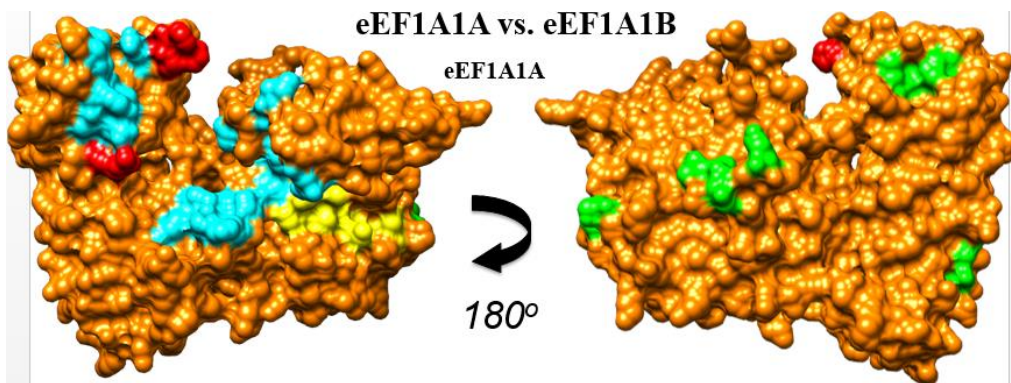
**eEF1A1L1 vs. eEF1A2**



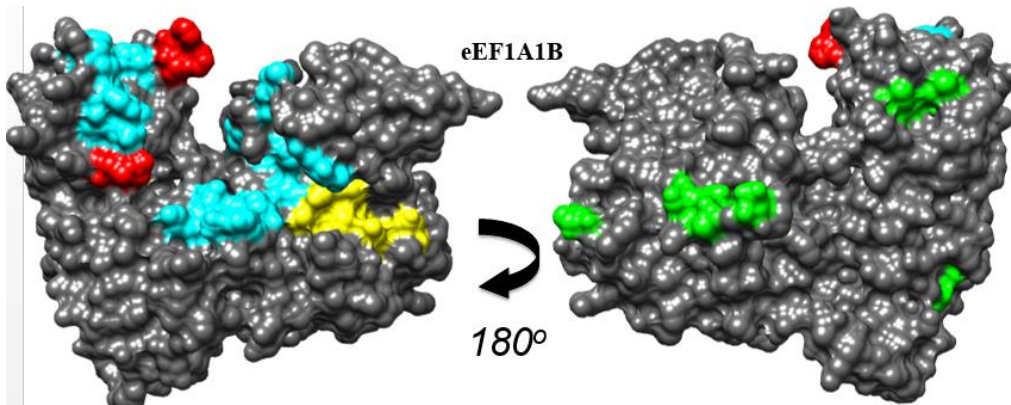
**eEF1A2**



**eEF1A1A vs. eEF1A1B**



**eEF1A1B**





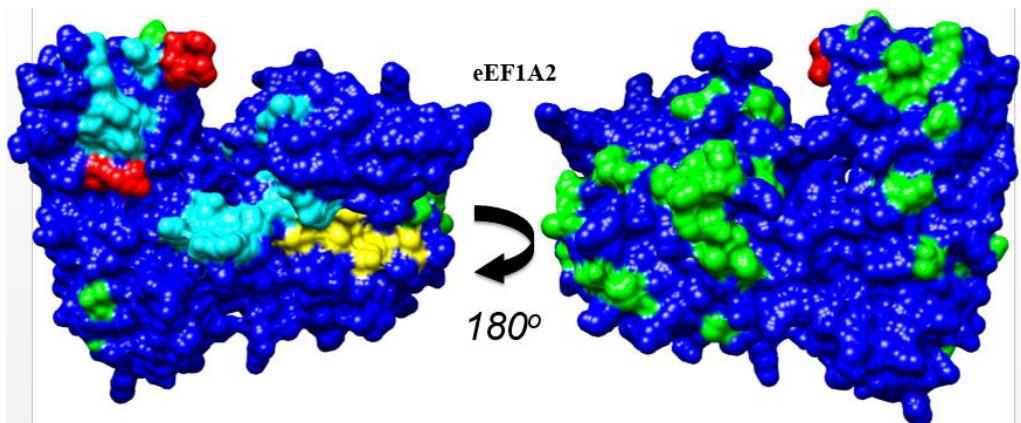
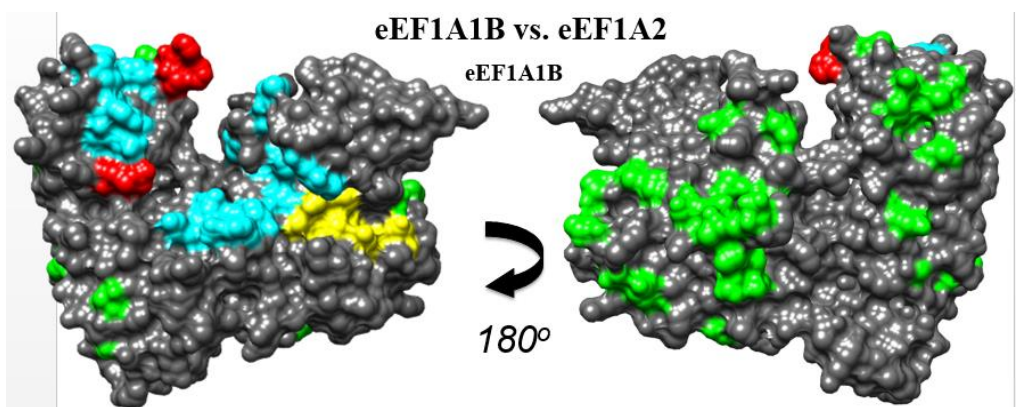
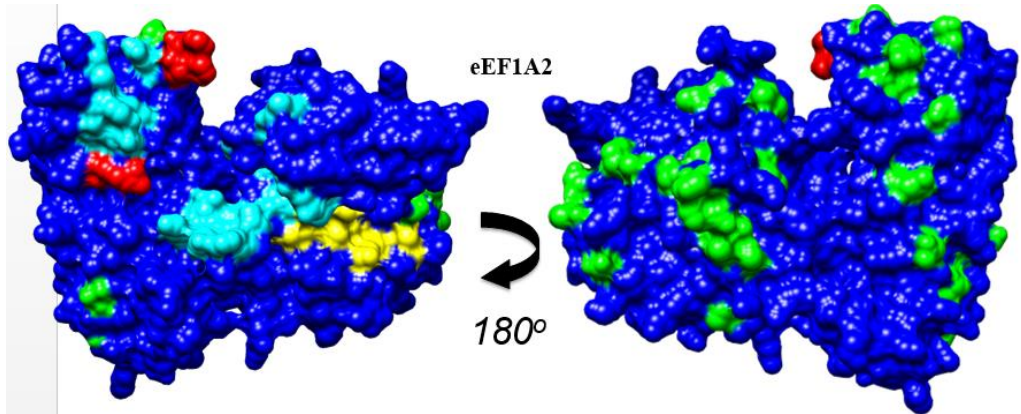
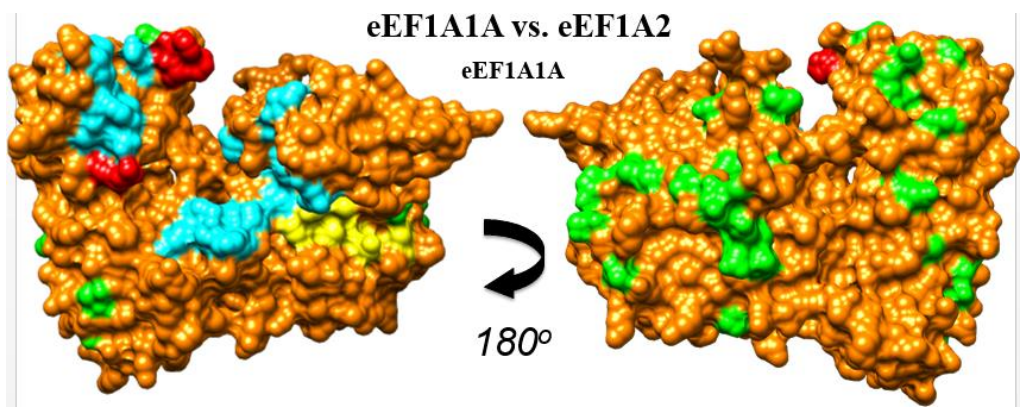


**Figure 3.6. Mapping of variant amino acids and known binding sites onto the surface of zebrafish eEF1A isoforms.** Two views rotated by 180° about the y-axis of the 3-D models of eEF1A1L1 (purple), eEF1A1A (orange), eEF1A1B (grey) and eEF1A2 (blue) shown with the location of exposed variant amino acids (green) mapped on the surface compared in a pairwise fashion. Also highlighted on the surface of the models are: location of the C-terminal eEF1B $\alpha$ -binding sites (cyan), GDP/GTP-binding sites (yellow) and aminoacyl-tRNA-binding residues (red). Residues His295 and Arg322 (equivalent to the yeast His293 and Arg320) are involved in both eEF1B $\alpha$  and aminoacyl-tRNA-binding but have been indicated as only aminoacyl-tRNA-binding residues and coloured red for the sake of clarity. Variant amino-acid present in the equivalent disordered region of the yeast eEF1A are not represented.

### 3.2.1.5 Prediction of phosphorylation sites in the zebrafish eEF1A variants

Protein phosphorylation is the most common type of post-translational modification used to regulate protein function in eukaryotic cells (Levy, Michnick and Landry, 2012). Phosphorylation is mediated by protein kinases which catalyses the transfer of the  $\gamma$ -phosphate from ATP to specific amino acids of the protein; which in eukaryotic cells are serine, threonine and tyrosine (Ubersax and Ferrell Jr, 2007). Interestingly, most of the differences between the zebrafish eEF1A proteins involved substitution of serine or threonine residues. Also, the tyrosine residues present at position 141 and 167 in eEF1A1A, eEF1A1B and eEF1A2 are substituted with phenylalanine in eEF1A1L1. This is similar to what was observed in the study by Soares *et al.*, 2009 in human eEF1A, although no change involved tyrosine in humans. Using an *in silico* approach, differential predicted phosphorylation profiles in human eEF1A1 and eEF1A2 were observed in their study. I therefore carried out a phosphorylation analysis of zebrafish eEF1A isoforms using the NetPhos 3.1 server (Blom, Gammeltoft and Brunak, 1999) (see section 2.2.10). The sequence of each variant was analysed using this server to identify likely serine, threonine or tyrosine residues that are phosphorylatable. A total of 27 out of 33 positions that involved change in serine or threonine residues within the eEF1A isoforms were predicted to be potential sites for phosphorylation. While 26 common phosphorylation sites were predicted, each eEF1A isoforms had their own specific predicted phosphorylation sites, with eEF1A2 having the most (12 in total). Seven out of nine residues which have been demonstrated experimentally to be phosphorylated in the human eEF1A variants are also predicted to be phosphorylatable in zebrafish (Figure 3.7). The isoform specific sites and the NetPhos prediction score for each position are shown in (Table 3.3). The higher the NetPhos score, the more likely that the predicted site is a true phosphorylation site. Some other predicted sites were shared by two or more of the eEF1A variants. Also,

one of the Tyr that was lost in eEF1A1L1 was predicted to be a phosphorylation site in eEF1A1A, eEF1A1B and eEF1A2 at position 167. The NetPhos score was high indicating Tyr167 to likely be a true phosphorylation site with eEF1A1A and eEF1A1B having a score of 0.659 and a higher score of 0.931 in eEF1A2. Also, worth noting is the high NetPhos score, >0.90 for all the four predicted eEF1A1B-specific sites indicating these sites are most likely true phosphorylation sites. The variant-specific residues and Tyr167 predicted as phosphorylation sites were present on the surface of the modeled structures except for Tyr183 (eEF1A1L1) and Tyr85 (eEF1A2). However, they all have their hydroxyl groups exposed (Figure 3.8) suggesting they are accessible to a kinase which is required for phosphorylation to occur. Although these prediction results will need to be validated, it provides preliminary findings that suggest the zebrafish eEF1A isoforms might be chemically different which will imply they may have some functional differences.

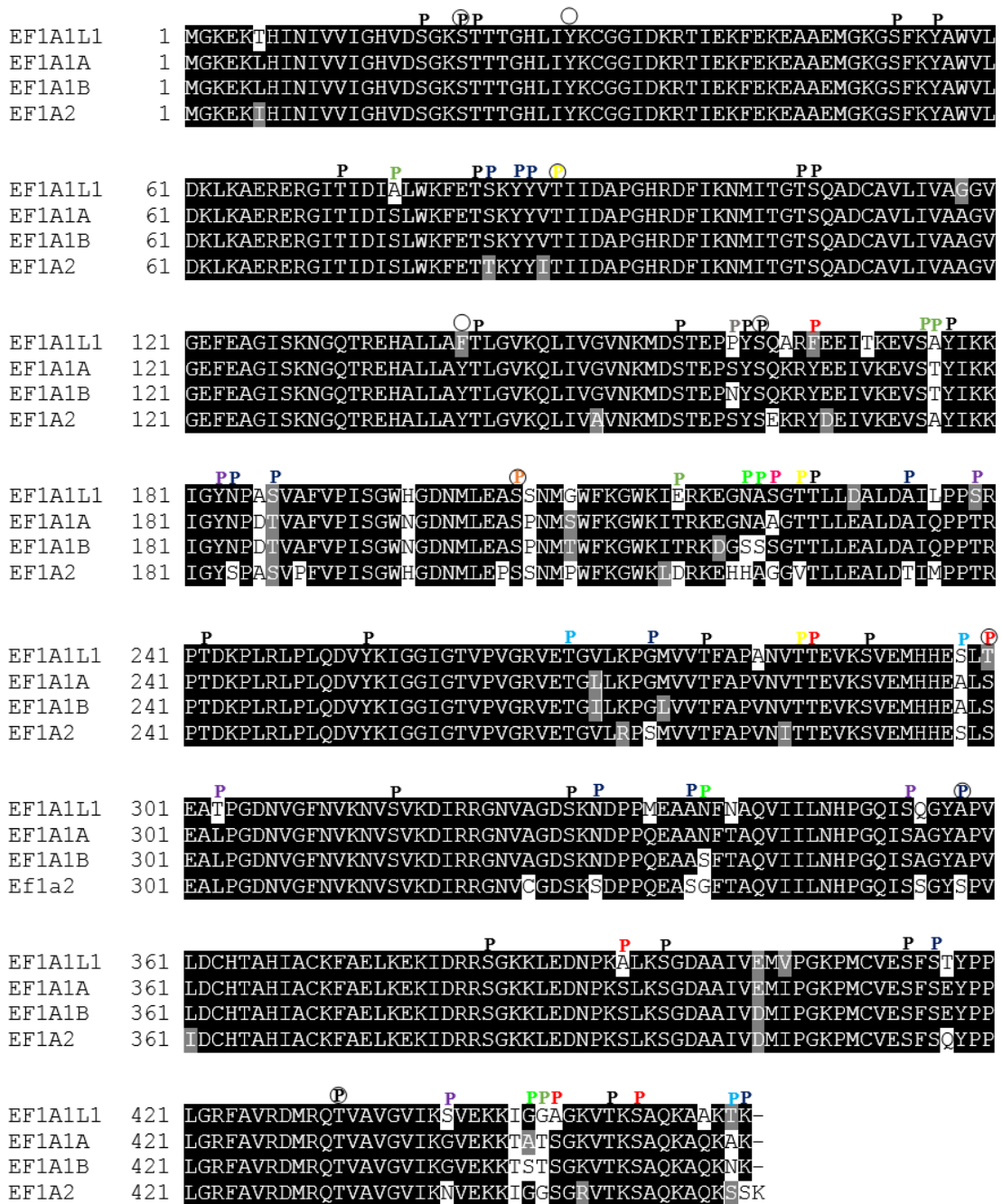


**Figure 3.7. Sequence alignment showing predicted phosphorylation sites for zebrafish eEF1A proteins.** Phosphorylation sites are indicated with P, colour coded according to variants. P = all eEF1A variants, P = eEF1A1L1-specific, P = eEF1A1A-specific, P = eEF1A1B-specific, P = eEF1A2-specific, P = eEF1A1L1, eEF1A1A and eEF1A1B, P = eEF1A1A and eEF1A1B, P = eEF1A1B and eEF1A1L1, P = eEF1A1A, eEF1A1B and eEF1A2, P = eEF1A1A and eEF1A2, P = eEF1A1L1 and eEF1A2. Equivalently positioned positions of the experimentally validated phosphorylated residues of the human eEF1A variants are denoted with black circles (see Table 1.1).

**Table 3.3: Predicted isoform-specific phosphorylation sites in zebrafish eEF1A proteins**

<b>Protein</b>	<b>Residue</b>	<b>Position</b>	<b>NetPhos Score</b>
<b>eEF1A1L1</b>	Tyrosine	183	0.544
	Serine	239	0.515
	Threonine	303	0.835
	Serine	354	0.522
	Serine	440	0.663
<b>eEF1A1A</b>	Serine	205	0.506
<b>eEF1A1B</b>	Serine	222	0.991
	Serine	223	0.964
	Serine	339	0.924
	Serine	440	0.932
<b>eEF1A2</b>	Threonine	83	0.541
	Tyrosine	85	0.586
	Tyrosine	86	0.509
	Serine	184	0.649
	Serine	187	0.567
	Threonine	234	0.660
	Serine	275	0.976
	Serine	331	0.558
	Serine	338	0.538
	Serine	358	0.881
	Serine	416	0.633
	Serine	462	0.576



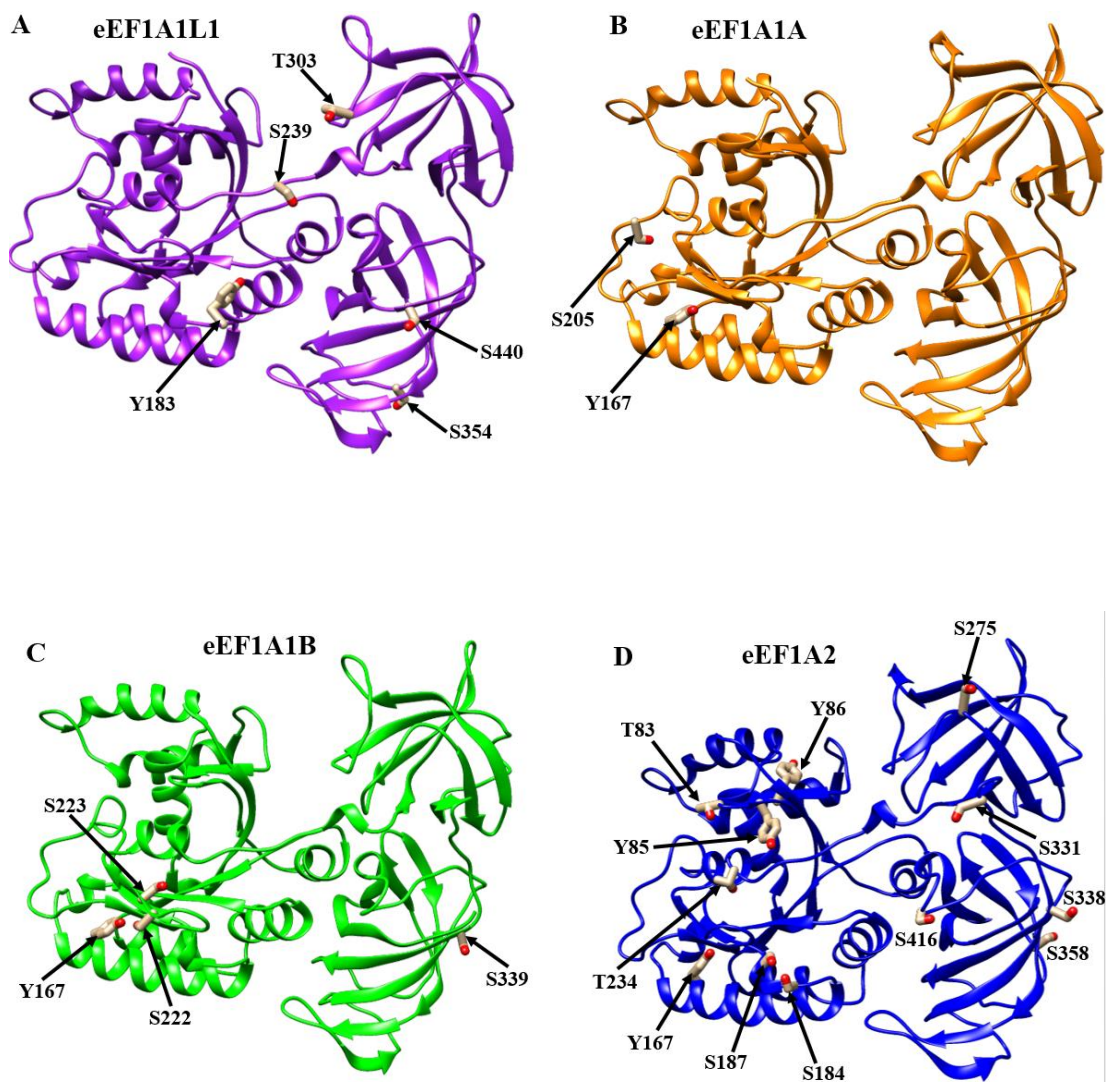


**Figure 3.8. Location of isoform-specific potential phosphorylation sites on the 3-D structure of the zebrafish eEF1A protein.** Ribbon representation of the 3-D model of zebrafish eEF1A isoforms showing predicted phosphorylation sites (side-chain of the residues at this sites are depicted with stick representation) calculated using the NetPhos 3.1 server (Blom, Gammeltoft and Brunak, 1999) specific for **A.** eEF1A1L1 (purple) **B.** eEF1A1A (orange) **C.** eEF1A1B (green) and **D.** eEF1A2 (blue). Ser-462 is not shown on eEF1A2 structure as it present within the equivalent disordered region in the yeast eEF1A structure. Predicted phosphorylated tyrosine residue at position 167 which is lost in eEF1A1L1 is also shown on the ribbon structure of eEF1A1A, eEF1A1B and eEF1A2 models.

### **3.2.2 Expression analysis of *eef1a* isoforms during zebrafish development and adult tissues**

To investigate the expression pattern and functional relationships of *eef1a* in zebrafish, I evaluated the expression of the four *eef1a* homologues during embryonic development and in various adult tissues. I performed both RT-PCR and quantitative PCR analyses on cDNA generated from RNA isolated from different developmental stages and adult tissues. At first, specific primers for each *eef1a* gene suitable for qRT-PCR were designed and their specificity were confirmed from results obtained from sequencing RT-PCR products amplified from whole adult fish (data not shown).

#### **3.2.2.1 Expression of *eef1a* isoforms during development**

Twelve different stages during embryogenesis and early development in zebrafish, namely 1-cell, 2-cell, 4-cell, 8-cell, 16-cell, 256-cell, high, 50%-epiboly, 90%-epiboly, 24 hours post-fertilisation (hpf), 48 hpf and 72 hpf stages, were analysed for *eef1a* mRNA using conventional RT-PCR (Figure 3.9). Expression of *eef1a111* was detected at all developmental stages analysed, including the one-cell zygotic stage, suggesting *eef1a111* is also maternally expressed. Expression of the other three *eef1a* genes, *eef1a1a*, *eef1a1b* and *eef1a2*, did not show any maternal expression as they were not detected during the early embryonic stages analysed from the one-cell to the 90%-epiboly stage which begins 9 hpf. Expression of *eef1a1a* and *eef1a1b* were detected at the 24 hpf, 48 hpf and 72 hpf developmental stages. While it cannot be concluded on which developmental stage *eef1a1a* and *eef1a1b* were first expressed, an increment in their expression level could be seen between 24 hpf and 48 hpf (Figure 3.9B), and it could be possible it is around the 24 hpf stage, rather than a stage much closer to the 90%-epiboly stage, that expression of these genes is induced. The *eef1a2* gene is first expressed at 48 hpf, being the last *eef1a* gene to be detected during development in the zebrafish.

To identify the expression pattern of *eef1a* genes during 24 hpf, 48 hpf and 72 hpf developmental stages, I performed whole-mount *in situ* hybridisation (ISH) using digoxigenin (DIG)-labelled antisense RNA probes to mark *eef1a*-expressing regions and DIG-labelled sense RNA probes as a control to check signal specificity (Figure 3.10). Probes for each *eef1a* gene were designed from the 3'UTR region of the gene



where there is maximum sequence difference between the genes. This helps to avoid cross-hybridisation further ensuring specificity of the hybridisation reaction. The WISH experiment for *eef1a111* showed that it is widely expressed from the head to the trunk at 24 hpf. At 48 hpf, its expression is enriched in the developing brain of the fish but is then reduced at 72 hpf and shows a more localised expression pattern with strong signal observed in the eye and tectum in the larva (Figure 3.10A). Simultaneous hybridisation with DIG-labelled sense RNA probe for all three stages was also performed and did not produce any signal and the fish remained clear (data shown for only 48 hpf embryo). For *eef1a1a*, *eef1a1b* and *eef1a2* (48 and 72 hpf), I was unable to obtain a clear expression pattern, likely as a result of low transcript levels, as a longer incubation time of a minimum of 10 hours was required when analysed. Although background signal was produced with the sense probe, some difference in the staining intensity around the head region can be seen with staining with the antisense probe being more pronounced than the sense probe. However, further optimisation of the hybridisation parameters for these probes would be required to obtain a much clearer spatial expression pattern for *eef1a1a*, *eef1a1b* and *eef1a2* genes.

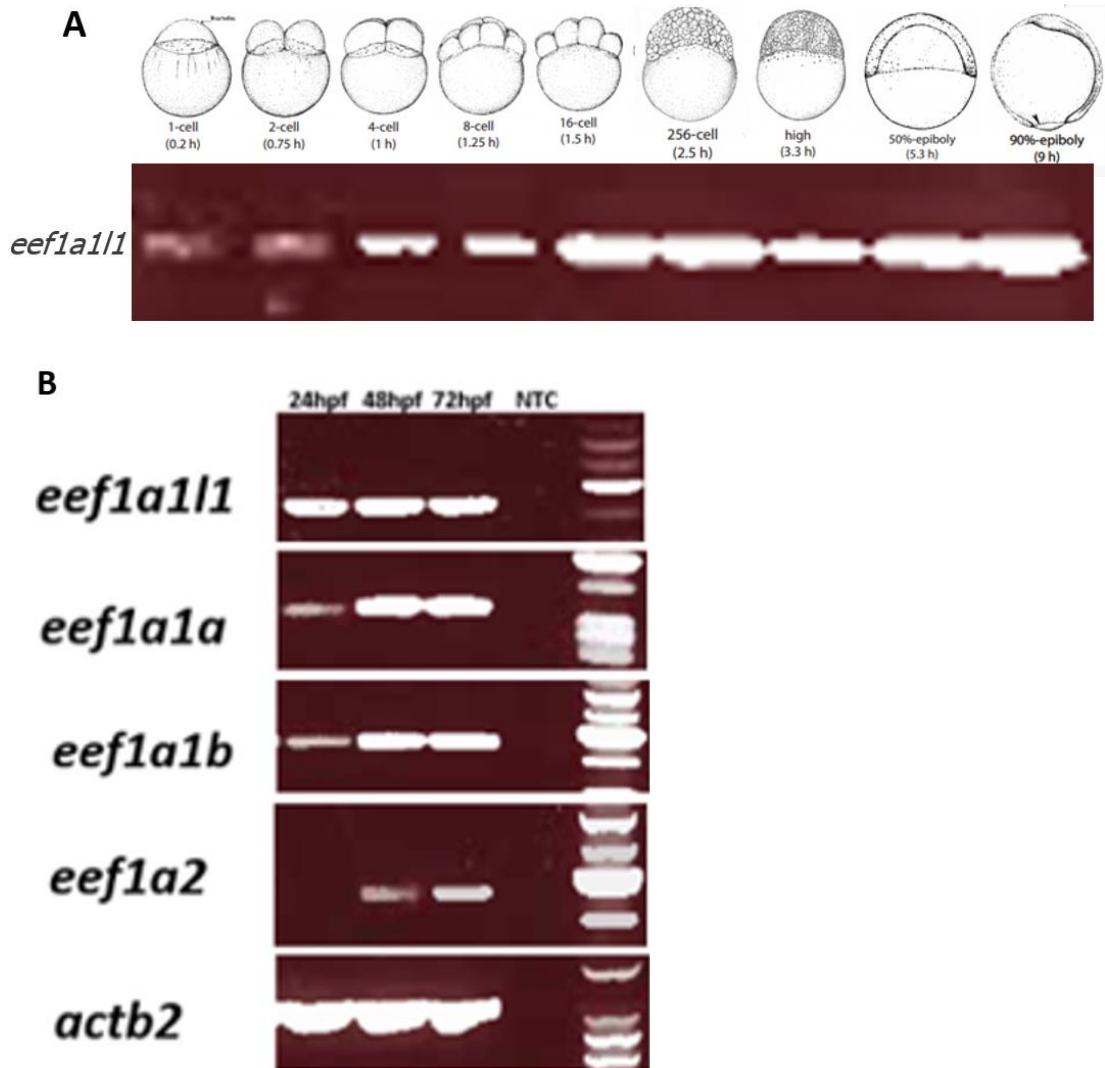
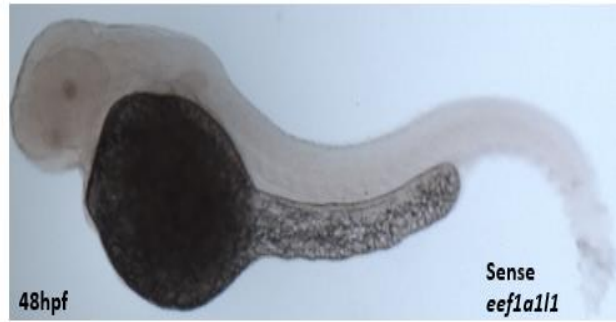
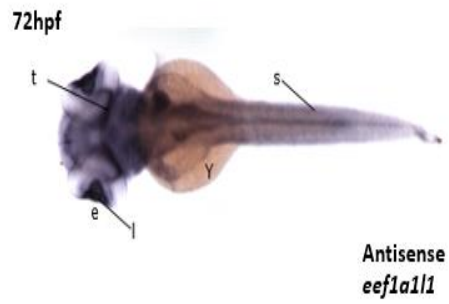
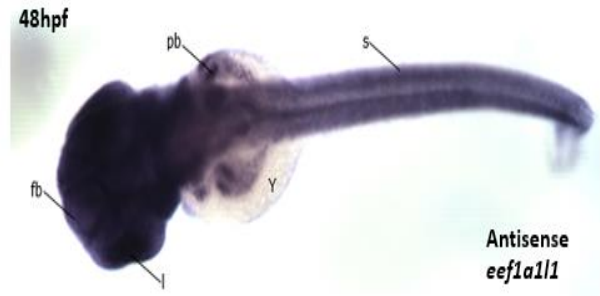
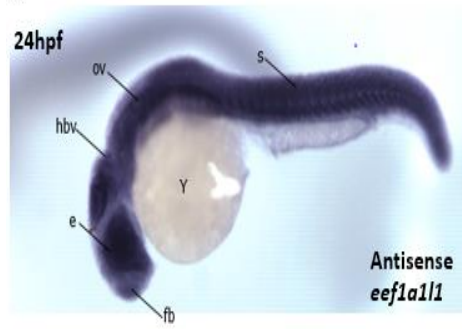
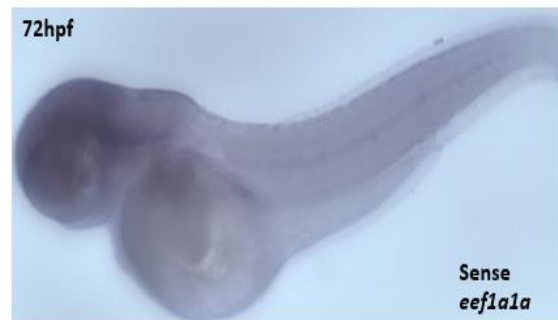
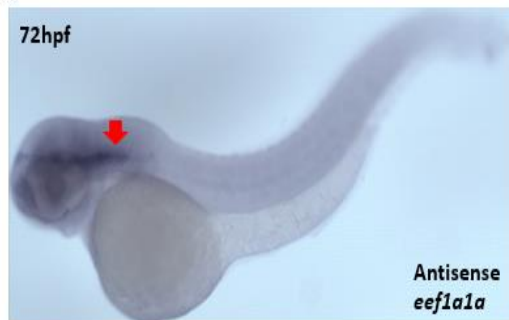


**Figure 3.9. Expression of *eef1a* genes during zebrafish development assayed by RT-PCR. A.** Gel pic showing expression of *eef1a1l1* in 1-cell, 2-cell, 4-cell, 8-cell, 16-cell, 256-cell, high, 50%-epiboly and 90%-epiboly embryonic stages. The other *eef1a* genes were undetected at these stages (data not shown). **B.** mRNA expression of *eef1a* in 24, 48 and 72 hpf stages. *eef1a1l1* was detected in all stages while *eef1a1a* and *eef1a1b* were detected in 24 and 48 hpf. *eef1a2* was the last isoform to be expressed during development at 48 hpf. As a loading control, expression of actin was also assessed in the same samples. RT-PCR was performed and gel run in duplicates using samples from the same cDNA. NTC – no template control.

**A**



**B**



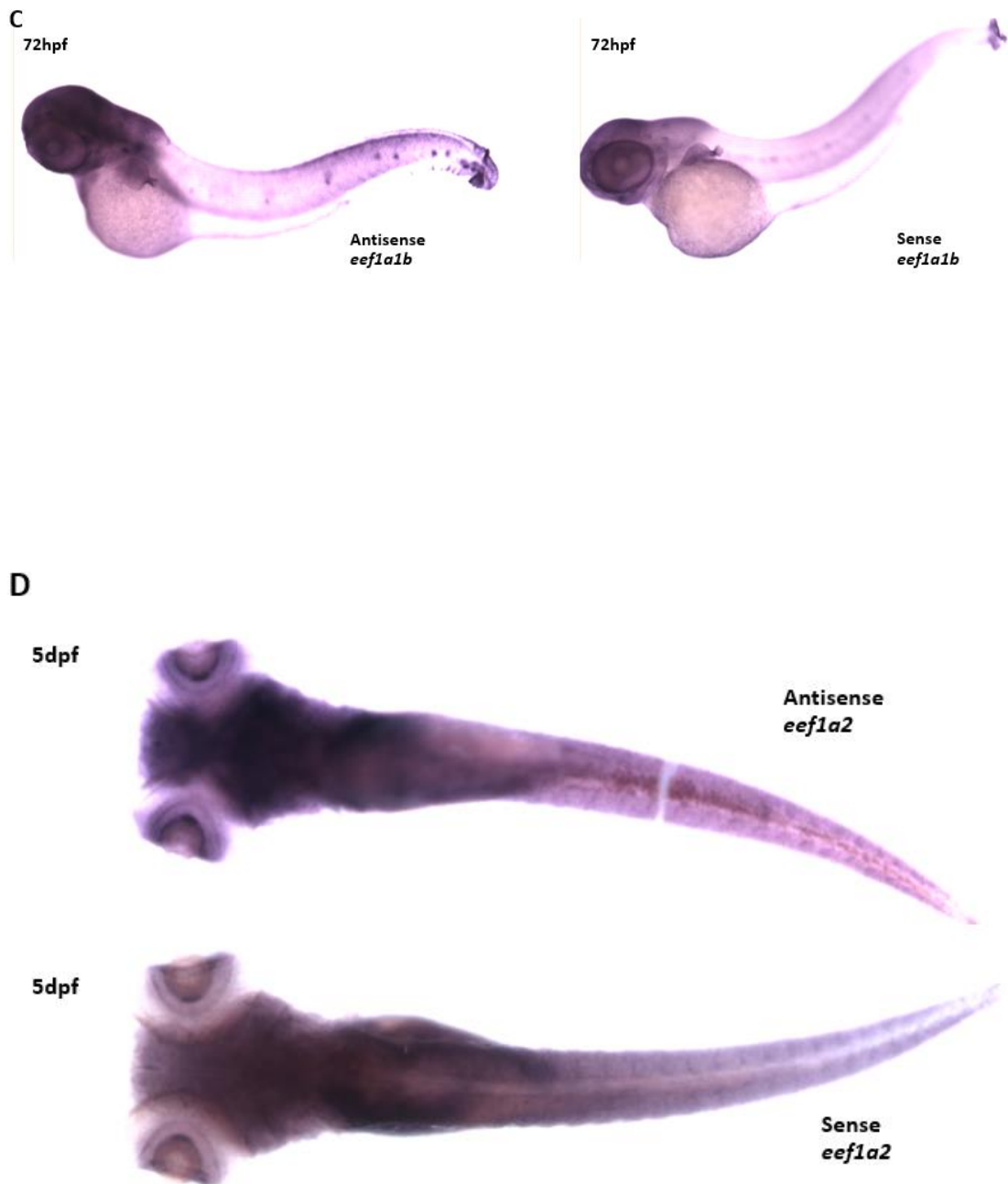


**Figure 3.10. Whole-mount *in situ* hybridisation analysis of *eef1a* expression in different developmental stages in zebrafish.** Expression of eEF1A mRNA was analysed at the indicated developmental stages **A**. At 24 hpf, *eef1a111* is expressed in the whole embryos and is then enriched in the brain at 48 hpf. At 72 hpf, its expression becomes more localised and is noticeable in the eyes and tectum of the larva. A representative larva hybridised with the sense probe do not show any staining indicating the *eef1a111* anti-sense probes are specific. **B-C**. Expression of *eef1a1a* and *eef1a1b* at 72 hpf. **D**. Expression of *eef1a2* at 5 dpf. Abbreviations: E- eye, fb- forebrain, hbv- hindbrain ventricle, l- lens, ov- otic vesicle, pb- pectoral fin bud, s- somite, t- tectum, y- yolk.

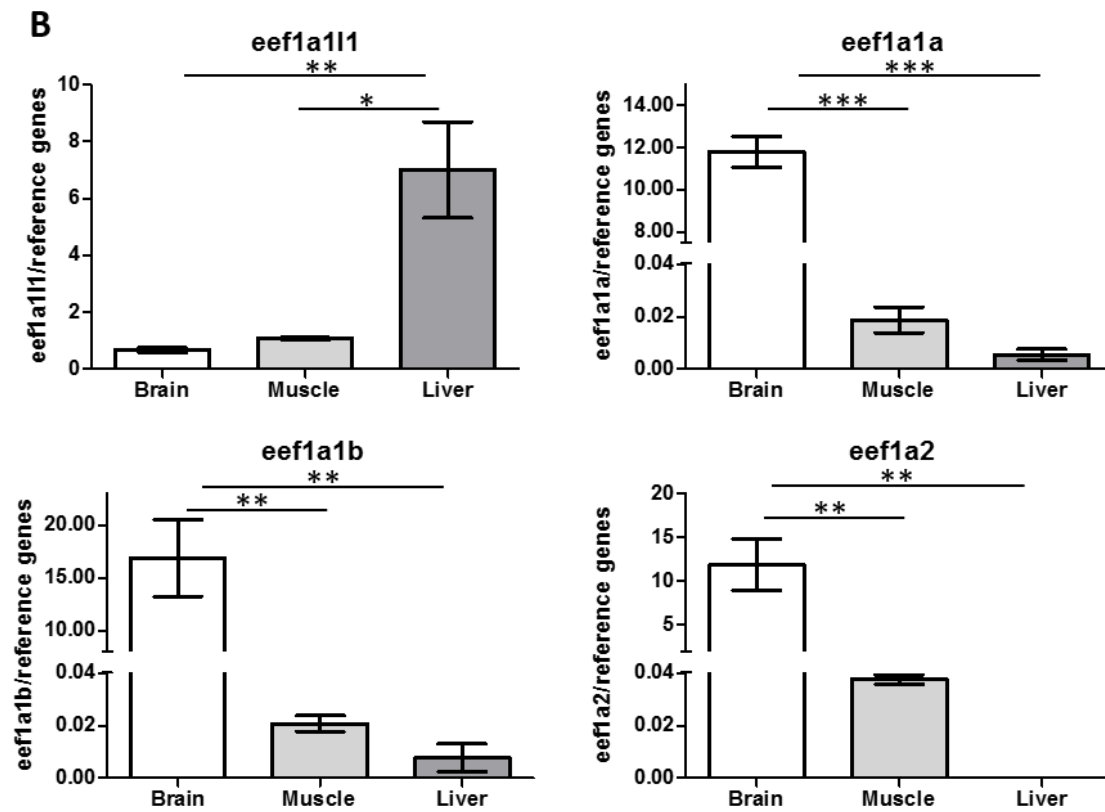
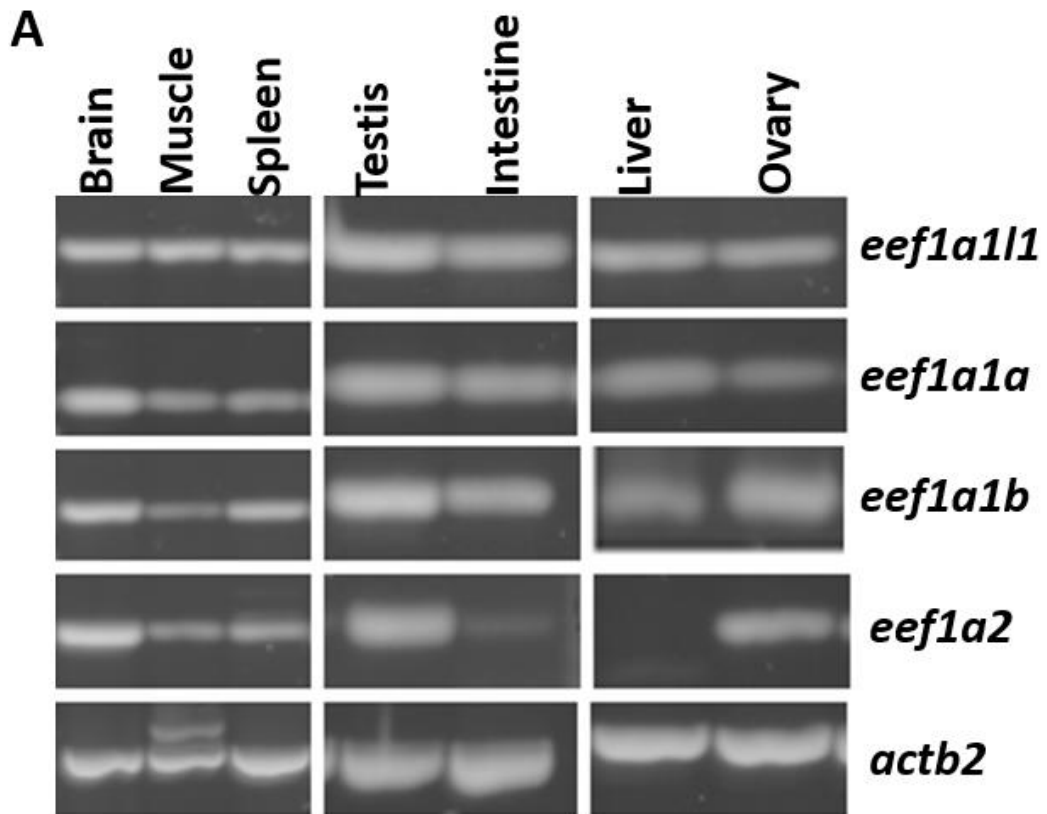
### 3.2.2.2 Expression of *eef1a* isoforms in adult tissues

Expression of all four *eef1a* genes in adult tissues was examined in total RNA isolated from brain, muscle, spleen, testis, intestine, liver and ovary by conventional RT-PCR analysis (Figure 3.11A). Three *eef1a* genes, *eef1a111*, *eef1a1a* and *eef1a1b*, were detected in all the adult tissues examined. Expression of *eef1a2* is readily observed in brain, muscle, spleen, testis and ovary tissues but only just detectable in the intestine. No expression is observed in liver for *eef1a2*.

Using q-PCR, I quantified the expression levels of the *eef1a* transcripts in adult brain, muscle and liver tissues with prevalidated primers designed by Primerdesign. Simultaneous detection of *ATPsynth*, *NADH* and *16S* expression was performed to be used as reference genes. Expression of these three genes were shown to be stable when measured in a representative set of cDNA samples from brain, muscle and liver tissues using the geNorm kit (Primerdesign, UK) (see Appendix figure 1). The geNorm analysis software ranks candidate reference genes by the stability measure M, where a lower M value indicates a more stable gene. A set of the three reference genes with the lowest M values were used to ensure accurate quantification of the *eef1a* transcripts in the tissues analysed. Each of the *eef1a* genes was normalised by the geometric mean of *ATPsynth*, *NADH* and *16S* to obtain their transcripts expression levels in the brain, muscle and liver tissues. Similar to the RT-PCR results, *eef1a111*, *eef1a1a* and *eef1a1b* are found in the brain, muscle and liver while *eef1a2* is only detected in the brain and muscle. However, the *eef1a* genes are not present in equal amount in the tissues in which they were detected. Expression of *eef1a111* is significantly higher in liver when compared with brain and muscle ( $p < 0.01$  for brain and  $p < 0.05$  for muscle, one-way ANOVA). On the other hand, *eef1a1a*, *eef1a1b* and *eef1a2* show similar expression level patterns with a higher expression level in brain tissue than in muscle and liver (in the case of *eef1a1a* and *eef1a1b*) tissues (Figure 3.11B).

The relative transcript levels of the four *eef1a* genes vary substantially across the three tissues examined above (Figure 3.11C). As a whole, *eef1a111* transcripts are the most abundant with about 7,980, 7,830 and 240-fold higher overall expression ratios than *eef1a1a*, *eef1a1b* and *eef1a2* respectively. However, expression levels of all the *eef1a* transcripts are similar in brain tissue with the higher expression level of *eef1a111* transcripts observed in the muscle (1,040, 1,280 and 490-fold higher than *eef1a1a*,

*eef1a1b* and *eef1a2* respectively) and liver (22,900 and 22,200-fold higher in *eef1a1a* and *eef1a1b* respectively) tissues. The expression level of *eef1a2* transcripts in muscle tissue is approximately two and three-fold higher than that of *eef1a1a* and *eef1a1b* respectively, both of which show similar expression levels in all three tissues examined.



C

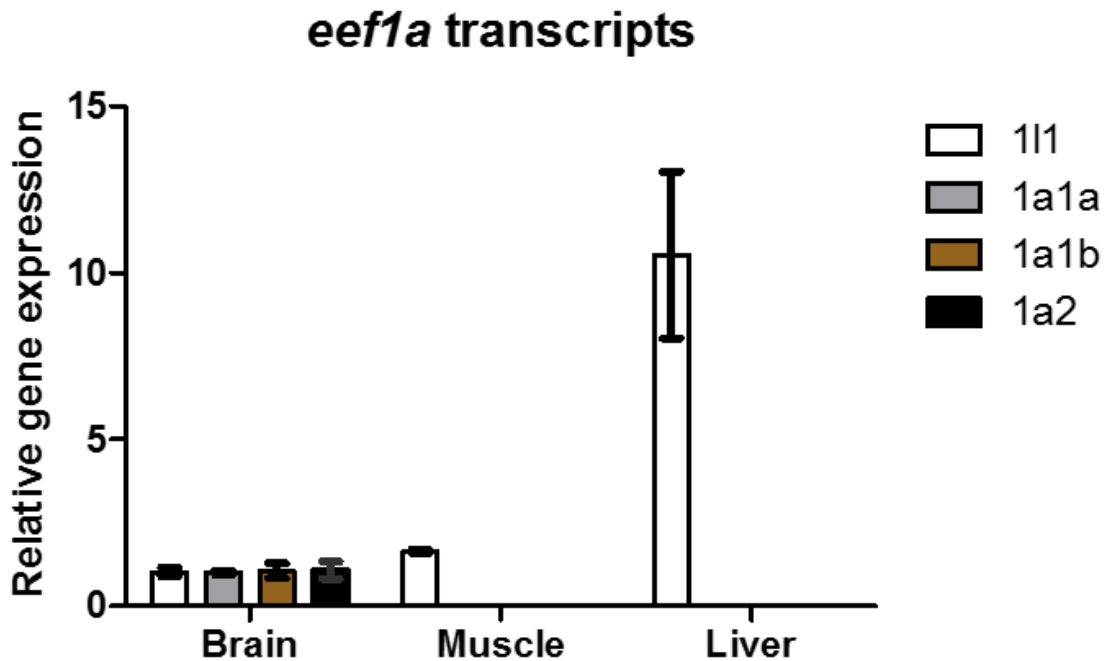


**Figure 3.11. Expression analysis of the four *eef1a* genes in adult tissues.** **A.** Expression of *eef1a1l1*, *eef1a1a*, *eef1a1b* and *eef1a2* in various adult tissues detected by RT-PCR. *eef1a1l1*, *eef1a1a* and *eef1a1b* are expressed in all the tissues analysed, while *eef1a2* is expressed in all the tissues except liver. As a loading control, expression of actin was also assessed in the same samples. RT-PCR was performed and gel run in duplicates using samples from the same cDNA. For each gene, -RT controls were included for all analysed tissues and showed no amplification. **B.** Expression levels of *eef1a* in brain, muscle and liver tissues. Data are presented as the expression levels normalised to the geometric mean of *ATPsynth*, *NADH* and *16S*. Results are means  $\pm$  S.E.M.; n=3 in each group. Asterisk show where there is a significant difference in transcript expression levels in the tissues (\* $p \leq 0.05$ , \*\* $p \leq 0.01$  and \*\*\* $p \leq 0.0001$ , one-way ANOVA) **C.** Comparison of the relative expression levels of *eef1a* transcripts in brain, muscle and liver tissues. Results are presented as the gene expression ratio of the target mRNA to the geometric mean of *ATPsynth*, *NADH* and *16S* for each tissue (means  $\pm$  S.E.M.; n=3).



### 3.2.2.3 Analysis of eEF1A2 antibodies specificity

Detection of *eef1a* mRNA expression does not necessarily indicate they are translated into stable proteins, especially given the findings of Newbery *et al.* 2011 which shows the expression of eEF1A in *Xenopus* to be regulated at the post-transcriptional level. It is therefore essential to be able to analyse expression of *eef1a* at the protein level in zebrafish. Using the available eEF1A2 antibodies, I investigated the expression of zebrafish eEF1A2 further. One in-house generated eEF1A2 antibody (hereafter referred to as eEF1A2-2) and three commercial antibodies against eEF1A2 were tested. The eEF1A2-2 antibody has previously been shown in our laboratory to be specific for mouse and *Xenopus* eEF1A2. Protein extracts from zebrafish and mouse brain, muscle and liver tissues were used to perform western blot following the method described in Newbery *et al.* 2011 and probed for eEF1A2 using the eEF1A2-2 antibody. A band was observed in protein lysates obtained from adult zebrafish and mouse liver tissues which were used as a negative control. This suggests a cross-reactivity of the antibody with other eEF1A variants, since eEF1A2 is not expressed in the liver in both species. It is worth mentioning that a different batch of eEF1A2-2 which had been purified by precipitation with ammonium sulphate only was used since the affinity purified eEF1A2-2 that was demonstrated to be specific in our laboratory was unavailable. This could explain why the lack of specificity of eEF1A2-2 was observed in my hands. Specificity of the three commercial antibodies (hereafter referred to as eEF1A2-Genetex, eEF1A2-Proteintech and eEF1A2-Abcam) were also tested using protein extracts from adult zebrafish brain, liver and muscle tissues. Since *eef1a2* expression was not detected at the mRNA level in the liver, it was used as a negative control while the muscle tissue from mouse which is known to express only eEF1A2 was used as a positive control. A band of the correct size was observed in the liver for both eEF1A2-Genetex and eEF1A2-Proteintech antibodies, suggesting these antibodies were not specific for eEF1A2 alone.

No band was recognised in the liver by eEF1A2-Abcam (Figure 3.12A) and it was then used to investigate the expression of eEF1A2 in different zebrafish tissues. Contrary to the findings of eEF1A2 expression at the mRNA level, no signal was detected for the muscle. No band was also observed in the other tissues: intestine, ovaries and heart which showed mRNA expression of eEF1A2 using eEF1A2-Abcam

antibody (data not shown). While a signal was readily detected in the brain, longer exposure time of about 30 minutes was required to produce a signal in the spinal cord using eEF1A2-Abcam antibody. To confirm the absence of a signal in the muscle was not due to the low abundance of *eef1a2* mRNA based on the qPCR results, protein extracts from muscle tissues at concentrations of 20 $\mu$ g, 30 $\mu$ g, 40 $\mu$ g and 50 $\mu$ g were probed with eEF1A2-Abcam antibody. No signal was observed even when the blot was exposed overnight during the detection process. Simultaneous probing of samples from the same muscle extract was carried out using an antibody against the zebrafish eEF1A (now known as eEF1A1L1) from GeneTex, anti-Ef1a (Figure 3.12B). A band was readily observed in the muscle samples at all concentrations. Bearing in mind that the specificity of the antibody for zebrafish has not been tested and also that there is no expression data available for the zebrafish eEF1A2 protein, it is important that validation of the eEF1A2-Abcam antibody be performed.

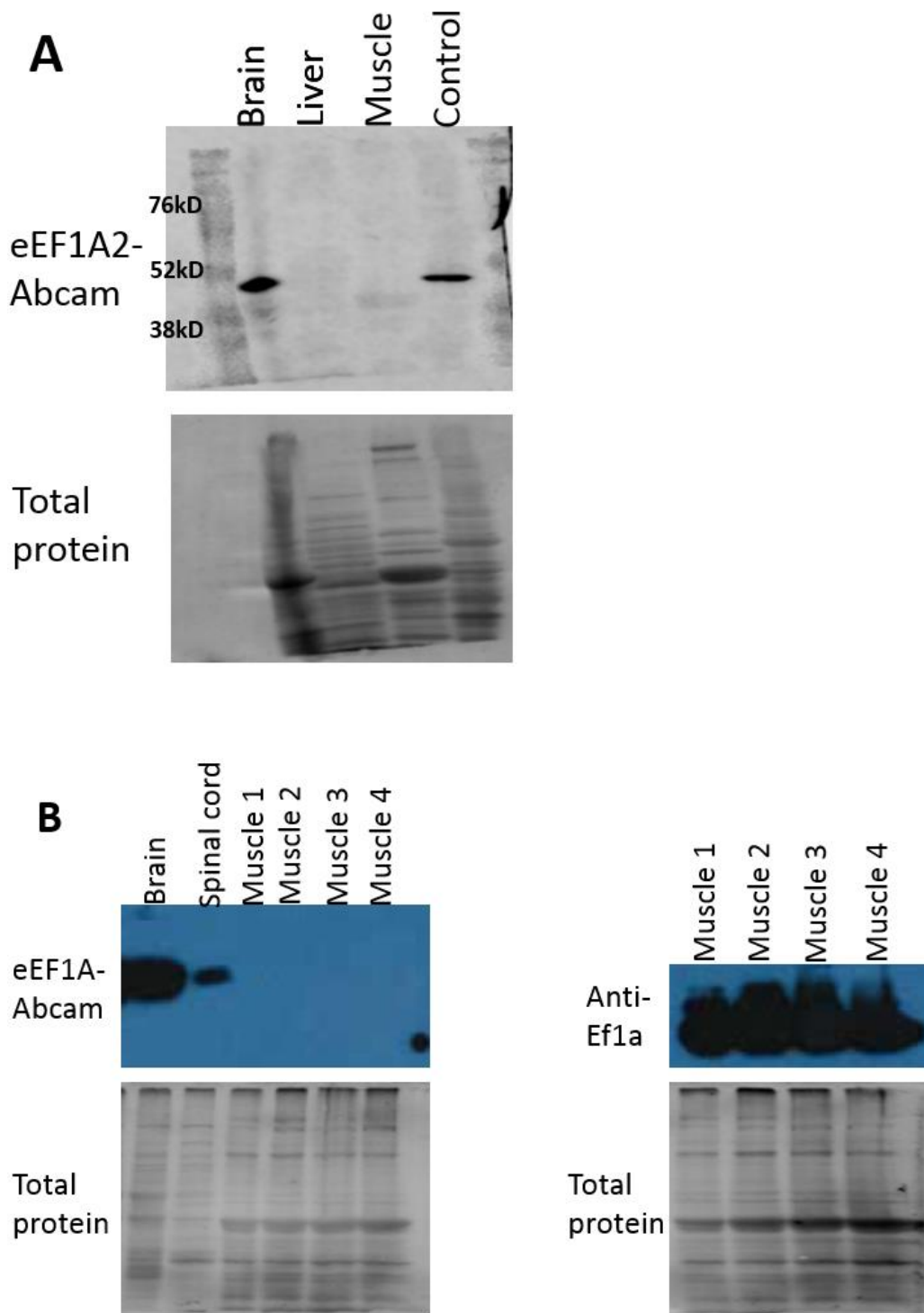


**Figure 3.12. eEF1A2 expression in zebrafish tissues using eEF1A2-Abcam antibody.** **A.** Western blot showing protein extracts from adult zebrafish brain, liver and muscle tissues probed with eEF1A2-Abcam at a concentration of 1:1000. Control is muscle tissue from mouse. **B.** Western blot showing protein extracts from adult zebrafish brain, spinal cord and muscle tissues (at different concentrations of 20 $\mu$ g, 30 $\mu$ g, 40 $\mu$ g and 50 $\mu$ g) probed with eEF1A2-Abcam (left). Samples of the different concentration of the muscle, run in parallel, were probed with eEF1A2-Abcam (left) and anti-Ef1a (right) antibodies at concentrations of 1:1000. Muscle 1, 2, 3 and 4 is samples at concentrations of 20 $\mu$ g, 30 $\mu$ g, 40 $\mu$ g and 50 $\mu$ g respectively. Transfer of protein were confirmed by staining blots with syproruby to visualise total protein on blots.

### **3.2.2.4 Cloning and expression of GFP-tagged *eef1a* construct and eEF1A2-Abcam antibody validation**

With the presence of four eEF1A proteins in the zebrafish which have highly similar amino acid sequences, it is crucial that antibodies against any of the eEF1A isoforms are validated to ensure they are specific. For this purpose, I generated full-length eEF1A1L1, eEF1A1A, eEF1A1B and eEF1A2 transcripts from cDNA synthesised from brain RNA extracts which were expressed with a GFP tag at the C-terminus. This is to help differentiate them from the endogenous eEF1A in the cell lines where they would be expressed as these zebrafish eEF1A proteins will have a higher molecular weight when expressed together with the GFP tag. Transcripts of all four eEF1A isoforms were confirmed by Sanger sequencing and then cloned into the pcDNA6.2/C-EmGFP-DEST expression vector using the Gateway® cloning technology (see section 2.2.3.1). Sequencing of constructs was performed to check sequences of the *eef1a* cDNA and that of the GFP tag were in frame. Each construct (hereafter referred to as eEF1A1L1-GFP, eEF1A1A-GFP, eEF1A1B-GFP and eEF1A2-GFP) were transfected into HEK293 cells and their expression were confirmed by western blot using an antibody, anti-EF1 $\alpha$  (Merck Milipore), which is known in our laboratory to pick up both mammalian eEF1A isoforms (Figure 3.13).

The specificity of eEF1A2-Abcam antibody was further investigated using protein extracts from HEK293 cells that were transfected with eEF1A1L1-GFP, eEF1A1A-GFP, eEF1A1B-GFP and eEF1A2-GFP constructs for western blot. Similar results were obtained using secondary antibodies for either LICOR or chemiluminescent detection of the eEF1A2 in the samples, with a clearer result obtained using the chemiluminescent method (Figure 3.14). A band of the correct size was observed for the cells transfected with eEF1A1A-GFP, eEF1A1B-GFP and eEF1A2-GFP but not eEF1A1L1-GFP suggesting that eEF1A2-Abcam is not specific for eEF1A2 in zebrafish but cross-reacts with eEF1A1A and eEF1A1B and likely does not recognise eEF1A1L1.

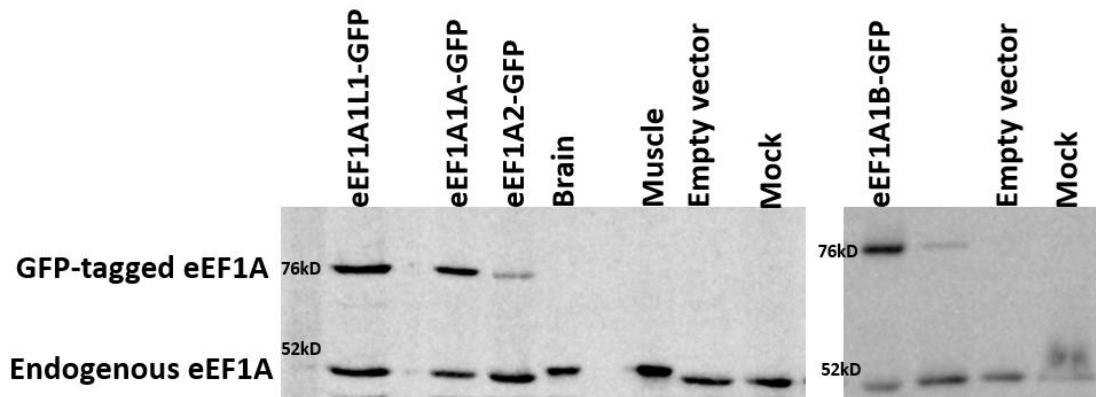


**Figure 3.13. Expression of eEF1A constructs confirmed by Western blot analysis.** eEF1A constructs tagged with GFP were transfected into HEK293 cells and their expression determined by western blot. Blots were probed for the tagged protein with anti-EF1 $\alpha$  (Merck Milipore), which recognises all eEF1A isoforms. Band of the right size was observed for all four eEF1A constructs. The GFP tag adds ~ 27kDa, therefore expected band size is ~ 77kDa (Mol. weight of eEF1A= 50kDa). Only endogenous eEF1A1 was observed in protein lysates from HEK293 cells transfected with the empty vector or water (mock) which acts as the negative controls.

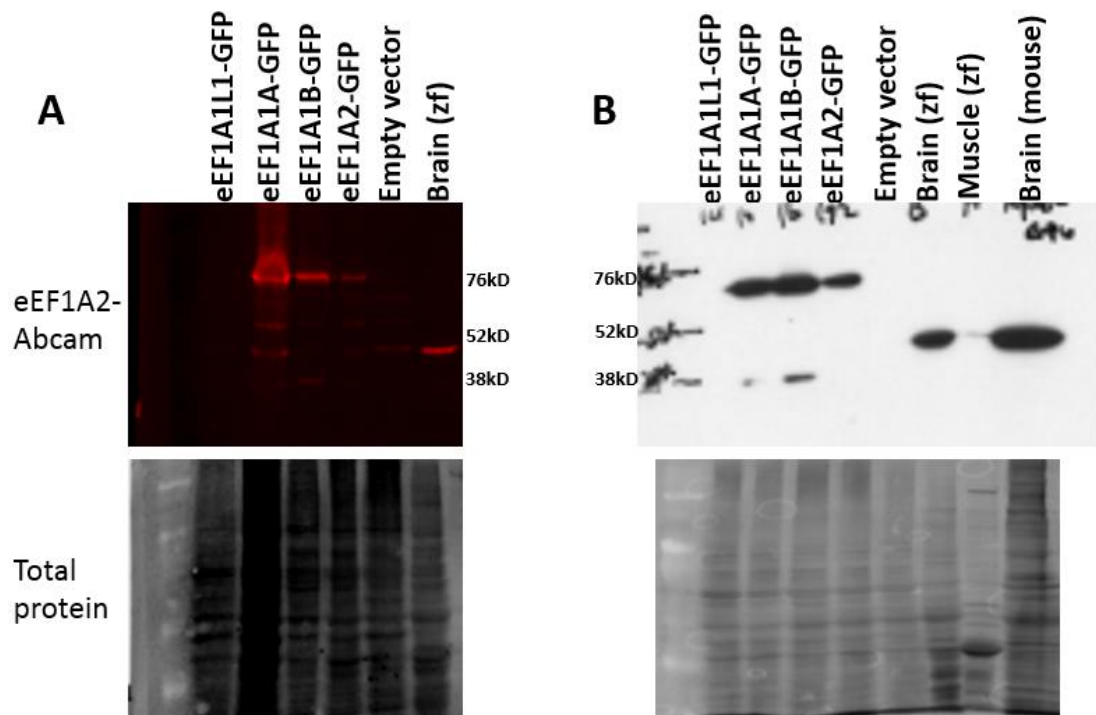


**Figure 3.14. Validation analysis of eEF1A2-Abcam antibody using the expression eEF1A constructs.** Specificity of eEF1A-Abcam was tested using the same lysates from HEK293 transfected with the different GFP-tagged eEF1A constructs. Immunoblotting was performed by **A.** LICOR and **B.** chemiluminescent detection method. Transfer of protein were verified by staining blots with syproruby to visualise total protein on blots. zf- zebrafish

### 3.3 Discussion

Initial studies suggested that the zebrafish has only one eEF1A gene in its genome (Gao *et al.*, 1997). However, the recent completion of the sequencing of the zebrafish genome has shown that more than one eEF1A genes exist in the zebrafish. Although the zebrafish sequencing project is still work in progress, it is clear that four eEF1A genes are present in the zebrafish genome. These genes, *eef1a111*, *eef1a1a*, *eef1a1b* and *eef1a2*, are located on chromosomes 19, 13, 1 and 23 respectively. The structure of these genes show that they are not processed (intronless) pseudogenes and are predicted to be actively transcribed, encoding different functional zebrafish eEF1A proteins. All of them share high sequence identity at both nucleotide and amino acid levels. Due to their high similarities, three different approaches were used to assign these genes to their appropriate human orthologue. All approaches gave strong support to the classification of *eef1a1a* and *eef1a1b* as co-orthologues of the human *EEF1A1*, while *eef1a2* is the orthologue of the human *EEF1A2*. The *eef1a1b* gene showed strong syntenic conservation with the genomic region containing the *eef1a1a* gene on chromosome 13 and is therefore a paralogue of *eef1a1a* and probably arose from the teleost-specific genome duplication that took place at the base of the teleost fish evolutionary lineage (Christoffels *et al.*, 2004). The *eef1a111* gene did not have any orthologue in the human genome but was clearly different from the other *eef1a* genes and is 92% identical to eEF1A1A and eEF1A1B and ~89% identical to eEF1A2 at the amino acid sequence level.

*In silico* functional analysis similar to the study of Soares *et al.* 2009, although less comprehensive, was carried out for the zebrafish eEF1A using their structural data calculated for the yeast eEF1A. Also 3-D models of the zebrafish eEF1A proteins were constructed using the yeast eEF1A crystal structure as the template. This showed that all four zebrafish eEF1A isoforms consists of three structural domains: I (1-240), II (241-336) and III (337-443) similar to the yeast eEF1A structure and the domain-domain contacts are almost conserved in them with variation at only two positions. At the two variable positions; 335 and 417, the variant residues still retain inter-domain interactions with their respective linker residues in domain III and II respectively. Also, the amino acid residues involved in the binding of the C-terminal fragment of eEF1B $\alpha$ , aminoacyl-tRNA and GDP/GTP were completely conserved in the zebrafish

eEF1A isoforms, which is in line with the functional importance of these residues in translation. It is reasonable to assume that all four zebrafish eEF1A isoforms have similar translational elongation activity and may adopt an identical conformation to that shown in the crystal structure for the complex of the yeast eEF1A with the C-terminal fragment of eEF1B $\alpha$  (Andersen *et al.*, 2000).

Structural differences between the zebrafish eEF1A isoforms was analysed using *in silico* approach to analyse the location of variant residues within known binding sites or in close proximity (within a distance of 5Å) to them. Noteworthy of mentioning is the non-conservative change Ala298Ser (eEF1A1A and eEF1A1B/eEF1A2 and eEF1A1L1) which is unique to the zebrafish and is invariant in the human isoforms and is equivalent to the yeast eEF1A Gln296. This position is close to the binding site for eEF1B $\alpha$  (Glu291 in yeast) and aminoacyl-tRNA (His294 in yeast). Interestingly, previous studies has implicated this position and others to be involved in actin-related functions in yeast (Gross and Kinzy 2007). They identified the mutant strains; one with a mutation at this site and 294 (H294A Q296R), K333E (equivalent to the variant position 335 in zebrafish eEF1A) and Y355C, (equivalent to 357 in zebrafish eEF1A), with normal translation function but that were able to reduce disorganisation of actin caused by overexpression of eEF1A. Similarly, a mutation N329S, which corresponds to the change that occur at position 331 (Asn331Ser) in the zebrafish isoforms, reduced the actin bundling activity with the translation function unaffected in yeast eEF1A (Gross and Kinzy, 2005). Two other position, 355 (unique to zebrafish) and 358 (identical change in zebrafish and human) lie close to Tyr357 (yeast eEF1A2 Tyr355). It is therefore most likely these differences in amino acids between the zebrafish eEF1A isoforms at these positions 298, 331, 335, 355 and 358 confers different actin interacting properties on the isoforms. This does not however rule out the possibility of the Ala298Ser change having an effect on the eEF1B and aminoacyl-tRNA binding properties of the four isoforms since it lies within 5Å of both binding sites.

A difference in the affinity of GDP and GTP between eEF1A1 and eEF1A2 has been reported, although it does not seem to influence protein synthesis using *in vitro* assays. While eEF1A1 binds more strongly to GDP, eEF1A2 shows more affinity for GTP than GDP (Kahns *et al.* 1998). They suggested that the non-conservative change (eEF1A1 Asn197His eEF1A2) could be one of the possible reasons for the difference

in guanine nucleotide binding between eEF1A1 and eEF1A2. Interestingly, this change also occurs in the zebrafish eEF1A isoforms, with eEF1A1A and eEF1A1B having an asparagine residue whereas eEF1A1L1 and eEF1A2 have a histidine residue at this position. Lying very close to 197, is Asp156, which is important for GDP/GTP binding and makes an hydrogen bond with Asn197 that is absent when this residue is replaced with a histidine in the structured eEF1A1L1 and eEF1A2 models as observed by Soares *et al*, 2009. The zebrafish isoforms may therefore exhibit differential affinity for guanine nucleotide binding which would further suggest likely functional differences within the isoforms.

There is evidence to suggest that post-translational modification of eEF1A isoforms might play a key role in the functional differences between the two isoforms (Kahns *et al*, 1998, Soares *et al*, 2009, Soares and Abbott, 2013). As it is likely the zebrafish eEF1A variants might have slightly different biological roles even though they share translational function, the pattern of post-translational modification will reflect this. Indeed this was the case as the eEF1A isoforms exhibited differential predicted phosphorylation patterns when analysed *in silico*. Predicted variant-specific phosphorylation sites are exposed and have their side chain exposed such that they can interact with a kinase (as this is obviously essential for phosphorylation to occur). Some of the predicted sites overlap with putative binding sites or variant residues that lie close to a functional site. For example, the eEF1A2-specific Ser358 which has a strong NetPhos score of 0.88, and is close to the actin-related residue mentioned above. Interestingly, phosphorylation of Ser358 in human eEF1A2 by c-Jun N-terminal kinase has been confirmed *in vitro* (Gandin *et al*. 2013). Other predicted phosphorylation sites for which experimental evidence of post-translational regulation also exists include Ser21, Thr88 and Ser300. Ser21, which is one of the residues involved in GDP/GTP-binding (Figure 3.5) was shown to modulate the half-life as well as the apoptotic roles of eEF1A isoforms (Sanges *et al.*, 2012). Interestingly, phosphorylated Thr88 (predicted for eEF1A1A, eEF1A1B and eEF1A1L1) was found only in the human eEF1A1 isoform (Sanges *et al.*, 2012). Although the score for Thr88 (0.53) is barely above the threshold for all the three zebrafish isoforms, the confidence of the prediction is increased by being in predictive agreement with findings from



Sanges *et al.*, 2012. Similar to Ser21, phosphorylation of Thr88 improved the stability of human eEF1A1 *in vivo*.

While all of the eEF1A1B-specific sites have been predicted with strong confidence and involves non-conserved serine residues, eEF1A1A specific site, Ser205 which is conserved in all the eEF1A variants has a score just on the threshold of 0.5. This suggests that eEF1A1B might have diverged in some other functions from eEF1A1A even though it is the most closely related paralogue compared with the other zebrafish isoforms. This possibility has been demonstrated by Chen *et al.*, 2017, where they found heterozygous mutation in eEF1A1B to cause infertility in male tilapia (*Oreochromis niloticus*). Unlike in human, the amino acid differences in the zebrafish eEF1A variants involves a loss of two tyrosine residues in eEF1A1L1. One of these positions, Tyr167 is likely a phosphorylation site in the eEF1A1A, eEF1A1B and eEF1A2, with a notably high prediction score of 0.9 in eEF1A2. Position 298, as mentioned above has been implicated in actin-related function in yeast and lies in close proximity to binding sites for eEF1B $\alpha$  and aminoacyl-tRNA, was predicted to be phosphorylated in eEF1A1L1 (NetPhos score, 0.75) and eEF1A2 (NetPhos score, 0.83). Interestingly, eEF1A1A and eEF1A1B has alanine at that position and this residue is very highly conserved with other higher vertebrates' eEF1A orthologues. Modification of Ser298 could likely regulate the translation and/or actin-binding functions of eEF1A1L1 and eEF1A2 and possibly serve as a molecular switch for these isoforms between these two functions similar to what was observed with Ser21 (Sanges *et al.*, 2012). It has been suggested that differences in phosphorylation may contribute to the different oligomeric state observed in human eEF1A with eEF1A1 having an enhanced ability to self-associate than eEF1A2 (Timchenko *et al.*, 2013). While Timchenko *et al.*, 2013 noted that the different oligomeric state did not affect the translation activity of the isoforms, it is likely to be of biological importance. For instance, in the study of Sanges *et al.*, 2012, phosphorylation of Ser21 residue which affects eEF1A stability and apoptotic activity was found to be more pronounced when both isoforms were preincubated before the kinase assay was performed. Whether this is the case with the zebrafish eEF1A isoforms will require separate investigation.

Gene expression analyses using RT-PCR confirms the presence of all four *eef1a* genes. Expression of the zebrafish *eef1a* genes were detected in a developmental-specific

manner which is a common feature of the different eEF1A genes in most species. During embryogenesis, *eef1a111* was the only gene shown to have maternal contribution as well as zygotic expression. Interestingly, *eef1a111* (formerly referred to as *eef1a*) has been shown to be an embryonic essential gene and is required for early embryonic development in zebrafish (Amsterdam *et al*, 2004). According to this study, mutation in *eef1a111* causes abnormal phenotypes which becomes apparent from 2dpf in the fish. At 3dpf, the larva develops small head and eyes, reduced growth and eventually die at 5dpf due to failure of the swim bladder to inflate. It is worth noting that ISH results presented in this work shows *eef1a111* to have a ubiquitous expression at 24hpf and an enriched expression in the head region and eyes of the fish at 48hpf. The next *eef1a* genes to be detected were *eef1a1a* and *eef1a1b*, while *eef1a2* was the last to be expressed. The detection of *eef1a2* at a later developmental stage is consistent with that of mammals, where its expression is observed much later in development gradually replacing eEF1A1 in skeletal muscle and neurons.

Expression of *eef1a* genes was also determined in adult zebrafish using a range of tissues. In all the tissues analysed, mRNA of *eef1a111*, *eef1a1a* and *eef1a1b* were detected. The *eef1a2* gene showed a tissue-specific expression pattern as its mRNAs was not present in the liver and was only just detected in the intestine. This is again another characteristics that appears to be conserved in vertebrates. The difference between the zebrafish *eef1a2* and the mammalian and *Xenopus* orthologue however, is the presence of *eef1a2* mRNA in the spleen and ovary tissues of the adult zebrafish. Whereas the expression pattern of *eef1a1a* and *eef1a1b* is in contrast to that of their mammalian orthologue, it is similar to that of *Xenopus* where eEF1A1 mRNA was also detected in the adult muscle (Newbery *et al*, 2011). Despite the co-expression of the *eef1a* genes in the tissues, quantification of transcripts levels in the brain, muscle and liver suggests that they are not present in equal amounts. While *eef1a111* mRNA was more abundant in muscle and liver compared to the other *eef1a* genes, the levels of all the *eef1a* mRNA were the same in the brain. Similar levels of *eef1a* mRNA in the brain might stem from the presence of a more heterogeneous cell types in this tissue compared to the liver and muscle tissues. A follow up experiment looking at cell-specific expression of these isoforms might shed more light on this. The *eef1a2* transcript was the second most abundant in the muscle but was only ~2-3 fold higher

than *eefla1a* and *eefla1b*. As expected and consistent with being paralogues, *eefla1a* and *eefla1b* exhibited the same expression pattern.

Regulation of eEF1A expression resulting in the switching of eEF1A variants in the muscle and neuron, though conserved, occurs through different mechanism in mammals and *Xenopus*. While in mammals, this occurs at the transcriptional level, regulation of eEF1A expression is post-transcriptional in *Xenopus* (Chambers, Peters and Abbott, 1998; Kahns *et al.*, 1998; Helen J Newbery *et al.*, 2011; Svobodová *et al.*, 2015). Although it is not yet understood why *Xenopus* shows a different mechanism from mammalian species, Newbery *et al* 2011 postulated that it could likely be an adaption for the need of a quick response of eEF1A switching during metamorphosis. This is reasonable considering the dramatic developmental changes that accompany this process and occur in the whole organism simultaneously. It is therefore possible that the post-transcriptional mode of regulating eEF1A expression does not only occur in *Xenopus* species but might be conserved in lower vertebrates. Unfortunately, the complexity of the zebrafish eEF1A coupled with the dearth of antibodies for zebrafish made it impossible to reach a definite conclusion for this hypothesis. However, results obtained using an antibody against eEF1A2 from Abcam (ab82912) advertised to be specific for zebrafish indicates it might also cross-react with the other eEF1A variants, particularly eEF1A1A and/or eEF1A1B. This stresses the need to validate antibodies first before employing it for further analysis particularly with zebrafish to avoid misleading results. This is particularly relevant as this antibody was used in a recent study by Cao *et al.* 2017 to show the absence of eEF1A2 in their knockdown zebrafish model at 2dpf. My RT-PCR results revealed that all of the *eefla* mRNA are already present at this stage and it is around this period that *eefla2* is first detected. A striking observation of my western blot results (summarised below) using the eEF1A2-abcam antibody was the absence of a band in a range of adult zebrafish tissues except brain where the four *eefla* genes are co-expressed at the mRNA level and spinal cord. Interestingly, the manufacturers (Abcam) also tested eEF1A2-abcam antibody using protein lysates from adult zebrafish brain, heart, and skeletal muscle tissues, but only observed a band with the brain lysate (personal communication) which is in line with my own results. Although the specificity of anti-Ef1a (GeneTex) which was raised against eEF1A1L1 is questionable, it does confirm the presence of eEF1A in muscle.

It is difficult to interpret this intriguing observation. It is however possible that eEF1A2 and eEF1A1A and /or eEF1A1B are not present in these other tissues assuming the eEF1A2-abcam recognises only these isoforms and not eEF1A1L1 and control of the zebrafish eEF1A occurs at the post-transcriptional level as in *Xenopus*. Alternatively, these isoforms might have different post-translational modification in the different tissue types which eEF1A2-abcam might not recognise.

**Summary of western blot results using different antibodies to probe tissues from adult zebrafish for eEF1A**

<b>Antibody</b>	<b>Brain</b>	<b>Muscle</b>	<b>Liver</b>	<b>Spinal cord</b>	<b>Intestine</b>	<b>Ovaries</b>	<b>Heart</b>
eEF1A2-2	Y	Y	Y	NA	NA	NA	NA
eEF1A2-Genetex	Y	Y	Y	NA	NA	NA	NA
eEF1A2-Proteintech	Y	Y	Y	NA	NA	NA	NA
eEF1A2-Abcam	Y	N	N	Y	N	N	N
Anti-Ef1a	NA	Y	NA	NA	NA	NA	NA

Y- Band of the correct size detected, N- no band detected, NA- Not analysed

Although, I was unable to investigate expression at the protein level, my findings suggest that while the zebrafish eEF1A isoforms have similar role in translation, the differences in residues, predicted phosphorylation sites and expression profile observed could possibly promote functional divergence in them thereby supporting a subfunctionalisation model for the four zebrafish eEF1A isoforms.

## Chapter 4: Modelling eEF1A2 disease-causing mutation in zebrafish

### 4.1 Introduction

Since 2012, twenty different mutations in *EEF1A2* have been identified in about 50 patients. These individuals usually present with epilepsy, intellectual disability and in some cases autism (discussed in section 1.2.2 in Chapter 1). Modeling of these mutations in different living models will not only provide insight into the underlying mechanism of these mutations but will also help in the identification of new treatment for these disorders.

Here, I describe experiments aimed at recreating the G70S mutation in zebrafish using CRISPR/Cas9 technology. Due to time constraints, this experiment was carried out concurrently with those described in chapter 5. I was however aware of the possibility that knocking out *eef1a2* might not have any phenotypic effect in zebrafish because the other *eef1a* genes might compensate for its loss. In which case, zebrafish carrying a heterozygous missense mutation will be non-informative if the G70S mutation acted through a loss of function mechanism. As there are studies that provide evidence that suggests eEF1A can form dimers (Bunai *et al.*, 2006; Sanges *et al.*, 2012), it is also possible that the G70S mutation could exert a dominant-negative effect on the wild-type eEF1A2 or even the other eEF1As present in zebrafish. Also, it is still unknown whether the missense mutations in eEF1A2 results in a loss or gain of function effect in humans. In the study of Davies *et al.*, 2017, four *Eef1a2*<sup>G70S/-</sup> mice generated from a CRISPR/Cas9-mediated gene editing experiment were found to show the typical wasted mouse phenotypes despite the expression of G70S protein in their brain at levels comparable to those of wild-type mice. This finding suggests that the function of eEF1A2 is compromised by the mutation since the G70S protein was unable to compensate for the loss of the wild-type *Eef1a2* in the other allele. Also, one *Eef1a2*<sup>G70S/G70S</sup> mouse had a more severe phenotype compared to its *Eef1a2* null littermates and had to be culled at 18 days which is earlier than that of wasted mice, which are usually culled at 21 days when the onset of the phenotype begins. This preliminary finding supports a gain-of-function mechanism is also at play with the G70S mutation.

These findings further stress the need to generate animal models that can accurately recapitulate the human phenotype as this will help inform decisions as regards developing new drug therapies. For example if these mutations are found to only lead to a loss of function of the mutant protein, then boosting wild-type eEF1A2 expression levels in the patients will be an efficient therapeutic strategy. However, this approach will be deleterious if the mutant protein has a dominant negative effect on the wild-type. For this reason, it is therefore important to generate zebrafish with the missense mutations as eEF1A2-null zebrafish models might not be sufficient to model the human disorder.

#### **4.1.1 Guide RNA (gRNA) synthesis**

Guide RNA (gRNA) was originally designed with the intention to generate *eef1a2* null zebrafish lines, however, for the sake of clarity it is described in here.

Guide RNA target sites for zebrafish *eef1a2* were designed using online target finders tools at <http://crispr.mit.edu/> and at <http://chopchop.cbu.uib.no/> (CHOPCHOP). To increase the chances of abolishing expression of *eef1a2*, the majority of the gRNAs were designed to target sites on early exons. Also, gRNAs with no predicted off-target sites found by the finder tools were selected. Target sequences were amplified from genomic DNA extracted from AB wild-type fish using the Phusion High-fidelity DNA polymerase and sequenced to confirm that no confounding sequence variants were present, as these can lead to a mismatch between the gRNAs and their target sites resulting in the inefficiency of the CRISPR/Cas9-mediated genome editing. Synthesised gRNAs were separately co-injected with nCas9 mRNA into 1-cell stage zebrafish embryos. For each gRNA, target sites were amplified from pooled genomic DNA isolated from 10-15 injected 3 days post fertilisation (dpf) embryos. As it is likely that injected embryos will be mosaic, PCR products were cloned into TOPO-A vector and used to transform competent *E. coli* cells. Between 22 and 48 individual colonies were sequenced and used to estimate the mutagenesis efficiency of the experiment by dividing the number of colonies with mutant sequence insert by the total number of colonies with insert sequence I was able to read (see Table 4.1). The nCas9 mRNA which was co-injected with gRNA1, gRNA2 and gRNA7 was found to be inefficient, which could explain the low mutation rate observed with these gRNAs. The other nCas9 mRNA (gift from Zhiqiang Zeng) co-injected with gRNA3 and gRNA5 proved to be more efficient (see section 2.2.5.3 in Chapter 2). Higher mutagenic activity was seen in embryos injected with gRNA3 compared with gRNA5 injected

embryos which nevertheless also generated several mutations (Figure 4.1). High survival rate was also observed in embryos injected with either gRNA3 or gRNA5.

**Table 4.1: Mutagenesis efficiency of CRISPR/Cas9 genome editing to target *eef1a2* in zebrafish**

<b>gRNA</b>	<b>Exon</b>	<b>Total colonies</b>	<b>Readable sequence</b>	<b>Mutant sequence</b>	<b>Mutagenic efficiency (%)</b>
*gRNA1	2	48	35	0	0/35 ( <b>0</b> )
*gRNA2	2	48	24	0	0/24 ( <b>0</b> )
gRNA3	3	38	31	24	24/31 ( <b>77.4</b> )
gRNA5	2	36	31	9	9/31 ( <b>29</b> )
*gRNA7	6	22	8	1	1/8 ( <b>12.5</b> )

\*indicates gRNA co-injected with the same source of nCas9 mRNA

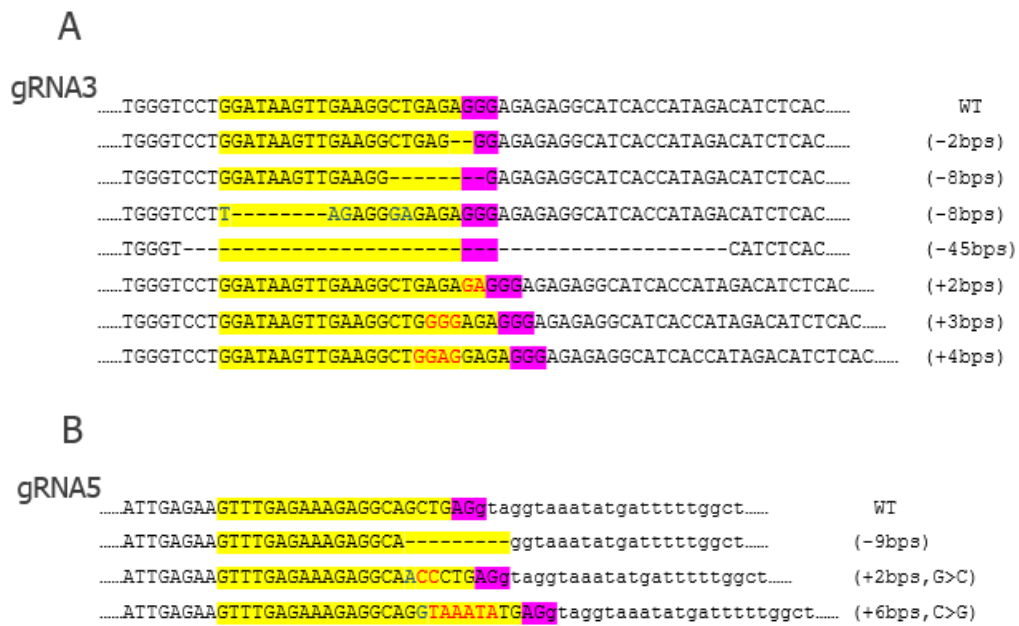


**Figure 4.1. Mutation rate analysis of gRNA3 and gRNA5 in CRISPR-Cas9 experiment. A-B.** Examples of mutation sequences recovered from genomic DNA clones of lysed injected F0 embryos. (A) Shows those generated by gRNA3 and (B) shows those generated by gRNA5. Sequences highlighted in yellow indicates gRNAs target sites with the PAM site highlighted in purple. Inserted bases are in red. Sequences that are located in exons or introns are represented in upper case and lower case respectively.



#### 4.1.2 CRISPR/Cas9-mediated HDR experimental design

The G70S (c.208G>A) mutation, which involves an amino acid residue that is highly conserved, was the first disease-causing *EEF1A2* mutation discovered and has been identified in the largest number of individuals. Patients with this mutation usually present with epilepsy, intellectual disability and hypotonia (see Table 1.2 in chapter 1). This mutation occurs on exon 3 and is only 8 base pairs away from the target site of gRNA3 which was also used in another CRISPR/Cas9 experiment described in chapter 5. Encouraged by the high mutagenic activity observed at this site with gRNA3, I speculated that it might be suitable to facilitate a targeted knock-in approach to recreate the G70S (c.208G>A) mutation in the zebrafish. To this end, I designed a single-stranded oligonucleotide (ssODN) repair template containing the G70S point mutation that spanned the same region targeted by gRNA3 as it is expected that is where DNA cleavage was likely to occur. Flanking the G>A point mutation in the ssODN template were 151 and 52 base pair homology arms on the 5' and 3' sides respectively. A silent mutation was introduced in the PAM site targeted by gRNA3 changing it from a NGG sequence (GGG) to a non-NGG sequence (GAG) on the ssODN repair template. This was done to avoid subsequent DNA cleavage from occurring following the incorporation of the repair template. Also, the repair template contained a two base substitution (CT→TC) 153 base pairs upstream of the G70S mutation site. This change does not affect *ef1a2* as it is situated well into the intron but it introduces a novel EcoRI restriction enzyme site to aid genotyping of the fish. The target region and repair template design are shown in figure 4.2.

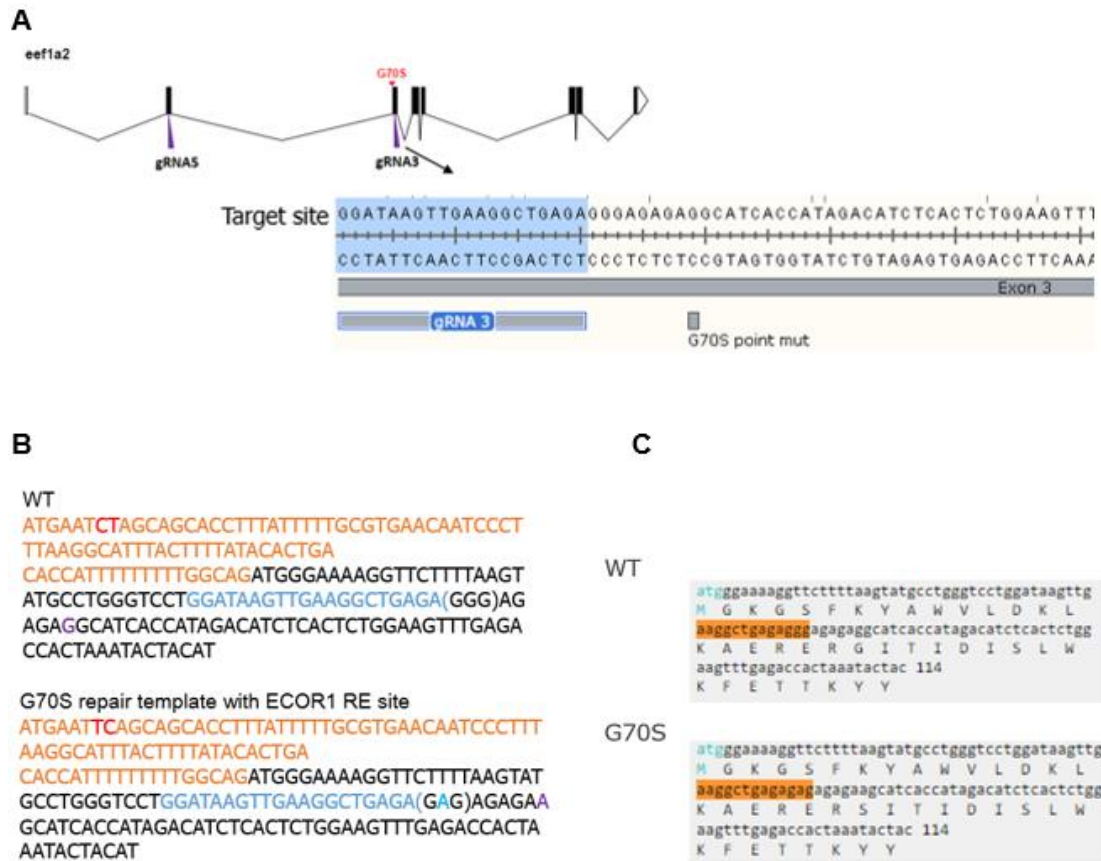


**Figure 4.2. G70S zebrafish CRISPR/Cas9 experimental design.** **A.** Schematic representation of zebrafish *eef1a2* showing the distance of the gRNA3 target site from the G70S point mutation in exon 3. **B.** Sequence of the 200bps repair template containing the point mutation (in purple). A novel restriction enzyme site (in red) was introduced into the intron which is represented by the orange nucleotides. Target site sequence is in blue. PAM site is mutated from GGG to GAG to avoid cleaving of the repair template once integrated. **C.** The translated amino acid sequence of WT and a G70S template showing that the PAM-blocking mutation (highlighted in orange) is silent and does not alter the coding potential of *eef1a2* and also the serine residue in the G70S repair temple.

## 4.1 Results

### 4.1.1 Microinjection and screening of founders for mutation

The ssODN repair template along with gRNA3 and Cas9 mRNA was microinjected into one-cell embryo stage by the fish facility Manager, Dr. Cameron Wyatt. The repair template was injected at two test concentrations; 92ng/μl and 183ng/μl into 108 and 131 embryos respectively. Injected embryos were placed in E3 solution in batches of 50 per 9cm Petri dish and kept in the incubator at ~ 28.5°C. Dead or deformed embryos were discarded and the healthy ones were placed in fresh E3 medium daily. At 5 days post fertilisation, injected embryos were transferred to tanks and raised until they were 2 months old. Table 4.2 summarises the number of injected fish at different ages that were alive during the course of the experiment.

**Table 4.2: Number of surviving fish at different ages injected with 92ng/μl and 183ng/μl ssODN**

ssODN concentration	Number of injected one-cell embryos	Number of injected embryos at 5dpf	Number of injected F0 at 2 months old
G70S 92ng/μl	108	100	46
G70S 183ng/μl	131	113	40

DNA was isolated from fin-clips of 2 month old injected fish (F0) and the region around the EcoRI restriction enzyme site and mutation site was amplified. Incorporation of the PAM-blocking and G70S silent mutation will result in the loss of the two MnlI site (Figure 4.2A), as such MnlI would fail to digest G70S mutant amplicons, thereby identifying founders with this mutation. Also, the amplified PCR product of 489 base pairs digested with EcoRI will generate bands of 429 and 60 base pairs if the repair template was incorporated by homology-directed repair (HDR) since this restriction enzyme site was engineered into the repair template only. The restriction enzymes, MnlI and EcoRI, were then used to digest PCR products to determine if the knock-in experiment was successful (Figure 4.3).

A total of eighty-six F0 fish were genotyped using both restriction enzymes but none of them were found to have incorporated the repair template or have the G70S missense mutation. Insertion and deletion mutations, mainly around the target site of

gRNA3, were consistently revealed on sequencing cloned PCR products obtained from a total of 21 founders (Figure 4.3C). These results, therefore suggests that the CRISPR/Cas9-mediated HDR experiment was unsuccessful.

Since no founder with the desired mutation was identified, this work could not be taken further and there was insufficient time to attempt another experiment to produce a G70S zebrafish line.

A

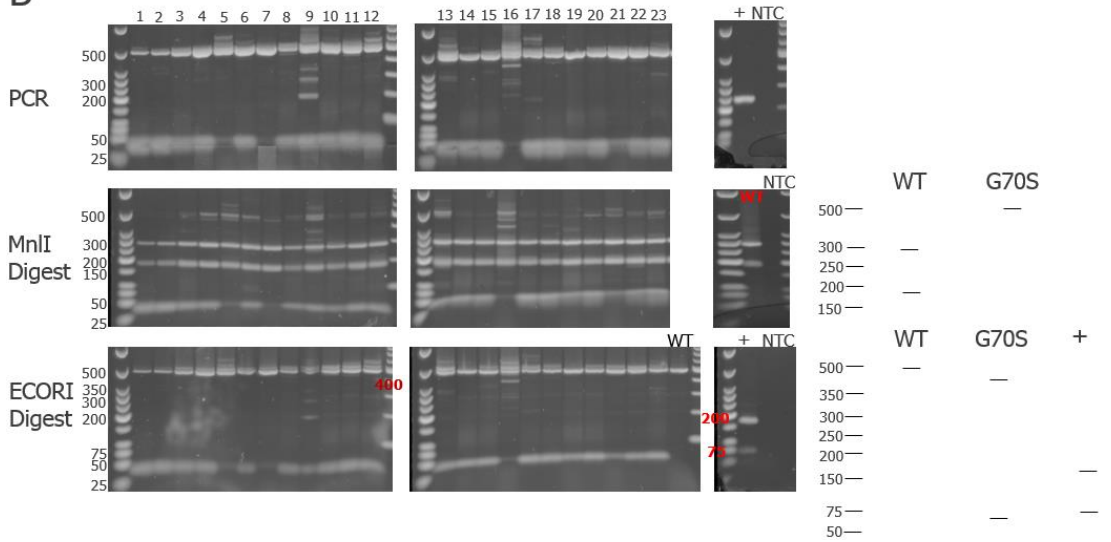
WT PCR PRODUCT

ggtaggcccggtcctataaataaagggcatagatttgcttttgccttactcttacctatgaatctagcagcacctttat  
 ttttgcgtgaacaatccctttaagggcatttacttttatacactgacaccattttttttggcagATGGGAAAAGGTCT  
 TTAAAGTATGCCTGGGTCCTGGATAAGTTGAAGGCTGAGAGGAGAGAGGCATCACCATAGACATCTCACTCTGGAAGT  
 TTGAGACCACTAAATACTACATAACCATAATAGATGCTCCAGGACATAGAGACTTATCAAAAACATGATCACTGGGAC  
 ATCTCAGgtaatgacttttaaaaaacttaataaaaaatgtacaaaaacttgctgctgggagactggtataacgcaggt  
 gtgctttaccctgttctggagatctacattcttttagacttcagctccaacctgatcaagcacaactaaactaacgg  
 tacattccaacaag

G70S PCR PRODUCT

ggtaggcccggtcctataaataaagggcatagatttgcttttgccttactcttacctatgaattcagcagcacctttat  
 ttttgcgtgaacaatccctttaagggcatttacttttatacactgacaccattttttttggcagATGGGAAAAGGTCT  
 TTAAAGTATGCCTGGGTCCTGGATAAGTTGAAGGCTGAGAGAGAGAGGCATCACCATAGACATCTCACTCTGGAAGT  
 TTGAGACCACTAAATACTACATAACCATAATAGATGCTCCAGGACATAGAGACTTATCAAAAACATGATCACTGGGAC  
 ATCTCAGgtaatgacttttaaaaaacttaataaaaaatgtacaaaaacttgctgctgggagactggtataacgcaggt  
 gtgctttaccctgttctggagatctacattcttttagacttcagctccaacctgatcaagcacaactaaactaacgg  
 tacattccaacaag

B



C

GGGTCCTGGATAAGTTGAAGGCTGAGAGGAGAGAGGCATCACCATAGACATCTCACTCTGG  
 GGGTCCTGGATAAGTTGAAGGCTG-GAGGGAGAGAGGCATCACCATAGACATCTCACTCTGG  
 GGGTCCTGGATAAGTTGAAGGCTGAG--GGAGAGAGGCATCACCATAGACATCTCACTCTGG  
 GGGTCCTGGATAAGTTGAAGG-----AGGGAGAGAGGCATCACCATAGACATCTCACTCTGG  
 GGGTCCTGGATAAGTGAAGGCTGTA-----TGGAGGCATCACCATAGACATCTCACTCTGG  
 GGGTCCTGGATAAGTTGAAGGCTGAG-----AGAGGCATCACCATAGACATCTCACTCTGG  
 GGGTCCTGGATAAGTTGAAGG-----GAGAGAGGCATCACCATAGACATCTCACTCTGG  
 GGGTCCTGGATAAG-----AGAGGGAGAGAGGCATCACCATAGACATCTCACTCTGG  
 GGGTCCTGGATAAGTTGAAGGCTGGA-----G-----G  
 -----GAGAGAGGCATCACCATAGACATCTCACTCTGG -54bp  
 GGGTCCTGGATAAGTTGAAGGCTTATCCAGGGAGAGAGGCATCACCATAGACATCTCACTCTGG  
 GGGTCCTGGATAAGTTGAAGGCTGTCTAGAGGGAGAGAGGCATCACCATAGACATCTCACTCTGG  
 GGGTCCTGGATAAGTTGAAGGCTGGGGAGAGAGGGAGAGAGGCATCACCATAGACATCTCACTCTGG  
 GGGTCCTGGATAAGTTGAAGTATTTAGTGGTCTCAAACCTCCAGAGTGAGAGAGGGGAGAGGG +46bp

**Figure 4.3. CRISPR/Cas9 experiment generated indels but failed to generate a G70S mutation in ssODN injected founders. A.** Sequence of PCR product for wild-type (WT) and G70S. Orange sequence indicates target site while PAM site is underlined. MnlI cut sites (highlighted in grey) is shown in the wild-type PCR product. These sites have been destroyed by the PAM-blocking mutation (G > A in the G70S product) and the G70S point mutation (shown in purple). Yellow highlight indicates EcoRI cut site contained in the repair template by a CT to TC substitution. **B.** Example gel electrophoresis of PCR products and restriction enzymes (MnlI and EcoRI) digest from 23 founders. NTC indicate a 'no template control' while '+' indicate a positive control that cuts with EcoRI. Predicted band sizes using NEBcutter V2.0 are shown to the right of the digest gels. PCR product size; 489bp. MnlI (middle) - WT band sizes: 291bp, 190bp and 8bp. G70S band uncut (489bp). EcoRI (bottom) - WT band uncut (489bp). G70S band sizes: 429bp and 60bp. + band sizes: 171bp and 73bp. **C.** Example sequence results from cloned PCR products from founders. Note that some of the generated indels destroy one or both of the MnlI cut sites which could explain the partial digest of some amplicons by MnlI.

## 4.2 Discussion

There has been a remarkable development of different tools for gene manipulation such as the zinc finger nucleases (ZFN), transcription activator-like effector nucleases (TALEN) and the more recent clustered regularly interspaced short palindromic repeat (CRISPR) system. With these genome editing technologies, mutations at a desired location in the genome can be efficiently generated in various model organisms. CRISPR/Cas9 has been shown to be highly efficient in inducing mutations at rates comparable or even exceeding that of ZFN and TALEN, which were the most used methods before the CRISPR/Cas9 system was adapted for use in the zebrafish (Hruscha *et al.* 2013, Hwang *et al.* 2013, Jao *et al.* 2013). However, CRISPR/Cas9 offers the advantage of being cheaper, easier to design and less time consuming than ZFN and TALEN, making it an excellent alternative to these other methods.

After successfully identifying a gRNA with high mutagenic activity which was fortunately in close proximity to the G70S mutation, I sought to use this gRNA in a CRISPR/Cas9-mediated HDR experiment to recreate the point mutation in the zebrafish *eef1a2*. The G70S (G>A) point mutation is only 8 base pairs away from the target site of gRNA3 with a mutagenic efficiency of 77.4%. A repair template was co-injected with gRNA3 and Cas9 mRNA to take advantage of the homology-directed repair (HDR) pathway to introduce our desired mutation. A ssODN was used as the donor repair template and designed to contain the point mutation and a silent mutation at the PAM site, to avoid further targeting once it has been integrated into the gene. In addition, a novel EcoRI restriction site was engineered into the ssODN to assist in genotyping the fish. Due to time and space constraints, screening for the G70S

mutation was carried out in the founders. Unlike non-homologous end joining (NHEJ) induced gene disruption, HDR requires screening for a precise mutation and can be time-consuming especially in zebrafish where there are high levels of mosaicism among founder fish. For this reason, founders were pre-screened using restriction fragment length polymorphism (RFLP) analysis. G70S founders were to be identified based upon their loss of MnlI sites and the ability of their PCR products to be digested when treated with EcoRI. Unfortunately, the expected cut pattern was not observed in any of the founders. Although a partial cut was observed when some of the PCR products were digested with MnlI, sequencing results obtained from some founders showed similar NHEJ-induced indel distribution which disrupted the MnlI sites. Also, EcoRI failed to digest the amplicons further supporting that the partial cut might be due to these indel mutations and not as a result of the G70S mutation being incorporated. There is, however, the possibility that fish with a point mutation could be missed using this approach as a result of the high null background. As such it is best to analyse F1 generation when possible to avoid this complication due to mosaicism in founders. However, the mutation must occur in the germline of the founders and breeding large number of fish for screening might be needed. Taken together, these results suggest that HDR did not occur and that the induced double-stranded breaks were likely repaired by the NHEJ pathway only.

HDR is a rare event with DSBs being predominantly repaired by the NHEJ pathway which occurs at least 10-fold higher than HDR during early embryonic development in the zebrafish (Dia *et al.* 2010, Li *et al.* 2015). Although the efficiency of the NHEJ pathway was high and reliably generated indels, none of the fish had incorporated the G70S point mutation. A similar experiment was performed by Armstrong *et al.*, 2016 where they successfully introduced a point mutation in *tardbp* and *fus* but with very low efficiencies. Surprisingly, the gRNA target sites for *tardbp* and *fus* used in their study had low efficiencies of 21% and 17% respectively. It is, however, possible that the position of their point mutation, being within the gRNA target sites, favoured the integration of the repair template. Interestingly, a systematic characterisation of the distance of the mutation to the cut site showed that a distance of 10bp reduces HDR efficiency by half in human IPS cells (Paquet *et al.* 2016). Several other studies have demonstrated the feasibility of precise gene modification using CRISPR/Cas9-

mediated HDR, but its efficiency is still considerably low in zebrafish and results have been inconsistent in zebrafish (Cornet, Di Donato and Terriente, 2018; Zhang, Zhang and Ge, 2018). This has become a limiting factor in harnessing the combined advantage of the CRISPR/Cas9 technology and the zebrafish model stressing the need for further investigations pertaining to the development of an efficient CRISPR/Cas9-mediated HDR protocol that could be routinely used in the laboratory. This might require a systematic approach to optimise the best conditions of the several factors showed to influence HDR efficiencies such as the activity rate of the gRNA, distance of mutation from the target site and design of repair template. Interestingly, in the study by Armstrong *et al*, 2016, two ssODN templates that differ in length showed different HDR efficiency, with the 100 base pairs template having a slightly higher efficiency than the one which was 23 base pairs in length. Also, while Armstrong *et al*, 2016 postulated that a higher HDR efficiency would have been achieved if gRNAs with high efficiencies were used, results from my study shows that several other factors other than the use of poor gRNAs might have been responsible.

Interestingly, a recent study by Zhang *et al*. 2018 demonstrated that employing a combination of the optimal condition of these factors significantly increased the rate of CRISPR/Cas9-mediated HDR. The approach used in this study that was most effective involved the use of a plasmid DNA donor, suppressing NHEJ and enhancing HDR rates by the use of drug antagonists: SCR7 (inhibits NHEJ) and RS-1 (HDR enhancer), Cas9 protein and a CRISPR/Cas9 blocking mutation. A combination of these parameters and a gRNA with a mutation rate of 80% resulted in a high HDR efficiency rate of about 74% and a germline transmission rate of 25%. Another advantage of this study is that it was designed such that point mutations can be easily identified in founders with a high background of indel mutations when screening, avoiding the need to breed large number of fish. The protocol described by Zang *et al*. 2018 could, therefore, be adapted as a guide in designing another round of CRISPR/Cas9 experiment to generate a G70S mutant zebrafish line. It is important to note that the point mutation incorporated in this study was within the target site which could have also contributed to the high level of efficiency obtained in this study. However, there is the possibility that the distance of the G70S point mutation from the target site might not dramatically reduce the expected level of efficiency reported as it



is only 8 base pairs away from the gRNA3 target site. Interestingly, it might even increase the chances of generating fish heterozygous for the G70S mutation which will be equivalent to the genotype seen in humans as well as other genotypes for comparative studies. This is because optimisation of the adequate distance between the target site and the mutation position by Paquet *et al.* 2016 showed that a distance of 5-20 base pair favours heterozygous editing, while a gRNA targeting <10 bp from the mutation was ideal for homozygous editing. Although Paquet *et al* 2016 carried out this work in human IPS cells, this relationship between the cut to mutation distance and zygosity might also be applicable to the zebrafish. It might, therefore, be possible to make use of gRNA3, avoiding the need to design and assess the mutation efficiency of another target site.

CRISPR/Cas9 genome editing was recently used in our laboratory to generate mice with G70S with a high level of efficiency (Davies *et al.*, 2017). Although no mice heterozygous for G70S mutation were recovered, this study provided some preliminary findings that suggest the G70S mutation might also act through a gain of function. Given the importance of the functional impact of the G70S mutation in developing treatment strategies, a G70S zebrafish mutant line will be useful as an additional model to confirm this finding. I will also be interested in modeling other disease-causing eEF1A2 mutations using the method from the study of Zhang *et al*, 2018 since it is possible these mutations might operate through different mechanisms as suggested by the phenotypic heterogeneity in the patients. For example, the D252H mutation which could be used in future studies together with our recently generated mice and LUHMES cells D252H models. Moreso, since I was able to generate and characterise a homozygous null zebrafish line (discussed in chapter 5), results on the effect of these missense mutations would be easier to interpret.

## Chapter 5: Generation and characterisation of *eef1a2* knockout zebrafish model

### 5.1 Introduction

Complete loss of *Eef1a2* in mouse causes motor neuron degeneration in the spinal cord anterior horn, muscle wasting and death by 4 weeks. More recently, a heterozygous null mutation in *Eef1a2* has been shown to cause a minor social discrimination in mice, even though these mice appear normal (J.E Hope, Ph.D. thesis). Studies using this model have no doubt provided valuable information on eEF1A2 function *in vivo*. However, homozygous *Eef1a2* null mice show postnatal mortality and are therefore not a suitable model for drug discovery studies. Also, the use of rodent models in the development of new drugs is costly, time-consuming, ethically challenging and usually performed at low-throughput. On the other hand, zebrafish has been shown to be an ideal model system for the screening of new drug molecules. This model provides a whole-animal system for investigating the onset and course of a pathological process *in vivo* and at the same time, allows for high-throughput screening of several small molecules simultaneously which saves time and is cost-effective, which is particularly useful in the pharmaceutical drug discovery field (Lieschke and Currie, 2007). For this reason, I aimed to investigate whether the zebrafish could be used as a complementary model to fill this need.

Bioinformatics and expression analysis described in chapter 3 identified four *eef1a* genes with a clear indication of the presence of a eEF1A2 orthologue in the zebrafish which is similar in amino acid sequence (94%) to that of the mouse. This also provides some evidence of sub functionality among these genes as they showed distinct expression profiles during the development of the zebrafish embryo. However, this interpretation is confounded by the co-expression of all the *eef1a* transcripts in a range of adult tissues which might also indicate functional redundancy. It is important to note that regulation of eEF1A expression in *Xenopus* occurred at the post-transcriptional level (Newbery *et al* 2011), therefore making the interpretation of the RNA level expression data not straightforward.

In this chapter, I describe work focused on *eef1a2* as this will provide an essential underpinning for assessing the suitability of the zebrafish as a model for our studies. This was achieved by

- Generating a *eef1a2* knockout zebrafish model using a CRISPR/Cas9 system shown to be efficient in zebrafish (Hwang *et al.*, 2013) and the subsequent validation of two independent mutant lines
- Characterising mutant lines to determine the effect of *eef1a2* disruption on phenotype and survival in zebrafish

## 5.2 Results

### 5.2.1 Generation of *eef1a2* null zebrafish lines

To generate a null *eef1a2* zebrafish model using CRISPR/Cas9, I designed and constructed five different guide RNA sequences (gRNAs) targeting the *eef1a2* gene. This is described in full details in section 4.1.1 in chapter 4. Two of these gRNAs; gRNA3 and gRNA5 which showed the highest mutagenic activity were then selected for further investigations. Embryos injected with gRNA3 and gRNA5 showed a high survival rate of 93% and 67% respectively. At 2 months old, nine CRISPR-injected fish for each gRNAs were genotyped using genomic DNA isolated from tail fin clipping to identify potential founders using the Agilent 2100 Bioanalyser. If mutagenesis is successful in the F0, PCR products will be made up of a mixture of wild-type and different mutant sequences since founders are usually mosaic. The presence of multiple sequences creates heteroduplex DNA which could be seen for all F0 genotyped (Figure 5.1).

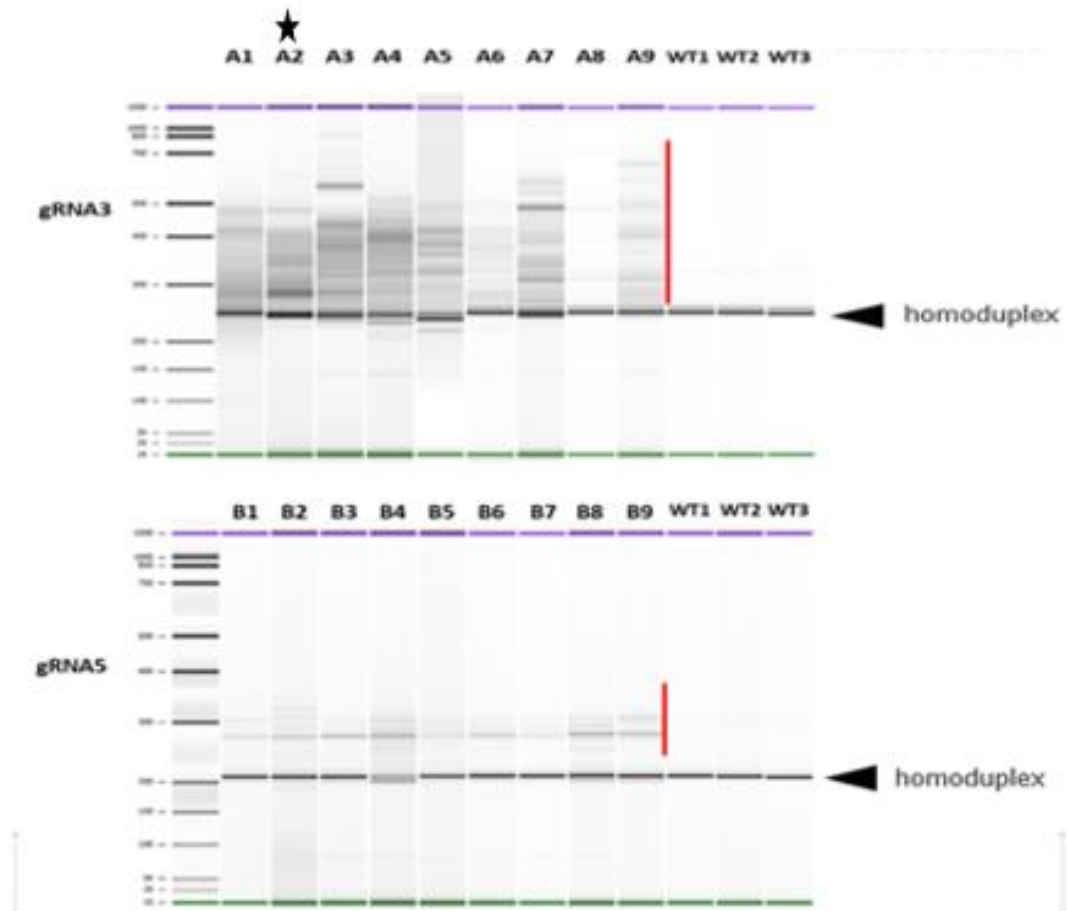
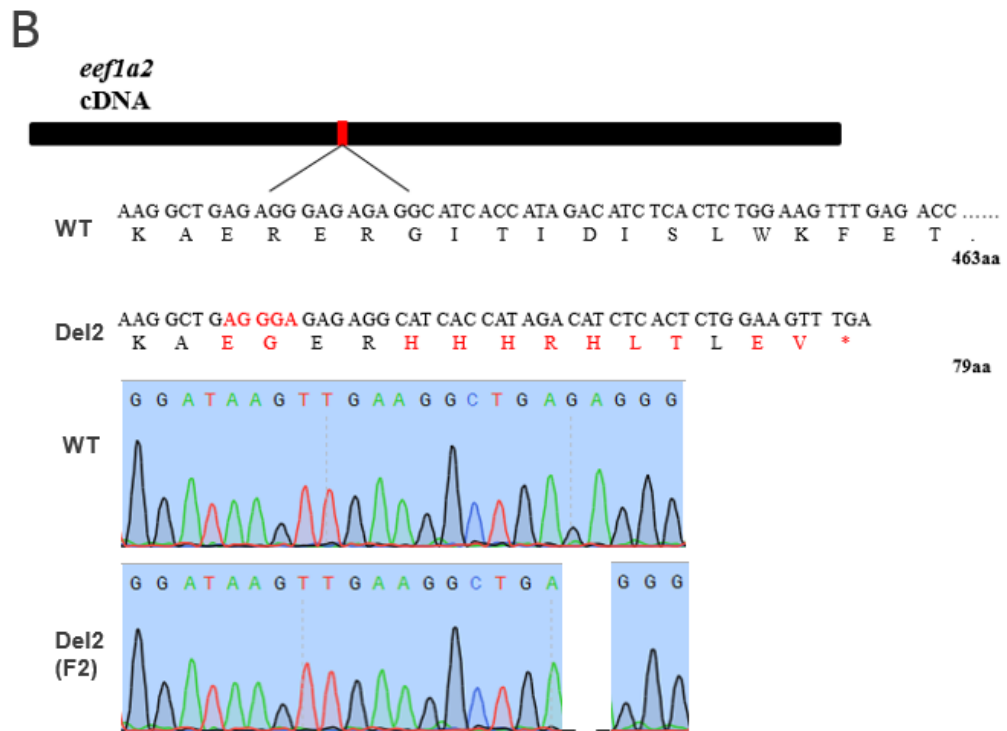
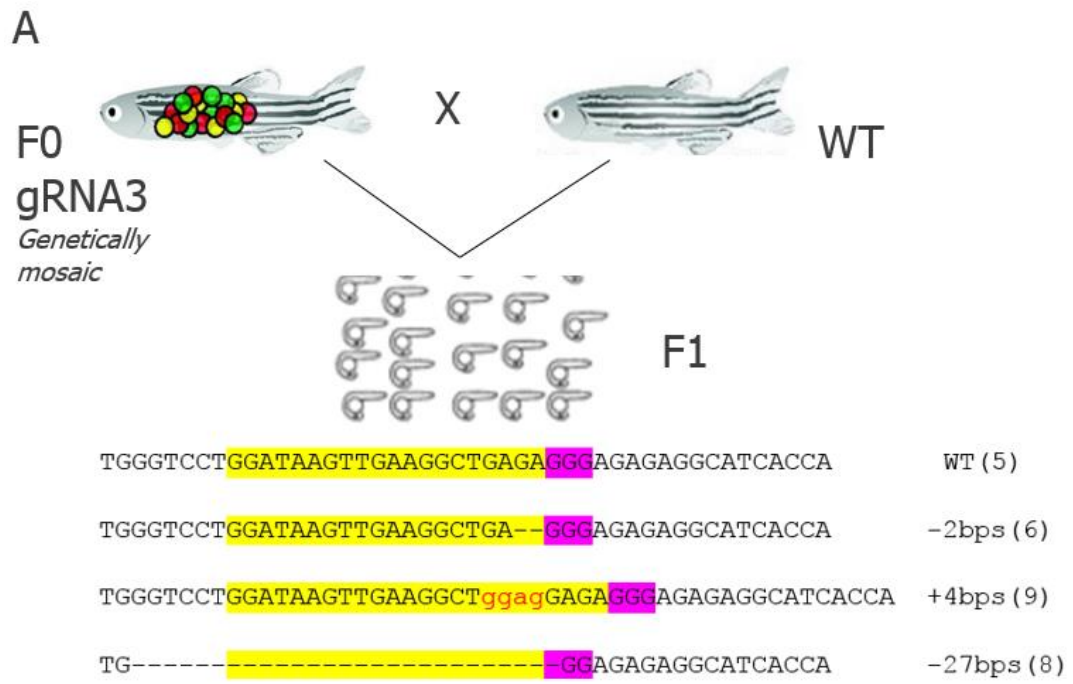


**Figure 5.1. PCR products amplified from F0 fish injected with gRNA3 or gRNA5 in the CRISPR-Cas9 experiment.** Screening of potential F0 mutants injected with gRNA3 (top) or gRNA5 (bottom). Level of mismatches forms heteroduplexes (red line). Black star indicates founder (F0) used to generate mutant lines. WT1, WT2 and WT3 indicate PCR products from fin clipping obtained from three different uninjected wild-type fish.

## 5.2.2 Germline transmission and establishing stable mutant lines

In order to employ these mutants for further characterisation, it is important to generate fish with identical mutations in every cell. This is only possible after germline transmission of the mutations of the putative founder fish, which are genetically mosaic. To confirm that mutations could be transmitted to their offspring, nine of the screened F0 of each gRNAs were in-crossed separately and individual F1 embryos were sequenced. gRNA5 injected F0 had a low germline transmission frequency of 18.8% (mutant F1/examined F1= 6/32) while a much higher germline transmission frequency of 82.9% (mutant F1/examined F1= 25/35) was observed in F0 injected with gRNA3.

To establish stable null mutant lines, putative founders were outcrossed with wild-type fish to avoid transmitting unlinked off-target mutations. Mating was successful with founder A2 (gRNA3) and three mutant alleles were recovered (Figure 5.2A). Two alleles, a 4 base pair insertion (hereafter referred to as Ins4) and 2 base pair deletion (hereafter referred to as Del2) were chosen for further analysis. Heterozygous fish carrying the same *eef1a2* mutation were crossed and the mutation was confirmed in F2 homozygote offspring using Phusion High fidelity DNA polymerase (Figure 5.2B-C). Complete loss of *Eef1a2* in mice causes a wasted phenotype from 21 days of age with rapid deterioration and the homozygous mice die by 28 days (Shultz, L.D, Sweet, H.O, Davisson, 1982). Interestingly, both *eef1a2* mutant lines reached adulthood without showing any obvious abnormal phenotypes and were fertile (Figure 5.2D). As a result, I was able to maintain them in homozygosity.



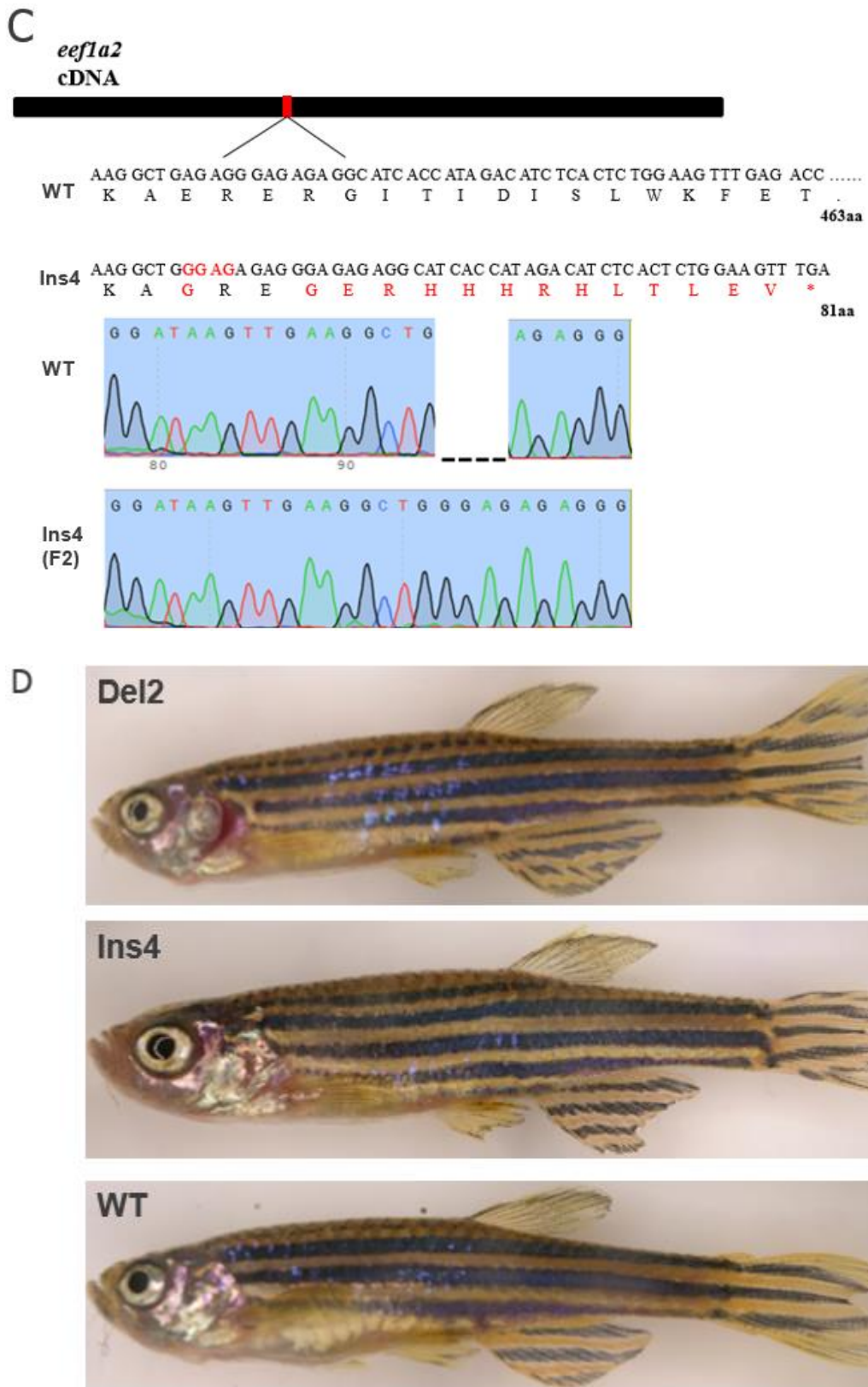


**Figure 5.2. Establishing *eef1a2* mutant zebrafish line.** A. Schematic of outcross mating of founder fish with wild-type showing recovered F1 sequences with the number for each sequence indicated in brackets. Target sequences (yellow highlight) and PAM site (purple) with red showing inserted bases. B-C. Predicted effect of the mutant allele (upper panel) and Sanger sequencing data from homozygous

fish which confirmed mutant alleles for Del2 and Ins4 mutant lines (bottom panel). Aberrant residues are shown in red **D**. No overt difference in homozygous Del2 (6 months) and Ins4 (8 months) adult fish from wild-type (6 months) adult fish.

### **5.2.3 Del2 and Ins4 mutant lines show reduced *eef1a2* transcript levels.**

Selected alleles are predicted to cause a frameshift lesion which introduces a premature stop codon. It is likely that the mRNA transcripts from these alleles would be subjected to nonsense-mediated decay, since the premature stop codon occurs early and is located  $\geq 50 - 55$  nucleotide upstream an exon-exon junction (Brojna and Wen, 2009; Popp and Maquat, 2016). The Del2 allele is predicted to encode a truncated polypeptide with 11 aberrant amino acid residues starting with an Arg to Gly substitution at position 67, while the Ins4 allele encodes a truncated polypeptide containing 14 aberrant amino acids (Figure 5.2B-C). To investigate the severity of these mutant alleles, I examined the levels of *eef1a2* transcript by real-time quantitative PCR in adult homozygous Del2 and Ins4 mutant zebrafish tissues. Two different set of primers, *eef1a2P* and 3'*eef1a2*, were used for both lines while a third primer set; *eef1a2S* was used only in Ins4. The location of the primers in relation to the target site is illustrated in figure 5.3. The 3'*eef1a2* primer set which is located further downstream from the target site was designed to assess nonsense-mediated decay efficiency. Both Del2 and Ins4 mutations lead to a decrease in transcripts levels compared with those seen in the wild-type siblings. Using primers *eef1a2P* and 3'*eef1a2*, *eef1a2* levels were reduced by approximately 81% and 92% in the Del2 homozygous adult brain compared to their wild-type siblings. On the other hand, *eef1a2P* and 3'*eef1a2* showed a *eef1a2* transcript level reduction of approximately 86% and 95% respectively in the Ins4 homozygous adult brain compared to wild-type. Similarly, *eef1a2S* showed a decrease of *eef1a2* mRNA of approximately 82% in F2 Ins4 homozygous adult brain and muscle tissues compared with wild-type (see Appendix figure 2A).

These primer sets were then used to assess the transcript levels of *eef1a2* in the brain of adult homozygous 12bp deletion mutants. As expected, there was no significant decrease in transcript levels as this is an in-frame mutation and is not predicted to cause a truncated protein (see Appendix figure 2B). These results suggest that the Del2 and



Ins4 allele leads to an increased messenger RNA degradation rate possibly through nonsense-mediated decay (NMD). It is, therefore, possible that Del2 and Ins4 are severe mutations and homozygous mutant fish could be null mutants.

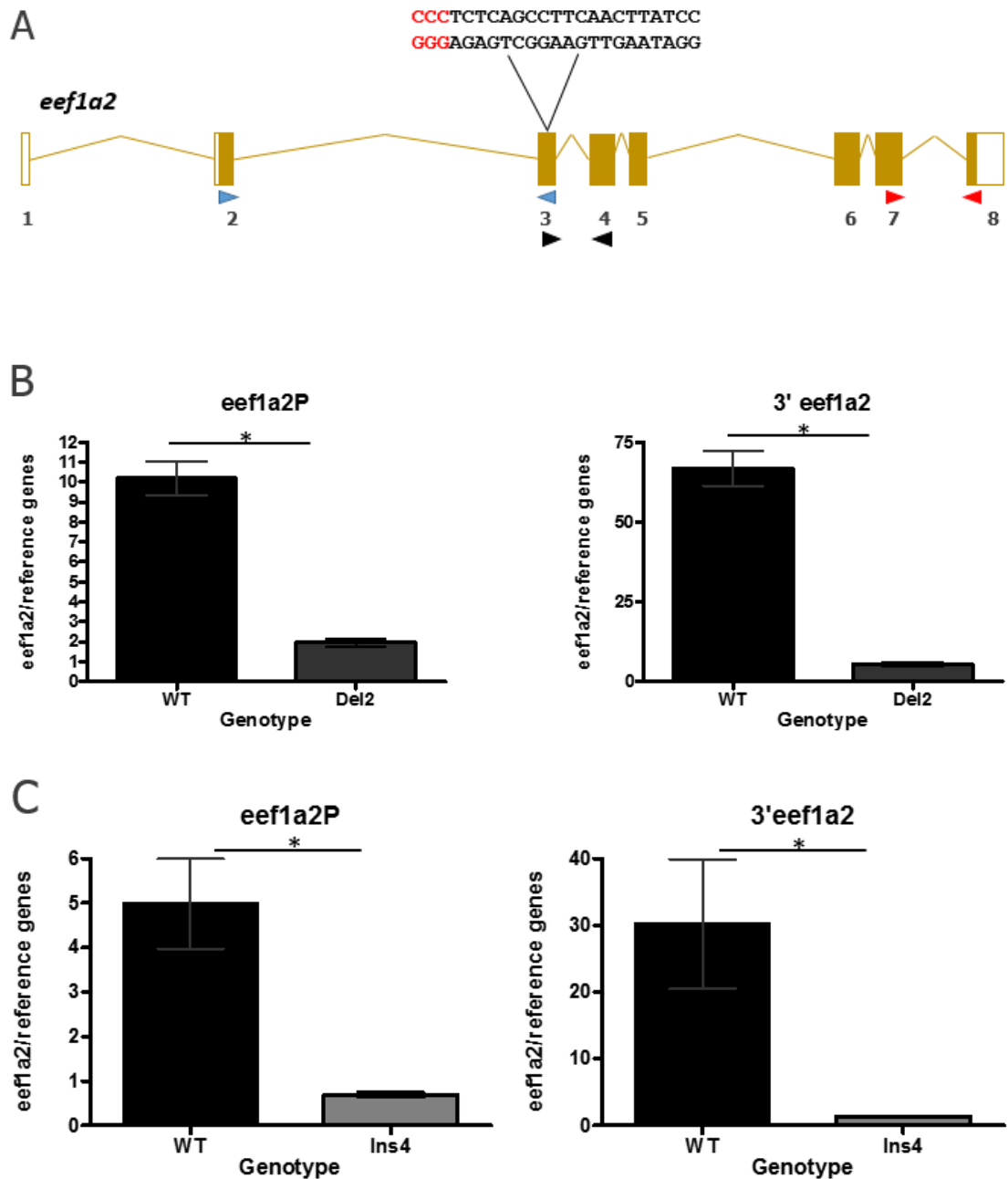


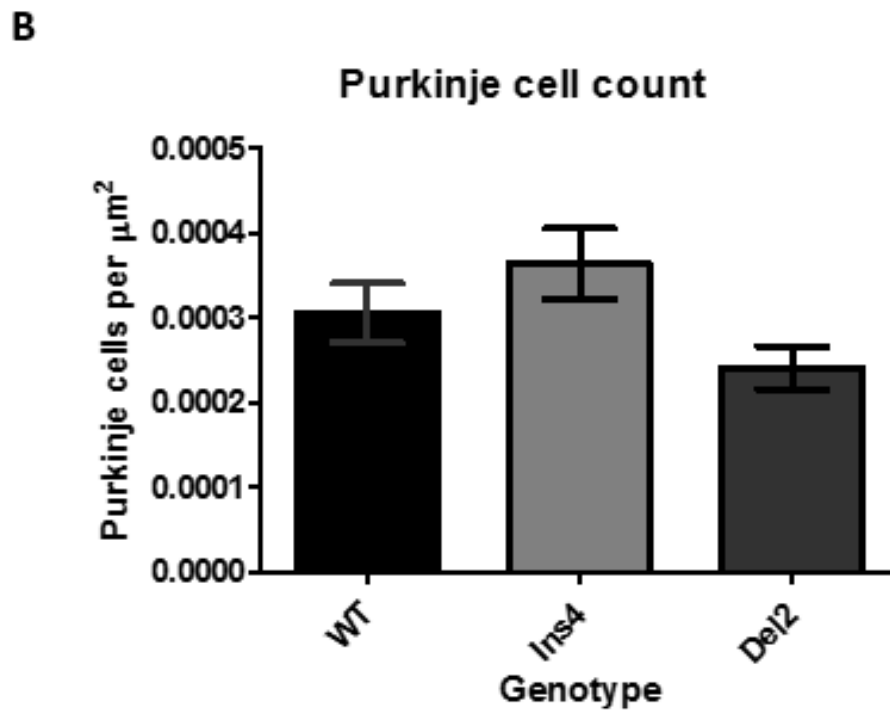
**Figure 5.3. Reduced *eef1a2* transcript levels in Del2 and Ins4 mutants.** **A.** Schematic of the *eef1a2* gene with untranslated region, exons and introns depicted as open box, filled box and line respectively. The position of the three different primer sets; eef1a2S (Blue triangle), eef1a2P (black triangle) and 3'eef1a2 (red triangle) is illustrated in relation to the gRNA3 target site (PAM site sequence in red). **B-C.** *eef1a2* mRNA expression (normalised to three reference genes: ATPsynth, NADH and 16S) as assessed by qPCR in (B) F2 Del2 homozygous (4 months) and (C) F3 Ins4 homozygous (3 months) and age-matched wild-type adult brain. Transcript levels of *eef1a2* were reduced in both lines using two different sets of primers suggesting NMD is taking place. Results are means  $\pm$  S.E.M.; n=3 in each group. \*p  $\leq$  0.05 (Mann Whitney test)

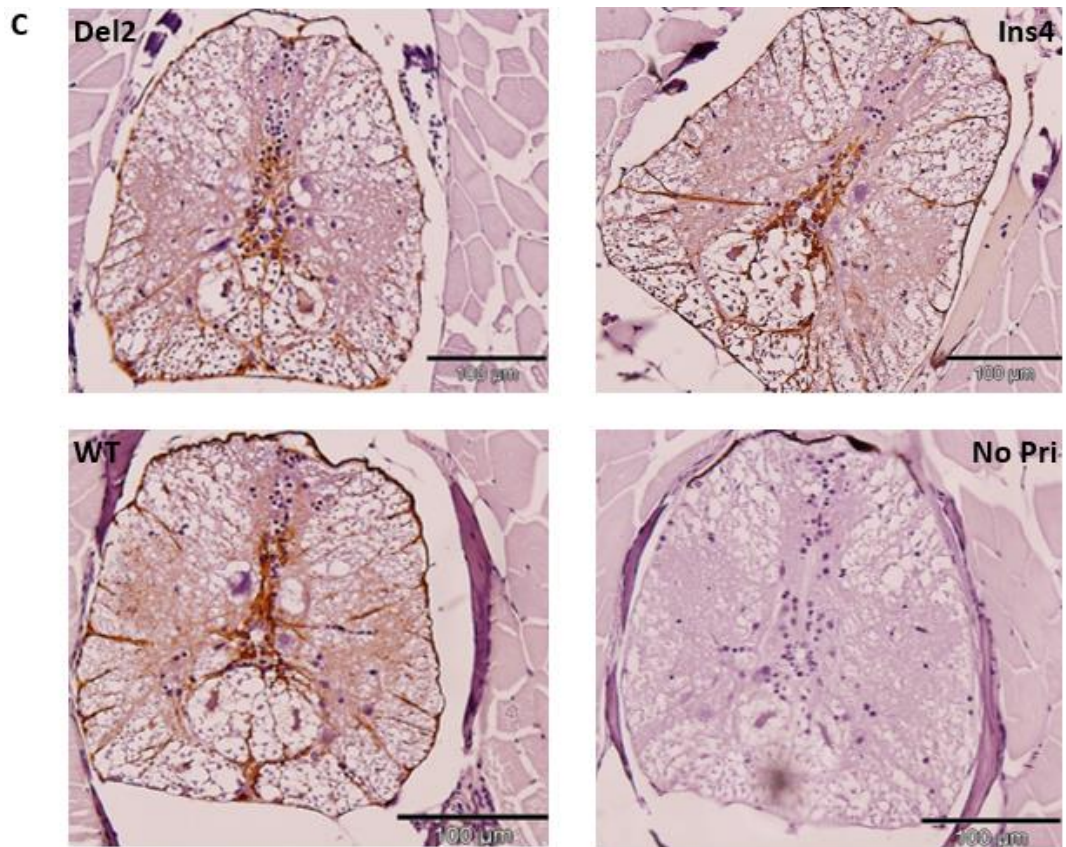
#### 5.2.4 Characterisation of mutant fish by histology

Since the *eef1a2* mutant zebrafish had a normal physical appearance and did not show any obvious phenotype, I decided to perform a histological analysis of the central nervous system in adult mutant fish to establish whether any changes could be identified at a cellular level. Loss of function of *Eef1a2* in mice has been well characterised and shown to cause severe neuromuscular abnormalities such as motor neuron degeneration of the anterior horn of the spinal cord and muscle wasting which is of neurogenic origin (Newbery *et al.*, 2005; Doig *et al.*, 2013). As a preliminary study, a detailed histological examination of longitudinal brain sections, 3µm-thick, obtained from one male homozygous Ins4 adult fish (5 months old) was carried out by Dr. Jorge del Pozo, a diagnostic pathologist at Easter Bush Veterinary Centre (EBVC). He observed lower neuronal density in the cerebellum and medulla oblongata in the Ins4 mutant compared with its age-matched male wild-type sibling (see Appendix figure 3). Interestingly, Shultz *et al* 1982 reported loss of Purkinje cells in the brain of wasted mouse. Therefore, a follow-up study was carried out using three male fish per genotype including the homozygous Del2 mutants as a complementary line which would also be predicted to be effectively null. Longitudinal brain sections of 3µm-thick were also generated from each fish and stained with H&E at the EBVC. For each fish, I analysed the number of Purkinje cells in the cerebellum at three areas around the corpus cerebelli (Figure 5.4A). This region was chosen as it was best represented in all the fish and allowed uniformity of sampled areas. Using one-way ANOVA, there was no significant difference in the density of Purkinje cells in the cerebellum of Ins4 and Del2 mutants when compared to wild-type (Figure 5.4B). It is, therefore, possible that the difference initially observed was artefactual.

Thin sections of spinal cord from homozygous Ins4 and Del2 adult fish were evaluated for gliosis. Gliosis is the reactive response to a variety of injuries to the central nervous system from trauma to neurodegeneration (Goc *et al.*, 2014). During this process, microglia and astrocytes are activated and expression of glial genes are upregulated, one of which is GFAP (O'Callaghan and Sriram, 2005). Glial fibrillary acidic protein (GFAP) is a widely used biomarker to evaluate gliosis and high level of staining of this protein has been shown to occur in the anterior horn of the spinal cord of wasted

mouse (Newbery *et al.*, 2005). I, therefore, stained spinal cord sections from homozygous Del2 and Ins4 mutants with an antibody against GFAP. Spinal cord sections of homozygous Del2 and Ins4 mutants did not show increased staining for GFAP when compared to wild-type (Figure 5.4C). These results suggest the absence of neurodegeneration in the spinal cord of both mutant lines.



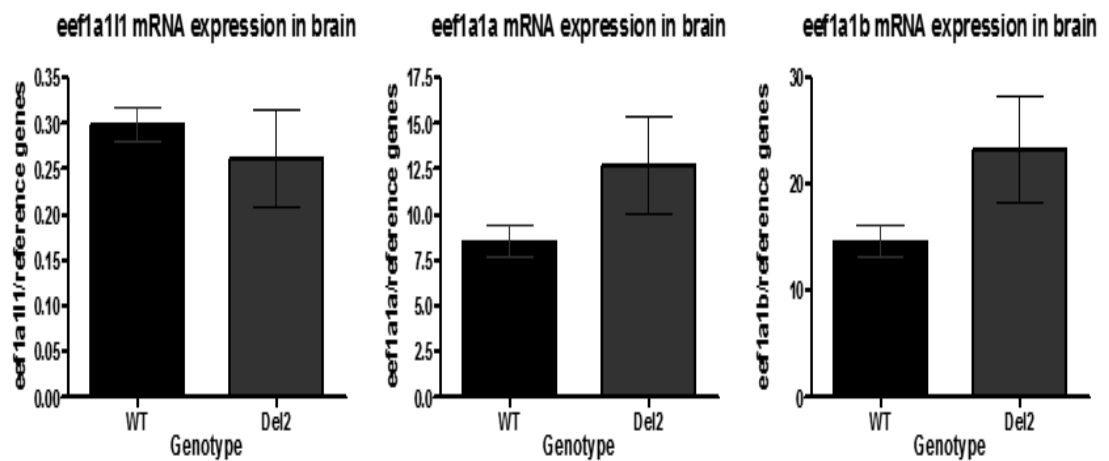
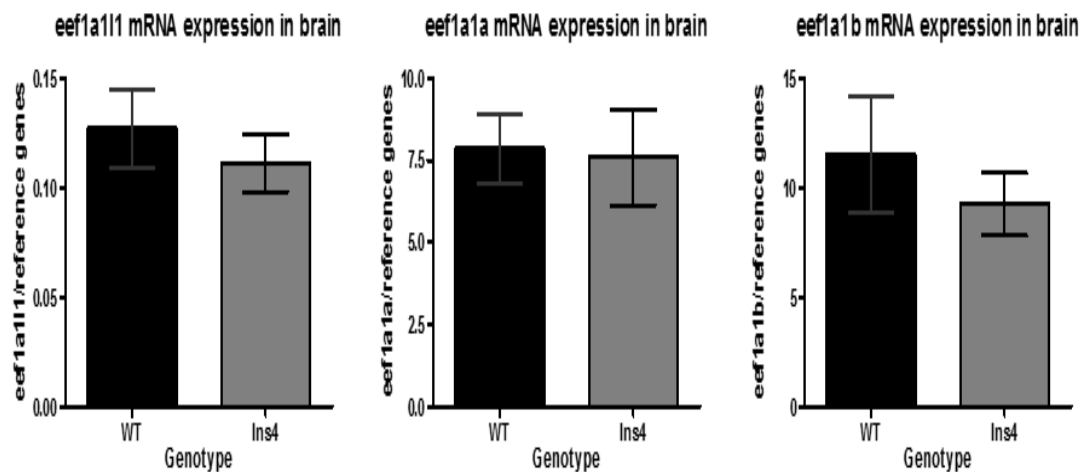


**Figure 5.4. Del2 and Ins4 characterisation by histology.** **A.** Representative Screenshot of ImageJ counter window used for analysing the Purkinje cell density in the cerebellum. The three sampled areas around the corpus cerebelli (CCe) (indicated with yellow squares) show individual Purkinje cells counted for square 1 (blue), square 2 (cyan) and square 3 (green) **B.** Graph showing average number of Purkinje cells per  $\mu\text{m}^2$  in homozygous Del2 and Ins4 fish compared to wild-type adult cerebellum. No significant difference was observed (One-way ANOVA). Results are means  $\pm$  S.E.M.; n=3 fish per genotype. **C.** Anti-GFAP antibody stained transverse sections of homozygous Del2 and Ins4 spinal cord shows no sign of neurodegeneration. Negative control of a no primary (No Pri) was included which showed no staining. Scale bar = 100 $\mu\text{m}$

### 5.2.5 Transcript levels of the other *eef1a* genes

To investigate whether there might be an underlying compensatory mechanism from the other *eef1a* genes leading to the healthy appearance of the two mutant lines generated, quantification of transcript level of the other *eef1a* genes (*eef1a111*, *eef1a1a* and *eef1a1b*) was performed in homozygous Del2 and Ins4 mutants. Pre-validated custom primers for *eef1a111*, *eef1a1a* and *eef1a1b* from Primerdesign and the same brain cDNA used to quantify *eef1a2* transcripts levels in section 5.2.3 were used for this experiment. Using the Mann Whitney test, transcripts level of the other *eef1a* in Del2 and Ins4 mutants were not significantly different from wild-type fish (Figure 5.5).

There is the possibility of the endonuclease activity of Cas9 to lead to random off-target mutations. The chances of this occurring are further favoured with the presence of four homologous *eef1a* genes and the use of a gRNA that targets exonic region which displays high similarities across the gene family. With this in mind, these data were also used to investigate any off-target effect of the CRISPR/Cas9 experiment involving the other *eef1a* genes. Since no significant change in the expression level of the other *eef1a* transcripts was observed, it suggests they were unaffected by the CRISPR experiment.

**A****B**

**Figure 5.5. Transcript levels of the other *eef1a* gene in *del2* and *Ins4* adult brain. A.** *eef1a111* (left), *eef1a1a* (middle) and *eef1a1b* (right) mRNA expression levels in *del2* homozygous adult brain. **B.** *eef1a111* (bottom left), *eef1a1a* (bottom middle) and *eef1a1b* (bottom right) mRNA expression levels in *Ins4* homozygous adult brain. Transcript levels of the other *eef1a* genes (normalised to three reference genes: *ATPsynth*, *NADH* and *16S*) were not significantly different compared to wild type. Results are means  $\pm$  S.E.M.; n=3 in each group.



### 5.2.6 Behavioural characterisation of homozygous *Ins4* mutant larvae

It was recently discovered in our laboratory that homozygous *Eef1a2* null mice on a pure C57BL/6 background, generated from a CRISPR/Cas9 experiment, were susceptible to audiogenic seizures. This finding was particularly interesting as epilepsy has been noted to occur in individuals with missense mutations in eEF1A2, with the mutation being *de novo* in almost all cases. Both of these findings suggest eEF1A2 to be an epilepsy susceptibility gene. I decided to investigate the susceptibility of *eef1a2* null fish to chemical-induced seizures especially as zebrafish are considered good models to study epileptic seizures in humans as they can be used for high-throughput screening for effective AEDs which has already been demonstrated by Baraban, Dinday and Hortopan, 2013 (discussed in section 1.3.3). For this experiment, pentylenetetrazole (PTZ) was chosen since it a common and well-established compound used to induce seizures in zebrafish. Also, PTZ-induced seizures in zebrafish larvae have been fully characterised and found to closely resemble seizure behaviour and changes evoked in rodents (Baraban *et al.*, 2005). Titration of five different PTZ concentrations; 1mM, 2mM, 2.5mM, 5mM and 15mM dissolved in normal E3 medium was carried out using 5 dpf wild-type larvae to identify the optimum concentration of PTZ that gives the best results of inducing a seizure phenotype in wild-type prior to performing the experiment on the mutants. The PTZ concentration at 2.5mM induced a mild increase in activity in the larvae and was selected as the working concentration. The rationale behind this was that an increase in hyperactivity by the *eef1a2* null mutants at this concentration compared to wild-type would be easily detected if a synergic effect of *eef1a2* knockout and PTZ treatment occurs. Only homozygous *Ins4* and wild-type larvae were used, as homozygous *Del2* mutants were not available at the time this experiment was conducted. Twenty four 5 dpf larvae per treatment group were placed in individual wells of a 96-well plate.

To quantify locomotor activity, zebrafish larvae were monitored using a mounted Nikon camera (Figure 5.6A) and EthoVision XT9 locomotion tracking software which was performed by Dr. Pia Lundergaard. Twenty minute baseline recordings were obtained from fish in E3 embryo medium alone. Afterward, for each genotype, 24 larvae were treated with 2.5mM PTZ dissolved in normal E3 medium and 24 larvae

maintained in normal E3 medium to serve as controls, and activity was monitored for 80 minutes divided into 4 blocks of 20 minutes. Activity did not differ significantly across the groups when in normal E3 medium after analysing the whole 20 minutes of baseline recording (Figure 5.6B). On the addition of 2.5mM PTZ, treated fish showed a marked increase in locomotor activity when compared to untreated controls (Figure 5.6C). Interestingly, a significant increase in activity was observed for 2.5mM PTZ treated Ins4 fish compared to 2.5mM PTZ treated wild-type fish in the first 20 minutes after treatment using repeated measures ANOVA. However, this difference is lost when activity is analysed for the rest of the video (Figure 5.6C). Notably, a decline in larval movement was observed in wild-type and Ins4 2.5mM PTZ treated fish from 40 to 80 minutes while untreated fish activity remained at a stable level for the entire monitoring session (Figure 5.6C).

To investigate whether these behaviours observed in the PTZ treated fish could be seizure related, the video for only the first 20 minutes following PTZ treatment was analysed by Dr. Rodanthi Lyraki who was blinded to genotype and treatment for seizure-like behaviour according to Baraban *et al*, 2005 (see section 2.2.8 for description) to obtain an unbiased result. All three stages of seizure were evoked in Ins4 and wild-type larvae treated with 2.5mM PTZ, with the least number of fish reaching stage III within 20 minutes of PTZ treatment (Figure 5.7). The latencies to the first sign of the stages of seizure-like activities were analysed for both PTZ treated group. Although all PTZ treated Ins4 and wild-type fish exhibited stage I behaviour, it was challenging for Dr. Rodanthi Lyraki, who performed the analysis, to accurately pinpoint the specific time some of them showed the first signs of stage I. Analysis of the available data using Two-way ANOVA showed no significant difference in the latency for both genotypes to show the first sign of any of the three stages of seizure behaviour scored within 20 minutes after treatment (Figure 5.7A).

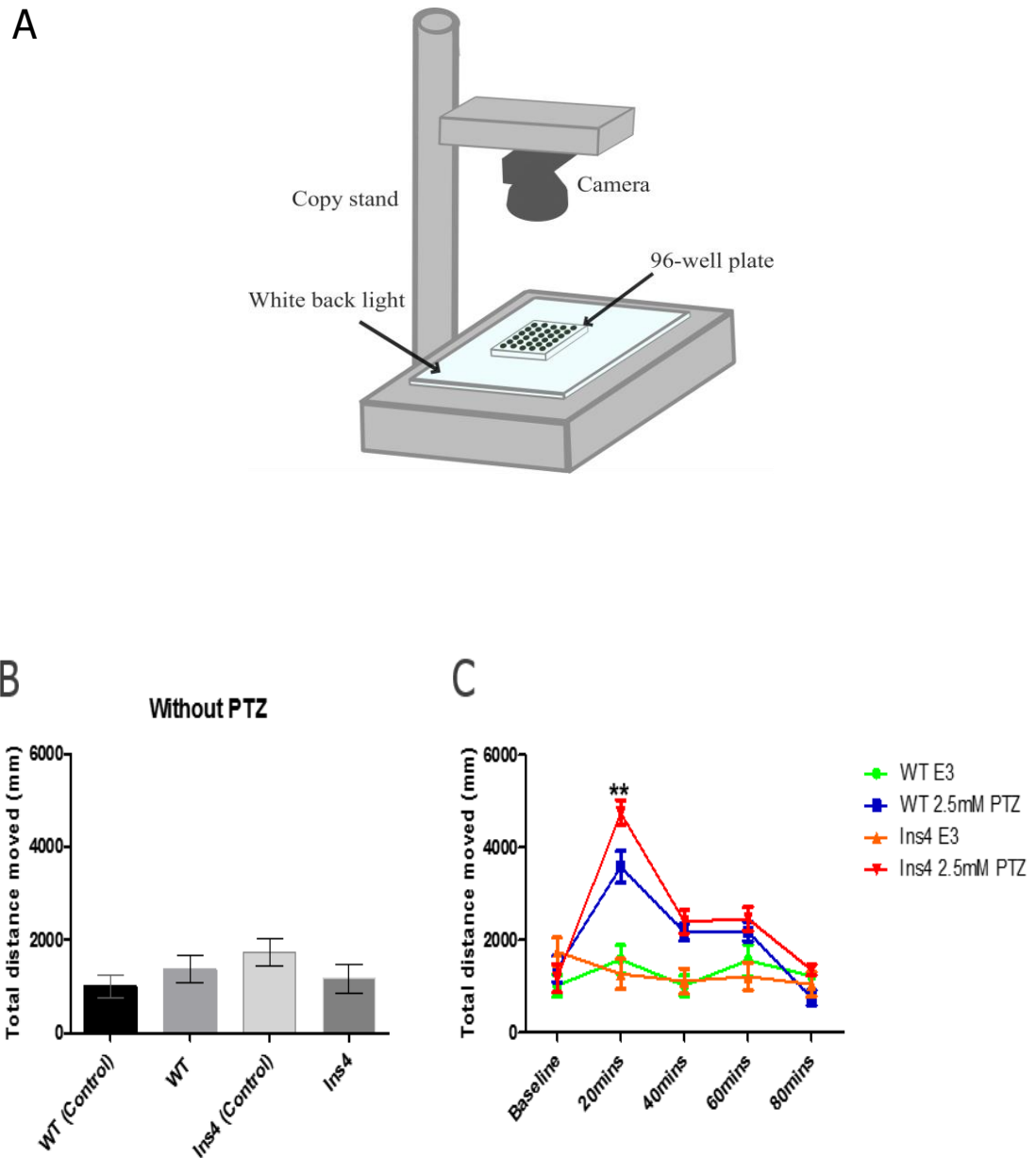


**Figure 5.6. Locomotor activity analysis of *Ins4* and wild-type zebrafish larvae exposed to 2.5mM PTZ or E3 medium.** **A.** Schematic of experimental set-up used for obtaining video recordings for analysis. **B.** Bar plot showing the average larval locomotor activity of 5 dpf *Ins4* and Wild-type larvae in E3 medium (baseline activity) over a 20 minutes period. In the absence of PTZ, no significant difference in the average total distance moved was observed among the group (One-way ANOVA,  $p$ -value 0.6). WT (control) and *Ins4* (control) were maintained in E3 medium, which was also the vehicle used in dissolving PTZ, for the entire recording sessions. **C.** graph showing the behavioural profile of larvae exposed to E3 only or with 2.5mM PTZ. The average total movement is shown per 20 minutes interval of the tracking session. \*\* is the confidence level for time point when the total distance moved for *Ins4* (2.5mM PTZ treated) was significantly increased compared to wild-type (2.5mM PTZ treated) using repeated measures ANOVA. (\*\*:  $p < 0.01$ ). Results are means  $\pm$  S.E.M.;  $n=24$  larvae per group.

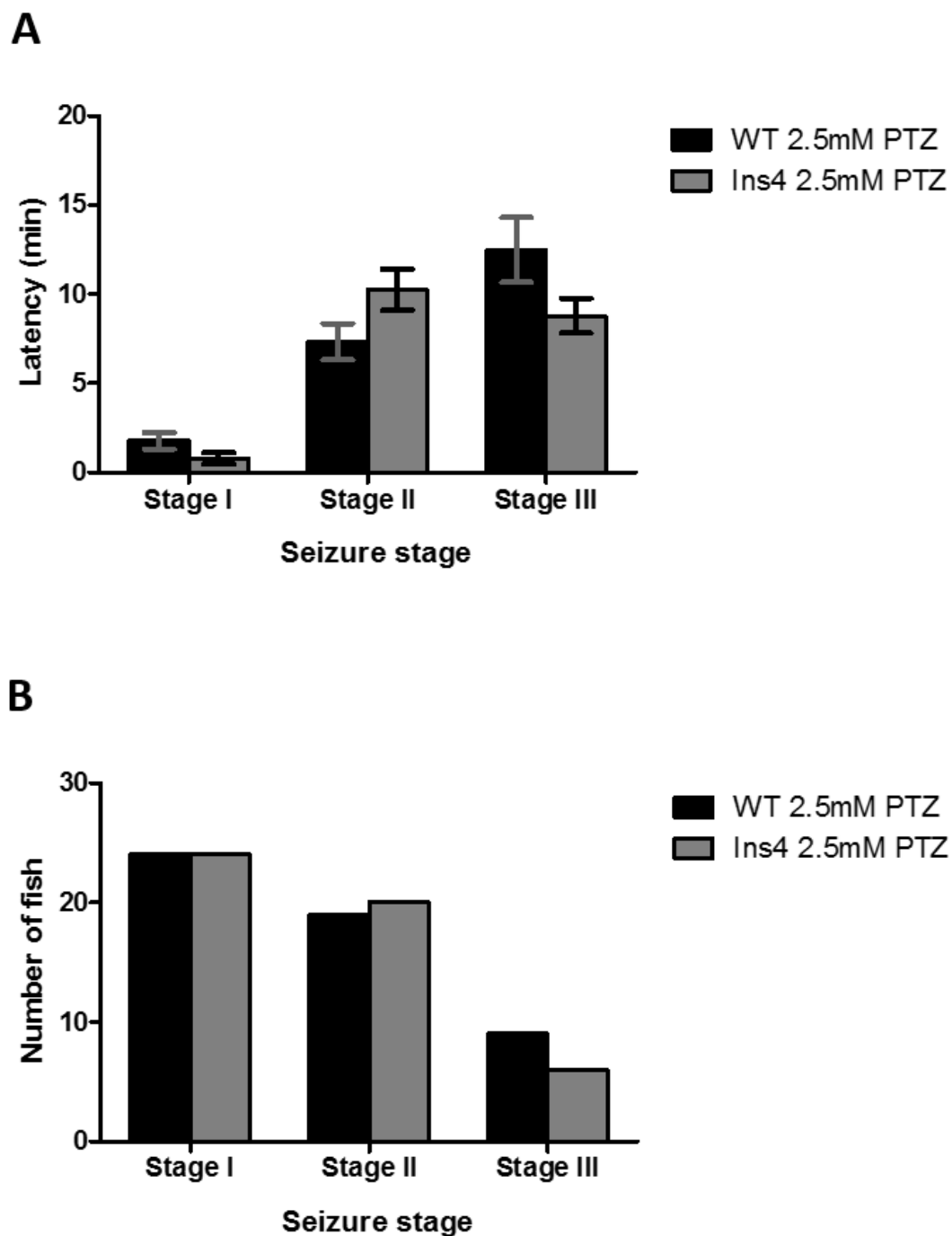


**Figure 5.7. Seizure behaviour analysis in Ins4 and wild-type zebrafish larvae.** **A.** Graph showing the latency to the first sign of seizure activity for three seizure stages in homozygous Ins4 and wild-type 5 dpf larvae after 20mins of treatment with 2.5mM PTZ. Seizure scoring was performed blind. Results are means  $\pm$  S.E.M.; n=24 larvae per genotype. **B.** graph showing number of Ins4 and wild-type larvae exposed to 2.5mM PTZ that reached each seizure stages. Note that PTZ evokes stage III behaviour at this concentration in few larvae.

### 5.3 Discussion

In this chapter, I aimed to investigate the function of *eef1a2* in zebrafish as a complementary animal model to mouse. To this end, I generated two mutant lines, namely Del2 and Ins4, using CRISPR/Cas9 technology. Both alleles are predicted to cause a frameshift mutation in exon 3 which if translated would encode a truncated polypeptide (79 and 81 amino acids long for Del2 and Ins4 respectively). However, the mRNA transcribed from both alleles is likely to be degraded through the activation of nonsense-mediated mRNA decay and would not be translated. This process is usually activated when a premature stop codon occurs early and is located  $\geq 50 - 55$  nucleotides upstream of an exon-exon junction (Broyna and Wen, 2009, Popp and Maquat, 2016) as is the case with both mutations. In line with this, Del2 and Ins4 mutant lines showed a significant decrease in *eef1a2* mRNA expression in adult brain and muscle. This does not preclude the possibility of translation re-initiation occurring downstream of the mutation. However, the 3' *eef1a2* primer set which was designed to amplify the 3' end of the gene showed a more dramatic decrease of *eef1a2* mRNA in both mutant lines, making the possibility of any other products less likely. The unavailability of a specific eEF1A2 antibody made it impossible to confirm whether these mutants were true null. Nevertheless, the findings that mutant transcripts are likely targets of nonsense-mediated decay suggests both the Del2 and Ins4 mutations are deleterious. Therefore, the *eef1a2* mutants I generated should be good models for investigating the role of eEF1A2 in disease.

In contrast to wasted mice, where complete loss of function of eEF1A2 is lethal, homozygous zebrafish *eef1a2* mutants appeared healthy and reached adulthood and showed no obvious abnormal phenotype. Adult homozygous Del2 and Ins4 mutants were fertile and produced viable embryos. With no observable phenotype displayed by fish of either the Del2 or Ins4 lines, they were further characterised for other phenotypes at the cellular level using immunohistological techniques. With the wasted mouse phenotype in mind, which has been shown to be of neurogenic origin (Doig *et al.*, 2013), a comparative analysis of the central nervous system was performed. Although Purkinje cell degeneration was shown to occur in the cerebral cortex of wasted mice by Shultz and colleagues, 1985, adult fish from both mutant lines did not show any Purkinje cell loss in the brain. It is worth mentioning, however, that this

observation by Schulz *et al.*, 1985 has not been replicated till date by other studies that have also characterised the wasted mouse model (Chambers, Peters and Abbott, 1998; Khalyfa *et al.*, 2001; Newbery *et al.*, 2005). No evidence of motor neuron degeneration was observed in the spinal cord of fish from both mutant lines, although this experiment was limited by the lack of a suitable control for gliosis.

One likely explanation for this difference could be due to species differences. As detailed in chapter 3 of this thesis, the zebrafish genome contains four *eef1a* genes that encode different closely related proteins which presumably retained the main function in protein synthesis. Also, *eef1a2* mRNA was found to be co-expressed with the other *eef1a* mRNAs. Although it was not possible to confirm this at the protein level, the apparent lack of phenotype is indicative of the possibility of paralogue redundancy and could explain why a deleterious mutation in *eef1a2* is well tolerated in zebrafish. Also, unlike mammals, the zebrafish CNS has regenerative capacity throughout its life. This confounding factor poses an obstacle especially as motor neuron degeneration is the benchmark outcome expected in the zebrafish *eef1a2* mutants. If regenerative responses are activated in these mutants, the neurodegenerative phenotypes might be subtle and easily masked by the continuous replacement of dead neurons with new ones. Interestingly, eEF1A genes have been identified to be differentially expressed during regeneration processes. A transcriptomic analysis of tail regeneration in *Anolis carolinensis* (green anole lizard) revealed eEF1A2 to be differentially expressed in the regenerating tail at the 25th day after autotomy and was upregulated 10-fold compared to lizard embryos (Hutchins *et al.*, 2014). Another study identified all four *eef1a* genes to be differentially expressed at five different time points of regeneration after crushed injury in the zebrafish spinal cord using genome-wide expression profiling technique (Hui *et al.*, 2014). From the regeneration data generated from this study, it was noted that the *eef1a* genes showed an expression pattern of up and down regulation across the five time points analysed. It is, therefore, possible that any of the *eef1a* genes could contribute to the regeneration process if this is the case. Another possible explanation could be that Del2 and Ins4 fish, unlike the wasted mice model, may not be true null mutants and may retain some degree of residual function of *eef1a2*. However, the consistency of the *eef1a2* reduction observed with three different set of primers makes it unlikely.

While this project was ongoing, a study was published where the authors suppressed *eef1a2* expression using morpholinos. Interestingly, Cao *et al*, 2017 observed skeletal muscle weakness, cardiac failure and small head phenotypes in *eef1a2* morphants. The discrepancy between my findings and those of Cao *et al*, 2017 may have to do with the different approaches used to disrupt *eef1a2* function. It is now a common occurrence that CRISPR-induced mutants fail to replicate morpholino-induced phenotypes since the development of efficient genome editing techniques in zebrafish. However, it is worth noting that the study by Cao *et al*, 2017 did not assess the possibility of an off-target mRNA effect involving another *eef1a* gene(s). It is therefore not clear if the observed phenotypes are specific to the knockdown of *eef1a2* alone or a combined effect of the knockdown of one or more of the other *eef1a* genes. It is important to note that an *eef1a111* mutant, from a large retroviral-mediated insertional mutagenesis screen, displayed a small head size (Amsterdam *et al*. 2004) which was one of the phenotypes observed in the *eef1a2* morphants in the study of Cao *et al*, 2017. Although the phenotypes observed were consistent using both translational and splice-site targeting morpholinos, it is still possible that they may have been the result of a common off-target toxic effect induced by both morpholinos. This type of situation has been demonstrated in the study by Robu *et al.*, 2007, where they observed that these two different types of morpholinos induced off-target effects mediated through p53 activation in the zebrafish embryo. Interestingly, a recent study showed that many morpholino-induced phenotypes, even though rescued by co-injecting with the wild-type mRNA, could still be due to off-target effects in zebrafish (Kok *et al.*, 2015). This study by Kok *et al*, 2015 also observed that off-target phenotypes induced by the use of morpholinos occurred much more frequently than was previously thought. This brings to light the dire need for a much better control to validate morpholino-mediated experiments. For example, validation of the morpholinos used in the Cao *et al*, 2017 study can be performed using embryos from the *eef1a2* mutant lines as a negative control. If a phenotype is observed in them, it could indicate an off-target effect and it might be possible to use these mutants background to identify the best concentration of the morpholinos that would not lead to off-target effects. Another validation approach is to check for p53 mRNA induction in the morpholino- injected

embryos as this usually points to the activation of non-specific effects by the morpholinos (Robu *et al.*, 2007).

On the other hand, CRISPR/Cas9 has been shown to have negligible off-target effects in zebrafish. Using next-generation sequencing (NGS), Hruscha *et al.*, 2013 demonstrated that the off-target effect was limited in founder fish. This study was small, analysing the gRNA target site for only one gene, but only 2.2-2.5% of all the reads were found to have mutations at the predicted off-targets in the pool of ten individual embryos injected with the gRNA (Hruscha *et al.*, 2013). Their observation of the limited off-target effect of CRISPR experiments in zebrafish was supported by another larger study. In this study, they analysed the target sites for five gRNAs of different genes. They performed NGS using PCR products pooled from five predicted off-target sites for each gRNA and detected a 3 base pair deletion in only one of the 25 off-target loci tested (Varshney *et al.*, 2015). Although no off-target sites were found for gRNA3, which was used to generate the mutant lines, by the online CRISPR design tool, CHOPCHOP at the time it was accessed, there is still the possibility of random off-target mutations at other sites particularly as annotation of the zebrafish genome is still work in progress. The presence or absence of these off-target mutations can be assessed in Del2 and Ins4 mutant lines by amplifying and sequencing DNA from regions with the highest homology to the target site of gRNA3. I did not analyse the Del2 and Ins4 lines for potential off-target mutations, but my use of fish starting from the F2 generation resulting from an outcross of the F0 with wild-type fish should minimise the possibility as these unintended mutations would segregate away from the Del2 and Ins4 *eef1a2* mutation. Also, evaluation of the other *eef1a* mRNAs levels in Del2 and Ins4 mutants were not significantly different when compared to wild-type fish. This provides strong evidence to suggest that *eef1a2* paralogues were not affected by the CRISPR/Cas9 experiment.

Another possible explanation for the inconsistencies could be that these two strategies induce different responses to *eef1a2* gene inactivation in zebrafish. For example, a study by Rossi *et al.*, 2015 found that severe mutations induced by a knockout approach, as is the case with Del2 and Ins4 mutants, resulted in compensatory upregulation of specific proteins which could account for the phenotypic rescue observed in knockdown experiments. Although the mutant lines I generated did not



show upregulation of the *eef1a2* paralogues suggesting no compensation occur in adult tissues at the mRNA level, this does not completely rule out this possibility. Perhaps there might be some compensation at the levels of specific cells, or during a critical developmental period in the fish or upregulation of these other *eef1a* genes occur at the protein level instead which will not reflect from analysing mRNA levels. Further experiments are needed to draw a conclusion on whether or not a compensatory response is activated in the mutant lines. However, this supports the idea of functional redundancy of *eef1a* genes as the more likely mechanism at play to compensate for the loss of *eef1a2* in Del2 and Ins4 mutants.

The identification of eEF1A2 as a likely epilepsy susceptibility gene in human and a recent observation in our laboratory of homozygous *Eef1a2* null mice showing vulnerability to audiogenic seizures prompted a behavioural analysis in the mutant lines. To test if *eef1a2* null fish were sensitised to seizure, 2.5mM PTZ was applied directly to the bathing E3 medium of the fish. Locomotor activity was found to significantly increase in 2.5mM treated 5 dpf homozygous Ins4 and wild-type larvae within 20 minutes after treatment compared to their baseline activity and to untreated fish. Homozygous Ins4 fish showed a significant increase in locomotor activity compared to wild-type when treated with 2.5mM PTZ in the first 20 minutes. Activity was not significantly different between the groups at the other time points. Interestingly, studies by Afrikanova *et al.* 2013 has shown that combining larval activity over longer time points could mask a subtle effect when performing the locomotor assay. Seizure analysis showed Ins4 and wild-type demonstrated all three stages of seizure behaviour within the first 20 minutes. The decline in total larval movement in both groups between 20 and 80 minutes could likely be as a result of the majority of treated larvae spending time in stage 3 with prolonged exposure to PTZ. This will result in a loss of posture and a subsequent decrease in swimming activity in those larvae. A similar trend was observed in the studies by Afrikanova *et al.* 2013. It was surprising to observe stage 3 behaviour using PTZ at a lower concentration (2.5mM) since this stage was reported in studies that routinely used a much higher PTZ concentration of 15-20mM (Baraban *et al.*, 2005; Afrikanova *et al.*, 2013). However, only a few larvae (about 37% and 25% wild-type and Ins4 respectively) exhibited stage 3 behaviour within 20 minutes of PTZ treatment compared to studies

of Baraban *et al.* 2005 (nearly 75%). As shown in these studies and initial pilot experiments I carried out, higher concentrations of PTZ induces a more severe and robust seizure activity within a short time frame, which will not allow the difference in PTZ response of wild-type and mutant larvae to be detected. One possible factor that could influence the outcome of this study is strain difference, with Baraban *et al.* 2005 and Afrikanova *et al.* 2013 using TL and Ekkwill fish respectively, whereas I used AB fish for this work. Another possibility could be the experimental protocol employed here. For example, in contrast to both studies, I performed this assay under constant light (as opposed to constant darkness in these other studies) due to the available apparatus and used younger larvae at 5 dpf (7 dpf, Baraban *et al.* 2005; 6 dpf, Afrikanova *et al.* 2013) since they are not regulated and do not require a license to work with. Although the nature of my experimental set-up could make the fish more vulnerable to external stimuli, the activity of untreated fish did not differ significantly for the entire recording sessions. Also, the stable level of activity of untreated fish was in line with the expected swimming pattern of zebrafish larvae tracked under constant light (MacPhail *et al.*, 2009). This suggests that the effect of unwanted external stimuli, if any, was negligible and did not greatly influence the outcome of the experiment.

The significant increase in locomotor activity observed in Ins4 larvae compared to wild-type within 20 minutes after PTZ treatment could indicate Ins4 larvae are spending more time in stage 1 and stage 2 or are more sensitised to PTZ-induced seizures, and hence move more during a seizure. It is tempting to assume the latter as the most likely reason particularly as stage 1 behaviour was more easily recognisable for Ins4 (21 out of 24) than wild-type (14 out of 24) by Dr. Lyraki who was blind to the genotype. However, a more detailed analysis of the 20 minutes tracking session into short intervals, for example, 5 minutes, will be valuable to better understand the kinetics of their response to PTZ more precisely. However, bearing in mind that only one mutant line; Ins4 was used to perform this assay, it is important that the PTZ-assay is first repeated using the Ins4 and also the Del2 mutant line. Furthermore, potential off-target events should be assessed in both mutant lines to ensure no other loci were affected by the CRISPR/Cas9 experiment. If after performing these experiments, seizure susceptibility is still observed, this could demonstrate a likely predisposing effect of the loss of function of *eef1a2* in zebrafish. A similar effect was seen in our

laboratory where homozygous *Eef1a2* null F0 mice generated from a CRISPR/Cas9-mediated HDR experiment were susceptible to audiogenic seizure in response to environmental sound (Davies *et al.*, 2017). Both of these models; mice and zebrafish, could then be used for complementary studies to understand the underlying mechanism by which mutation in eEF1A2 results in epilepsy. Drug screening with the zebrafish mutant lines can also be performed to identify efficient AEDs.

## Chapter 6: Summary and future directions.

### 6.1 Summary

The unequivocal role of eEF1A2 in neurodevelopment was first evident in the wasted mouse model. More recently, missense mutations in eEF1A2 have also been identified in WES data obtained from about 50 patients with severe cases of neurodevelopmental disorders. Up until now, work in our laboratory has focused on the use of mice and cell lines as model systems to better understand the relationship between eEF1A2 and neuronal diseases. With the mounting evidence of the utility of the zebrafish in neuroscience research, this animal was chosen as a model to be used for further complementary studies, with particular interest in its high-throughput screening capacity as a whole organism which is quick, easier and cost-efficient compared to rodents (Kalueff *et al.*, 2014).

#### 6.1.1 Bioinformatics and expression analysis of Zebrafish eEF1A

The first step taken to determine if the zebrafish was an appropriate model for research into eEF1A2 was to re-evaluate information on eEF1A genes in zebrafish, as previous literature worked on the premise that only one eEF1A was present in its genome. Using bioinformatics and gene expression analysis, I showed that the zebrafish has four eEF1A genes; *eef1a1ll*, *eef1a1a*, *eef1a1b* and *eef1a2*. While *eef1a1ll* did not have an orthologue in the human genome, *eef1a1a* and *eef1a1b* were identified as the co-orthologues of the human *EEF1A1* gene. In addition, *eef1a2* was identified as the orthologue of the human *EEF1A2* and the two were shown to be 94% identical at the amino acid sequence level. *In silico* functional analysis of the zebrafish eEF1A isoforms suggest that they all share a similar translational function but could likely have other functional differences between them. In support of this finding, isoform-specific phosphorylation sites were predicted for each eEF1A isoform which could further strengthen their functional differences. The eEF1A genes were developmentally regulated as their expression was detected at different developmental stages. Consistent with the expression pattern of the mammalian eEF1A2 gene, *eef1a2* was expressed much later than the other *eef1a* genes in development, around 48hpf. Although it is difficult to directly compare developmental stages between the zebrafish

and mammalian species, *eef1a2* could be regarded as the ‘adult’ form of the eukaryotic elongation factor in zebrafish as is the case for eEF1A2 in mammals (Knudsen *et al.*, 1993; Lee, Wolfrain and Wang, 1993; Chambers, Peters and Abbott, 1998; Khalyfa *et al.*, 2001; Svobodová *et al.*, 2015).

I also investigated the expression pattern of the *eef1a* genes in adult fish using a range of adult tissues. The zebrafish *eef1a2* appear to have a tissue-specific expression pattern as it was not detected in the liver, another feature it has in common with eEF1A2 gene in mammalian species. However, one difference between eEF1A from these species, is that the zebrafish *eef1a2* transcripts were detected in some other tissues such as the spleen and ovary which are negative for eEF1A2 expression both at the mRNA and protein level in mammals (Khalyfa *et al.*, 2001; Anand *et al.*, 2002; Newbery *et al.*, 2007; Svobodová *et al.*, 2015). Since I was unable to determine expression of eEF1A2 at the protein level in these tissues, it is still unknown if these transcripts are actually translated in which case, a conclusion could be made on whether the zebrafish eEF1A2 shows a completely different expression pattern from that of mammals. Another difference was observed with the expression pattern of the eEF1A1 orthologues. In zebrafish, expression of *eef1a1a* and *eef1a1b* mRNA was noted in all the adult tissues analysed including muscle which is known to be negative for their mammalian orthologue. However, this is consistent with the *Xenopus* eEF1A expression pattern at the mRNA level, where regulation of eEF1A occurs at the post-transcriptional level instead (Helen J. Newbery *et al.*, 2011). Since eEF1A isoform switching is biologically important as it appears to be evolutionarily conserved in vertebrates, it is most likely that this also occurs at the translational level in the zebrafish. Unfortunately, I was unable to test this hypothesis due to the lack of specific antibodies for each of the eEF1A proteins. However, the results from the analysis of the specificity of antibodies against eEF1A2 demonstrate the value of validating commercial antibodies even if advertised as specific for a particular species, before using them for further investigation.

Another key difference is the presence of an eEF1A gene, *eef1a111*, which has no corresponding orthologue in mammalian species. My expression data suggests this gene to be the ‘embryonic’ form of the eukaryotic elongation factor in zebrafish. Furthermore, *eef1a111* transcript is the major form detected in the adult muscle and

liver tissues, in contrast to mammalian species where only eEF1A2 and eEF1A1 are expressed in the mature adult muscle and liver tissue respectively. It is possible that eEF1A1L1 has some of the non-canonical functions in common with these other eEF1A isoforms. However, equivalent amounts of each *eef1a* transcripts were noted in adult brain tissue. Since brain tissue is made up of a more heterogeneous cell population than liver and muscle, it is also possible that there are other isoform-specific ‘moonlighting’ functions between the zebrafish eEF1A isoforms. It is however worth noting that this results are based on the mRNA expression of the eEF1A isoforms and should be confirmed at the protein level.

All the findings presented here suggest that functional diversification might have occurred among the zebrafish eEF1A isoforms while presumably retaining their main role in protein elongation, which is somewhat similar to the case of the eEF1A isoforms in mammals. These additional functions could be biologically important and confer some evolutionary advantage in the zebrafish, which could explain why all four eEF1A isoforms were positively selected for their maintenance in its genome. Studies by Kinoshita *et al.*, 2001 also showed two eEF1A gene was present in medaka (*Oryzias latipes*) which displayed a tissue and stage-specific pattern of expression. In the flatfish (*Solea senegalensis*), five eEF1A genes were isolated which also showed differential expression in ten different tissues examined and during larval development (Infante *et al.*, 2008). One of the eEF1A genes, termed *SseEF1A4*, was suggested to have a role in metamorphosis as its expression was upregulated by thyroid hormones in larvae. More recently, a heterozygous mutation of eEF1A1B in tilapia (*Oreochromis niloticus*) has been demonstrated to give rise to viable fish but caused spermatogenesis arrest and infertility in males (Chen *et al.*, 2017).

### **6.1.2 Modelling an eEF1A2 disease-causing mutation in zebrafish**

I attempted to knock-in the G70S epilepsy causing mutation in the zebrafish eEF1A2 using a gRNA originally generated and used in creating eEF1A2 null zebrafish. Unfortunately, I was unable to identify any fish with the G70S encoding mutation incorporated and most of the mutants carried indel mutations. The high rate of indel mutations is in itself not surprising, considering they are generated by the NHEJ pathway which occurs at a much higher rate than HDR (Dai *et al.*, 2010; Li *et al.*,

2015). However, together with the low efficiency of the knock-in, this posed a challenge in the screening process to identify any point mutations. Low HDR efficiencies and the high rate of indel mutations are common pitfalls in CRISPR/Cas9-mediated HDR in zebrafish (Armstrong *et al.*, 2016; Zhang, Zhang and Ge, 2018). It is, therefore, necessary to determine optimum conditions that will combat these two factors. The recent CRISPR/Cas9-mediated HDR protocol for zebrafish described by Zhang *et al.* 2018, seems to show more promise as it is the only study that has reported a high efficiency. Another attractive feature of Zhang *et al.* 2018 study is that it was also designed to make screening for the point mutation a less challenging task by generating specific primers that only amplified the HDR-induced mutation, which is useful if one's efficiency is not as high as was obtained in their study. Since this protocol shows some promise, it will be a good starting point to attempt another knock-in experiment in the zebrafish. However bearing in mind the lack of reproducibility of other studies which have also demonstrated the successful use of the CRISPR-Cas9 technique for HR in zebrafish, it should be tested first with only one eEF1A2 epilepsy-causing mutation. Once a working protocol is obtained and the protocol optimised, generating mutant lines with the other missense mutations would be worthwhile since it is possible they may perturb function via a different mechanistic pathway.

If I were able to generate a G70S zebrafish mutant, I would characterise this mutant line with a focus initially on seizure activity, which is an easier and more valid human-relevant phenotype to model in the zebrafish and can be performed in the first instance on larval stages which are not regulated. This can be achieved by using automated video locomotion tracking devices to screen for seizure-like behaviours as well as using electrophysiology to look for spontaneous electrographic seizure discharges. If these mutants do not exhibit spontaneous seizure behaviours, seizure susceptibility can also be investigated using the PTZ-induced seizure assay (Baraban *et al.*, 2005). It will also be interesting to carry out a microarray-based transcriptomic analysis to identify if any differentially expressed genes including the other eEF1A genes, which could compensate for the loss of eEF1A2 function, occur in the mutants. This could also provide insights into the molecular pathways underlying the epileptic phenotypes. Another epilepsy-causing mutation I would like to generate and characterise alongside the G70S in zebrafish is the D252H mutation. The advantage of generating these two

mutant lines is that they will be useful for further complementary studies since the G70S and D252H mutation have already been modelled in mouse (Davies *et al.*, 2017 and unpublished data) and LUHMES cells (only D252H in LUHMES) in our laboratory. This will hopefully contribute immensely to disentangling the role of eEF1A2 in epilepsy and ultimately to provide better treatment strategies especially as they can be employed for high throughput screening of different small molecules.

### **6.1.3 Generation and characterisation of *eef1a2* null zebrafish model**

Having confirmed the presence of an eEF1A2 orthologue in the zebrafish, it was essential to investigate the function of this gene in the zebrafish and determine if loss of function mutation of *eef1a2* would result in a similar phenotype to that seen in wasted mice, a well-characterised model for early onset motor neuron degeneration. For this purpose, I generated two mutant lines, Del2 and Ins4, using CRISPR/Cas9 gene editing. Although I was unable to confirm these lines as true nulls because of the lack of a specific antibody against eEF1A2, a marked decrease of *eef1a2* at the mRNA level was noted in both lines, suggesting these mutations could lead to a loss of function similar to that seen in the wasted mouse. However, my results show that loss of *eef1a2* does not lead to any obvious defects and that the fish are viable as adults. No evidence of neurodegeneration was noted in the spinal cord as assessed using immunohistological examination. I have proposed at least three possible confounding factors that could explain this discrepancy; (i) Del2 and Ins4 might not be true nulls as seen in wasted mice and could retain some residual eEF1A2 function (ii) the presence of multiple *eef1a* genes, any of which could compensate for the loss of *eef1a2* as they are co-expressed at the mRNA level leading to redundancy and (iii) the ability of the zebrafish CNS to regenerate throughout its life which could mask any neuronal loss caused by these mutations.

One mutant line, Ins4, was characterised behaviourally and was found to show significant susceptibility to PTZ-induced seizures compared to their wild-type siblings. As I was unable to carry out a complementary testing using the Del2 line in the seizure behaviour analysis, caution must be taken when interpreting this results. However, this finding seems to corroborate a recent observation in our laboratory, where eEF1A2-null mice showed susceptibility to audiogenic seizures which resulted



in the death of these mice (Davies *et al*, 2017). It is, therefore, possible that the seizure phenotypes observed in humans are mediated by conserved mechanisms in these other species. If this is the case, further complementary studies with the zebrafish and mice models will be invaluable in future research.

## **6.2 Future directions**

### **6.2.1 Potential of using the zebrafish and its eEF1A isoforms to understand the functions of eEF1A in vertebrates**

The fundamental question as to why there are two eEF1A isoforms with very high sequence identity in mammals has remained unanswered. Resolving this question could likely help us understand how mutation or dysregulation in the expression of eEF1A2 causes disease. The most reasonable explanation for the existence of different isoforms is the presence of some other isoform-specific non-canonical functions that may be suitable for only certain cells types or at certain developmental stages. Results from characterising the zebrafish eEF1A genes have shown that some features are conserved with mammalian species and could offer insights into understanding the functional differences within the eEF1A family. However, one important feature that will be interesting to confirm in the zebrafish is the occurrence of eEF1A isoform switching in different tissues. With evidence that this process is a biologically important one demonstrated by its conservation in different vertebrate species (Lee, Wolfrain and Wang, 1993; Chambers, Peters and Abbott, 1998; Helen J. Newbery *et al.*, 2011; Svobodová *et al.*, 2015), it is tempting to assume that this is also the case in the zebrafish. We hypothesised that similar to what was observed in the *Xenopus* (Newbery *et al*, 2011), this process will occur at the translational level if it does occur in the zebrafish. Generation of isoform-specific antibodies will be invaluable for testing this hypothesis since any switch will not necessarily be reflected in the expression pattern at the RNA level. Determining which tissue type and the point of development where this switch occurs could contribute towards providing an answer to the question above.

Further investigation into the expression pattern of the zebrafish eEF1A isoforms at the cellular level is also required to shed more light on these ‘moonlighting’ functions.

If isoform-specific antibodies could successfully be generated, they could also be used for immunohistochemistry (IHC) or immunofluorescence examination of different tissues to determine cell type-specific expression and also the subcellular localisation of the different isoforms. However, generating specific antibodies for these eEF1A isoforms can be a challenging task due to their sequence similarities and there is the possibility, they may be specific for Western blotting but not IHC applications from experience in our laboratory. Alternatively, individual cell types could be isolated from zebrafish transgenic lines expressing different fluorescent protein reporters in any of the tissue types using fluorescence-activated cell sorting (FACS) assay. These predefined cell populations could then be used for subsequent gene expression analysis using techniques such as qRT-PCR or Western blotting if specific antibodies are available. More recently, large scale single-cell RNA sequencing (scRNA-seq) is being explored with data generated from different embryonic stages in the zebrafish currently available (Farrell *et al.*, 2018; Wagner *et al.*, 2018). I examined the datasets from these two studies, but none of the *eef1a* genes was found. Although scRNA-seq is more expensive than ISH, it offers the opportunity to generate transcriptome-wide data of individual cells and will facilitate the exploration of different developmental stages and adult tissues compared to ISH. This may be useful in constructing an atlas of the expression patterns and the dynamics of the eEF1A genes in adult fish in future, as well as being able to examine other known interacting partners at a single-cell resolution.

Differences in the PTMs between eEF1A1 and eEF1A2 isoforms have been noted and could likely contribute to the functional divergence of these proteins. Mapping of these PTM sites, both from experimental and predicted studies, to the modelled 3-D structures showed they are mostly present on the surfaces with clusters of sequence variation between the isoforms suggesting the proteins are differentially regulated (Soares and Abbott, 2013). Using the NetPhos 3.1 server (Blom, Gammeltoft and Brunak, 1999), I was able to predict likely phosphorylation sites for the zebrafish eEF1A isoforms. While these isoforms share some of the predicted sites, likely unique sites were also noted for each of them. Bearing in mind the possibility of predicting some false-positive sites using this method, it would be ideal to compare predicted sites for the zebrafish eEF1A isoforms to that of human to select candidate sites for

further investigation in the first instance. One candidate site that may be suitable for future studies is the Ser300 predicted to be phosphorylated in the zebrafish eEF1A1A, eEF1A1B and eEF1A2. Although these sites have a borderline NetPhos probability score of 0.5, these sites are readily accessible by a kinase on the modelled structure and Ser300 has been experimentally confirmed in eEF1A1, thus increasing the confidence of the prediction. Phosphorylation of Ser300 by type 1 TGF- $\beta$  receptor (T $\beta$ R-1) has been demonstrated to interfere with the binding activity of aminoacylated-tRNAs in eEF1A1, thus inhibiting protein synthesis and cell proliferation (Lin *et al.*, 2010). Although eEF1A111 was not predicted to be phosphorylated at this site, it has a threonine residue at this position which can also interact with a kinase. To test that this is not a false- negative site, it should also be investigated. Another site that might have implications for the translation rate is Ser298 (in eEF1A2 and eEF1A1L1) since it lies very close to residues involved in eEF1B $\alpha$  and aminoacyl-tRNA binding. This position is also equivalent to Gln296 in yeast, which has been implicated in actin-related functions (Gross and Kinzy, 2007), therefore phosphorylation could potentially affect actin-eEF1A interaction(s) as well. It is interesting that opposite these two sites (298 and 300) is an exposed and most likely phosphorylatable eEF1A1L1 specific site (>0.84 probability score), Thr303, which could perhaps help with understanding the role of both sites and is therefore worth further investigation. Other sites that could also be considered and have experimental support include: Ser21 and Thr88, which modulate the stability of eEF1A (Sanges *et al.*, 2012) and Ser358, a phosphorylation site on eEF1A2 but not eEF1A1 in both zebrafish and human, in which it has been shown to have a role in stress-induced quality control of newly synthesized polypeptides (Gandin *et al.*, 2013). Further studies of these sites could contribute towards understanding how eEF1A switches between its main role in protein translation to other non-canonical functions. This will be particularly useful in understanding the functional difference between eEF1A isoforms in human and perhaps provide insights on some disease related to them, for example, the oncogenic ability of eEF1A2.

Confirmation of the phosphorylation status of these sites can be achieved using mass spectrometry. It will also be useful to generate phosphorylation mimics by mutating Ser or Thr to either Glu or Asp (phospho-positive) and also to a non-phosphorylatable residue such as alanine (phospho-negative) to determine if similar functional

significance occurs with the zebrafish. If these sites are validated as true phosphorylation sites, *in vitro* kinase assays should be performed to establish if phosphorylation is mediated by the same kinase. If the expected results are observed after these experiments, phospho-specific antibodies could be raised and used to determine if the eEF1A isoform is phosphorylated *in vivo* in the zebrafish. It will also be interesting to determine if the genes encoding these kinases are expressed at the same time as the eEF1A isoforms. Similar experiments as outlined above could also be performed for some of the isoform-specific sites predicted with high confidence as indicated with the NetPhos score >0.5 (Table 3.3 in chapter 3) with the hope that these could contribute to the evolutionary understanding of the eEF1A family in vertebrates.

### **6.2.2 Translational validity of the *eef1a2* mutant lines for neurological diseases**

With the aim of using the zebrafish for drug discovery studies, I generated two lines with different deleterious mutations in *eef1a2*. Since the role of *eef1a2* in zebrafish was unknown during the course of this project, phenotyping of the mutant zebrafish lines was carried out using the wasted mouse model as a guide. However, the severe phenotypes such as motor neurodegeneration of the spinal cord in the wasted mouse model were absent in both mutant lines which were viable and fertile as adults. Further experiments are still required which might elucidate the reason behind the discrepancy between these models. I have outlined above three possible factors that could be responsible and will require further investigation as understanding the reason for the different phenotypes will contribute towards the validation of these models for neurological diseases.

Generation of specific antibodies could help establish whether these models are true nulls as they could be used to perform Western blot analysis to detect the presence of any residual protein. Alternatively, Del2 and Ins4 could be further characterised to confirm that their transcripts are indeed targets of NMD as suggested by the qRT-PCR results (see Figure 5.3 in chapter 5). Expression of Del2 and Ins4 alleles could be evaluated *in vitro* by generating constructs for each allele. These constructs should then be separately transfected into cell lines and their expression measured using Western blotting. Since there is the possibility of the antibody cross-reacting with the

endogenous eEF1A, expressing the mutant cDNA with a tag protein would allow the effect of the mutation to be easily detected. The wild-type *eef1a2* construct generated during this project would serve as a useful positive control for this experiment. If the protein from cells transfected with the mutant constructs is mostly absent, this will confirm the severity of these potential null alleles.

The presence of multiple *eef1a* genes in the zebrafish genome encoding separate proteins with almost identical amino acid sequence and presumably functional equivalence in translation might imply functional redundancy occurring in both mutant lines. At the same time, it also poses a challenge to determine which isoform(s) could be playing this compensatory role. While the suggested future work described in section 6.2.1 could help identify the isoform(s) responsible, a systematic analysis of the compensatory effect of the other *eef1a* genes could also be performed. Loss of function mutations should be induced using similar CRISPR/Cas9 technique described herein in both Del2 and Ins4 lines and the phenotypes compared to the *eef1a2* mutant lines. Bearing in mind that eEF1A1L1, which appears to share some features with eEF1A2, is the only eEF1A present in the zebrafish during early development, global loss of *eef1a1ll* could likely be embryonic lethal as observed in the study of Amsterdam *et al.* 2004. To overcome this caveat, the generation of a time-dependent conditional knockout (Maddison, Li and Chen, 2014) should be considered.

The regenerative capacity of the zebrafish CNS imposes a major drawback in developing any zebrafish model of neurodegeneration. Since motor neurodegeneration in the spinal cord is a benchmark outcome, this phenotype might be subtle in the mutant lines if these dead neurons are constantly replaced. For this reason, a good positive control is important for the immunohistological assay with GFAP which I used in phenotyping these lines. Another alternative to the GFAP-immunostaining would be to perform a choline acetyltransferase (ChAT) immunostaining instead on spinal cord sections. The total number, as well as the size of ChAT-positive motor neurons, could then be quantified and compared between the mutant and wild-type fish. Generally, the smaller the motor neuron, the younger it is thought to be, as it gets larger with maturation (Da Costa *et al.*, 2014). If a decrease in the number of large (mature) ChAT-positive motor neurons are observed in the mutant fish spinal cord, this could suggest that neuronal loss occur in them as well. However, if the rate at

which neurons are lost is similar to that at which they are replaced, performing these immunohistochemical analyses with fish that are more than 24 months, when a decline in neurogenesis and regenerative response is expected (Fleisch, Fraser and Allison, 2011), may be best to make it easier to detect any neuronal death in the mutant lines. Alternatively, cell death assays that involve staining with fluorescent markers for neuronal death such as TUNEL or Fluoro-Jade can be performed on mutant larval and younger adult stages as it is usually difficult to breed fish beyond 24 months without a project license. Both of these assays are simple, quick and well-established techniques for qualitative and quantitative assessment of neurons undergoing apoptosis. If more cells stained with either of these dyes are observed in the mutant lines, this would suggest they are undergoing an increased rate of neuronal death than that seen in WT fish. Data from the cell-specific expression analysis of the eEF1A isoforms in the zebrafish CNS will also be extremely useful in this regard. If a cycle of degeneration and regeneration is noted, these mutant lines will be an invaluable model to dissect the underlying molecular and cellular pathways involved in replacing dead neurons during disease progression, and perhaps identify potential therapeutic targets for degenerative diseases.

Finally, the observation that loss of eEF1A2 in zebrafish might make them susceptible to chemical-induced seizures is worth exploring further, especially as it is in line with findings in our laboratory with eEF1A2 null mice models (Davies *et al.*, 2017). Since I was only able to use the Ins4 lines for this experiment, it will be interesting to follow this up using both mutant lines; Del2 and Ins4, to confirm if indeed the seizure phenotype is caused by a mutation in *ee1a2*. Although the set-up I used to carry out this assay did not appear to be affected by other external stimuli, it might be worth repeating this experiment using the automated larval tracking devices, for example, DanioVision<sup>TM</sup> ([www.noldus.com](http://www.noldus.com)). This would ensure the testing environment is uniform for all rounds of biological replicates performed and an unbiased qualitative and quantitative behavioural analysis could be obtained. Using this equipment, Ins4 and Del2 mutant larvae could also be exposed to other forms of epileptogenic stimuli in a controlled manner. For example, an in-built tapping device could be used to provide sound/vibration stimulus especially as eEF1A2 null mice were observed to show susceptibility to audiogenic seizure in our laboratory (Davies *et al.*, 2017). Visual

stimulus can also be employed by varying the lighting conditions providing alternating cycles of light and dark conditions. This is similar to flashing light which is the most common trigger for reflex seizures. Mutant larvae could be exposed to these stimuli alone and/or in combination with PTZ treatment and analysed for any difference in seizure behaviour compared to wild-type larvae.

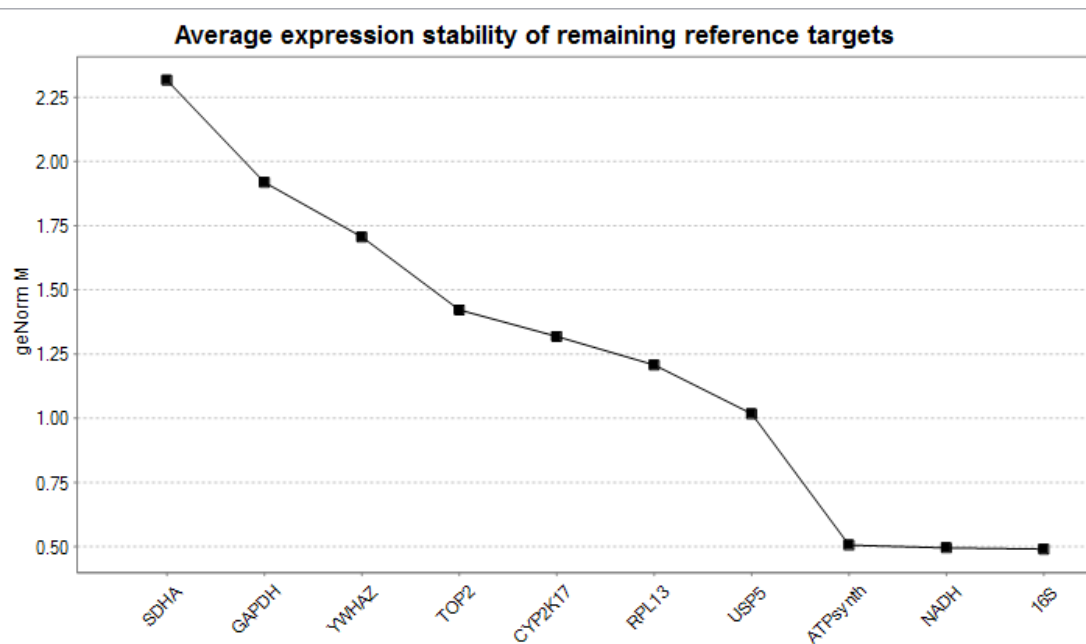
Depending on the outcome, it might be worth performing other seizure analysis assays as the locomotor assay may not be robust enough (Afrikanova *et al.*, 2013; Ingebretson and Masino, 2013) even though it served as a useful easy and quick initial screening tool for seizure activity. Alternatively, the epileptiform activity can be monitored by taking extracellular recordings from the brain of larval fish exposed to PTZ (Baraban *et al.*, 2005, 2007; Afrikanova *et al.*, 2013). Electrophysiological recordings obtained from larval zebrafish brain is comparable to electroencephalographic (EEG) monitoring which is the gold standard for the diagnosis of seizures (Baraban, 2013). This provides a more sensitive readout for seizure-like behaviour compared to using locomotor activity, however, it cannot be performed in a high-throughput multiwell-format as the locomotor assay. Abnormal brain activity can also be monitored by analysing expression levels of *cfos*, a robust marker for neuronal activity, using qPCR or *in situ* hybridisation assays in PTZ-treated larvae (Baraban *et al.*, 2005; Baxendale *et al.*, 2012). Establishing Del2 and Ins4 lines expressing a genetically encoded calcium indicator marker such as GFP-Calmodulin fusion protein (GCaMP) will enable the spatiotemporal visualisation of neuronal activity *in vivo* within the larval CNS. A new GCaMP variant known as NBT:GCaMP3 has recently been developed that allows the *in vivo* visualisation of neural activity in the CNS of larval stages up to the age of 21 dpf (Bergmann *et al.*, 2018). Electrophysiological analysis can also be performed on both transgenic mutant and wild-type PTZ-treated larvae to obtain a quantitative neural activity measurement *in vivo*. If my initial observation of susceptibility of the mutant larvae to PTZ-induced seizure is confirmed using any of the approaches described above, the *ee1a2* mutant lines will serve as an invaluable tool to be used to elucidate the mechanisms of epilepsy and an *in vivo* platform for high-throughput screens for better and safer AEDs for these patients.

## **6.3 Conclusion**

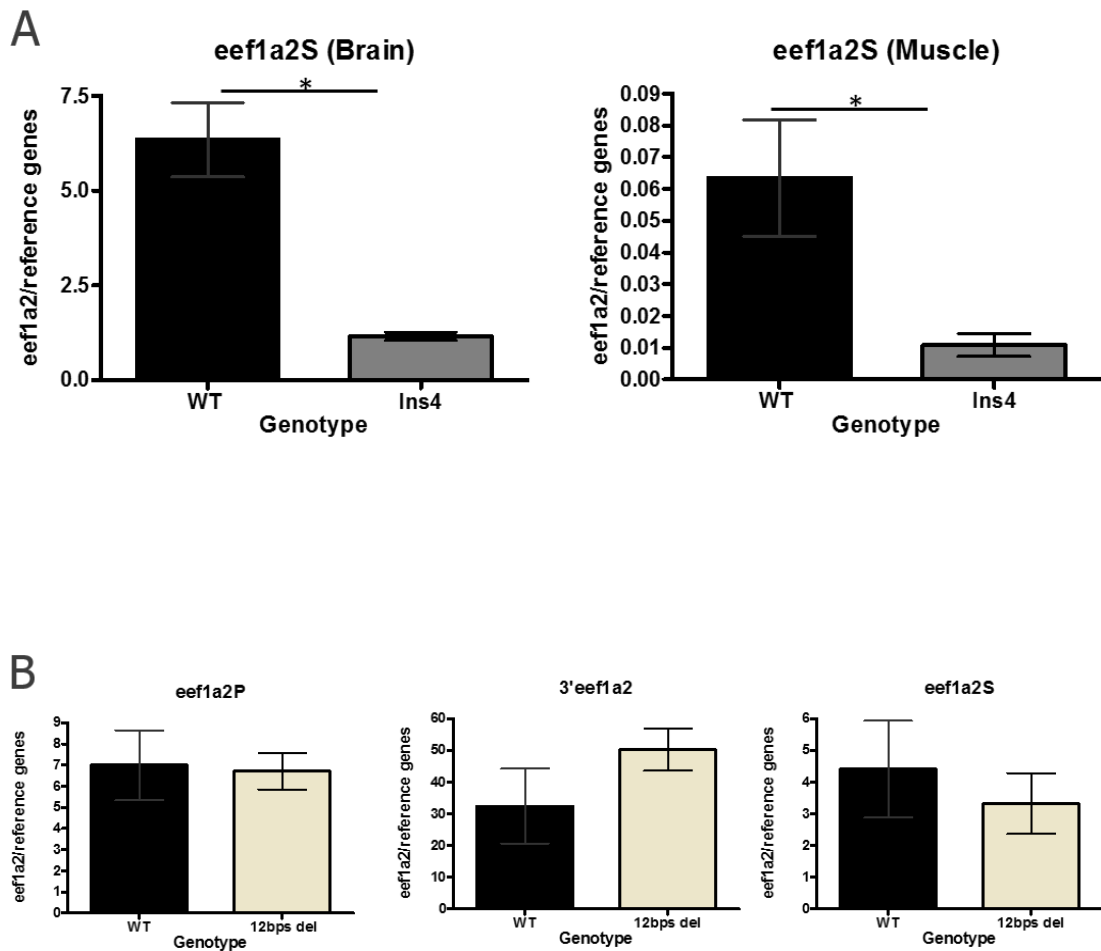
With this work, I have provided an up to date expression profile of the eEF1A genes in the zebrafish as well generated two mutant lines for *eef1a2*. The findings reported in this thesis provides groundwork information that can be used in the laboratory to further assess the fitness of the zebrafish model for our research. This is particularly useful as the success of translating research benefits to the patients depends largely on the use of well-validated animal models that correctly recapitulate the human condition.

## **Appendices**

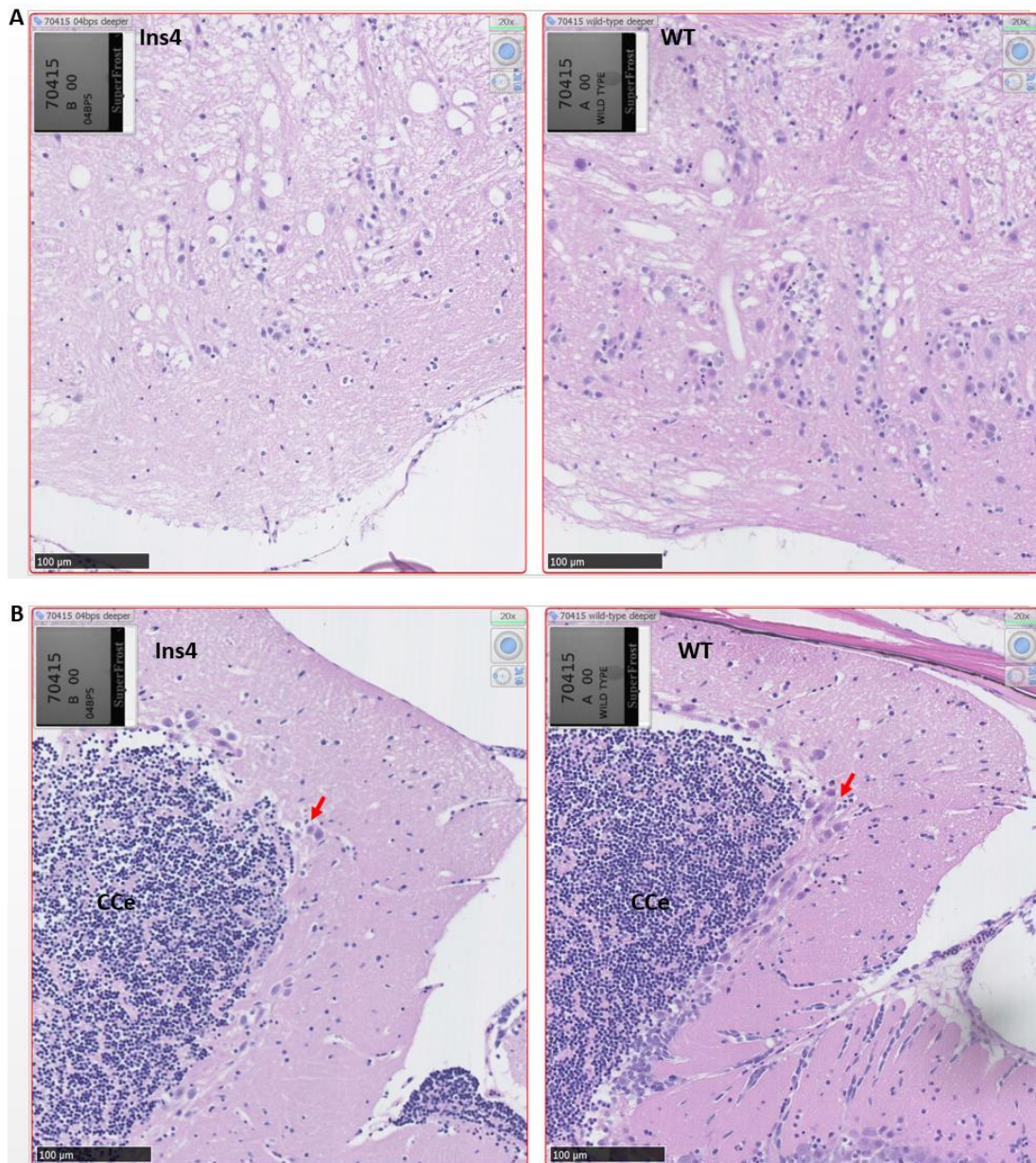




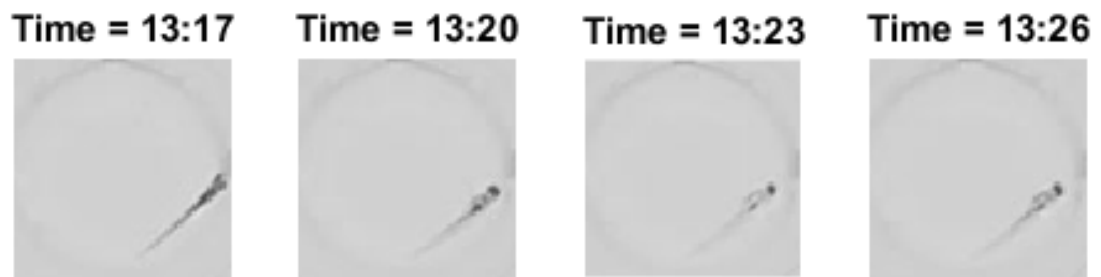
**Appendix figure 1: geNorm analysis for selecting reference genes for qPCR experiments.** geNorm M graph generated by qbase<sup>+</sup> software indicating the average expression stability value (M) of the reference genes tested. The stability of the genes are ranked with the least stable gene starting from the left and ending with the most stable gene on the right. *ATPsynth*, *NADH* and *16S* are the three most stable genes and were selected as reference genes for qPCR analyses.



**Appendix figure 2: Analysis of *eef1a2* transcripts in *Ins4* and confirmation of the possibility of *Del2* and *Ins4* mutations leading to nonsense-mediated decay. **A.** Reduced *eef1a2* transcript was noted in F2 *Ins4* homozygous (3 months) brain and muscle tissues. **B.** The three different primer sets; *eef1a2P*, 3'*eef1a2* and *eef1a2S* that were used in the molecular characterisation of *Del2* and *Ins4* mutant lines did not show any significant reduction in *eef1a2* mRNA expression when tested with brain cDNA from adult fish with a homozygous 12 bps deletion. This is an in-frame mutation and theoretically should not cause a truncated protein to be translated. Since the result is in agreement, it suggests that the observed decrease in *eef1a2* transcript levels in the *Del2* and *Ins4* are likely due to NMD which leads to the increased degradation of the mutant mRNA. cDNA samples from age-matched wild-type fish were used as controls. *eef1a2* mRNA expression was normalised to three reference genes: *ATPsynth*, *NADH* and *16S*. Results are presented as means  $\pm$  S.E.M.; n=3 in each group. \*p < 0.05 (Mann Whitney test)**



**Appendix figure 3: Preliminary histological examination of the brain from one homozygous Ins4 fish (5 months old) and age-matched wild-type zebrafish. A.** Representative image from the medulla oblongata showing lower neuronal density in Ins4 **B.** Representative image from the cerebellum with sparsely arranged Purkinje cells (indicated with red arrow) noted in Ins4 fish. However, follow-up investigation using more number of fish and the Del2 line was carried out and did not support preliminary findings, suggesting these were likely artefacts possible from the preparation of the sections. Longitudinal sectioning (3μm-thick) and H&E staining were carried out by the staffs at Easter Bush Veterinary Centre (EBVC). Histological observation and images were provided by Dr. Jorge del Pozo. CCe- Corpus cerebelli. Scale bar = 100μm.



**Appendix figure 4: Time evolution of a representative larva showing a pattern of activity consistent with stage III seizure behaviour.** Black arrow shows the larva treated with 2.5mM PTZ which was followed in the 96-well plate. Larva remained stationary at 13mins 17secs and then loses posture and fell on its side at 13mins 20secs and remained in that position for few seconds.

**Appendix Table 1: Positions with amino acid variation and the respective residues in the four zebrafish eEF1A isoforms.**

<b>Position</b>	<b>eEF1A1L1</b>	<b>eEF1A1A</b>	<b>eEF1A1B</b>	<b>eEF1A2</b>
6	Threonine (T)	Leucine (L)	Leucine (L)	Isoleucine (I)
76	Alanine (A)	Serine (S)	Serine (S)	Serine (S)
83	Serine (S)	Serine (S)	Serine (S)	Threonine (T)
87	Valine (V)	Valine (V)	Valine (V)	Isoleucine (I)
118	Glycine (G)	Alanine (A)	Alanine (A)	Alanine (A)
141	Phenylalanine (F)	Tyrosine (Y)	Tyrosine (Y)	Tyrosine (Y)
151	Glycine (G)	Glycine (G)	Glycine (G)	Alanine (A)
161	Proline (P)	Serine (S)	Asparagine (N)	Serine (S)
164	Glutamine (Q)	Glutamine (Q)	Glutamine (Q)	Glutamic acid (E)
165	Alanine (A)	Lysine (K)	Lysine (K)	Lysine (K)
167	Phenylalanine (F)	Tyrosine (Y)	Tyrosine (Y)	Tyrosine (Y)
168	Glutamic acid (E)	Glutamic acid (E)	Glutamic acid (E)	Aspartic acid (D)
171	Threonine (T)	Valine (V)	Valine (V)	Valine (V)
176	Alanine (A)	Threonine (T)	Threonine (T)	Alanine (A)
184	Asparagine (N)	Asparagine (N)	Asparagine (N)	Serine (S)
186	Alanine (A)	Aspartic acid (D)	Aspartic acid (D)	Alanine (A)
187	Serine (S)	Threonine (T)	Threonine (T)	Serine (S)
189	Alanine (A)	Alanine (A)	Alanine (A)	Proline (P)
197	Histidine (H)	Asparagine (N)	Asparagine (N)	Histidine (H)
204	Alanine (A)	Alanine (A)	Alanine (A)	Proline (P)
206	Serine (S)	Proline (P)	Proline (P)	Serine (S)
209	Glycine (G)	Serine (S)	Threonine (T)	Proline (P)
216	Isoleucine (I)	Isoleucine (I)	Isoleucine (I)	Leucine (L)
217	Glutamic acid (E)	Threonine (T)	Threonine (T)	Aspartic acid (D)
220	Glutamic acid (E)	Glutamic acid (E)	Aspartic acid (D)	Glutamic acid (E)

221	Glycine (G)	Glycine (G)	Glycine (G)	Histidine (H)
222	Asparagine (N)	Asparagine (N)	Serine (S)	Histidine (H)
223	Alanine (A)	Alanine (A)	Serine (S)	Alanine (A)
224	Serine (S)	Alanine (A)	Serine (S)	Glycine (G)
226	Threonine (T)	Threonine (T)	Threonine (T)	Valine (V)
230	Aspartic acid (D)	Glutamic acid (E)	Glutamic acid (E)	Glutamic acid (E)
234	Alanine (A)	Alanine (A)	Alanine (A)	Threonine (T)
236	Leucine (L)	Glutamine (Q)	Glutamine (Q)	Methionine (M)
239	Serine (S)	Threonine (T)	Threonine (T)	Threonine (T)
271	Valine (V)	Leucine (L)	Isoleucine (I)	Valine (V)
273	Lysine (K)	Lysine (K)	Lysine (K)	Arginine (R)
275	Glycine (G)	Glycine (G)	Glycine (G)	Serine (S)
276	Methionine (M)	Methionine (M)	Leucine (L)	Methionine (M)
283	Alanine (A)	Valine (V)	Valine (V)	Valine (V)
285	Valine (V)	Valine (V)	Valine (V)	Isoleucine (I)
298	Serine (S)	Alanine (A)	Alanine (A)	Serine (S)
300	Threonine (T)	Serine (S)	Serine (S)	Serine (S)
303	Threonine (T)	Leucine (L)	Leucine (L)	Leucine (L)
326	Alanine (A)	Alanine (A)	Alanine (A)	Cysteine (C)
331	Asparagine (N)	Asparagine (N)	Asparagine (N)	Serine (S)
335	Methionine (M)	Glutamine (Q)	Glutamine (Q)	Glutamine (Q)
338	Alanine (A)	Alanine (A)	Alanine (A)	Serine (S)
339	Asparagine (N)	Asparagine (N)	Serine (S)	Glycine (G)
341	Asparagine (N)	Threonine (T)	Threonine (T)	Threonine (T)
355	Glutamine (Q)	Alanine (A)	Alanine (A)	Serine (S)
358	Alanine (A)	Alanine (A)	Alanine (A)	Serine (S)
361	Leucine (L)	Leucine (L)	Leucine (L)	Isoleucine (I)
393	Alanine (A)	Serine (S)	Serine (S)	Serine (S)
403	Glutamic acid (E)	Glutamic acid (E)	Aspartic acid (D)	Aspartic acid (D)

405	Valine (V)	Isoleucine (I)	Isoleucine (I)	Isoleucine (I)
417	Threonine (T)	Glutamic acid (E)	Glutamic acid (E)	Glutamine (Q)
440	Serine (S)	Glycine (G)	Glycine (G)	Asparagine (N)
445	Isoleucine (I)	Threonine (T)	Threonine (T)	Isoleucine (I)
446	Glycine (G)	Alanine (A)	Serine (S)	Glycine (G)
447	Glycine (G)	Threonine (T)	Threonine (T)	Glycine (G)
448	Alanine (A)	Serine (S)	Serine (S)	Serine (S)
450	Lysine (K)	Lysine (K)	Lysine (K)	Arginine (R)
459	Alanine (A)	Glutamine (Q)	Glutamine (Q)	Glutamine (Q)
461	Threonine (T)	Alanine (A)	Asparagine (N)	Serine (S)
462	Lysine (K)	Lysine (K)	Lysine (K)	Serine (S)
463	-	-	-	Lysine (K)

**Appendix Table 2: Slope, intercept and correlation coefficient (R<sup>2</sup>) output from SDS software to estimate efficiency of primers used for qPCR analyses.**

<b>Primer</b>	<b>Slope</b>	<b>Y-Intercept</b>	<b>Correl. Coeff. (R<sup>2</sup>)</b>
eef1a1l1	-3.296	11.766	0.997
eef1a1a	-3.223	19.571	0.997
eef1a1b	-3.283	20.197	0.996
eef1a2P	-3.294	21.767	0.994
eef1a2S	-3.495	20.357	0.981
3' eef1a2	-3.208	22.445	0.992
ATPsynth	-3.237	14.832	0.999
NADH	-3.227	16.500	0.996
16S	-3.018	10.194	0.991



## References

- Abbas, W., Kumar, A. and Herbein, G. (2015) 'The eEF1A Proteins: At the Crossroads of Oncogenesis, Apoptosis, and Viral Infections', *Frontiers in Oncology*, 5(April), pp. 1–10. doi: 10.3389/fonc.2015.00075.
- Adab, N., Kini, U., Vinten, J., Ayres, J., Baker, G., Clayton-Smith, J., Coyle, H., Fryer, A., Gorry, J., Gregg, J., Mawer, G., Nicolaides, P., Pickering, L., Tunnicliffe, L. and Chadwick, D. W. (2004) 'The longer term outcome of children born to mothers with epilepsy', *Journal of Neurology, Neurosurgery and Psychiatry*, 75(11), pp. 1575–1583. doi: 10.1136/jnnp.2003.029132.
- Afrikanova, T., Serruys, A.-S. K., Buenafe, O. E. M., Clinckers, R., Smolders, I., de Witte, P. A. M., Crawford, A. D. and Esguerra, C. V (2013) 'Validation of the Zebrafish Pentylentetrazol Seizure Model: Locomotor versus Electrographic Responses to Antiepileptic Drugs', *PLOS ONE*. Public Library of Science, 8(1), p. e54166. Available at: <https://doi.org/10.1371/journal.pone.0054166>.
- Aguilar Martínez, N., Aguado Carrillo, G., Saucedo Alvarado, P. E., Mendoza García, C. A., Velasco Monroy, A. L. and Velasco Campos, F. (2017) 'Clinical importance of olfactory function in neurodegenerative diseases', *Revista Médica del Hospital General de México*. doi: 10.1016/j.hgmx.2017.05.007.
- Alunni, A., Vaccari, S., Torcia, S., Meomartini, M. E., Nicotra, A. and Alfei, L. (2005) 'Characterization of glial fibrillary acidic protein and astroglial architecture in the brain of a continuously growing fish, the rainbow trout.', *European journal of histochemistry : EJH.*, 49(2), pp. 157–166.
- Amsterdam, A., Nissen, R. M., Sun, Z., Swindell, E. C., Farrington, S. and Hopkins, N. (2004) 'Identification of 315 genes essential for early zebrafish development', *Proceedings of the National Academy of Sciences*, 101(35), pp. 12792–12797. doi: 10.1073/pnas.0403929101.
- Anand, N., Murthy, S., Amann, G., Wernick, M., Porter, L. a, Cukier, I. H., Collins, C., Gray, J. W., Diebold, J., Demetrick, D. J. and Lee, J. M. (2002) 'Protein elongation factor EEF1A2 is a putative oncogene in ovarian cancer.', *Nature genetics*, 31(3), pp. 301–5. doi: 10.1038/ng904.
- Andersen, G. R., Pedersen, L., Valente, L., Chatterjee, I., Kinzy, T. G., Kjeldgaard, M. and Nyborg, J. (2000) 'Structural basis for nucleotide exchange and competition with tRNA in the Yeast elongation factor complex eEF1A:eEF1B $\alpha$ ', *Molecular Cell*, 6(5), pp. 1261–1266. doi: 10.1016/S1097-2765(00)00122-2.
- Ann, D. K., Lin, H. H., Lee, S., Tu, Z. J. and Wang, E. (1992) 'Characterization of the statin-like S1 and rat elongation factor 1 $\alpha$  as two distinctly expressed messages in rat', *Journal of Biological Chemistry*, 267(2), pp. 699–702.
- Armstrong, G. A. B., Liao, M., You, Z., Lissouba, A., Chen, B. E. and Drapeau, P. (2016) 'Homology Directed Knockin of Point Mutations in the Zebrafish *tardbp* and *fus* Genes in ALS Using the CRISPR/Cas9 System', *PLOS ONE*. Public Library of Science, 11(3), p. e0150188. Available at:

<https://doi.org/10.1371/journal.pone.0150188>.

Babin, P. J., Goizet, C. and Raldúa, D. (2014) 'Zebrafish models of human motor neuron diseases: Advantages and limitations', *Progress in Neurobiology*. Pergamon, 118, pp. 36–58. doi: 10.1016/J.PNEUROBIO.2014.03.001.

Bae, Y. K., Kani, S., Shimizu, T., Tanabe, K., Nojima, H., Kimura, Y., Higashijima, S. ichi and Hibi, M. (2009) 'Anatomy of zebrafish cerebellum and screen for mutations affecting its development', *Developmental Biology*, 330(2), pp. 406–426. doi: 10.1016/j.ydbio.2009.04.013.

Bagni, C., Tassone, F., Neri, G. and Hagerman, R. (2012) 'Fragile X syndrome: causes, diagnosis, mechanisms, and therapeutics', *The Journal of clinical investigation*. 2012/12/03. American Society for Clinical Investigation, 122(12), pp. 4314–4322. doi: 10.1172/JCI63141.

Baraban, S. C. (2013) 'Forebrain electrophysiological recording in larval zebrafish.', *Journal of Visualized Experiments*, (71), pp. 2–5. Available at: <http://www.ncbi.nlm.nih.gov/pubmed/23380808>.

Baraban, S. C., Dinday, M. T., Castro, P. A., Chege, S., Guyenet, S. and Taylor, M. R. (2007) 'A Large-scale Mutagenesis Screen to Identify Seizure-resistant Zebrafish', *Epilepsia*, 48(6), pp. 1151–1157. doi: 10.1111/j.1528-1167.2007.01075.x.

Baraban, S. C., Dinday, M. T. and Hortopan, G. a (2013) 'Drug screening in Scn1a zebrafish mutant identifies clemizole as a potential Dravet syndrome treatment.', *Nature communications*. Nature Publishing Group, 4, p. 2410. Available at: <http://www.pubmedcentral.nih.gov/articlerender.fcgi?artid=3891590&tool=pmcentre&rendertype=abstract>.

Baraban, S. C., Taylor, M. R., Castro, P. A. and Baier, H. (2005) 'Pentylentetrazole induced changes in zebrafish behavior, neural activity and c-fos expression', *Neuroscience*, 131(3), pp. 759–768. doi: 10.1016/j.neuroscience.2004.11.031.

Batulan, Z., Shinder, G. a, Minotti, S., He, B. P., Doroudchi, M. M., Nalbantoglu, J., Strong, M. J. and Durham, H. D. (2003) 'High threshold for induction of the stress response in motor neurons is associated with failure to activate HSF1.', *The Journal of neuroscience : the official journal of the Society for Neuroscience*, 23(13), pp. 5789–5798. doi: 23/13/5789 [pii].

Baxendale, S., Holdsworth, C. J., Meza Santoscoy, P. L., Harrison, M. R. M., Fox, J., Parkin, C. A., Ingham, P. W. and Cunliffe, V. T. (2012) 'Identification of compounds with anti-convulsant properties in a zebrafish model of epileptic seizures', *Disease Models & Mechanisms*, 5(6), pp. 773–784. doi: 10.1242/dmm.010090.

Beckelman, B. C., Day, S., Zhou, X., Donohue, M., Gouras, G. K., Klann, E., Keene, C. D. and Ma, T. (2016) 'Dysregulation of Elongation Factor 1A Expression is Correlated with Synaptic Plasticity Impairments in Alzheimer's Disease', *Journal of Alzheimer's disease : JAD*, 54(2), pp. 669–678. doi: 10.3233/JAD-160036.

Beckelman, B. C., Zhou, X., Keene, C. D. and Ma, T. (2016) 'Impaired Eukaryotic Elongation Factor 1A Expression in Alzheimer's Disease', *Neuro-degenerative*

*diseases*. 2015/11/10, 16(1–2), pp. 39–43. doi: 10.1159/000438925.

Bender, A. C., Morse, R. P., Scott, R. C., Holmes, G. L. and Lenck-Santini, P.-P. (2012) ‘SCN1A mutations in Dravet syndrome: Impact of interneuron dysfunction on neural networks and cognitive outcome’, *Epilepsy & Behavior*. Academic Press, 23(3), pp. 177–186. doi: 10.1016/J.YEBEH.2011.11.022.

Berberich, T., Sugawara, K., Harada, M. and Kusano, T. (1995) ‘Short communication Molecular cloning, characterization and expression of an elongation factor 1 $\alpha$  gene in maize Laboratory of Plant Genetic Engineering, Biotechnology Institute, Akita Prefectural College of Agriculture, Ohgata, Akita 010-04, Japan’, *Plant molecular biology*, 45407, pp. 611–615.

Bergmann, K., Meza Santoscoy, P., Lygdas, K., Nikolaeva, Y., MacDonald, R. B., Cunliffe, V. T. and Nikolaev, A. (2018) ‘Imaging Neuronal Activity in the Optic Tectum of Late Stage Larval Zebrafish’, *Journal of developmental biology*. MDPI, 6(1), p. 6. doi: 10.3390/jdb6010006.

Blom, N., Gammeltoft, S. and Brunak, S. (1999) ‘Sequence and structure-based prediction of eukaryotic protein phosphorylation sites’, *Journal of Molecular Biology*, 294(5), pp. 1351–1362. doi: 10.1006/jmbi.1999.3310.

Bluem, R., Schmidt, E., Corvey, C., Karas, M., Schlicksupp, A. and Kirsch, J. (2007) ‘Components of the Translational Machinery Are Associated with Juvenile Glycine Receptors and Are Redistributed to the Cytoskeleton upon Aging and Synaptic Activity \*’, 282(52), pp. 37783–37793. doi: 10.1074/jbc.M708301200.

Bootorabi, F., Manouchehri, H., Changizi, R., Barker, H., Palazzo, E., Saltari, A., Parikka, M., Pincelli, C. and Aspatwar, A. (2017) ‘Zebrafish as a model organism for the development of drugs for skin cancer’, *International Journal of Molecular Sciences*, 18(7), pp. 1–15. doi: 10.3390/ijms18071550.

Bosutti, A., Scaggiante, B., Grassi, G., Guarnieri, G. and Biolo, G. (2007) ‘Overexpression of the elongation factor 1A1 relates to muscle proteolysis and proapoptotic p66(ShcA) gene transcription in hypercatabolic trauma patients’, *Metabolism: Clinical and Experimental*, 56(12), pp. 1629–1634. doi: 10.1016/j.metabol.2007.07.003.

Boyce, M., Bryant, K. F., Jousse, C., Long, K., Harding, H. P., Scheuner, D., Kaufman, R. J., Ma, D., Coen, D. M., Ron, D. and Yuan, J. (2005) ‘A Selective Inhibitor of eIF2 $\alpha$  Dephosphorylation Protects Cells from ER Stress’, *Science*, 307(5711), p. 935 LP-939. Available at: <http://science.sciencemag.org/content/307/5711/935.abstract>.

Bradford, Y., Conlin, T., Dunn, N., Fashena, D., Frazer, K., Howe, D. G., Knight, J., Mani, P., Martin, R., Moxon, S. A. T., Paddock, H., Pich, C., Ramachandran, S., Ruef, B. J., Ruzicka, L., Schaper, H. B., Schaper, K., Shao, X., Singer, A., Sprague, J., Sprunger, B., Van Slyke, C. and Westerfield, M. (2011) ‘ZFIN: Enhancements and updates to the zebrafish model organism database’, *Nucleic Acids Research*, 39(SUPPL. 1).

Brogna, S. and Wen, J. (2009) ‘Nonsense-mediated mRNA decay (NMD)

mechanisms', *Nature Structural and Molecular Biology*. doi: 10.1038/nsmb.1550.

Bunai, F., Ando, K., Ueno, H. and Numata, O. (2006) 'Tetrahymena Eukaryotic Translation Elongation Factor 1A (eEF1A) Bundles Filamentous Actin through Dimer Formation', *The Journal of Biochemistry*, 140(3), pp. 393–399. Available at: <http://dx.doi.org/10.1093/jb/mvj169>.

Bustin, S. A., Benes, V., Garson, J. A., Hellems, J., Huggett, J., Kubista, M., Mueller, R., Nolan, T., Pfaffl, M. W., Shipley, G. L., Vandesompele, J. and Wittwer, C. T. (2009) 'The MIQE Guidelines: Minimum Information for Publication of Quantitative Real-Time PCR Experiments', *Clinical Chemistry*, 55(4), p. 611 LP-622. Available at: <http://clinchem.aaccjnl.org/content/55/4/611.abstract>.

Byrne, S., Walsh, C., Lynch, C., Bede, P., Elamin, M., Kenna, K., McLaughlin, R. and Hardiman, O. (2011) 'Rate of familial amyotrophic lateral sclerosis: A systematic review and meta-analysis', *Journal of Neurology, Neurosurgery and Psychiatry*, 82(6), pp. 623–627. doi: 10.1136/jnnp.2010.224501.

Cao, H., Zhu, Q., Huang, J., Li, B., Zhang, S., Yao, W. and Zhang, Y. (2009) 'Regulation and functional role of eEF1A2 in pancreatic carcinoma', *Biochemical and Biophysical Research Communications*. Elsevier Inc., 380(1), pp. 11–16. doi: 10.1016/j.bbrc.2008.12.171.

Cao, S., Smith, L. L., Padilla-Lopez, S. R., Guida, B. S., Blume, E., Shi, J., Morton, S. U., Brownstein, C. A., Beggs, A. H., Kruer, M. C. and Agrawal, P. B. (2017) 'Homozygous EEF1A2 mutation causes dilated cardiomyopathy, failure to thrive, global developmental delay, epilepsy and early death', *Human molecular genetics*, 26(18), pp. 3545–3552. doi: 10.1093/hmg/ddx239.

Cao, X.-J., Arnaudo, A. M. and Garcia, B. A. (2013) 'Large-scale global identification of protein lysine methylation in vivo', *Epigenetics*. Landes Bioscience, 8(5), pp. 477–485. doi: 10.4161/epi.24547.

Catchen, J. M., Conery, J. S. and Postlethwait, J. H. (2009) 'Automated identification of conserved synteny after whole genome duplication.', *Genome research*, pp. 1–18. doi: 10.1101/gr.090480.108.

Chambers, D. M., Peters, J. and Abbott, C. M. (1998) 'The lethal mutation of the mouse wasted (wst) is a deletion that abolishes expression of a tissue-specific isoform of translation elongation factor 1, encoded by the Eef1a2 gene', *Proceedings of the National Academy of Sciences*, 95(8), pp. 4463–4468. doi: 10.1073/pnas.95.8.4463.

Chang, R. and Wang, E. (2007) 'Mouse translation elongation factor eEF1A-2 interacts with Prdx-I to protect cells against apoptotic death induced by oxidative stress', *Journal of Cellular Biochemistry*, 100(2), pp. 267–278. doi: 10.1002/jcb.20969.

Charlier, C., Singh, N. A., Ryan, S. G., Lewis, T. B., Reus, B. E., Leach, R. J. and Leppert, M. (1998) 'A pore mutation in a novel KQT-like potassium channel gene in

- an idiopathic epilepsy family', *Nature Genetics*, 18(1), pp. 53–55. doi: 10.1038/ng0198-53.
- Chege, S. W., Hortopan, G. A., Dinday, M. T. and Baraban, S. C. (2012) 'Expression and function of KCNQ channels in larval zebrafish', *Developmental Neurobiology*, 72(2), pp. 186–198. doi: 10.1002/dneu.20937.
- Chen, J., Jiang, D., Tan, D., Fan, Z., Wei, Y., Li, M. and Wang, D. (2017) 'Heterozygous mutation of eEF1A1b resulted in spermatogenesis arrest and infertility in male tilapia, *Oreochromis niloticus*', *Scientific Reports*. The Author(s), 7, p. 43733. Available at: <http://dx.doi.org/10.1038/srep43733>.
- Christoffels, A., Koh, E. G. L., Chia, J. M., Brenner, S., Aparicio, S. and Venkatesh, B. (2004) 'Fugu genome analysis provides evidence for a whole-genome duplication early during the evolution of ray-finned fishes', *Molecular Biology and Evolution*, 21(6), pp. 1146–1151. doi: 10.1093/molbev/msh114.
- Cioni, J.-M., Koppers, M. and Holt, C. E. (2018) 'Molecular control of local translation in axon development and maintenance', *Current Opinion in Neurobiology*, 51, pp. 86–94. doi: <https://doi.org/10.1016/j.conb.2018.02.025>.
- Clark, K. J., Balciunas, D., Pogoda, H. M., Ding, Y., Westcot, S. E., Bedell, V. M., Greenwood, T. M., Urban, M. D., Skuster, K. J., Petzold, A. M., Ni, J., Nielsen, A. L., Patowary, A., Scaria, V., Sivasubbu, S., Xu, X., Hammerschmidt, M. and Ekker, S. C. (2011) 'In vivo protein trapping produces a functional expression codex of the vertebrate proteome', *Nature Methods*, 8(6), pp. 506–512. doi: 10.1038/nmeth.1606.
- Condeelis, J. (1995) 'Elongation factor 1 alpha, translation and the cytoskeleton', *Trends in Biochemical Sciences*, (May), pp. 169–170.
- Corcia, P., Couratier, P., Blasco, H., Andres, C. R., Beltran, S., Meininger, V. and Vourc'h, P. (2017) 'Genetics of amyotrophic lateral sclerosis', *Revue Neurologique*. Elsevier Masson SAS, 173(5), pp. 254–262. doi: 10.1016/j.neurol.2017.03.030.
- Cornet, C., Di Donato, V. and Terriente, J. (2018) 'Combining Zebrafish and CRISPR/Cas9: Toward a More Efficient Drug Discovery Pipeline', *Frontiers in Pharmacology*, 9, p. 703. doi: 10.3389/fphar.2018.00703.
- Costa, C. J. and Willis, D. E. (2018) 'To the end of the line: Axonal mRNA transport and local translation in health and neurodegenerative disease', *Developmental Neurobiology*. John Wiley & Sons, Ltd, 78(3), pp. 209–220. doi: 10.1002/dneu.22555.
- Da Costa, M. M. J., Allen, C. E., Higginbottom, A., Ramesh, T., Shaw, P. J. and McDermott, C. J. (2014) 'A new zebrafish model produced by TILLING of SOD1-related amyotrophic lateral sclerosis replicates key features of the disease and represents a tool for in vivo therapeutic screening', *Disease Models & Mechanisms*, 7(1), pp. 73–81. doi: 10.1242/dmm.012013.
- Cunliffe, V. T. (2016) 'Building a zebrafish toolkit for investigating the pathobiology of epilepsy and identifying new treatments for epileptic seizures', *Journal of Neuroscience Methods*. Elsevier B.V., 260, pp. 91–95. doi: 10.1016/j.jneumeth.2015.07.015.

Dai, J., Cui, X., Zhu, Z. and Hu, W. (2010) 'Non-homologous end joining plays a key role in transgene concatemer formation in transgenic zebrafish embryos', *International Journal of Biological Sciences*, 6(7), pp. 756–768. doi: 10.7150/ijbs.6.756.

Van Damme, P., Robberecht, W. and Van Den Bosch, L. (2017) 'Modelling amyotrophic lateral sclerosis: progress and possibilities', *Disease Models & Mechanisms*, 10(5), pp. 537–549. doi: 10.1242/dmm.029058.

Daneman, R., Zhou, L., Kebede, A. A. and Barres, B. A. (2010) 'Pericytes are required for blood-brain barrier integrity during embryogenesis', *Nature*. Nature Publishing Group, 468(7323), pp. 562–566. doi: 10.1038/nature09513.

Darnell, J. C., Van Driesche, S. J., Zhang, C., Hung, K. Y. S., Mele, A., Fraser, C. E., Stone, E. F., Chen, C., Fak, J. J., Chi, S. W., Licatalosi, D. D., Richter, J. D. and Darnell, R. B. (2011) 'FMRP stalls ribosomal translocation on mRNAs linked to synaptic function and autism', *Cell*, 146(2), pp. 247–261. doi: 10.1016/j.cell.2011.06.013.

Davies, F. C. J., Hope, J. E., McLachlan, F., Nunez, F., Doig, J., Bengani, H., Smith, C. and Abbott, C. M. (2017) 'Biallelic mutations in the gene encoding eEF1A2 cause seizures and sudden death in F0 mice', *Scientific Reports*. Nature Publishing Group, 7(April), pp. 1–11. doi: 10.1038/srep46019.

Demma, M., Warren, V., Hock, R., Dharmawardhane, S. and Condeelis, J. (1990) *Isolation of an abundant 50,000-dalton actin filament bundling protein from Dictyostelium amoebae*, *The Journal of biological chemistry*.

Deng, H., Shi, Y., Furukawa, Y., Zhai, H., Fu, R., Liu, E., Gorrie, G. H., Khan, M. S., Hung, W., Bigio, E. H., Lukas, T., Canto, M. C. D., Halloran, T. V. O. and Siddique, T. (2006) 'Conversion to the amyotrophic lateral sclerosis phenotype is associated with intermolecular linked insoluble aggregates of SOD1 in mitochondria', pp. 1–6.

Dever, T. E., Costello, C. E., Owens, C. L., Rosenberry, T. L. and Merrick, W. C. (1989) 'Location of seven post-translational modifications in rabbit elongation factor 1 $\alpha$  including dimethyllysine, trimethyllysine, and glycerylphosphorylethanolamine', *Journal of Biological Chemistry*, 264(34), pp. 20518–20525.

Djé, M. K., Mazabraud, A., Viel, A., Le Maire, M., Denis, H., Crawford, E. and Brown, D. D. (1990) 'Three genes under different developmental control encode elongation factor 1- $\alpha$  in *Xenopus laevis*.', *Nucleic Acids Research*, 18(12), pp. 3489–3493. doi: 10.1093/nar/18.12.3489.

Doble, A. and Kennel, P. (2000) 'Animal models of amyotrophic lateral sclerosis', *Amyotrophic Lateral Sclerosis*, 1(5), pp. 301–312. doi: 10.1080/146608200300079545.

Doig, J., Griffiths, L. A., Peberdy, D., Dharmasaroja, P., Vera, M., Davies, F. J. C., Newbery, H. J., Brownstein, D. and Abbott, C. M. (2013) 'In vivo characterization of the role of tissue-specific translation elongation factor 1A2 in protein synthesis reveals insights into muscle atrophy', *FEBS Journal*, 280(24), pp. 6528–6540. doi:

10.1111/febs.12554.

Dravet, C. (2011) 'The core Dravet syndrome phenotype', *Epilepsia*, 52(SUPPL. 2), pp. 3–9. doi: 10.1111/j.1528-1167.2011.02994.x.

Durso, N. a and Cyr, R. J. (1994) 'A calmodulin-sensitive interaction between microtubules and a higher plant homolog of elongation factor-1 alpha.', *The Plant cell*, 6(June), pp. 893–905. doi: 10.1105/tpc.6.6.893.

Duttaroy, A., Bourbeau, D., Wang, X. L. and Wang, E. (1998) 'Apoptosis rate can be accelerated or decelerated by overexpression or reduction of the level of elongation factor-1 $\alpha$ ', *Experimental Cell Research*, 238(1), pp. 168–176. doi: 10.1006/excr.1997.3819.

Dzialo, M. C., Travaglini, K. J., Shen, S., Loo, J. A. and Clarke, S. G. (2014) 'A new type of protein lysine methyltransferase trimethylates Lys-79 of elongation factor 1A', *Biochemical and biophysical research communications*, 455(0), pp. 382–389. doi: 10.1016/j.bbrc.2014.11.022.

Eckhardt, K., Tröger, J., Reissmann, J., M, D., Wagner, K. F., Stengel, P., Paasch, U., Hunziker, P., Borter, E., Barth, S., Schläfli, P., Spielmann, P., Stiehl, D. P., Camenisch, G. and Wenger, H. (2007) 'Cellular Physiology Biochemistry and Biochemistr y Male Germ Cell Expression of the PAS Domain Kinase PASKIN and its Novel Target Eukaryotic Translation Elongation Factor eEF1A1', *Cellular Physiology and Biochemistry*.

Edmonds, B. T., Murray, J. and Condeelis, J. (1995) 'pH regulation of the F-actin binding properties of Dictyostelium elongation factor 1 $\alpha$ ', *Journal of Biological Chemistry*, pp. 15222–15230. doi: 10.1074/jbc.270.25.15222.

EJIRI, S. (2002) 'Moonlighting Functions of Polypeptide Elongation Factor 1: From Actin Bundling to Zinc Finger Protein R1-Associated Nuclear Localization', *Bioscience, Biotechnology, and Biochemistry*, 66(1), pp. 1–21. doi: 10.1271/bbb.66.1.

Farrell, J. A., Wang, Y., Riesenfeld, S. J., Shekhar, K., Regev, A. and Schier, A. F. (2018) 'Single-cell reconstruction of developmental trajectories during zebrafish embryogenesis', *Science*, 360(6392). doi: 10.1126/science.aar3131.

Fleisch, V. C., Fraser, B. and Allison, W. T. (2011) 'Investigating regeneration and functional integration of CNS neurons: Lessons from zebrafish genetics and other fish species', *Biochimica et Biophysica Acta - Molecular Basis of Disease*, 1812(3), pp. 364–380. doi: 10.1016/j.bbadis.2010.10.012.

Flicek, P., Amode, M. R., Barrell, D., Beal, K., Billis, K., Brent, S., Carvalho-Silva, D., Clapham, P., Coates, G., Fitzgerald, S., Gil, L., Girón, C. G., Gordon, L., Hourlier, T., Hunt, S., Johnson, N., Juettemann, T., Kähäri, A. K., Keenan, S., Kulesha, E., Martin, F. J., Maurel, T., McLaren, W. M., Murphy, D. N., Nag, R., Overduin, B., Pignatelli, M., Pritchard, B., Pritchard, E., Riat, H. S., Ruffier, M., Sheppard, D., Taylor, K., Thormann, A., Trevanion, S. J., Vullo, A., Wilder, S. P., Wilson, M., Zadissa, A., Aken, B. L., Birney, E., Cunningham, F., Harrow, J., Herrero, J., Hubbard, T. J. P., Kinsella, R., Muffato, M., Parker, A., Spudich, G.,

- Yates, A., Zerbino, D. R. and Searle, S. M. J. (2014) 'Ensembl 2014.', *Nucleic acids research*, 42(Database issue), pp. D749-55. doi: 10.1093/nar/gkt1196.
- Frost, W. N., Castellucci, V. F., Hawkins, R. D. and Kandel, E. R. (1985) 'Monosynaptic connections made by the sensory neurons of the gill- and siphon-withdrawal reflex in *Aplysia* participate in the storage of long-term memory for sensitization', *Proceedings of the National Academy of Sciences of the United States of America*, 82(23), pp. 8266–8269. Available at: <https://www.ncbi.nlm.nih.gov/pubmed/16593630>.
- Gandin, V., Gutierrez, G. J., Brill, L. M., Varsano, T., Feng, Y., Aza-Blanc, P., Au, Q., McLaughlan, S., Ferreira, T. A., Alain, T., Sonenberg, N., Topisirovic, I. and Ronai, Z. A. (2013) 'Degradation of Newly Synthesized Polypeptides by Ribosome-Associated RACK1/c-Jun N-Terminal Kinase/Eukaryotic Elongation Factor 1A2 Complex', *Molecular and Cellular Biology*, 33(13), pp. 2510–2526. doi: 10.1128/MCB.01362-12.
- Gao, D. Y., Li, Z. F., Murphy, T. and Sauerbier, W. (1997) 'Structure and transcription of the gene for translation elongation factor 1 subunit alpha of zebrafish (*Danio rerio*)', *Biochimica et Biophysica Acta-Gene Structure and Expression*, pp. 1–5.
- Giustetto, M., Hegde, A. N., Si, K., Casadio, A., Inokuchi, K., Pei, W., Kandel, E. R. and Schwartz, J. H. (2003) 'Axonal transport of eukaryotic translation elongation factor 1alpha mRNA couples transcription in the nucleus to long-term facilitation at the synapse', *Proceedings of the National Academy of Sciences of the United States of America*. 2003/10/24. National Academy of Sciences, 100(23), pp. 13680–13685. doi: 10.1073/pnas.1835674100.
- Goc, J., Liu, J. Y. W., Sisodiya, S. M. and Thom, M. (2014) 'A spatiotemporal study of gliosis in relation to depth electrode tracks in drug-resistant epilepsy', *European Journal of Neuroscience*, 39(12), pp. 2151–2162. doi: 10.1111/ejn.12548.
- Goldsmith, P., Golder, Z., Hunt, J., Berghmans, S., Jones, D., Stables, J. P., Murphree, L., Howden, D., Newton, P. E. and Richards, F. M. (2007) 'GBR12909 possesses anticonvulsant activity in zebrafish and rodent models of generalized epilepsy but cardiac ion channel effects limit its clinical utility', *Pharmacology*, 79(4), pp. 250–258. doi: 10.1159/000102061.
- Golling, G., Amsterdam, A., Sun, Z., Antonelli, M., Maldonado, E., Chen, W., Burgess, S., Haldi, M., Artzt, K., Farrington, S., Lin, S.-Y., Nissen, R. M. and Hopkins, N. (2002) 'Insertional mutagenesis in zebrafish rapidly identifies genes essential for early vertebrate development.', *Nature genetics*, 31(2), pp. 135–40. doi: 10.1038/ng896.
- Grassi, G., Scaggiante, B., Farra, R., Dapas, B., Agostini, F., Baiz, D., Rosso, N. and Tiribelli, C. (2007) 'The expression levels of the translational factors eEF1A 1/2 correlate with cell growth but not apoptosis in hepatocellular carcinoma cell lines with different differentiation grade', *Biochimie*, 89(12), pp. 1544–1552. doi: 10.1016/j.biochi.2007.07.007.
- Griffiths, L. A., Doig, J., Churchhouse, A. M. D., Davies, F. C. J., Squires, C. E.,



- Newbery, H. J. and Abbott, C. M. (2012) ‘Haploinsufficiency for translation elongation factor eEF1A2 in aged mouse muscle and neurons is compatible with normal function’, *PLoS ONE*, 7(7). doi: 10.1371/journal.pone.0041917.
- Gross, S. R. and Kinzy, T. G. (2005) ‘Translation elongation factor 1A is essential for regulation of the actin cytoskeleton and cell morphology’, *Nature Structural and Molecular Biology*, 12(9), pp. 772–778. doi: 10.1038/nsmb979.
- Gross, S. R. and Kinzy, T. G. (2007) ‘Improper Organization of the Actin Cytoskeleton Affects Protein Synthesis at Initiation’, *Molecular and Cellular Biology*, 27(5), pp. 1974–1989. doi: 10.1128/MCB.00832-06.
- Guo, A., Gu, H., Zhou, J., Mulhern, D., Wang, Y., Lee, K. A., Yang, V., Aguiar, M., Kornhauser, J., Jia, X., Ren, J., Beausoleil, S. A., Silva, J. C., Vemulapalli, V., Bedford, M. T. and Comb, M. J. (2014) ‘Immunoaffinity Enrichment and Mass Spectrometry Analysis of Protein Methylation’, *Molecular & Cellular Proteomics : MCP*. The American Society for Biochemistry and Molecular Biology, 13(1), pp. 372–387. doi: 10.1074/mcp.O113.027870.
- Hamey, J. J., Winter, D. L., Yagoub, D., Overall, C. M., Hart-Smith, G. and Wilkins, M. R. (2016) ‘Novel N-terminal and Lysine Methyltransferases That Target Translation Elongation Factor 1A in Yeast and Human’, *Molecular & Cellular Proteomics : MCP*. The American Society for Biochemistry and Molecular Biology, 15(1), pp. 164–176. doi: 10.1074/mcp.M115.052449.
- Harris, W. A., Holt, C. E. and Bonhoeffer, F. (1987) ‘Retinal axons with and without their somata, growing to and arborizing in the tectum of *Xenopus* embryos: a time-lapse video study of single fibres in vivo’, *Development*, 101(1), p. 123 LP-133. Available at: <http://dev.biologists.org/content/101/1/123.abstract>.
- Haschemeyer, A. E. V. (1985) ‘Multiple aminoacyl-tRNA synthetases (translases) in temperature acclimation of eurythermal fish’, *Journal of Experimental Marine Biology and Ecology*, 87(2), pp. 191–198. doi: 10.1016/0022-0981(85)90090-5.
- Hill, J. T., Demarest, B. L., Bisgrove, B. W., Su, Y., Smith, M. and Yost, H. J. (2014) ‘Poly Peak Parser: Method and software for identification of unknown indels using Sanger Sequencing of PCR products’, *Developmental dynamics : an official publication of the American Association of Anatomists*, 243(12), pp. 1632–1636. doi: 10.1002/dvdy.24183.
- Hirano, A. (1996) ‘Neuropathology of ALS: An overview’, *Neurology*, 47(Issue 4, Supplement 2), p. 63S–66S. doi: 10.1212/WNL.47.4\_Suppl\_2.63S.
- Van Hoecke, A., Schoonaert, L., Lemmens, R., Timmers, M., Staats, K. A., Laird, A. S., Peeters, E., Philips, T., Goris, A., Dubois, B., Andersen, P. M., Al-Chalabi, A., Thijs, V., Turnley, A. M., Van Vught, P. W., Veldink, J. H., Hardiman, O., Van Den Bosch, L., Gonzalez-Perez, P., Van Damme, P., Brown, R. H., Van Den Berg, L. H. and Robberecht, W. (2012) ‘EPHA4 is a disease modifier of amyotrophic lateral sclerosis in animal models and in humans’, *Nature Medicine*, 18(9), pp. 1418–1422. doi: 10.1038/nm.2901.
- Holt, C. E. and Schuman, E. M. (2013) ‘The Central Dogma Decentralized: New

Perspectives on RNA Function and Local Translation in Neurons', *Neuron*, 80(3), pp. 648–657. doi: <https://doi.org/10.1016/j.neuron.2013.10.036>.

Hovemann, B., Richter, S., Walldorf, U. and Cziepluch, C. (1988) 'Two genes encode related cytoplasmic elongation factors 1 alpha (EF-1 alpha) in *Drosophila melanogaster* with continuous and stage specific expression.', *Nucleic acids research*, 16(8), pp. 3175–94. Available at: <http://www.pubmedcentral.nih.gov/articlerender.fcgi?artid=336487&tool=pmcentrez&rendertype=abstract>.

Howe, D. G., Bradford, Y. M., Conlin, T., Eagle, A. E., Fashena, D., Frazer, K., Knight, J., Mani, P., Martin, R., Moxon, S. A. T., Paddock, H., Pich, C., Ramachandran, S., Ruef, B. J., Ruzicka, L., Schaper, K., Shao, X., Singer, A., Sprunger, B., Van Slyke, C. E. and Westerfield, M. (2013) 'ZFIN, the Zebrafish Model Organism Database: increased support for mutants and transgenics', *Nucleic Acids Research*, 41(D1), pp. D854–D860. Available at: <http://dx.doi.org/10.1093/nar/gks938>.

Howe, K., Clark, M. D., Torroja, C. F., Torrance, J., Berthelot, C., Muffato, M., Collins, J. E., Humphray, S., McLaren, K., Matthews, L., McLaren, S., Sealy, I., Caccamo, M., Churcher, C., Scott, C., Barrett, J. C., Koch, R., Rauch, G.-J., White, S., Chow, W., Kilian, B., Quintais, L. T., Guerra-Assunção, J. a, Zhou, Y., Gu, Y., Yen, J., Vogel, J.-H., Eyre, T., Redmond, S., Banerjee, R., Chi, J., Fu, B., Langley, E., Maguire, S. F., Laird, G. K., Lloyd, D., Kenyon, E., Donaldson, S., Sehra, H., Almeida-King, J., Loveland, J., Trevanion, S., Jones, M., Quail, M., Willey, D., Hunt, A., Burton, J., Sims, S., McLay, K., Plumb, B., Davis, J., Clee, C., Oliver, K., Clark, R., Riddle, C., Elliot, D., Elliott, D., Threadgold, G., Harden, G., Ware, D., Begum, S., Mortimore, B., Mortimer, B., Kerry, G., Heath, P., Phillimore, B., Tracey, A., Corby, N., Dunn, M., Johnson, C., Wood, J., Clark, S., Pelan, S., Griffiths, G., Smith, M., Glithero, R., Howden, P., Barker, N., Lloyd, C., Stevens, C., Harley, J., Holt, K., Panagiotidis, G., Lovell, J., Beasley, H., Henderson, C., Gordon, D., Auger, K., Wright, D., Collins, J., Raisen, C., Dyer, L., Leung, K., Robertson, L., Ambridge, K., Leongamornlert, D., McGuire, S., Gilderthorp, R., Griffiths, C., Manthavadi, D., Nichol, S., Barker, G., Whitehead, S., Kay, M., Brown, J., Murnane, C., Gray, E., Humphries, M., Sycamore, N., Barker, D., Saunders, D., Wallis, J., Babbage, A., Hammond, S., Mashreghi-Mohammadi, M., Barr, L., Martin, S., Wray, P., Ellington, A., Matthews, N., Ellwood, M., Woodmansey, R., Clark, G., Cooper, J. D., Cooper, J., Tromans, A., Grafham, D., Skuce, C., Pandian, R., Andrews, R., Harrison, E., Kimberley, A., Garnett, J., Fosker, N., Hall, R., Garner, P., Kelly, D., Bird, C., Palmer, S., Gehring, I., Berger, A., Dooley, C. M., Ersan-Ürün, Z., Eser, C., Geiger, H., Geisler, M., Karotki, L., Kirn, A., Konantz, J., Konantz, M., Oberländer, M., Rudolph-Geiger, S., Teucke, M., Lanz, C., Raddatz, G., Osoegawa, K., Zhu, B., Rapp, A., Widaa, S., Langford, C., Yang, F., Schuster, S. C., Carter, N. P., Harrow, J., Ning, Z., Herrero, J., Searle, S. M. J., Enright, A., Geisler, R., Plasterk, R. H. a, Lee, C., Westerfield, M., de Jong, P. J., Zon, L. I., Postlethwait, J. H., Nüsslein-Volhard, C., Hubbard, T. J. P., Roest Crolius, H., Rogers, J. and Stemple, D. L. (2013) 'The zebrafish reference genome sequence and its relationship to the human genome.', *Nature*, 496(7446), pp. 498–503. doi: [10.1038/nature12111](https://doi.org/10.1038/nature12111).

- Hruscha, A., Krawitz, P., Rechenberg, A., Heinrich, V., Hecht, J., Haass, C. and Schmid, B. (2013) 'Efficient CRISPR/Cas9 genome editing with low off-target effects in zebrafish.', *Development (Cambridge, England)*, 140(24), pp. 4982–7. Available at: <http://www.ncbi.nlm.nih.gov/pubmed/24257628>.
- Huang, F., Chotiner, J. K. and Steward, O. (2005) 'The mRNA for Elongation Factor 1 $\alpha$  Is Localized in Dendrites and Translated in Response to Treatments That Induce Long-Term Depression', *The Journal of Neuroscience*, 25(31), p. 7199 LP-7209. doi: 10.1523/JNEUROSCI.1779-05.2005.
- Hui, S. P., Sengupta, D., Lee, S. G. P., Sen, T., Kundu, S., Mathavan, S. and Ghosh, S. (2014) 'Genome wide expression profiling during spinal cord regeneration identifies comprehensive cellular responses in zebrafish', *PLoS ONE*, 9(1). doi: 10.1371/journal.pone.0084212.
- Hutchins, E. D., Markov, G. J., Eckalbar, W. L., George, R. M., King, J. M., Tokuyama, M. A., Geiger, L. A., Emmert, N., Ammar, M. J., Allen, A. N., Siniard, A. L., Corneveaux, J. J., Fisher, R. E., Wade, J., DeNardo, D. F., Rawls, J. A., Huentelman, M. J., Wilson-Rawls, J. and Kusumi, K. (2014) 'Transcriptomic Analysis of Tail Regeneration in the Lizard *Anolis carolinensis* Reveals Activation of Conserved Vertebrate Developmental and Repair Mechanisms', *PLOS ONE*. Public Library of Science, 9(8), p. e105004. Available at: <https://doi.org/10.1371/journal.pone.0105004>.
- Hwang, W. Y., Fu, Y., Reyon, D., Maeder, M. L., Tsai, S. Q., Sander, J. D., Peterson, R. T., Yeh, J. R. J. and Joung, J. K. (2013) 'Efficient genome editing in zebrafish using a CRISPR-Cas system', *Nature Biotechnology*. Nature Publishing Group, 31(3), pp. 227–229. doi: 10.1038/nbt.2501.
- Infante, C., Asensio, E., Cañavate, J. P. and Manchado, M. (2008) 'Molecular characterization and expression analysis of five different elongation factor 1 alpha genes in the flatfish Senegalese sole (*Solea senegalensis* Kaup): Differential gene expression and thyroid hormones dependence during metamorphosis', *BMC Molecular Biology*. BioMed Central, 9, p. 19. doi: 10.1186/1471-2199-9-19.
- Ingebretson, J. J. and Masino, M. A. (2013) 'Quantification of locomotor activity in larval zebrafish: considerations for the design of high-throughput behavioral studies', *Frontiers in neural circuits*. Frontiers Media S.A., 7, p. 109. doi: 10.3389/fncir.2013.00109.
- Inui, T., Kobayashi, S., Ashikari, Y., Sato, R., Endo, W., Uematsu, M., Oba, H., Saitsu, H., Matsumoto, N., Kure, S. and Haginoya, K. (2016) 'Two cases of early-onset myoclonic seizures with continuous parietal delta activity caused by *EEF1A2* mutations', *Brain and Development*. The Japanese Society of Child Neurology, 38(5), pp. 520–524. doi: 10.1016/j.braindev.2015.11.003.
- Iwaniuk, A. N. and Whishaw, I. Q. (2000) 'On the origin of skilled forelimb movements', *Trends in Neurosciences*, 23(8), pp. 372–376. doi: 10.1016/S0166-2236(00)01618-0.
- Jakobsson, M. E., Malecki, J., Nilges, B. S., Moen, A., Leidel, S. A. and Falnes, P. (2017) 'Methylation of human eukaryotic elongation factor alpha (eEF1A) by a

member of a novel protein lysine methyltransferase family modulates mRNA translation', *Nucleic acids research*, 45(14), pp. 8239–8254. doi: 10.1093/nar/gkx432.

Janzer, R. C. and Raff, M. C. (1987) 'Astrocytes induce blood-brain barrier properties in endothelial cells', *Nature*, pp. 253–257. doi: 10.1038/325253a0.

Jeganathan, S., Morrow, A., Amiri, A. and Lee, J. M. (2008) 'Eukaryotic Elongation Factor 1A2 Cooperates with Phosphatidylinositol-4 Kinase III To Stimulate Production of Filopodia through Increased Phosphatidylinositol-4,5 Bisphosphate Generation', *Molecular and Cellular Biology*, 28(14), pp. 4549–4561. doi: 10.1128/MCB.00150-08.

Jeong, J. Y., Kwon, H. B., Ahn, J. C., Kang, D., Kwon, S. H., Park, J. A. and Kim, K. W. (2008) 'Functional and developmental analysis of the blood-brain barrier in zebrafish', *Brain Research Bulletin*, 75(5), pp. 619–628. doi: 10.1016/j.brainresbull.2007.10.043.

Kabashi, E., Bercier, V., Lissouba, A., Liao, M., Brustein, E., Rouleau, G. A. and Drapeau, P. (2011) 'Fus and tardbp but not sod1 interact in genetic models of amyotrophic lateral sclerosis', *PLoS Genetics*, 7(8), pp. 17–28. doi: 10.1371/journal.pgen.1002214.

Kabashi, E., Brustein, E., Champagne, N. and Drapeau, P. (2011) 'Zebrafish models for the functional genomics of neurogenetic disorders', *Biochimica et Biophysica Acta - Molecular Basis of Disease*. Elsevier B.V., 1812(3), pp. 335–345. doi: 10.1016/j.bbdis.2010.09.011.

Kahns, S., Lund, A., Kristensen, P., Knudsen, C. R., Clark, B. F. C., Cavallius, J. and Merrick, W. C. (1998) 'The elongation factor 1 A-2 isoform from rabbit: Cloning of the cDNA and characterization of the protein', *Nucleic Acids Research*, 26(8), pp. 1884–1890. doi: 10.1093/nar/26.8.1884.

Kalueff, A. V, Stewart, A. M., Gerlai, R. and Court, P. (2014) 'Zebrafish as an emerging model for studying complex brain disorders', *Trends in Pharmacological Sciences*, 35(2), pp. 63–75. doi: 10.1016/j.tips.2013.12.002.Zebrafish.

Kanibolotsky, D. S., Novosyl'na, O. V., Abbott, C. M., Negrutskii, B. S. and El'skaya, A. V. (2008) 'Multiple molecular dynamics simulation of the isoforms of human translation elongation factor 1A reveals reversible fluctuations between "open" and "closed" conformations and suggests specific for eEF1A1 affinity for Ca<sup>2+</sup>-calmodulin', *BMC Structural Biology*, 8, pp. 1–16. doi: 10.1186/1472-6807-8-4.

Kawai, H., Arata, N. and Nakayasu, H. (2001) 'Three-dimensional distribution of astrocytes in zebrafish spinal cord', *Glia*, 36(3), pp. 406–413. doi: 10.1002/glia.1126.

Khalyfa, A., Bourbeau, D., Chen, E., Petroulakis, E., Pan, J., Xu, S. and Wang, E. (2001) 'Characterization of Elongation Factor-1A (eEF1A-1) and eEF1A-2/S1 Protein Expression in Normal and wasted Mice', *Journal of Biological Chemistry*, 276(25), pp. 22915–22922. doi: 10.1074/jbc.M101011200.

Khalyfa, A., Carlson, B. M., Dedkov, E. I. and Wang, E. (2003) 'Changes in protein

levels of elongation factors, eEF1A-1 and eEF1A-2/S1, in long-term denervated rat muscle.’, *Restorative neurology and neuroscience*, 21(1–2), pp. 47–53.

Kiernan, M. C., Vucic, S., Cheah, B. C., Turner, M. R., Eisen, A., Hardiman, O., Burrell, J. R. and Zoing, M. C. (2011) ‘Amyotrophic lateral sclerosis’, *The Lancet*. Elsevier Ltd, 377(9769), pp. 942–955. doi: 10.1016/S0140-6736(10)61156-7.

Kimmel, C. B., Ballard, W. W., Kimmel, S. R., Ullmann, B. and Schilling, T. F. (1995) ‘Stages of embryonic development of the zebrafish.’, *Developmental Dynamics*, 203(3), pp. 253–310. doi: 10.1002/aja.1002030302.

Kinoshita, M., Kani, S., Ozato, K. and Wakamatsu, Y. (2001) ‘Activity of the medaka translation elongation factor 1 $\alpha$ -A promoter examined using the GFP gene as a reporter’, *Development, Growth & Differentiation*. Wiley/Blackwell (10.1111), 42(5), pp. 469–478. doi: 10.1046/j.1440-169x.2000.00530.x.

Kirby, B. B., Takada, N., Latimer, A. J., Shin, J., Carney, T. J., Kelsh, R. N. and Appel, B. (2006) ‘In vivo time-lapse imaging shows dynamic oligodendrocyte progenitor behavior during zebrafish development’, *Nature Neuroscience*, 9(12), pp. 1506–1511. doi: 10.1038/nn1803.

Knudsen, S. M., Frydenberg, J., Clark, B. F. C. and Leffers, H. (1993) ‘Tissue-dependent variation in the expression of elongation factor-lor isoforms : Isolation and characterisation of a cDNA encoding a novel variant of human elongation-factor lor’, 554, pp. 549–554.

Kok, F. O., Shin, M., Ni, C.-W., Gupta, A., Grosse, A. S., van Impel, A., Kirchmaier, B. C., Peterson-Maduro, J., Kourkoulis, G., Male, I., DeSantis, D. F., Sheppard-Tindell, S., Ebarasi, L., Betsholtz, C., Schulte-Merker, S., Wolfe, S. A. and Lawson, N. D. (2015) ‘Reverse genetic screening reveals poor correlation between Morpholino-induced and mutant phenotypes in zebrafish’, *Developmental cell*, 32(1), pp. 97–108. doi: 10.1016/j.devcel.2014.11.018.

Kulkarni, G., Turbin, D. A., Amiri, A., Jeganathan, S., Andrade-Navarro, M. A., Wu, T. D., Huntsman, D. G. and Lee, J. M. (2007) ‘Expression of protein elongation factor eEF1A2 predicts favorable outcome in breast cancer’, *Breast Cancer Research and Treatment*, 102(1), pp. 31–41. doi: 10.1007/s10549-006-9315-8.

Kurosinski, P., Biol, D. and Götz, J. (2002) ‘Glial cells under physiologic and pathologic conditions’, *Archives of Neurology*, 59(10), pp. 1524–1528. doi: 10.1001/archneur.59.10.1524.

Laird, A. S., van Hoecke, A., De Muynck, L., Timmers, M., van den Bosch, L., Van Damme, P. and Robberecht, W. (2010) ‘Progranulin is neurotrophic in vivo and protects against a mutant TDP-43 induced axonopathy’, *PLoS ONE*, 5(10), pp. 1–7. doi: 10.1371/journal.pone.0013368.

Lam, W. W. K., Millichap, J. J., Soares, D. C., Chin, R., McLellan, A., FitzPatrick, D. R., Elmslie, F., Lees, M. M., Schaefer, G. B. and Abbott, C. M. (2016) ‘Novel de novo *EEF1A2* missense mutations causing epilepsy and intellectual disability’, *Molecular Genetics & Genomic Medicine*, 4(4), pp. 465–474. doi: 10.1002/mgg3.219.

- Lambrechts, D., Storkebaum, E., Morimoto, M., Del-Favero, J., Desmet, F., Marklund, S. L., Wyns, S., Thijs, V., Andersson, J., Van Marion, I., Al-Chalabi, A., Bornes, S., Musson, R., Hansen, V., Beckman, L., Adolfsson, R., Pall, H. S., Prats, H., Vermeire, S., Rutgeerts, P., Katayama, S., Awata, T., Leigh, N., Lang-Lazdunski, L., Dewerchin, M., Shaw, C., Moons, L., Vlietinck, R., Morrison, K. E., Robberecht, W., Van Broeckhoven, C., Collen, D., Andersen, P. M. and Carmeliet, P. (2003) 'VEGF is a modifier of amyotrophic lateral sclerosis in mice and humans and protects motoneurons against ischemic death', *Nature Genetics*, 34(4), pp. 383–394. doi: 10.1038/ng1211.
- Lee, M. H. and Surh, Y. J. (2009) 'eEF1A2 as a putative oncogene', *Annals of the New York Academy of Sciences*, 1171, pp. 87–93. doi: 10.1111/j.1749-6632.2009.04909.x.
- Lee, S., Wolfrum, L. A. and Wang, E. (1993) 'Differential expression of S1 and elongation factor-1 $\alpha$  during rat development', *Journal of Biological Chemistry*, 268(32), pp. 24453–24459.
- Lemmens, R., Van Hoecke, A., Hersmus, N., Geelen, V., D'Hollander, I., Thijs, V., Van Den Bosch, L., Carmeliet, P. and Robberecht, W. (2007) 'Overexpression of mutant superoxide dismutase 1 causes a motor axonopathy in the zebrafish', *Human Molecular Genetics*, 16(19), pp. 2359–2365. doi: 10.1093/hmg/ddm193.
- Levy, E. D., Michnick, S. W. and Landry, C. R. (2012) 'Protein abundance is key to distinguish promiscuous from functional phosphorylation based on evolutionary information', *Philosophical Transactions of the Royal Society B: Biological Sciences*. The Royal Society, 367(1602), pp. 2594–2606. doi: 10.1098/rstb.2012.0078.
- Li, D., Wei, T., Abbott, C. M. and Harrich, D. (2013) 'The Unexpected Roles of Eukaryotic Translation Elongation Factors in RNA Virus Replication and Pathogenesis', *Microbiology and Molecular Biology Reviews*, 77(2), pp. 253–266. doi: 10.1128/MMBR.00059-12.
- Li, J., Zhang, B., Ren, Y., Gu, S., Xiang, Y., Huang, C. and Du, J. (2015) 'Intron targeting-mediated and endogenous gene integrity-maintaining knockin in zebrafish using the CRISPR/Cas9 system', *Cell Research*. The Author(s), 25, p. 634. Available at: <http://dx.doi.org/10.1038/cr.2015.43>.
- Li, R., Wang, H., Bekele, B. N., Yin, Z., Caraway, N. P., Katz, R. L., Stass, S. A. and Jiang, F. (2006) 'Identification of putative oncogenes in lung adenocarcinoma by a comprehensive functional genomic approach', *Oncogene*, 25(18), pp. 2628–2635. doi: 10.1038/sj.onc.1209289.
- Li, Z., Qi, C. F., Shin, D. M., Zingone, A., Newbery, H. J., Kovalchuk, A. L., Abbott, C. M. and Morse, H. C. (2010) 'Eef1a2 promotes cell growth, inhibits apoptosis and activates JAK/STAT and AKT signaling in mouse plasmacytomas', *PLoS ONE*, 5(5).
- Lieschke, G. J. and Currie, P. D. (2007) 'Animal models of human disease: Zebrafish swim into view', *Nature Reviews Genetics*, 8(5), pp. 353–367. doi: 10.1038/nrg2091.
- de Ligt, J., Willemsen, M. H., van Bon, B. W. M., Kleefstra, T., Yntema, H. G.,

- Kroes, T., Vulto-van Silfhout, A. T., Koolen, D. a, de Vries, P., Gilissen, C., del Rosario, M., Hoischen, A., Scheffer, H., de Vries, B. B. a, Brunner, H. G., Veltman, J. a and Vissers, L. E. L. M. (2012) ‘Diagnostic exome sequencing in persons with severe intellectual disability.’, *The New England journal of medicine*, 367(20), pp. 1921–9. doi: 10.1056/NEJMoa1206524.
- Lin, K. W., Yakymovych, I., Jia, M., Yakymovych, M. and Souchelnytskyi, S. (2010) ‘Phosphorylation of eEF1A1 at Ser300 by TβR-I results in inhibition of mRNA translation’, *Current Biology*, 20(18), pp. 1615–1625. doi: 10.1016/j.cub.2010.08.017.
- Lindquist, S. and Craig, E. A. (1988) ‘The Heat-Shock Proteins’, *Annual Review of Genetics*. Annual Reviews, 22(1), pp. 631–677. doi: 10.1146/annurev.ge.22.120188.003215.
- Lipson, R. S., Webb, K. J. and Clarke, S. G. (2010) ‘Two novel methyltransferases acting upon eukaryotic elongation factor 1A in *Saccharomyces cerevisiae*’, *Archives of biochemistry and biophysics*, 500(2), pp. 137–143. doi: 10.1016/j.abb.2010.05.023.
- Liu, G., Tang, J., Edmonds, B. T., Murray, J., Levin, S. and Condeelis, J. (1996) ‘F-actin sequesters elongation factor 1 $\alpha$  from interaction with aminoacyl-tRNA in a pH-dependent reaction’, *Journal of Cell Biology*, 135(4), pp. 953–963. doi: 10.1083/jcb.135.4.953.
- Livingstone, M., Atas, E., Meller, A. and Sonenberg, N. (2010) ‘Mechanisms governing the control of mRNA translation’, *Physical Biology*, 7(2). doi: 10.1088/1478-3975/7/2/021001.
- Logroscino, G., Traynor, B. J., Hardiman, O., Chió, A., Mitchell, D., Swingler, R. J., Millul, A., Benn, E. and Beghi, E. (2010) ‘Incidence of amyotrophic lateral sclerosis in Europe’, *Journal of Neurology, Neurosurgery and Psychiatry*, 81(4), pp. 385–390. doi: 10.1136/jnnp.2009.183525.
- Lopes, F., Barbosa, M., Ameer, A., Soares, G., De Sá, J., Dias, A. I., Oliveira, G., Cabral, P., Temudo, T., Calado, E., Cruz, I. F., Vieira, J. P., Oliveira, R., Esteves, S., Sauer, S., Jonasson, I., Syvänen, A. C., Gyllensten, U., Pinto, D. and Maciel, P. (2016) ‘Identification of novel genetic causes of Rett syndrome-like phenotypes’, *Journal of Medical Genetics*, 53(3), pp. 190–199. doi: 10.1136/jmedgenet-2015-103568.
- Loreni, F., Francesconi, A. and Amaldi, F. (1993) ‘Coordinate translational regulation in the syntheses of elongation factor 1 alpha and ribosomal proteins in *Xenopus laevis*’, *Nucleic Acids Res*, 21(20), pp. 4721–4725. Available at: [http://www.ncbi.nlm.nih.gov/entrez/query.fcgi?cmd=Retrieve&db=PubMed&dopt=Citation&list\\_uids=8233819](http://www.ncbi.nlm.nih.gov/entrez/query.fcgi?cmd=Retrieve&db=PubMed&dopt=Citation&list_uids=8233819).
- Lutsep, Helmi L. ; Rodriguez, M. (1989) ‘Ultrastructural, morphometric, and immunocytochemical study of anterior horn cells in mice with “wasted” mutation.’, *Journal of Neuropathology and Experimental Neurology*, 48(5), pp. 519–533. Available at: <https://ohsu.pure.elsevier.com/en/publications/ultrastructural-morphometric-and-immunocytochemical-study-of-ante-2>.

- Lyons, D. A. and Talbot, W. S. (2015) 'Glial Cell Development and Function in Zebrafish', *Cold Spring Harbor Perspectives in Biology*. Cold Spring Harbor Laboratory Press, 7(2), p. a020586. doi: 10.1101/cshperspect.a020586.
- MacPhail, R. C., Brooks, J., Hunter, D. L., Padnos, B., Irons, T. D. and Padilla, S. (2009) 'Locomotion in larval zebrafish: Influence of time of day, lighting and ethanol', *NeuroToxicology*, 30(1), pp. 52–58. doi: <https://doi.org/10.1016/j.neuro.2008.09.011>.
- Maddison, L. A., Li, M. and Chen, W. (2014) 'Conditional Gene-Trap Mutagenesis in Zebrafish', *Methods in molecular biology (Clifton, N.J.)*, 1101, pp. 393–411. doi: 10.1007/978-1-62703-721-1\_19.
- Małeckı, J., Aileni, V. K., Ho, A. Y. Y., Schwarz, J., Moen, A., Sørensen, V., Nilges, B. S., Jakobsson, M. E., Leidel, S. A. and Falnes, P. Ø. (2017) 'The novel lysine specific methyltransferase METTL21B affects mRNA translation through inducible and dynamic methylation of Lys-165 in human eukaryotic elongation factor 1 alpha (eEF1A)', *Nucleic Acids Research*. Oxford University Press, 45(8), pp. 4370–4389. doi: 10.1093/nar/gkx002.
- Maragakis, N. J. and Galvez-Jimenez, N. (2018) 'Epidemiology and pathogenesis of amyotrophic lateral sclerosis', *UpToDate*, pp. 1–20. doi: 10.1007/s11920-014-0463-y.
- Mateyak, M. K. and Kinzy, T. G. (2010) 'eEF1A: Thinking outside the ribosome', *Journal of Biological Chemistry*, 285(28), pp. 21209–21213. doi: 10.1074/jbc.R110.113795.
- McGown, A., McDearmid, J. R., Panagiotaki, N., Tong, H., Al Mashhadi, S., Redhead, N., Lyon, A. N., Beattie, C. E., Shaw, P. J. and Ramesh, T. M. (2013) 'Early interneuron dysfunction in ALS: Insights from a mutant sod1 zebrafish model', *Annals of Neurology*, 73(2), pp. 246–258. doi: 10.1002/ana.23780.
- Mead, R. J., Higginbottom, A., Allen, S. P., Kirby, J., Bennett, E., Barber, S. C., Heath, P. R., Coluccia, A., Patel, N., Gardner, I., Brancale, A., Grierson, A. J. and Shaw, P. J. (2013) 'S[+] Apomorphine is a CNS penetrating activator of the Nrf2-ARE pathway with activity in mouse and patient fibroblast models of amyotrophic lateral sclerosis', *Free Radical Biology and Medicine*. Elsevier, 61, pp. 438–452. doi: 10.1016/j.freeradbiomed.2013.04.018.
- Meeker, N. D., Hutchinson, S. A., Ho, L. and Trede, N. S. (2007) 'Method for isolation of PCR-ready genomic DNA from zebrafish tissues', *BioTechniques*. Future Science, 43(5), pp. 610–614. doi: 10.2144/000112619.
- Merrick, W. C., Dever, T. E., Kinzy, T. G., Conroy, S. C., Cavallius, J. and Owens, C. L. (1990) 'Characterization of protein synthesis factors from rabbit reticulocytes', *BBA - Gene Structure and Expression*, 1050(1–3), pp. 235–240. doi: 10.1016/0167-4781(90)90173-Y.
- Miceli, F., Soldovieri, M. V., Ambrosino, P., De Maria, M., Migliore, M., Migliore, R. and Tagliatela, M. (2015) 'Early-Onset Epileptic Encephalopathy Caused by Gain-of-Function Mutations in the Voltage Sensor of Kv7.2 and Kv7.3 Potassium



- Channel Subunits', *Journal of Neuroscience*, 35(9), pp. 3782–3793. doi: 10.1523/JNEUROSCI.4423-14.2015.
- Molina, H., Horn, D. M., Tang, N., Mathivanan, S. and Pandey, A. (2007) 'Global proteomic profiling of phosphopeptides using electron transfer dissociation tandem mass spectrometry', *Pnas*, 104(7), pp. 2199–204. doi: 10.1073/pnas.0611217104.
- Morrow, J., Russell, A., Guthrie, E., Parsons, L., Robertson, I., Waddell, R., Irwin, B., McGivern, R. C., Morrison, P. J. and Craig, J. (2006) 'Malformation risks of antiepileptic drugs in pregnancy: A prospective study from the UK Epilepsy and Pregnancy Register', *Journal of Neurology, Neurosurgery and Psychiatry*, 77(2), pp. 193–198. doi: 10.1136/jnnp.2005.074203.
- Nagashima, K., Nagata, S. and Kaziro, Y. (1986) 'Structure of the two genes coding for polypeptide chain elongation factor Ia (EF-Ia) from *Saccharomyces cerevisiae*', *Gene*, 45, pp. 265–273. doi: 10.1016/0378-1119(86)90024-7.
- Nagata, S., Nagashima, K., Tsunetsugu, Y., Fujimura, K., Miyazaki, M. and Kaziro, Y. (1984) 'Polypeptide chain elongation factor', 3(8), pp. 1825–1830.
- Nakajima, J., Okamoto, N., Tohyama, J., Kato, M., Arai, H., Funahashi, O., Tsurusaki, Y., Nakashima, M., Kawashima, H., Saitsu, H., Matsumoto, N. and Miyake, N. (2014) 'De novo EEF1A2 mutations in patients with characteristic facial features, intellectual disability, autistic behaviors and epilepsy.', *Clinical genetics*, pp. 1–6. doi: 10.1111/cge.12394.
- Newbery, H. J., Gillingwater, T. H., Dharmasaroja, P., Peters, J., Wharton, S. B., Thomson, D., Ribchester, R. R. and Abbott, C. M. (2005) 'Progressive Loss of Motor Neuron Function in Wasted Mice: Effects of a Spontaneous Null Mutation in the Gene for the eEF1A2 Translation Factor', *Journal of Neuropathology & Experimental Neurology*, 64(4), pp. 295–303. doi: 10.1093/jnen/64.4.295.
- Newbery, H. J., Loh, D. H., O'Donoghue, J. E., Tomlinson, V. A. L., Chau, Y. Y., Boyd, J. A., Bergmann, J. H., Brownstein, D. and Abbott, C. M. (2007) 'Translation elongation factor eEF1A2 is essential for post-weaning survival in mice', *Journal of Biological Chemistry*, 282(39), pp. 28951–28959. doi: 10.1074/jbc.M703962200.
- Newbery, H. J., Stancheva, I., Zimmerman, L. B. and Abbott, C. M. (2011) 'Evolutionary importance of translation elongation factor eEF1A variant switching: eEF1A1 down-regulation in muscle is conserved in *Xenopus* but is controlled at a post-transcriptional level.', *Biochemical and biophysical research communications*. Elsevier Inc., 411(1), pp. 19–24. doi: 10.1016/j.bbrc.2011.06.062.
- Newbery, H. J., Stancheva, I., Zimmerman, L. B. and Abbott, C. M. (2011) 'Evolutionary importance of translation elongation factor eEF1A variant switching: eEF1A1 down-regulation in muscle is conserved in *Xenopus* but is controlled at a post-transcriptional level', *Biochemical and Biophysical Research Communications*. Elsevier Inc., 411(1), pp. 19–24. doi: 10.1016/j.bbrc.2011.06.062.
- Nieuwenhuys, R., Pouwels, E. and Smulders-Kersten, E. (1974) 'The Neuronal Organization of Cerebellar Lobe C1 in the Mormyrid Fish *Gnathonemus petersii* (Teleostei)', *Zeitschrift für Anatomie und Entwicklungsgeschichte*, 144(3), pp. 315–

336. doi: 10.1007/BF00522813.

Novosylina, O., Doyle, A., Vlasenko, D., Murphy, M., Negrutskii, B. and El'Skaya, A. (2017) 'Comparison of the ability of mammalian eEF1A1 and its oncogenic variant eEF1A2 to interact with actin and calmodulin', *Biological Chemistry*, 398(1), pp. 113–124. doi: 10.1515/hsz-2016-0172.

O'Callaghan, J. P. and Sriram, K. (2005) 'Glial fibrillary acidic protein and related glial proteins as biomarkers of neurotoxicity', *Expert Opinion on Drug Safety*, 4(3), pp. 433–442. doi: 10.1517/14740338.4.3.433.

Patten, S. A., Aggad, D., Martinez, J., Tremblay, E., Petrillo, J., Armstrong, G. A. B., La Fontaine, A., Maios, C., Liao, M., Ciura, S., Wen, X.-Y., Rafuse, V., Ichida, J., Zinman, L., Julien, J.-P., Kabashi, E., Robitaille, R., Korngut, L., Parker, J. A. and Drapeau, P. (2017) 'Neuroleptics as therapeutic compounds stabilizing neuromuscular transmission in amyotrophic lateral sclerosis', *JCI Insight*, 2(22), pp. 1–20. doi: 10.1172/jci.insight.97152.

Patten, S. A., Armstrong, G. A. B., Lissouba, A., Kabashi, E., Parker, J. A. and Drapeau, P. (2014) 'Fishing for causes and cures of motor neuron disorders', *Disease Models & Mechanisms*, 7(7), p. 799 LP-809. Available at: <http://dmm.biologists.org/content/7/7/799.abstract>.

Pecorari, L., Marin, O., Silvestri, C., Candini, O., Rossi, E., Guerzoni, C., Cattelani, S., Mariani, S. A., Corradini, F., Ferrari-Amorotti, G., Cortesi, L., Bussolari, R., Raschella, G., Federico, M. R. and Calabretta, B. (2009) 'Elongation Factor 1 alpha interacts with phospho-Akt in breast cancer cells and regulates their proliferation, survival and motility', *Molecular Cancer*, 8, pp. 1–11. doi: 10.1186/1476-4598-8-58.

Peri, F. and Nüsslein-Volhard, C. (2008) 'Live Imaging of Neuronal Degradation by Microglia Reveals a Role for v0-ATPase a1 in Phagosomal Fusion In Vivo', *Cell*, 133(5), pp. 916–927. doi: 10.1016/j.cell.2008.04.037.

Pettersen, E. F., Goddard, T. D., Huang, C. C., Couch, G. S., Greenblatt, D. M., Meng, E. C. and Ferrin, T. E. (2004) 'UCSF Chimera - A visualization system for exploratory research and analysis', *Journal of Computational Chemistry*, 25(13), pp. 1605–1612. doi: 10.1002/jcc.20084.

Pfaffl, M. W. (2001) 'A new mathematical model for relative quantification in real-time RT-PCR', *Nucleic Acids Research*. Oxford, UK: Oxford University Press, 29(9), pp. e45–e45. Available at: <http://www.ncbi.nlm.nih.gov/pmc/articles/PMC55695/>.

Popp, M. W. and Maquat, L. E. (2016) 'Leveraging rules of nonsense-mediated mRNA decay for genome engineering and personalized medicine', *Cell*. Elsevier Inc., 165(6), pp. 1319–1332. doi: 10.1016/j.cell.2016.05.053.

Rink, E. and Wullimann, M. F. (2004) 'Connections of the ventral telencephalon (subpallium) in the zebrafish (*Danio rerio*)', *Brain Research*, 1011(2), pp. 206–220. doi: 10.1016/j.brainres.2004.03.027.

Robu, M. E., Larson, J. D., Nasevicius, A., Beiraghi, S., Brenner, C., Farber, S. A. and Ekker, S. C. (2007) 'p53 Activation by Knockdown Technologies', *PLoS*

*Genetics*. Edited by M. Mullins. San Francisco, USA: Public Library of Science, 3(5), p. e78. doi: 10.1371/journal.pgen.0030078.

Rosander, C. and Hallböök, T. (2015) 'Dravet syndrome in Sweden: A population-based study', *Developmental Medicine and Child Neurology*, 57(7), pp. 628–633. doi: 10.1111/dmcn.12709.

Rosen, D. R., Siddique, T., Patterson, D., Figlewicz, D. A., Sapp, P., Hentati, A., Donaldson, D., Goto, J., O'Regan, J. P. and Deng, H. X. (1993) 'Mutations in Cu/Zn superoxide dismutase gene are associated with familial amyotrophic lateral sclerosis.', *Nature*, 362(6415), pp. 59–62. doi: 10.1038/362059a0.

Rosenberry, T. L., Krall, J. A., Dever, T. E., Haas, R., Louvard, D. and Merrick, W. C. (1989) 'Biosynthetic incorporation of [3H]ethanolamine into protein synthesis elongation factor 1 $\alpha$  reveals a new post-translational protein modification', *Journal of Biological Chemistry*, 264(13), pp. 7096–7099.

Rossi, A., Kontarakis, Z., Gerri, C., Nolte, H., Hölper, S., Krüger, M. and Stainier, D. Y. R. (2015) 'Genetic compensation induced by deleterious mutations but not gene knockdowns', *Nature*. Nature Publishing Group, a division of Macmillan Publishers Limited. All Rights Reserved., 524, p. 230. Available at: <http://dx.doi.org/10.1038/nature14580>.

Ruest, L.-B., Marcotte, R. and Wang, E. (2002) 'Peptide elongation factor eEF1A-2/S1 expression in cultured differentiated myotubes and its protective effect against caspase-3-mediated apoptosis.', *The Journal of biological chemistry*, 277(7), pp. 5418–25. doi: 10.1074/jbc.M110685200.

Rush, J., Moritz, A., Lee, K. A., Guo, A., Goss, V. L., Spek, E. J., Zhang, H., Zha, X. M., Polakiewicz, R. D. and Comb, M. J. (2005) 'Immunoaffinity profiling of tyrosine phosphorylation in cancer cells', *Nature Biotechnology*, 23(1), pp. 94–101. doi: 10.1038/nbt1046.

Sanges, C., Scheuermann, C., Zahedi, R. P., Sickmann, A., Lamberti, A., Migliaccio, N., Baljuls, A., Marra, M., Zappavigna, S., Rapp, U., Abbruzzese, A., Caraglia, M. and Arcari, P. (2012) 'Raf kinases mediate the phosphorylation of eukaryotic translation elongation factor 1A and regulate its stability in eukaryotic cells', *Cell Death and Disease*. Nature Publishing Group, 3(3), pp. e276-9. doi: 10.1038/cddis.2012.16.

Sanner, M. F., Olson, A. J. and Spehner, J.-C. (2018) 'Reduced surface: An efficient way to compute molecular surfaces', *Biopolymers*. Wiley-Blackwell, 38(3), pp. 305–320. doi: 10.1002/(SICI)1097-0282(199603)38:3<305::AID-BIP4>3.0.CO;2-Y.

Sarlette, A., Krampfl, K., Grothe, C., Neuhoff, N. Von, Dengler, R. and Petri, S. (2008) 'Nuclear erythroid 2-related factor 2-antioxidative response element signaling pathway in motor cortex and spinal cord in amyotrophic lateral sclerosis', *Journal of Neuropathology and Experimental Neurology*, 67(11), pp. 1055–1062. doi: 10.1097/NEN.0b013e31818b4906.

Sathasivam, S. (2010) 'Motor neurone disease : clinical features , diagnosis , diagnostic pitfalls and prognostic markers', 51(5), pp. 367–373.

- Saxena, S., Cabuy, E. and Caroni, P. (2009) 'A role for motoneuron subtype-selective ER stress in disease manifestations of FALS mice', *Nature Neuroscience*, 12(5), pp. 627–636. doi: 10.1038/nn.2297.
- Schlaeger, C., Longerich, T., Schiller, C., Bewerunge, P., Mehrabi, A., Toedt, G., Kleeff, J., Ehemann, V., Eils, R., Lichter, P., Schumacher, P. and Radlwimmer, B. (2008) 'Etiology-dependent molecular mechanisms in human hepatocarcinogenesis', *Hepatology*, 47(2), pp. 511–520. doi: 10.1002/hep.22033.
- Shamovsky, I., Ivannikov, M., Kandel, E. S., Gershon, D. and Nudler, E. (2006) 'RNA-mediated response to heat shock in mammalian cells', *Nature*, 440(7083), pp. 556–560. doi: 10.1038/nature04518.
- Shamovsky, I. and Nudler, E. (2008) 'New insights into the mechanism of heat shock response activation', *Cellular and Molecular Life Sciences*, 65(6), pp. 855–861. doi: 10.1007/s00018-008-7458-y.
- Shiina, N., Gotoh, Y., Kubomura, N., Iwamatsu, A. and Nishida, E. (1994) 'Microtubule severing by elongation factor 1 alpha', *Science*, 266(5183), p. 282 LP-285. Available at: <http://science.sciencemag.org/content/266/5183/282.abstract>.
- Shimazu, T., Barjau, J., Sohtome, Y., Sodeoka, M. and Shinkai, Y. (2014) 'Selenium-Based S-Adenosylmethionine Analog Reveals the Mammalian Seven-Beta-Strand Methyltransferase METTL10 to Be an EF1A1 Lysine Methyltransferase', *PLoS ONE*. Edited by A. Jeltsch. Public Library of Science, 9(8), p. e105394. doi: 10.1371/journal.pone.0105394.
- Shorvon, S. D. (2011) 'The etiological classification of epilepsy', *The Causes of Epilepsy: Common and Uncommon Causes in Adults and Children*, 9780521114(6), pp. 21–23. doi: 10.1017/CBO9780511921001.004.
- Shultz, L.D, Sweet, H.O, Davisson, M. . and C. D. . (1982) "'Wasted", a new mutant of the mouse with abnormalities characteristics of ataxia telangiectasia'. *Nature*, 297, pp. 402–404.
- Sievers, F., Wilm, A., Dineen, D., Gibson, T. J., Karplus, K., Li, W., Lopez, R., McWilliam, H., Remmert, M., Söding, J., Thompson, J. D. and Higgins, D. G. (2011) 'Fast, scalable generation of high-quality protein multiple sequence alignments using Clustal Omega', *Molecular systems biology*. School of Medicine and Medical Science, UCD Conway Institute of Biomolecular and Biomedical Research, University College Dublin, Dublin, Ireland., p. 539. doi: 10.1038/msb.2011.75.
- Simon, E. (1987) 'Effect of acclimation temperature on the elongation step of protein synthesis in different organs of rainbow trout', *Journal of Comparative Physiology B: Biochemical, Systemic and Environmental Physiology*, 157(2), pp. 201–207. doi: 10.1007/BF00692364.
- Singh, N. A., Charlier, C., Stauffer, D., DuPont, B. R., Leach, R. J., Melis, R., Ronen, G. M., Bjerre, I., Quattlebaum, T., Murphy, J. V., McHarg, M. L., Gagnon, D., Rosales, T. O., Peiffer, A., Elving Anderson, V. and Leppert, M. (1998) 'A novel potassium channel gene, KCNQ2, is mutated in an inherited epilepsy of newborns',

*Nature Genetics*, 18(1), pp. 25–29. doi: 10.1038/ng0198-25.

Soares, D. C. and Abbott, C. M. (2013) ‘Highly homologous eEF1A1 and eEF1A2 exhibit differential post-translational modification with significant enrichment around localised sites of sequence variation’, *Biology Direct*. *Biology Direct*, 8(1), p. 1. doi: 10.1186/1745-6150-8-29.

Soares, D. C., Barlow, P. N., Newbery, H. J., Porteous, D. J. and Abbott, C. M. (2009) ‘Structural models of human eEF1A1 and eEF1A2 reveal two distinct surface clusters of sequence variation and potential differences in phosphorylation.’, *PLoS one*, 4(7), p. e6315. doi: 10.1371/journal.pone.0006315.

Stewart, A. M., Desmond, D., Kyzar, E., Gaikwad, S., Roth, A., Riehl, R., Collins, C., Monnig, L., Green, J. and Kalueff, A. V. (2012) ‘Perspectives of zebrafish models of epilepsy: What, how and where next?’, *Brain Research Bulletin*. Elsevier Inc., 87(2–3), pp. 135–143. doi: 10.1016/j.brainresbull.2011.11.020.

Storkebaum, E., Lambrechts, D., Dewerchin, M., Moreno-Murciano, M. P., Appelmans, S., Oh, H., Van Damme, P., Rutten, B., Man, W. Y., De Mol, M., Wyns, S., Manka, D., Vermeulen, K., Van Den Bosch, L., Mertens, N., Schmitz, C., Robberecht, W., Conway, E. M., Collen, D., Moons, L. and Carmeliet, P. (2005) ‘Treatment of motoneuron degeneration by intracerebroventricular delivery of VEGF in a rat model of ALS’, *Nature Neuroscience*, 8(1), pp. 85–92. doi: 10.1038/nn1360.

Al Sultan, A., Waller, R., Heath, P. and Kirby, J. (2016) ‘The genetics of amyotrophic lateral sclerosis: current insights’, *Degenerative Neurological and Neuromuscular Disease*, 6, pp. 49–64. doi: 10.2147/DNND.S84956.

Sun, Y., Du, C., Wang, B., Zhang, Y., Liu, X. and Ren, G. (2014) ‘Up-regulation of eEF1A2 promotes proliferation and inhibits apoptosis in prostate cancer’, *Biochemical and Biophysical Research Communications*. Elsevier Inc., 450(1), pp. 1–6. doi: 10.1016/j.bbrc.2014.05.045.

Sung, Y. J., Dolzhanskaya, N., Nolin, S. L., Brown, T., Currie, J. R. and Denman, R. B. (2003) ‘The Fragile X Mental Retardation Protein FMRP Binds Elongation Factor 1A mRNA and Negatively Regulates Its Translation in Vivo \*’, 278(18), pp. 15669–15678. doi: 10.1074/jbc.M211117200.

Svobodová, K., Horák, P., Stratil, A., Bartenschlager, H., Van Poucke, M., Chalupová, P., Dvořáková, V., Knorr, C., Stupka, R., Čítek, J., Šprysl, M., Palánová, A., Peelman, L. J., Geldermann, H. and Knoll, A. (2015) ‘Porcine EEF1A1 and EEF1A2 genes: genomic structure, polymorphism, mapping and expression’, *Molecular Biology Reports*, 42(8), pp. 1257–1264. doi: 10.1007/s11033-015-3866-x.

Talapatra, S., Wagner, J. D. O. and Thompson, C. B. (2002) ‘Elongation factor-1 alpha is a selective regulator of growth factor withdrawal and ER stress-induced apoptosis’, *Cell Death and Differentiation*, 9(8), pp. 856–861. doi: 10.1038/sj.cdd.4401078.

Tamura, K., Stecher, G., Peterson, D., Filipowski, A. and Kumar, S. (2013) ‘MEGA6: Molecular evolutionary genetics analysis version 6.0’, *Molecular Biology and Evolution*, 30(12), pp. 2725–2729.

- Teng, Y., Xie, X., Walker, S., Rempala, G., Kozlowski, D. J., Mumm, J. S. and Cowell, J. K. (2010) 'Knockdown of zebrafish *Igi1a* results in abnormal development, brain defects and a seizure-like behavioral phenotype', *Human Molecular Genetics*, 19(22), pp. 4409–4420. doi: 10.1093/hmg/ddq364.
- Teng, Y., Xie, X., Walker, S., Saxena, M., Kozlowski, D. J., Mumm, J. S. and Cowell, J. K. (2011) 'Loss of zebrafish *Igi1b* leads to hydrocephalus and sensitization to pentylentetrazol induced seizure-like behavior', *PLoS ONE*, 6(9). doi: 10.1371/journal.pone.0024596.
- Thisse, C. and Thisse, B. (2007) 'High-resolution in situ hybridization to whole-mount zebrafish embryos', *Nature Protocols*. Nature Publishing Group, 3, p. 59. Available at: <http://dx.doi.org/10.1038/nprot.2007.514>.
- Thornton, S., Anand, N., Purcell, D. and Lee, J. (2003) 'Not just for housekeeping: Protein initiation and elongation factors in cell growth and tumorigenesis', *Journal of Molecular Medicine*, 81(9), pp. 536–548. doi: 10.1007/s00109-003-0461-8.
- Timchenko, A. A., Novosylina, O. V., Prituzhalov, E. A., Kihara, H., El'Skaya, A. V., Negrutskii, B. S. and Serdyuk, I. N. (2013) 'Different oligomeric properties and stability of highly homologous A1 and proto-oncogenic A2 variants of mammalian translation elongation factor eEF1', *Biochemistry*, 52(32), pp. 5345–5353. doi: 10.1021/bi400400r.
- Tomlinson, V. A. L., Newbery, H. J., Bergmann, J. H., Boyd, J., Scott, D., Wray, N. R., Sellar, G. C., Gabra, H., Graham, A., Williams, A. R. W. and Abbott, C. M. (2007) 'Expression of eEF1A2 is associated with clear cell histology in ovarian carcinomas: Overexpression of the gene is not dependent on modifications at the EEF1A2 locus', *British Journal of Cancer*, 96(10), pp. 1613–1620. doi: 10.1038/sj.bjc.6603748.
- Tomlinson, V. A. L., Newbery, H. J., Wray, N. R., Jackson, J., Larionov, A., Miller, W. R., Dixon, J. M. and Abbott, C. M. (2005) 'Translation elongation factor eEF1A2 is a potential oncoprotein that is overexpressed in two-thirds of breast tumours.', *BMC cancer*, 5, p. 113.
- Tropepe, V. and Sive, H. L. (2003) 'Can zebrafish be used as a model to study the neurodevelopmental causes of autism?', *Genes, Brain and Behavior*, 2(5), pp. 268–281. doi: 10.1034/j.1601-183X.2003.00038.x.
- Tsai, N.-P., Wilkerson, J. R., Guo, W., Maksimova, M. A., DeMartino, G. N., Cowan, C. W. and Huber, K. M. (2012) 'Multiple autism-linked genes mediate synapse elimination via proteasomal degradation of a synaptic scaffold PSD-95', *Cell*, 151(7), pp. 1581–1594. doi: 10.1016/j.cell.2012.11.040.
- Tsaytler, P., Harding, H. P., Ron, D. and Bertolotti, A. (2011) 'Selective Inhibition of a Regulatory Subunit of Protein Phosphatase 1 Restores Proteostasis', *Science*, 332(6025), pp. 91–94. doi: 10.1126/science.1201396.
- Tsokas, P., Grace, E. A., Chan, P., Ma, T., Sealfon, S. C., Iyengar, R., Landau, E. M. and Blitzer, R. D. (2005) 'Local Protein Synthesis Mediates a Rapid Increase in Dendritic Elongation Factor 1A after Induction of Late Long-Term Potentiation', *The*

*Journal of Neuroscience*, 25(24), p. 5833 LP-5843. doi: 10.1523/JNEUROSCI.0599-05.2005.

Tuchman, R. and Cuccaro, M. (2011) 'Epilepsy and autism: Neurodevelopmental perspective', *Current Neurology and Neuroscience Reports*, 11(4), pp. 428–434. doi: 10.1007/s11910-011-0195-x.

Ubersax, J. A. and Ferrell Jr, J. E. (2007) 'Mechanisms of specificity in protein phosphorylation', *Nature Reviews Molecular Cell Biology*. Nature Publishing Group, 8, p. 530. Available at: <http://dx.doi.org/10.1038/nrm2203>.

Untergasser, A., Cutcutache, I., Koressaar, T., Ye, J., Faircloth, B. C., Remm, M. and Rozen, S. G. (2012) 'Primer3—new capabilities and interfaces', *Nucleic Acids Research*. Oxford University Press, 40(15), pp. e115–e115. doi: 10.1093/nar/gks596.

Vaccaro, A., Patten, S. A., Aggad, D., Julien, C., Maios, C., Kabashi, E., Drapeau, P. and Parker, J. A. (2013) 'Pharmacological reduction of ER stress protects against TDP-43 neuronal toxicity in vivo', *Neurobiology of Disease*. Elsevier B.V., 55, pp. 64–75. doi: 10.1016/j.nbd.2013.03.015.

Vaccaro, A., Patten, S. A., Ciura, S., Maios, C., Therrien, M., Drapeau, P., Kabashi, E. and Parker, J. A. (2012) 'Methylene blue protects against TDP-43 and FUS neuronal toxicity in *C. elegans* and *D. rerio*', *PLoS ONE*, 7(7). doi: 10.1371/journal.pone.0042117.

Vandesompele, J., De Preter, K., Pattyn, F., Poppe, B., Van Roy, N., De Paepe, A. and Speleman, F. (2002) 'Accurate normalization of real-time quantitative RT-PCR data by geometric averaging of multiple internal control genes', *Genome Biology*. London: BioMed Central, 3(7), p. research0034.1-research0034.11. Available at: <http://www.ncbi.nlm.nih.gov/pmc/articles/PMC126239/>.

Vargas, M. R., Johnson, D. A., Sirkis, D. W., Messing, A. and Johnson, J. A. (2008) 'Nrf2 activation in astrocytes protects against neurodegeneration in mouse models of familial amyotrophic lateral sclerosis', *The Journal of neuroscience : the official journal of the Society for Neuroscience*, 28(50), pp. 13574–13581. doi: 10.1523/JNEUROSCI.4099-08.2008.

Varshney, G. K., Pei, W., LaFave, M. C., Idol, J., Xu, L., Gallardo, V., Carrington, B., Bishop, K., Jones, M., Li, M., Harper, U., Huang, S. C., Prakash, A., Chen, W., Sood, R., Ledin, J. and Burgess, S. M. (2015) 'High-throughput gene targeting and phenotyping in zebrafish using CRISPR/Cas9', *Genome Research*. Cold Spring Harbor Laboratory Press, 25(7), pp. 1030–1042. doi: 10.1101/gr.186379.114.

Veeramah, K. R., Johnstone, L., Karafet, T. M., Wolf, D., Salogiannis, J., Barthmaron, A., Greenberg, M. E., Stuhlmann, T., Weinert, S., Jentsch, T., Pazzi, M., Restifo, L. L., Erickson, R. P. and Hammer, M. F. (2014) 'Exome sequencing reveals new causal mutations in children with epileptic encephalopathies', *Epilepsia*, 54(7), pp. 1270–1281. doi: 10.1111/epi.12201.Exome.

Vera, M., Pani, B., Griffiths, L. A., Muchardt, C., Abbott, C. M., Singer, R. H. and Nudler, E. (2014) 'The translation elongation factor eEF1A1 couples transcription to translation during heat shock response', *eLife*, 3, p. e03164. doi:

10.7554/eLife.03164.

Vlasenko, D. O., Novosylina, O. V., Negrutskii, B. S. and El'skaya, A. V. (2015) 'Truncation of the A,A\*,A' helices segment impairs the actin bundling activity of mammalian eEF1A1', *FEBS Letters*. Federation of European Biochemical Societies, 589(11), pp. 1187–1193. doi: 10.1016/j.febslet.2015.03.030.

Vriend, G. and Sander, C. (1993) 'Quality control of protein models: directional atomic contact analysis', *Journal of Applied Crystallography*, 26(1), pp. 47–60. doi: 10.1107/S0021889892008240.

Wagner, D. E., Weinreb, C., Collins, Z. M., Briggs, J. A., Megason, S. G. and Klein, A. M. (2018) 'Single-cell mapping of gene expression landscapes and lineage in the zebrafish embryo', *Science*, 360(6392), pp. 981–987. doi: 10.1126/science.aar4362.

Webb, B. and Sali, A. (2016) 'Comparative Protein Structure Modeling Using MODELLER', *Current protocols in bioinformatics / editorial board, Andreas D. Baxevanis ... [et al.]*, 54, p. 5.6.1-5.6.37. doi: 10.1002/cpbi.3.

Wullimann, M. F. (1997) *The Central Nervous System, The Physiology of Fishes*. doi: 10.1016/j.jcv.2009.08.012.Neurodevelopmental.

Xu, C., Hu, D. and Zhu, Q. (2013) 'eEF1A2 promotes cell migration, invasion and metastasis in pancreatic cancer by upregulating MMP-9 expression through Akt activation', *Clinical & Experimental Metastasis*, 30(7), pp. 933–944. doi: 10.1007/s10585-013-9593-6.

Yamamoto, N., Nakayama, T. and Hagio, H. (2017) 'Descending pathways to the spinal cord in teleosts in comparison with mammals, with special attention to rubrospinal pathways', *Development Growth and Differentiation*, 59(4), pp. 188–193. doi: 10.1111/dgd.12355.

Yang, F., Demma, M., Warren, V., Dharmawardhane, S. and Condeelis, J. (1990) 'Identification of an actin-binding protein from Dictyostelium as elongation factor 1a', *Nature*, 347(6292), pp. 494–496. doi: 10.1038/347494a0.

Zappulo, A., Bruck, D. Van Den, Mattioli, C. C., Franke, V., Imami, K., Mcshane, E., Moreno-estelles, M., Calviello, L., Filipchuk, A., Peguero-sanchez, E., Müller, T., Woehler, A., Birchmeier, C., Merino, E., Rajewsky, N., Ohler, U., Mazzoni, E. O., Selbach, M., Akalin, A. and Chekulaeva, M. (2017) 'RNA localization is a key determinant of neurite-enriched proteome', *Nature Communications*. Springer US, 8, p. 583. doi: 10.1038/s41467-017-00690-6.

Zhang, Y., Zhang, Z. and Ge, W. (2018) 'An efficient platform for generating somatic point mutations with germline transmission in the zebrafish by CRISPR/Cas9-mediated gene editing', *Journal of Biological Chemistry*, 293(17), pp. 6611–6622. doi: 10.1074/jbc.RA117.001080.

Zhong, J., Zhang, T. and Bloch, L. M. (2006) 'Dendritic mRNAs encode diversified functionalities in hippocampal pyramidal neurons', *BMC neuroscience*. BioMed Central, 7, p. 17. doi: 10.1186/1471-2202-7-17.



Zhu, H., Lam, D. C. L., Han, K. C., Tin, V. P. C., Suen, W. S., Wang, E., Lam, W. K., Cai, W. W., Chung, L. P. and Wong, M. P. (2007) 'High resolution analysis of genomic aberrations by metaphase and array comparative genomic hybridization identifies candidate tumour genes in lung cancer cell lines', *Cancer Letters*. Elsevier Ireland Ltd, 245(1–2), pp. 303–314. doi: 10.1016/j.canlet.2006.01.020.

Zuckerkindl, E. and Pauling, L. (1965) 'Evolutionary divergence and convergence in proteins', in Bryson, V. and Vogel, H. (eds) *Evolving Genes and Proteins*. Academic Press, pp. 97–166.